1-1-2018

Cation Clock Reactions For The Determination Of Relative Reaction Kinetics In Glycosylation Reactions

Philip Adero
Wayne State University,

CATION CLOCK REACTIONS FOR THE DETERMINATION OF RELATIVE REACTION KINETICS IN GLYCOSYLATION REACTIONS

by

PHILIP OUMA ADERO

DISSERTATION

Submitted to the Graduate School

of Wayne State University,

Detroit, Michigan

in the partial fulfillment of the requirements

for the degree of

DOCTOR OF PHILOSOPHY

2018

MAJOR: CHEMISTRY (Organic)

Approved By:

_____

Advisor Date

_____

_____

_____

_____

DEDICATION

This dissertation is dedicated to God for his providence and mercy,

and to my family for the unconditional love and support

ACKNOWLEDGMENTS

I would like to express my profound gratitude to my graduate adviser, Professor David Crich for his guidance and encouragement throughout my research work in his laboratory at Wayne State University. I thank him for the confidence he had in me, for his constant unwavering support for my academic excellence and for inspiration and mentorship throughout my Ph.D studies.

I wish to thank my committee members comprising; Prof. Jennifer Stockdill, Prof. Sarah Trimpin and prof. Jianlong Zhu for contributing their time, energy and suggestions to this dissertation and defense.

I would like to thank my previous advisor, Prof. Peter Norris for his immense work in shaping my career by encouraging me to pursue Ph.D studies at Wayne State University. This has totally transformed my scientific knowledge.

I would like to give great gratitude to my past and present labmates. First, to the postdoc in our: Dr. Takayuki Furukawa, for the collaborative work, Dr. Takayuki Kato, Dr. Takahiko Matzushita. Dr. Szyman Buda, Dr. Suresh Dharuman, Dr. Oskar Popik, Dr. Parasuraman, Dr. Vikram Sarpe and Dr. Govind. They had great laboratory techniques. Many thanks to my batchmates, Dr. Amr Sonusi, Dr. Peng Wen, Dr. Girish Sati, and Dr. Harsha Amarasekhara. Without their encouragement and support I would not have been be able to finish this Ph.D. I would like to thank my labmates: Sandeep Dhanju, Bibek Dhakal, Guanyu Yang, Michael Pirrone, Jonny Quirke, Dean Jarios, Tim Mcmillan, Philemon Ngoje, Mohammad Hawsawi, Nuwan Kondasinghe, Sameera Jayanath, Onobun Emmanuel, Fathima Rukshana, Kondor Courtney and Samarbakhsh Amirreza. They are amazing and very responsible people who constantly maintained the operations of the Crich lab. I feel short of words to express a deep sense of respect and gratitude

for my friend and benchmate Dr. Amr Sonusi. In all my difficult moments, I always found him on my side to guide me in every way possible.we not only shared a good rapport with him but also find his criticism and suggestion fruitful in my graduate career.

My special thanks are due to my siblings; Nicholas Adero, Rose Akinyi and Hellen Adhiambo for their unconditional support since the death of my parents. They saw me through my life after the death of my parents and endless encouragement. I always found them standing by my side through thick and thin. I owe more gratitude than I can express to my cousin Dr. James Onyona and for their financial support. I feel short of words to express a deep sense of respect and gratitude for my friend and senior Erick Amuka. My special thanks to my beloved wife Dinah Akinyi for her unconditional love and support in the last five years, I am deeply indebted to her for their unwavering faith in me.

TABLE OF CONTENTS

Dedication ii

Acknowledgments iii

Table of Contents v

List of Figures ix

List of Schemes xi

List of Tables xv

List of Abbreviations xvi

CHAPTER 1: INTRODUCTION 1

1.1 Glycochemistry Significance and Challenges 1

1.2 General Aspects of Chemical *O*-Glycoside Bond Formation 2

1.3 Some Common Chemical *O*-Glycosylation Methods 2

1.3.1 The Koenigs-Knorr Method 2

1.3.2 The Trichloroacetimidate Method 6

1.3.3 Other *O*-Glycosylation Methods 9

1.4 General Mechanism of Chemical *O*-Glycosylation Reaction 10

1.4.1 Mechanistic Studies of Glycosylation 11

1.4.2 NMR Spectroscopic Studies 11

1.4.3 Computational Studies 13

1.4.4 Kinetic Isotope Effects 15

1.5 Clock Reactions 19

1.5.1 Jencks Azide Clock Reaction 19

1.5.2 Radical Clocks 20

1.6 Intramolecular Aglycon Delivery 21

1.6.1 Silicon Mediated Intramolecular Aglycon Delivery. 23

1.6.2 para-Methoxybenzyl Mediated Intramolecular Aglycon Delivery 24

1.6.3 Iodonium-mediated Intamolecular Aglycone Delivery 28

1.7 The Cyclization Concept 30

1.8 Previous Studies in Cation Clock Reactions for the Determination of Relative Kinetics in Pyranosyl Sulfoxide Systems and their Limitations. 32

1.9 Problem Statement. 35

1.10 Main Objectives: 36

CHAPTER 2: CATION CLOCK REACTIONS FOR THE DETERMINATION OF RELATIVE KINETICS IN GLYCOSYLATION REACTIONS: APPLICATIONS TO GLUCO AND MANNOPYRANOSYL TRICHLOROACETIMIDATE DONORS 38

2.1 Introduction 38

2.2 Cation Clock Reactions for the Determination of Relative Kinetics in Glycosylation Reactions: Mannopyranosyl clock system. 40

2.2.1 Synthesis of the 4,6-*O*-Benzylidene-protected Mannopyranosyl Clock 40

2.1.2 Reductive Lithiation 42

2.1.3 Clock Cyclization Reaction 44

2.1.4 *O*-Glycoside Formation in Competition with Cyclization 45

2.1.5 Kinetic Data 46

2.1.6 *C*-Glycosylation in competition with cyclization 48

2.1.7 β-*C*-Mannoside Selectivity 51

2.1.8 Conclusions on *O* and *C*-Mannosylation 52

2.3 Cation Clock Reactions for the Determination of Relative Kinetics in Glycosylation Reactions: Glucopyranosyl Clocks 53

2.3.1 Synthesis of the 4,6-*O*-Benzylidene-protected Glucopyranosyl Clock 53

2.3.2 Clock Cyclization Reaction 55

2.3.3 Conformation and Selectivity of the Glucopyranosyl Oxocarbenium Ion 55

2.3.4 Competition Kinetics (*O*-Glycoside in Competition with Cyclization) 56

2.3.5 Competition Kinetics (*C*-Glucoside Formation in Competition with Cyclization) 58

2.4 Overall Conclusions 63

CHAPTER 3: USE OF CATION CLOCK REACTIONS FOR THE DETERMINATION OF RELATIVE REACTION KINETICS IN ARABINOFURANOSYLATION 64

3.1 Introduction 64

3.2 Synthesis of Phenyl 3,5-*O*-(di-*tert*-Butylsilylene) 2-*O*-((2-Hydroxymethyl) Benzyl)-1-Thio-α-D-Arabinofuranoside 66

3.2.1 Clock Cyclization Reaction 68

3.2.2 Competition Kinetics 71

3.2.3 Kinetic Analysis 72

3.3 Synthesis of Phenyl 3,5-*O*-Dibenzyl-2-*O*-(2-Hydroxymethyl) Benzyl-1-thio-α-D-Arabinofuranoside 74

3.3.1 Clock cyclization reaction with donor **91** 75

3.3.2 *O*-Glycoside Synthesis 76

3.4 Conclusions 81

CHAPTER 4: USE OF THE CATION CLOCK METHOD TO DETERMINE THE INFLUENCE OF ACCEPTOR NUCLEOPHILICITY ON THE ARABINOFURANOSYLATION MECHANISM 82

4.1 Introduction 82

4.2 Synthesis of 1,3-Difluoropropan-2-yl 3,5-*O*-(Di-*tert*-Butylsilylene)-2-*O*-((2-Hydroxymethyl) Benzyl)-1-Thio-D-Arabinofuranosides 84

4.3 Competition Kinetics Using 1,3-Difluoroisopropanol as Acceptor in the 3,5-Di-*O*-*tert*-Butylsilylene Protected Arabinofuranosyl System 85

4.4 Competition Kinetics Using 2-Fluoroethenol as an Acceptor in the 3,5-Di-*O*-*tert*-Butylsilylene Protected Arabinofuranosyl System 87

4.5 Conclusions 92

CHAPTER 5: HYDROGENOLYTIC CLEAVAGE OF NAPHTHYLMETHYL ETHERS IN THE PRESENCE OF SULFIDES 93

5.1 Introduction 93

5.2 Chemistry 95

5.2.1 Synthesis and Hydrogenolytic Cleavage of Naphthylmethyl Ethers in Aliphatic Model Substrates 95

5.2.2 Synthesis and Hydrogenolytic Cleavage of Napthylmethyl Ethers in Thiomannoside Substrates 96

5.2.3 Synthesis and Hydrogenolytic Cleavage of Naphthylmethyl Ethers in Thioglucoside Substrates 98

5.2.4 Synthesis and Hydrogenolytic Cleavage of Naphthylmethyl Ethers in Peptides..... 100
5.3 Conclusions..... 102
CHAPTER 6: EXPERIMENTAL SECTION..... 103
REFERENCES..... 139
ABSTRACT..... 150
AUTOBIOGRAPHICAL STATEMENT..... 152

LIST OF FIGURES

Figure **1**. Pull-push mechanism..... 5

Figure **2.** Whitfield's transition states for glycosylation reactions 13

Figure **3.** Preferred conformations of manno- and glucosyl oxocarbenium ion triflate ion pairs. 15

Figure **4**. Examples of radical clock reactions 20

Figure **5.** 1,2-*cis* and 1,2-*trans* mannosides and glucosides 22

Figure **6.** General mechanism for intramolecular aglycon delivery 22

Figure **7**. Possible approaches to the determination of glycosylation reaction mechanism..... 39

Figure **8.** Common aromatic radical-anions..... 43

Figure **9**. *O*-Glycosides from competition kinetics..... 46

Figure **10.** *O*-Glycoside in competition with cyclization..... 48

Figure **11.** *C*-glycoside from competition kinetics. 48

Figure **12.** Concentration dependence of the formation of *C*-mannosides in competition with cyclization. 50

Figure **13.** *O*- and *C*-Mannosylation with trichloroacetimidate donor 50

Figure **14.** Graphic representation of clock reactions. a) *O*- and *C*-Mannosylation with trichloroacetimidate donor. b) *O*- and *C*-Mannosylation with sulfoxide donor 51

Figure **15.** *O*-Glucoside products from competition reaction 56

Figure **16.** *O*-Glucosylation in competition with cyclization..... 58

Figure **17.** *C*-Glucoside..... 58

Figure **18.** Graphical representation of *C*-glucoside formation in competition with cyclization as a function of concentration 60

Figure **19**. Graphical representation of concentration dependence in *O*- and *C*-glucosylations with trichloroacetimidate donor **70** 60

Figure **20.** Superposition of *C*-glycosylation with mannosyl and glucosyl donors 61

Figure **21**. Structures of D- and L-arabinofuranosides and their anomers..... 64

Figure **22**. Isolated 3,5-di-tert-butylsilylene protected α- and β-O-glycosides..... 72

Figure **23**. Graphical representation of *O*-glycoside formation in competition with cyclization reaction for the 3,5-di-*tert*-butylsilylene donor **84**. 74

Figure **24**. Graphical representation of *O*-glycoside formation in competition with cyclization reaction in 3,5-dibenzyl protected arabinofuranosyl donor series. 79

Figure **25**. Comparison of graphical representation of *O*-glycoside formation in competition with cyclization reaction in both 3,5-di-*tert*-butylsilylene donor and 3,5-dibenzyl donor series. 80

Figure **26**. Selected acceptors for the kinetics study. 83

Figure **27**. 1,3-Difluoroisopropyl glycosides in the 3,5-di-*O*-*tert*-butylsilylene protected arabinofuranosyl system. 84

Figure **28**. Graphical representation of *O*-glycoside formation in competition with cyclization reaction in 3, 5-di-*tert*-butylsilylene protected arabinofuranosyl donor series using 1,3-difluoroisopronanol as the acceptor. 87

Figure **29**. 2-Fluoroethanol glycosides in the 3,5-di-*O*-*tert*-butylsilylene protected arabinofuranosyl system 88

Figure **30**. Graphical representation of *O*-glycoside formation in competition with cyclization reaction in 3,5-di-*tert*-butylsilylene protected arabinofuranosyl donor series using 2-fluoroethanol as the acceptor. 90

Figure **31**. The influence of acceptor nucleophilicity on arabinofuranosylation mechanism..... 91

LIST OF SCHEMES

Scheme **1**. Glycosylation reaction 2

Scheme **2**. Koenigs-Knorr glycosylation using neighboring group participation 3

Scheme **3**. Koenigs-Knorr Glycosylation 4

Scheme **4.** 1,2-*trans* glycoside product formation without neighboring group participation 4

Scheme **5.** 1,2-*cis* Glycoside product formation 5

Scheme **6.** Lemieux bromide ion catalysis concept for the synthesis of α-glycosides 5

Scheme **7.** Mukaiyama catalytic α-glucoside formation 6

Scheme **8**. General synthesis and use of trichloroacetimidates 7

Scheme **9.** Fructofuranoside synthesis using an *N*-phenyltrifluoroacetimidate 8

Scheme **10.** In(III)-promoted glycosylation. 8

Scheme **11.** Example of lanthanide salt activation of trichloroacetimidates 9

Scheme **12.** $Bi(OTf)_3$ promoted glycosylation 9

Scheme **13**. General glycosylation mechanism 10

Scheme **14.** Formation, structure and irreversible quenching of the fully protonated triacetyl 2-deoxy-D-glucopyranosyl oxocarbenium ion 12

Scheme **15**. Formation, structure and irreversible quenching of the fully protonated triacetyl 2-bromo-2-deoxy-D-glucopyranosyl oxocarbenium ion 13

Scheme **16.** Intermediates and transition states involved in reactions of Manno- and Glucose systems 14

Scheme **17**. Natural abundance ^{13}C NMR KIE study, on formation of; a) β and α-mannosides, b) β and α-glucosides 17

Scheme **18.** Formation of the β- and α-glycosides in the reaction of oxetane with acyclic mannosyl iodide 18

Scheme **19**. Exclusive β-mannosylation; the benzylidene effect 18

Scheme **20**. Jencks azide clock reaction 19

Scheme **21.** Radical clock reaction in competition kinetics 21

Scheme **22.** Hindsgaul's acid-catalysed tethering and glycosylations..... 23

Scheme **23**. Stork's silicon-tethered β-mannosylation..... 24

Scheme **24:** Ogawa's p-Methoxybenzyl mediated intramolecular aglycon delivery 25

Scheme **25.** Ogawa and Ito's PMB mediated β-mannosylation using thioglycoside donor..... 25

Scheme **26.** Mechanism of 4-methoxybenzylidene- tethered intermediates 26

Scheme **27:** β-Fructosylation with the PMB IAD method 27

Scheme **28.** β-Arabinofuranosylation with the PMB IAD method..... 27

Scheme **29.** Bertozzi's DMB-mediated IAD for the synthesis of trehaloses..... 28

Scheme **30.** Iodinium-mediated tethering and intramolecular glycosylation in gluco and manno systems..... 29

Scheme **31.** Fairbanks' allyl-derived IAD with thioglycoside donors..... 30

Scheme **32**. Cyclization of protecting groups at the 2-position. 31

Scheme **33.** Denmark's use of an intramolecular allylsilane-acetal reaction as a probe of mechanism. 32

Scheme **34.** Initial clock cyclization design..... 32

Scheme **35**. Clock reaction for mannosyl sulfoxide donor 33

Scheme **36**. Proposed reaction mechanism for the formation of clock products..... 34

Scheme **37**. Competition glycosylation reaction in mannose system 35

Scheme **38.** The sulfenyl transfer product complicating use of the original clock in the glucose series. 36

Scheme **39.** The cation clock reaction 39

Scheme **40**. Synthesis of a 4,6-*O*-benzylidene-protected mannopyranosyl clock 40

Scheme **41.** Initial alkylation of the thioglycoside..... 41

Scheme **42.** Synthesis of iodomethylallylsilane..... 41

Scheme **43.** Cleavage of the phenylethyl thioglycoside 42

Scheme **44.** Generation of the aromatic radical anion reducing agent 42

Scheme **45.** General mechanism of reduction cleavage of phenylether thioethers..... 42

Scheme **46**. Proposed mechanism of reductive cleavage of compound **50** 43

Scheme **47.** Clock cyclization reaction (mannosyl unimolecular clock reaction)..... 44

Scheme **48.** Conformation and selectivity of the mannopyranosyl oxocarbenium ion in the cyclization reaction 45

Scheme **49.** Rationalization of selectivity in 4,6-*O*-benzylidene protected β-*C*-mannosyl formation..... 52

Scheme **50.** Synthesis of the 4,6-*O*-benzylidene-protected glucopyranosyl clock. 54

Scheme **51**. Glucopyranosyl unimolecular clock reaction..... 55

Scheme **52**. Conformation and selectivity of the glucopyranosyl oxocarbenium ion 56

Scheme **53.** Synthesis of a 3,5-*O*-di-*tert*-butylsilylene protected arabinofuranoside donor..... 66

Scheme 54. Synthesis of 2-((naphthalen-2-ylmethoxy) methyl) benzyl bromide 67

Scheme **55**. Hydogenolytic cleavage of the naphthymethyl protecting group 68

Scheme **56**. Clock cyclization reaction..... 69

Scheme **57**. Cyclization of the clock system. 70

Scheme **58**. Inside attack on the furanosyl oxocarbenium ion leading to the major product, and outside attack leading to the minor product. 71

Scheme **59**. Synthesis of phenyl 3,5-*O*-dibenzyl-2-*O*-(2-hydroxymethyl) benzyl-1-thio-α-D-arabinofuranoside..... 75

Scheme **60** The clock cyclization reaction in the 3,5-di-*O*-benzyl series..... 76

Scheme **61**. Model for the selectivity of the cyclization..... 76

Scheme **62**. The synthesis and characterization of *O*-glycosides in the 3,5-di-*O*-benzyl arabinofuranoside series..... 77

Scheme **63**. The formation of both β- and α-glycosides due to rapidly equilibrating arabinofuranosyl triflates. 92

Scheme **64.** Selective hydrogenolysis of a naphthylmethyl ether in presence of a benzyl ether.. 94

Scheme **65**. Selective hydrogenolytic cleavage of a naphthylmethyl carbamate in presence of a benzyl carbamate. 94

Scheme **66**. Hydogenolytic cleavage of the naphthymethyl ether in presence of benzyl ether and phenyl thioether. 95

Scheme **67**. Model aliphatic substrate synthesis 95

Scheme **68**. Hydrogenolytic cleavage of aliphatic a naphthylmethyl ether in presence of a sulfide..... 96

Scheme **69**. Synthesis of phenyl 2, 3, 4-tri-*O*-benzyl-6-*O*-(2-naphthyl)methyl-1-thio-α-D-mannopyranoside 96

Scheme **70**. Synthesis of phenyl 3, 4, 6-tri-*O*-benzyl-2-*O*-(2-naphthyl)methyl-1-thio-α-D-mannopyranoside 97

Scheme **71**. *tert*-Butyl 2,3,4-tri-*O*-benzyl-6-*O*-(2-naphthyl)methyl-1-thio-β-D-mannopyranoside 97

Scheme **72**. Synthesis of naphthylmethyl and benzyl ethers containing thioglucosides **116** and **118.**..... 99

Scheme **73**. Hydrogenolytic cleavage of napthylmethyl ethers in thioglucosides..... 100

Scheme **74**. Synthesis of the naphthylmethyl and benzyl containing tripeptide **124**..... 101

Scheme **75**. Hydrogenolytic cleavage of napthylmethyl ethers peptides. 101

LIST OF TABLES

Table **1**. *O*-Mannosylation with trichloroacetimidates donor **55**. 47

Table **2**. *C*-Mannosylation with trichloroacetimidates donor 49

Table **3.** *O*-Glucosylation with trichloroacetimidate donor **70**. 57

Table **4.** *C*-Glucoside in competition with cyclization 58

Table **5**. *O*-Glycoside formation in competition with cyclization for the 3,5-*O*-di-*tert*-butylsilylene protected donor..... 73

Table **6**. *O*-Glycoside formation in competition with cyclization reaction for the 3,5-dibenzyl protected donor **91** 78

Table **7**. *O*-Glycoside formation in competition with cyclization reaction for the 3,5-di-*tert*-silylene protected donor **84** using 1,3-difluoroisopronol as acceptor. 86

Table **8**. *O*-Glycoside formation in competition with cyclization reaction for the 3,5-di-*tert*-butylsilylene protected donor **84** using 2-fluoroethanol acceptor..... 89

Table **9**. Hydrogenolytic cleavage of napthylmethyl ethers in thiomannoside systems 98

LIST OF ABBREVIATIONS

AgOTf	Silver trifluoromethanesulfonate
Bn	Benzyl
BnBr	Benzyl bromide
CSA	Camphorsulfonic acid
CIP	Contact ion pair
DBU	1,8-Diazabicyclo[5.4.0]undec-7-ene
DCM	Dichloromethane
DDQ	2,3-Dichloro-5,6-dicyano-1,4-benzoquinone
DIPEA	*N*,*N*-Diisopropylethylamine
DMAP	4-(Dimethylamino)pyridine
DMF	*N*,*N*-Dimethylformamide
DMSO	Dimethyl sulfoxide
equiv.	Equivalent
Et	Ethyl
ESI-HRMS	Electrospray ionization high resolution mass spectroscopy
h	Hour
H	Half boat
HATU	*O*-(7-Azabenzotriazol-1-yl)-1,1,3,3-tetramethyluronium hexafluorophosphate
HPLC	High performance liquid chromatography
Hz	Hertz
IDCP	Iodonium dicollidine perchlorate

i-Pr	Isopropyl
i-PrOH	Isopropyl alcohol
Me	Methyl
min	Minutes
mmol	Millimole
M.p.	Melting point
MS	Molecular sieves
Nap	2-Naphthylmethyl
NIS	*N*-Iodosuccinimide
NMR	Nuclear magnetic resonance
PMB	*p*-Methoxybenzyl
PG	Protecting group
Ph	Phenyl
ppm	Parts per million
PTSA	*p*-Toluenesulfonic acid
Py	Pyridine
quant.	Quantitative
r.t.	Room temperature
sat.	Saturated
SSIP	Solvent separated ion pair
TBAF	Tetrabutylammonium fluoride
temp.	Temperature
Tf	Trifluoromethanesulfonyl

TFA	Trifluoroacetic acid
THF	Tetrahydrofuran
TLC	Thin layer chromatography
TTBP	2,4,6-Tri-*tert*-butylpyrimidine
TMSOTf	Trimethylsilyl trifluoromethanesulfonate
UPLC	Ultra high-pressure liquid chromatography
UV/Vis	Ultraviolate-visible

CHAPTER 1: INTRODUCTION

1.1 Glycochemistry Significance and Challenges

Carbohydrates represent the largest class of naturally occurring compounds that are found as essential components of bioactive molecules on earth. They were initially assumed to serve as energy storage materials, structural components, and primary metabolites.[1] Currently, it is known that carbohydrates mediate many fundamental biochemical processes,[2] such as molecular recognition, cell–cell interaction, immunological recognition, transmission of biological information, and so on.[3] Carbohydrates also play crucial roles in life threatening events like pathogenesis of diabetes, bacterial and viral infections, inflammation, development and growth of cancers, and many other diseases. Clearly, the importance of carbohydrates in biology and the potential for their exploitation in medicine has made glycoscience one of the most vibrant and dynamic fields at the interface of chemistry and biology.[4,5]

In nature, carbohydrates exist as polysaccharides, glycoconjugates, or glycosides. Major challenges in studying natural carbohydrates are the difficulties in isolating and characterizing these molecules from their natural sources. While some scientists have been able to successfully isolate and characterize certain classes of natural carbohydrates, the availability of pure isolates is still low. Consequently, the ever-expanding field of glycoscience depends critically on the development of improved synthetic methods for the supply of natural and artificial oligosaccharides and their conjugates. The central reaction in glycochemistry is that of glycosidic bond formation, or glycosylation,[6, 7, 8] but surprisingly the details of this critical reaction remain relatively poorly understood.

The notable challenges involved in the synthesis of complex oligosaccharides and glycoconjugates include branched structures, anomeric stereochemistry, regiochemistry and

coupling efficiency. This diversity, and the complexity of oligosaccharides and glycoconjugates, demands the use of a range of the most efficient synthetic methods with sufficient scope.

1.2 General Aspects of Chemical *O*-Glycoside Bond Formation

Glycosylation is one of the most important reactions in the field of glycochemistry. It is the substitution of a leaving group in a glycosyl donor by an acceptor alcohol, often supported by a promoter, for which there are two extreme mechanisms, uni- and bimolecular nucleophilic substitution, that are bridged by a continuum of more or less tightly bound ion pairs leading to generation of a glycosidic bond.[9,10] As a general principle of most glycosylation methods, a glycosyl donor is formed by combining a leaving group with the anomeric centre of one appropriately protected glycosyl building block. Once the glycosyl donor is activated, it reacts with one hydroxyl group of the completely or partially protected glycosyl acceptor. There are two anomers of *O*-glycosides (Scheme 1), which are commonly defined as the α- and β glycosides.

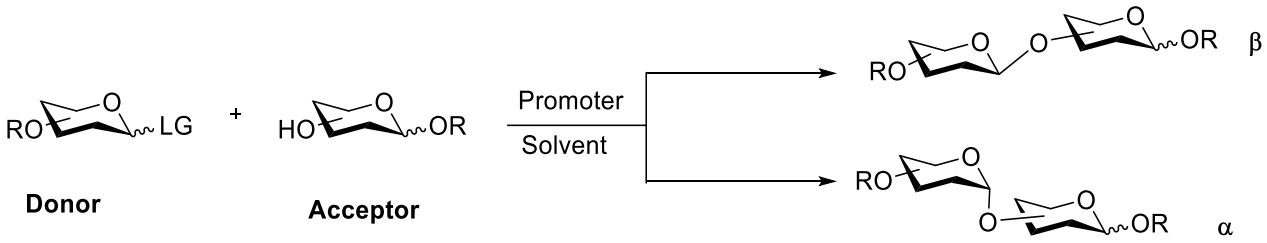

Scheme **1**. Glycosylation reaction

1.3 Some Common Chemical *O*-Glycosylation Methods

1.3.1 The Koenigs-Knorr Method

Published by Koenigs and Knorr in 1901,[11] this is one of the oldest glycosylation methods. It has gone through various modifications and is still currently being used.[11] In this method, glycosyl halides (Br, Cl) are activated by various silver salts like $AgCO_3$, Ag_2O as well as those

soluble salts like AgOTf, $AgClO_4$ to give glycoside products. The use of heavy metal salts like $HgBr_2$, $Hg(CN)_2$ was also successfully reported by Helferich.

One of the advantages of glycosyl halides is that, they can easily be synthesized in few steps. Glycosyl bromides are obtained from the treatment of per-acetylated sugars with HBr-AcOH, while glycosyl chlorides are synthesized from the same staring material as bromides using tin tetrachloride as promoter and chloride source.

Classical examples of Koenigs-Knorr, used 2,3,4,6-tetra-acetyl-α-D-glucopyranoside bromide, activated it with Ag_2CO_3 in dichloromethane and observed a β-glycoside as major product (Scheme 2).

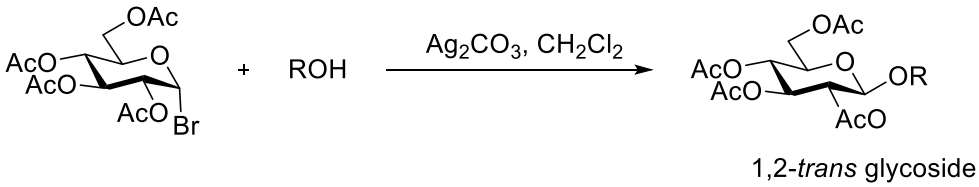

Scheme **2**. Koenigs-Knorr glycosylation using neighboring group participation

The observed stereochemistry (1,2-*trans* type) is attributed to neighboring group participation. The acetate protecting group at C (2) results in an intramolecular nucleophilic attack of the oxocarbenium ion leading to the formation of an acetoxonium ion intermediate. The trapping of the acetoxonium ion by the alcohol on the β-face (path **a**) gave the desired 1,2-*trans* *O*-glycoside as major product. While attack via path **b** leads to the formation of the orthoester (Scheme 3).

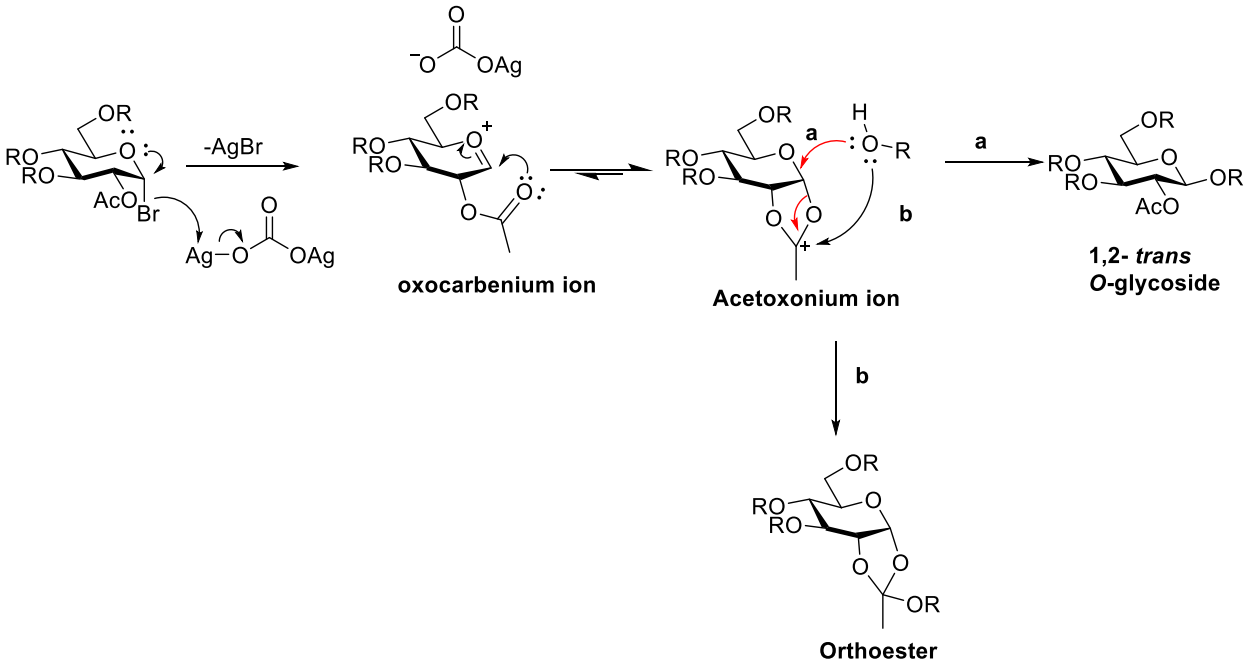

Scheme **3**. Koenigs-Knorr Glycosylation

Reaction under same conditions but with ether protecting groups, 2,3,4,6-tetra-benzyl-α-D-glucopyranoside bromide, a similar stereochemical outcome was observed despite the absence of neighboring group participation (Scheme 4).

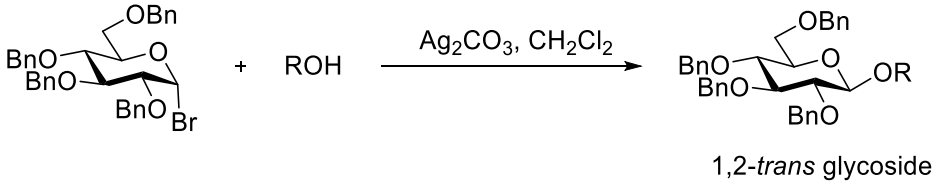

Scheme **4.** 1,2-*trans* glycoside product formation without neighboring group participation

The observation can be understood from the view point of the 'push and pull mechanism,' a more S_N2-like reaction taking place on the promoter surface (Figure 1).

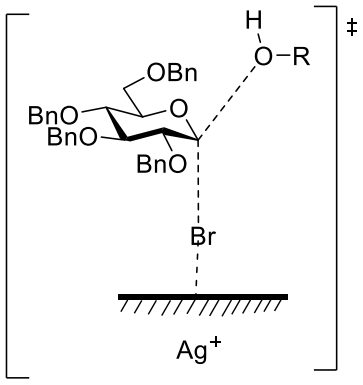

Figure **1**. Pull-push mechanism

Interestingly, the use of a more soluble catalyst, AgOTf gave a 1,2-*cis* glycoside (Scheme 5). This prompted more mechanistic studies to explain the stereochemical outcome.

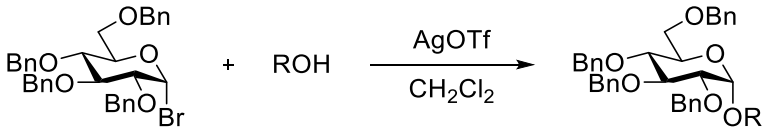

Scheme **5.** 1,2-*cis* Glycoside product formation

Lemieux and coworkers used the additive tetraethylammonium bromide in their halide-ion catalyzed approach to axial glycosides from glycosyl bromides. In this seminal work, in what amounts to a demonstration of the Curtin-Hammett principle, the added bromide was considered to displace bromide from the initial axial donor to populate the less stable but more reactive equatorial bromide, which itself was subsequently displaced by the alcohol (Scheme 6).[12]

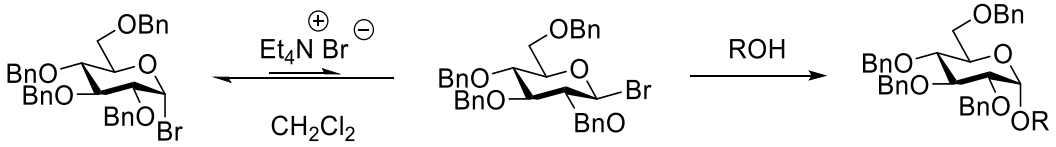

Scheme **6.** Lemieux bromide ion catalysis concept for the synthesis of α-glycosides

Other modifications of the Koenigs-Knorr reaction include preparation of the sugar hemiacetals with PPh_3/N-halosuccinimide reported by Hanessian and co-workers[13] or with PBr_3 as reported by Smith group.[14]

The development of the Koenigs-Knorr reaction is still under active investigation to avoid the two main disadvantages; the instability of glycosyl halides and the use of stoichiometric heavy metal salts of silver and mercury. Other critical developments of the method include the stereocontrolled synthesis of 1-2-*cis*-*O*-glycosides while improving the thermal stability of the glycosyl donor and the stoichiometric use of the promoters. To this end, Mukaiyama and co-workers reported a catalytic and stereoselective glycosylation with β-glycosyl fluorides. They used a fluorophilic promoter ($SnCl_2$-$AgClO_4$), which gave a predominantly the α-glucoside (Scheme 7).[15] They also reported instances in which the avoided they use of metals; by using activated glycoside fluorides and catalytic protic promoters like TfOH, $HClO_4$, or $C_4F_9SO_3H$.[16]

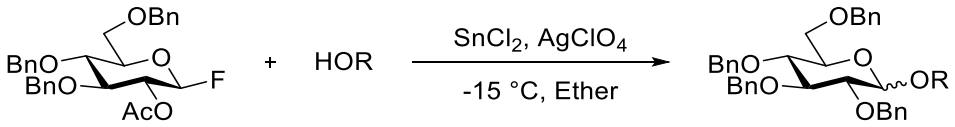

α : β = (80: 20 –92:8)

Scheme **7.** Mukaiyama catalytic α-glucoside formation

1.3.2 The Trichloroacetimidate Method

This glycosylation method that avoids the use of heavy metal salts as promoters, was developed by Schmidt and Michel in 1980, and relies on *O*-glycosyl trichloroacetimidates as a new type of glycosyl donors.[14] The main advantages of the method are; easy preparation of sufficiently stable donors that can be activated for the glycosylation reactions with catalytic amounts of Lewis acids such as boron trifluoride etherate and trimethylsilyl trifluoromethane

sulfonate (TMSOTf).[17] The installation of the trichloroacetimidate starts with the base (NaH, K_2CO_3, or DBU) treatment of the anomeric hydroxyl leading to the formation of anomeric oxyanion (Scheme 8). The electron-deficient nitriles are known to undergo direct and reversible base-catalyzed addition of alcohols to the triple-bond system, thereby providing *O*-alkyl imidates.[18] Trichloroacetimidates can be isolated in pure form and often in high yields. After the installation of the imidate, the glycosylation reaction is initiated by the addition of the catalytic Lewis acid (Scheme 8). The well-established promoters are Lewis acids as mentioned above. However, there has been tremendous development of both promoters and imidate derivative for efficient glycosylation reaction.

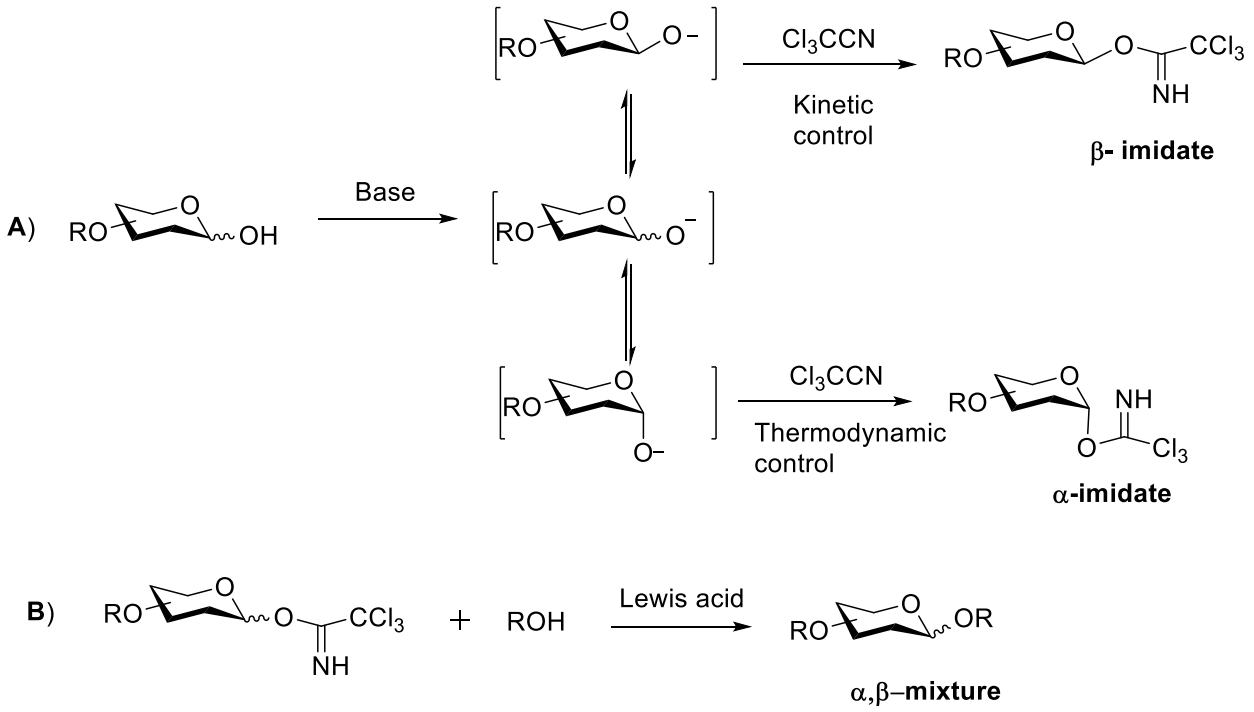

Scheme **8**. General synthesis and use of trichloroacetimidates

The synthesis of trichloroacetimidates can be difficult in some cases, especially the synthesis of fructofuranosides. In that case, Lin and coworkers made an effective use of *N*-

phenyltrifluoroacetimidates as efficient trichloroacetimidate substitutes (Scheme 9).[19] They showed effective α-selectivity when performing glycosylations with various flavonoids.[20]

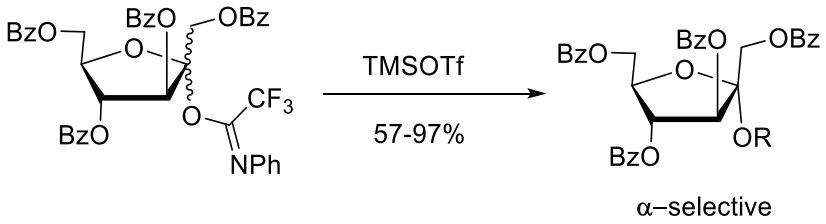

Scheme **9.** Fructofuranoside synthesis using an N-phenyltrifluoroacetimidate

Whereas $BF_3{\cdot}Et_2O$ and TMSOTf have been widely used as promoters in the activation of tricholoracetimidates donors, Cloninger and coworkers reported in 2012 the use of In(III)-based promoters; $InCl_3$, $InBr_3$, and $In(OTf)_3$ in the preparation of glycosides from trichloroacetimidate donors with a range of protecting groups and alcohol acceptors (Scheme 10). They showed that In(III) compounds were better than the widely used promoter BF_3OEt_2.[21] Their versatility has also been effectively established in the synthesis of kaempferol derivations by virtue of its subsequent activation with $BF_3{\cdot}Et_2O$.[22]

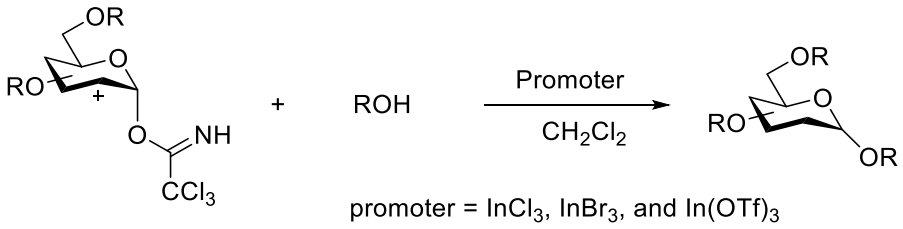

Scheme **10.** In(III)-promoted glycosylation.

The versatility of $BF_3{\cdot}Et_2O$ over TMSOTf for the activation of trichloroacetimidate or (*N*-phenyl)trifluoroacetimidate donors, leading to the selective formation of 1,2-*trans* glycosides in high yields, has been widely studied.[23]

Another activation method reported by Adinolfi and coworkers uses catalytic amounts of $Sm(OTf)_3$ to activate armed glycosyl trichloroacetimides. Activation by lanthanide salts like $Sc(OTf)_3$, $Tb(OTf)_3$, and $Yb(OTf)_3$ at room temperature was also reported (Scheme 11).[24] To reduce the toxicity involved in the use of lanthanide salts, they also reported the alternate use of $Bi(OTf)_3$ for the activation of perbenzylated trichloroacetimidates and (*N*-phenyl)trifluoroacetimidate glycosyl donors (Scheme 12).[25]

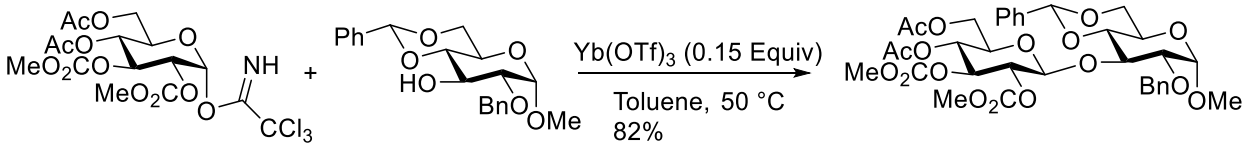

Scheme **11.** Example of lanthanide salt activation of trichloroacetimidates

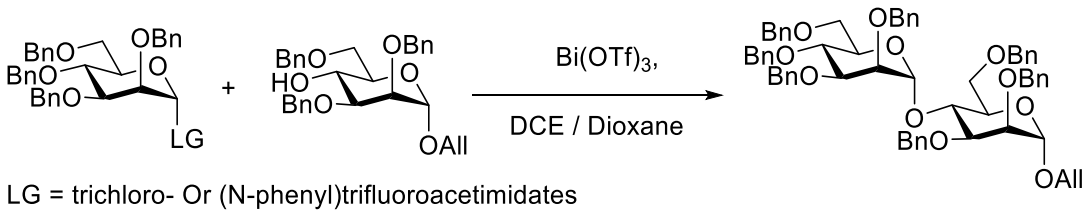

Scheme **12.** $Bi(OTf)_3$ promoted glycosylation

1.3.3 Other *O*-Glycosylation Methods

The need for the improved glycosylation and stereoselectivity of the glycosylation reactions has prompted the development of additional functional groups such as thioglycosides, glycals,[26] sugar epoxides,[27] phosphites, phosphates, sulfinates, etc as donors. Although all the above methods have been employed for chemical *O*-glycoside bond formation, the trichloroacetimidate method is the most widely applied and is considered one of the most efficient methods for the *O*-glycoside bond formation in both simple and complex synthesis of oligosaccharides.

1.4 General Mechanism of Chemical *O*-Glycosylation Reaction

The mechanism of glycosylation displays a lot of complexity beyond the involvement of an oxocarbenium ion intermediate, due to the many variables like the nature of the glycosyl donor, of the glycosyl acceptor and of the promoter. However, mechanistically, the concept revolves around equilibrating contact and solvent-separated oxocarbenium ion/ counterion pairs as initially reported by Winstien and co-workers in solvolysis reactions.[28] The concept was first applied to glycosylation by Rhind-Tutt and Vernon,[12] and consequently further advanced by Lemieux.[27] Subsequently, a more systematic mechanistic study was done in the Crich lab, which drew a demarcation and finally the conclusion that glycosylation mechanisms can occur via two extreme pathways namely S_N1 and S_N2. Scheme 13 shows the borderline existence of glycosyl cations in the general glycosylation mechanism.

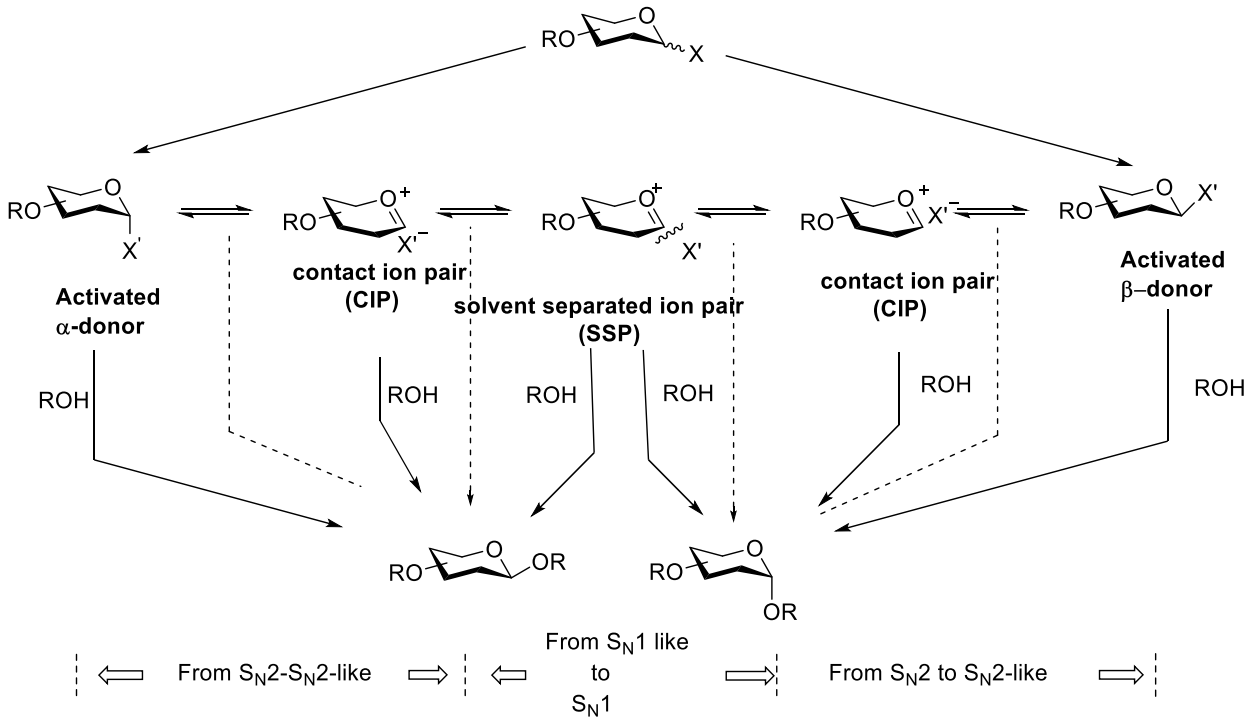

Scheme **13**. General glycosylation mechanism

1.4.1 Mechanistic Studies of Glycosylation

A knowledge of reactive intermediates and the transition states is crucial for the development of improved synthetic methods, which avoid side reactions and give quantitative yields and selectivity. The investigation of these transition states or reactive intermediates has been reported by three significant types of studies that have led to some important hypotheses for such species: namely, kinetic isotope effects, computational studies of hypothetical transition states and nuclear magnetic (NMR) studies of the donor under activation conditions.

1.4.2 NMR Spectroscopic Studies

Despite the tremendous strides in the study of many different reactive glycosyl intermediates of many different carbohydrates in the recent past, it is still very difficult to predict whether these intermediates are truly involved in the product-forming step or merely serve as a reservoir for a more reactive species. NMR spectroscopy has transformed this field, and no other technique has been able to give the same insight into what goes on once the glycosyl intermediate is activated. Olah used superacidity to generate, stabilize and study carbocations[29] by low-temperature NMR (including simple oxocarbenium ions).[30] However, the concept of a 'cation-pool' approach based on an electrochemical oxidation reaction which favors the accumulation and low-temperature NMR analysis of acyclic and cyclic oxocarbenium ions in organic solvents (dichloromethane), has been applied with little success to glycosyl cations, since they have been found to be too unstable under these conditions. The major break-through in characterization of glycosyl cations was recorded by Blériot and co-workers using NMR spectroscopic characterization, and preliminary reactions of free 2-deoxy and 2-bromo- 2-deoxy glucopyranosyl oxocarbenium ions liberated from close proximity with any counterion by the hydrofluoric acid–antimony pentafluoride (HF/SbF_5) superacidic medium.[31] In this paper, the authors reported that

on dissolution in an approximately 4:1 mixture of HF and SbF_5 at −40 °C, 2-deoxy-β-D-glucopyranose tetraacetate gave ^{1}H and ^{13}C NMR spectra consistent with conversion to the fully protonated form of the tri-*O*-acetyl-2-deoxyglucopyranosyl oxocarbenium ion as characterized by the anomeric proton and carbon resonances with chemical shifts (δ) of 8.89 and 229.1, respectively (Scheme 14). The also reported density functional theory (DFT) calculations and coupling constant analysis pointing to the preferential adoption of a ^{4}E envelope conformation in which the three protonated substituents take up pseudoequatorial positions. V-T NMR spectroscopy demonstrated the cation to be stable to at least 20 °C in the HF/SbF_5 mixture.

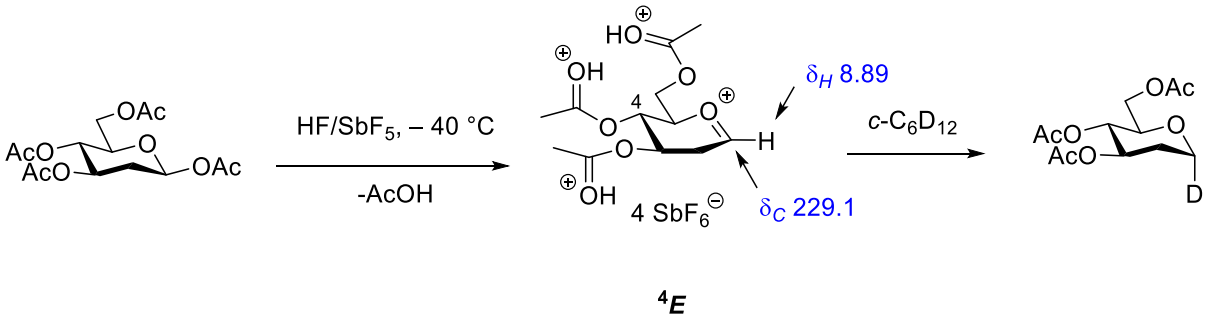

Scheme **14.** Formation, structure and irreversible quenching of the fully protonated triacetyl 2-deoxy-D-glucopyranosyl oxocarbenium ion.

According to Blériot, peracetyl-2-bromo-2-deoxy-β-D-glucopyranose (Scheme 15) on dissolution in the same HF/SbF_5 mixture lost the anomeric acetate and afforded a triprotonated cation assigned to a $^{4}H_5$ half-chair conformation containing a loose unsymmetrical cyclic bromonium ion, whose presence was revealed by the anomeric proton and carbon resonances of δ 8.36 and 198.1, respectively. These revelations have certainly enhanced the mechanistic understanding of the intermediacy of oxocarbenium ions.

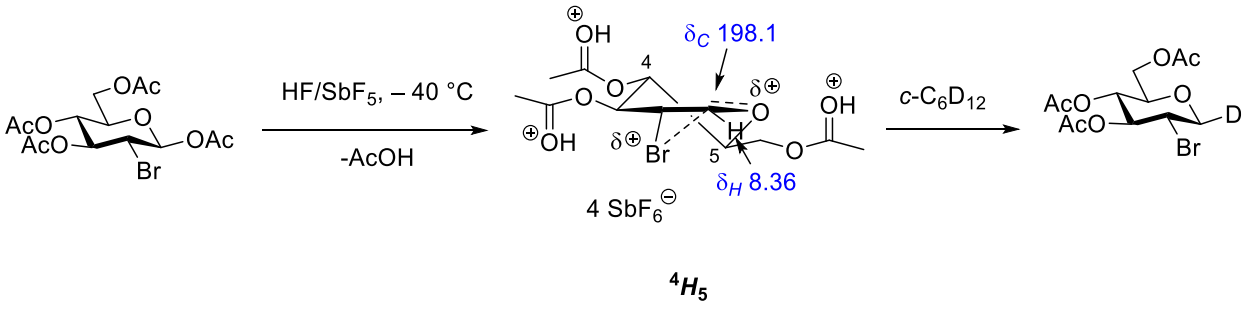

Scheme **15**. Formation, structure and irreversible quenching of the fully protonated triacetyl 2-bromo-2-deoxy-D-glucopyranosyl oxocarbenium ion

1.4.3 Computational Studies

In the absence of direct observation of glycosyl oxocarbenium ions themselves, computational studies have been advanced to predict their conformations.[32] Whitefield and co-workers, using density functional theory calculations further showed plausible transition states for glycosylation reactions (Figure 2).[33] In the work, they used glycosyl triflate as the intermediate, dichloromethane as the solvent, methanol. They observed that the bond length (C-1-OTf) was greater that 2Å before the nucleophilic attack, suggesting the dissociative nature of glycosylation process.

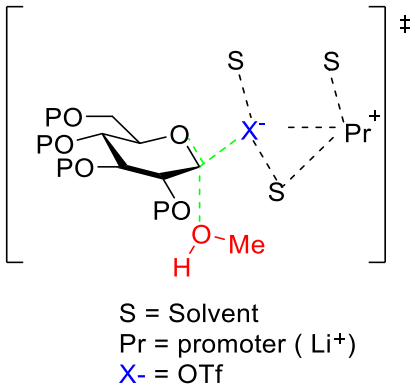

Figure **2.** Whitfield's transition states for glycosylation reactions

Another tremendous work was reported by Li and coworkers, in which they used computational studies to explain the effect of cyclic protecting groups in controlling stereochemical outcome.[34] Computational methods also were used to study the effect of benzylidene acetal and cyclic carbonate protecting groups in glycosylation reactions. Methylidene acetal- and methyl ether-protected mannosyl triflate intermediates were used to mimic the benzylidene acetal-protected mannosyl donor and glucosyl triflate intermediates. Using methanol as acceptor in all cases, they reported the relative energies of transition states and concluded that ring strain plays a major role in stereoselectivity glycosylation reaction, as was earlier demonstrated experimentally.[35,36,37]

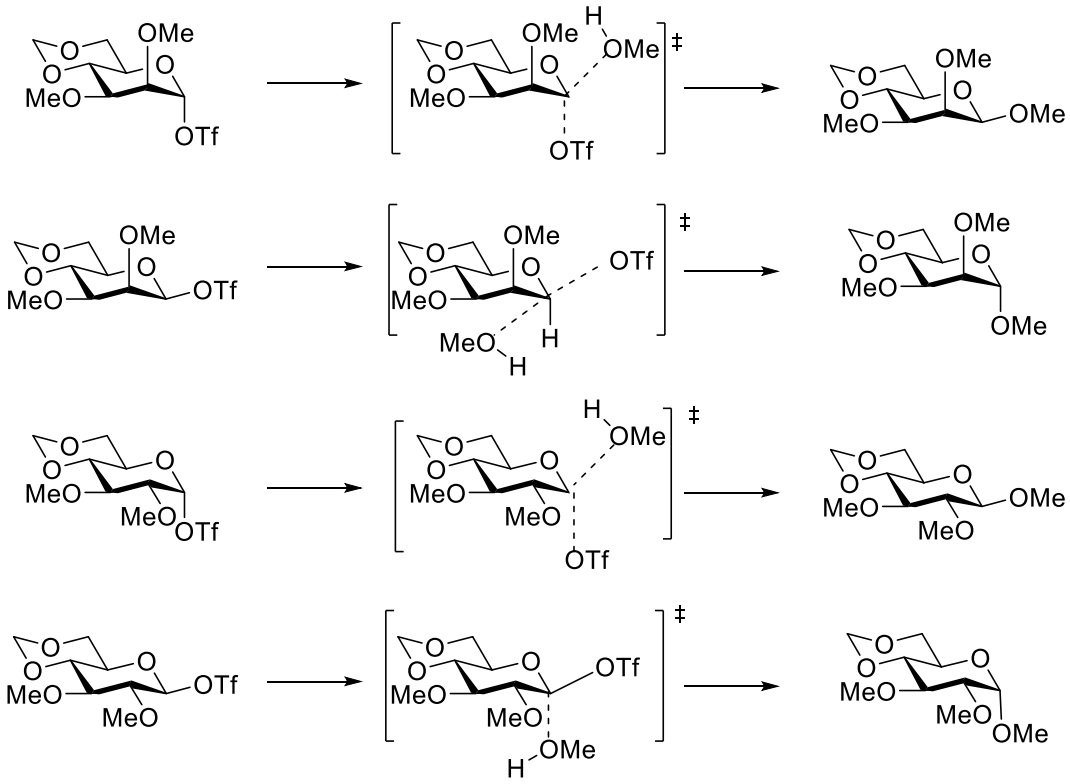

Scheme **16.** Intermediates and transition states involved in reactions of Manno- and Glucose systems

In recent mechanistic studies, Kosma and co-workers,[38] using computational studies unveiled two major differences between the D-mannopyranosyl and D-glucopyranosyl ion pairs.

They reported that the ion pairs from the D-mannopyranosyl triflate adopt $B_{2,5}$-like conformations unlike the D-glucopyranosyl triflate which adopts the $^4H_3$ conformation (Figure 3). This study also revealed that dioxacarbenium ion with the 1,6-anhydo structure is more stable in the D-mannopyranosyl series, and hence more likely to play roles in mannosylation reactions. They asserted that the stability and the geometries of the ion pairs play key roles in the determination of stereochemical outcome of glycoside synthesis. They also noted other factors like the chemical properties of the acceptor, i.e, steric properties, nucleophilicity, acceptor type (*O*- or *C*-glycosylation) and the influence of the protecting group on the chemical nature of ion pairs.

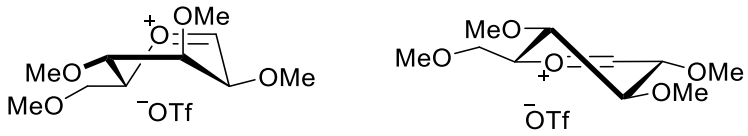

($B_{2,5}$) ($^4H_3$)

Figure **3.** Preferred conformations of manno- and glucosyl oxocarbenium ion triflate ion pairs

1.4.4 Kinetic Isotope Effects

The use of kinetic isotope effects (KIE) in probing reaction mechanisms has well been appreciated by the synthetic community especially in the light of the distinction between S_N1 and S_N2 mechanisms. Singleton and coworkers developed a method for precise measurement of ^{13}C and ^2H KIEs at natural abundance simultaneously for every atom in the molecule of interest using high field NMR.[39] Crich and coworkers using a benzylidene protected mannosyl sulfoxide partially enriched by deuterium at the anomeric position and in the benzylidene position successfully studied the formation of a β-mannosyl linkage to a relatively unreactive glucopyranosyl 4-H via the corresponding α-mannosyl triflate.[40] The KIE data was consistent with a loosely associative mechanism for this displacement.[41] Crich and coworkers, working at natural abundance with 800

MHz NMR reported the KIE values for the glycosylation reaction of 4,6-*O*-benzylidene protected mannosyl and glycosyl triflates with isopropanol in CD_2Cl_2 giving α and β glycosides in both manno and gluco-type systems (Scheme 17).[41] Based on the KIE data, the formation of the β-manno- and glucosides can be rationalized as a direct displacements on the α-triflates, whereas the α-glucoside is viewed as formed by associative displacement of a minor but more reactive β-glucosyl triflate in dynamic equilibrium with its β-anomer. According to Crich, α-mannoside formation, displays a distinctly different mechanisms ^{13}C primary KIE data is more consistent with the operation of an S_N1-type mechanism.

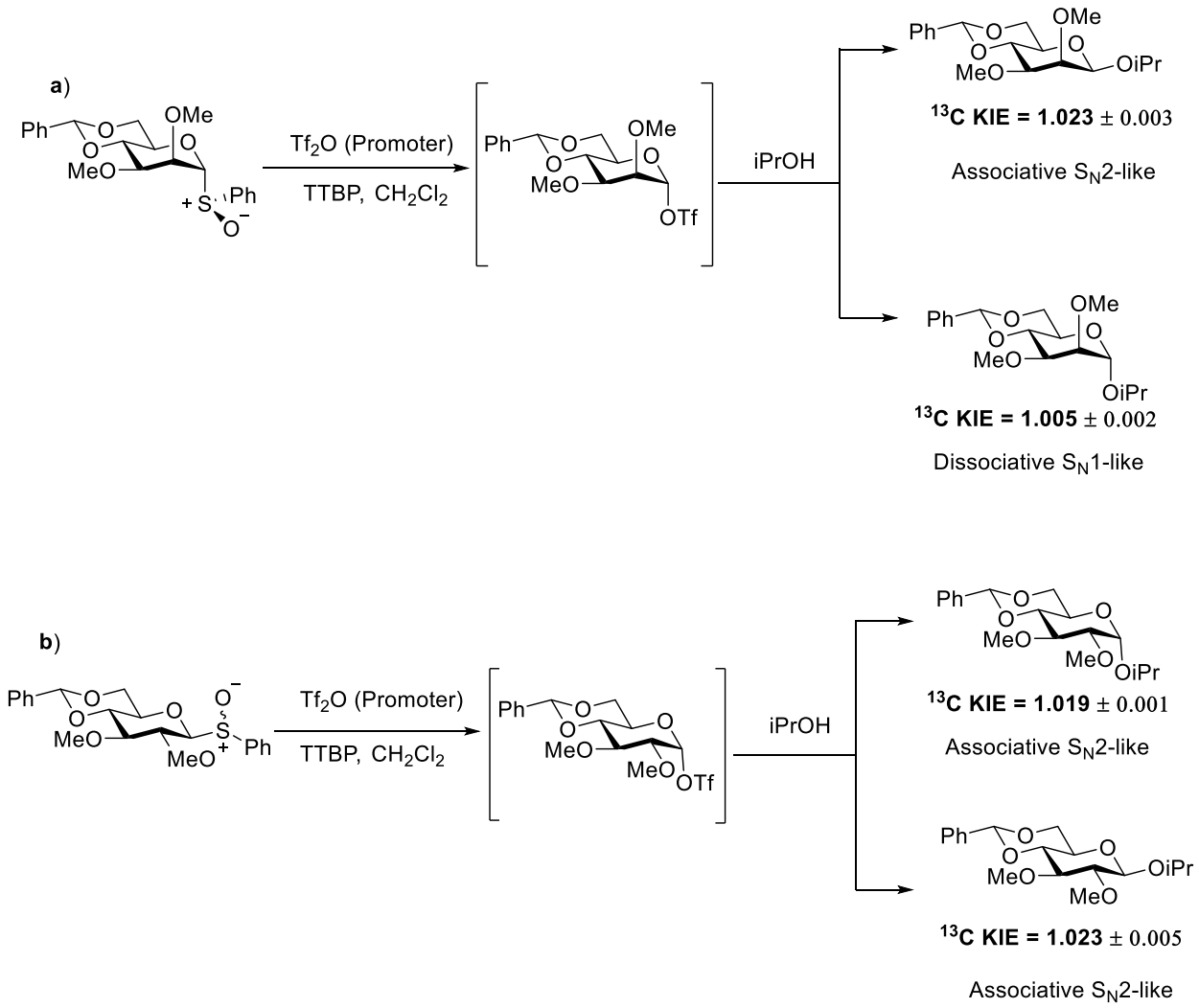

Scheme **17**. Natural abundance ^{13}C NMR KIE study, on formation of; a) β and α-mannosides, b) β and α-glucosides

In another account, Gervay-Hague and coworkers studied the formation of the β- and α-glycosides in the reaction of oxetane with a 6-*O*-acetyl-2,3,4-tri-*O*-benzyl-α-mannosyl iodide in deuteriobenzene at room temperature (Scheme 18).[42] After comparison with the computed transition states for associative displacements they concluded that both reactions proceeded via exploded S_N2-like transition states, however formation of the α-glycoside displayed a significantly longer partial C-I bond than the β-anomer. Since both anomers of the product formed via S_N2-like

transition states with inversion of configuration,the reaction mechanism requires the rapid in situ anomerization of the α-mannosyl iodide used as substrate.

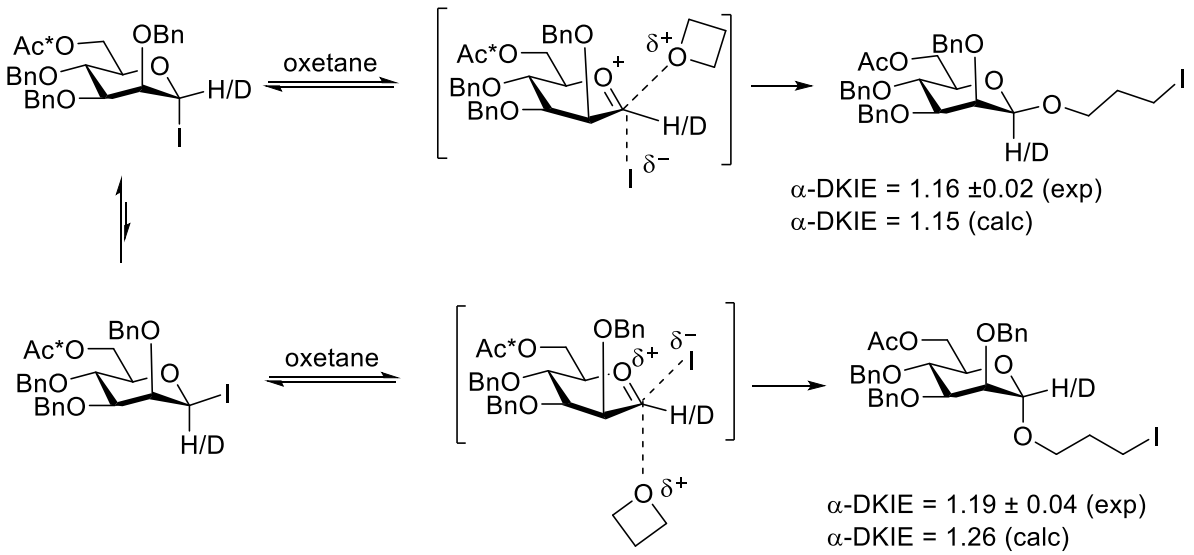

Scheme **18.** Formation of the β- and α-glycosides in the reaction of oxetane with acyclic mannosyl iodide

The authors also computed secondary α-deuterium KIEs for the reaction 4,6-*O*-methylidene protected α-and β-mannosyl iodides as 1.01 and 1.31 respectively; the data revealed a looser process for the formation of the α-anomer.[42] The reaction of the 4,6-*O*-benzylidene protected donor gave exclusively β-mannosides. Therefore, it was suggested that the presence of the cyclic acetal suppresses in situ anomerization of the iodide (Scheme 19).

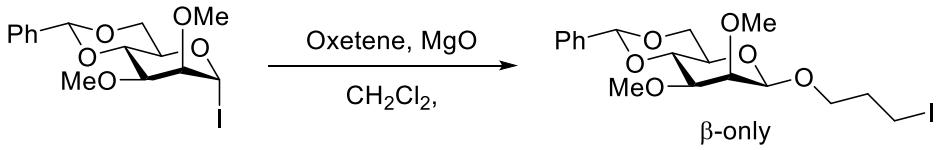

Scheme **19**. Exclusive β-Mannosylation; the Benzylidene effect

From the above discussions, it is evident that KIE data are very informative in the distinction between S_N1 and S_N2 reaction mechanism, however, the method is highly instrument

intensive and expensive, and consequently is not routinely applicable. Therefore, it is necessary to seek a much simpler alternative method for the determination of the relative kinetics and molecularity of glycosylation reactions, which can be applied in synthetic glycochemistry laboratories, and to inform the rational optimization of glycosylation reactions.

The development of competition experiments for assessing the relative kinetics of two reactions is a concept that is deeply ingrained in the field of organic chemistry. Clock reactions therefore have been applied and reported in many instances. Example of clock reactions in literature are the Jencks clock and radical clocks.

1.5 Clock Reactions

1.5.1 Jencks Azide Clock Reaction

Jencks and co-workers, developed the diffusion-controlled trapping by external azide together with common ion inhibition as a clock for the solvolysis of the corresponding α-azido ethers (Scheme 20).[43] They applied this method to estimate the lifetime of glycosyl cations and of the methoxymethyl cation as 1 x 10^{-12} s^{-1} and between 10^{12}-10^{15} s^{-1} respectively. They concluded that the glycosyl cation has a short but significant lifetime in aqueous solution and that there is little or no barrier for hydration of the methoxymethyl cation.[43] This concept of the determination of oxocarbenium ion lifetimes in water also been applied subsequently by Horenstein[44] and by Bennet.[45]

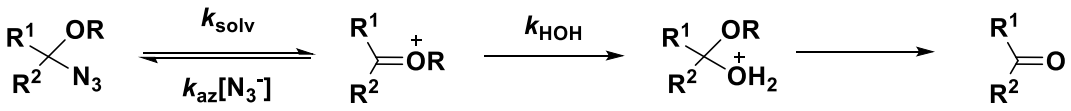

Scheme **20**. Jencks azide clock reaction

The competition kinetics technique is a much simpler way of solving complex mechanistic problems that would otherwise use complex and expensive methods. It is worth noting however that the azide clock method cannot be applied to actual glycosidic bond-forming reactions conducted at low temperature in organic solution.

1.5.2 Radical Clocks

Mechanistic studies on the kinetics of radical processes has become increasingly important to synthetic organic chemists. The recognition that radical intermediates are common in both chemical and enzymatic pathways drives the measurement of rates of these radical processes. Standard methods employed to measure the rates of radical reactions include electron spin resonance (ESR), time-resolved laser flash photolysis, and pulse radiolysis. The simplest way for investigating these reactions however is the radical clock.[46] Radical clocks are compounds that undergo a unimolecular radical reaction at a known rate. The application of these compounds in competition reactions with bimolecular radical reactions allows the measurement of unknown rates, thus functioning as a molecular "clock". Examples of radical clock reactions include: cyclizations, ring openings, and 1,2-migrations (Figure 4).[47] The impact of the rearrangements as clocks for the determination of relative kinetics in radical chemistry has been considerable.[48]

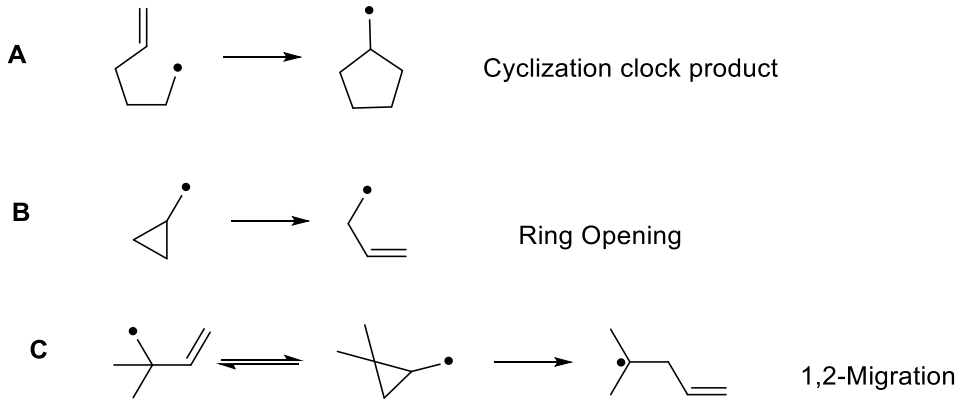

Figure **4**. Examples of radical clock reactions

The application of radical clocks in competition kinetics allows for the determination of rate constants of the bimolecular reaction (Scheme 21). In this scheme, after the radical intermediate formation, the 5-hexenyl radical cyclization (intramolecular reaction) competes with trapping by reagent XY (intermolecular reaction), leading to the formation of two products (unimolecular and bimolecular. The rate constant for the trapping reaction can be determined from the ratio of acyclic to cyclic products, the concentration of XY, and the known rate constant for cyclization.

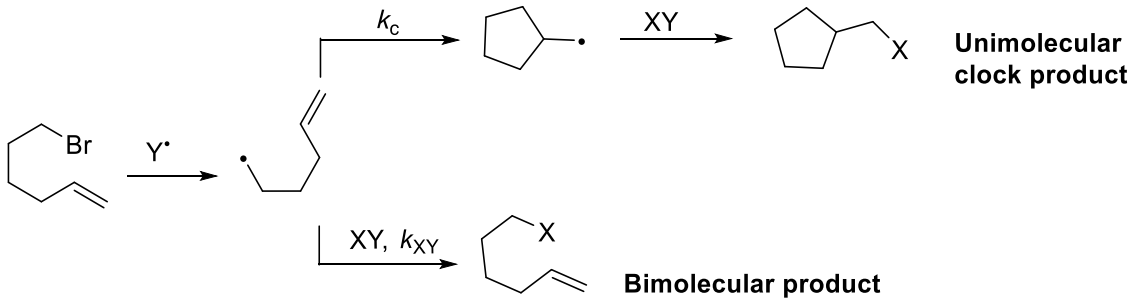

Scheme **21.** Radical clock reaction in competition kinetics

1.6 Intramolecular Aglycon Delivery

The chemical synthesis of 1,2-*cis* glycosidic linkages, such as β-mannosides, α-glucopyranosides and β-arabinfuranosides, which are found in natural glycans, has been an active challenge in the field of glycochemistry. While the 1,2-t*rans*-isomers have been obtained stereoselectively through the effect of neighboring group participation of the C-2 substituent, stereoselective synthesis of 1,2-*cis* glycosides is still under active investigations (Figure 5).

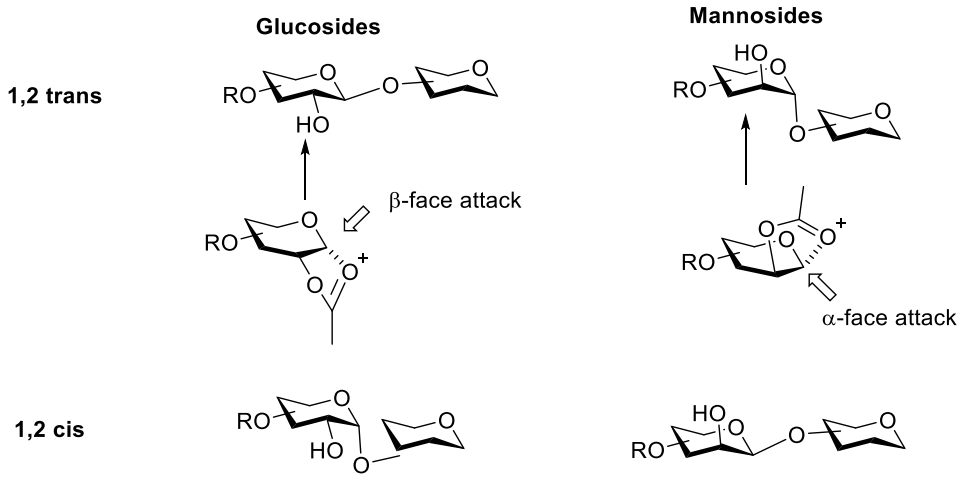

Figure **5.** 1,2-*cis* and 1,2-*trans* mannosides and glucosides

The intramolecular aglycon delivery (IAD) strategy to the stereoselective synthesis of 1,2-*cis* glycosidic linkages has been employed for several decades. In this case the C-2 substituent participates in a two-step glycosylation process. Initially, the aglycon is temporarily tethered to C-2 to give an intermediate product. The collapse of this intermediate upon activation of the donor leads to a 1,2-*cis* product according to the general mechanism (Figure 6). The success of the method is attributed to the use of efficient tethering method and the intramolecular nature of the acetal glycosidic bond forming reaction.

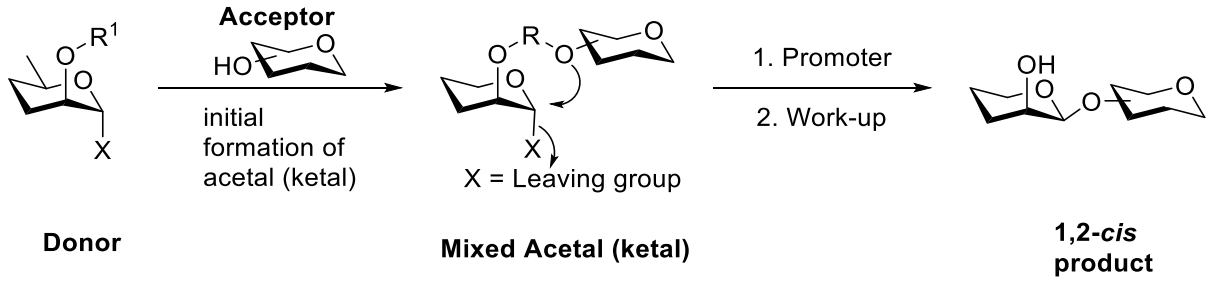

Figure **6.** General mechanism for intramolecular aglycon delivery

Hindsgual and Barresi pioneered the concept of intramolecular aglycon delivery leading to exclusive formation of β-mannosides:[49] the tethering was carried out using acid catalysis followed

by the addition of accepter to an enol ether intermediate. The modification of the acetate **1** by Tebbe methylenation[50] followed by acid activation in the presence of the acceptor alcohol gave a mixed acetal **3**. The intermediate thioglycoside successfully underwent intramolecular glycosylation to give β-manoside after activation under *N*-iodosuccinimide (NIS) conditions (Scheme 22). The enhanced yield was achieved by suppressing the breakdown of the mixed acetal intermediate by addition of hindered base, di-*tert*-butylmethylpyridine (DTBMP) to the acidic reaction mixture.[51]

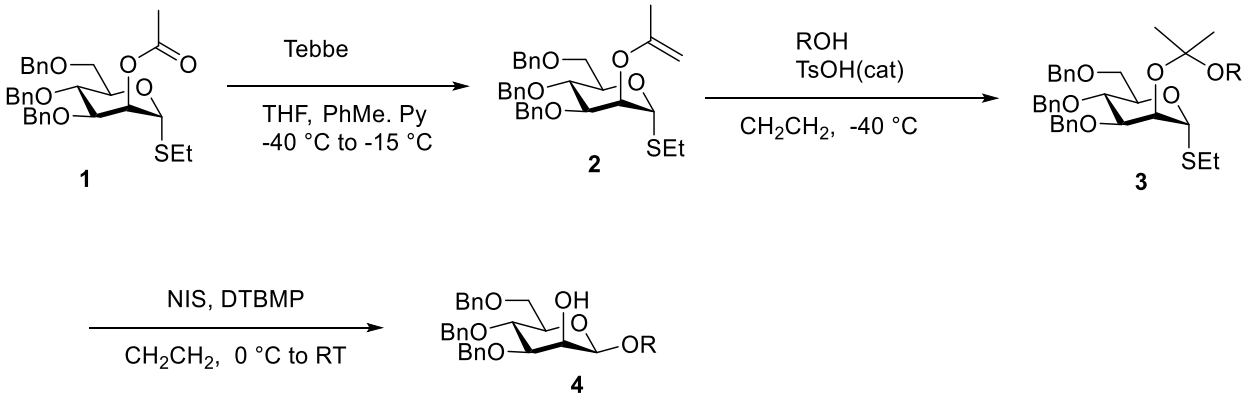

Scheme **22.** Hindsgaul's acid-catalysed tethering and glycosylations

1.6.1 Silicon Mediated Intramolecular Aglycon Delivery.

The importance of β-mannosylation prompted Stork to introduce silicon-tethered β-mannosylation using sulfoxides as the donors (Scheme 23).[52] Route **A** applied the use of dimethylchlorosilyl ethers derived from the aglycon alcohol and coupling to OH-2 of a mannosyl thioglycoside **5** to give mixed silyl acetal **6**. The tethered intermediates were oxidized to the glycosyl sulfoxide **8**, which, upon activation with triflic anhydride in the presence of the hindered base DTBMP underwent intramolecular glycosylation to give exclusively the β-mannoside **9**. The process gave β-mannosides in similar yields by starting from either the α- or β-configured

thiomannoside donor starting material. Stock also applied the Me_2SiCl_2 in route **B** to give mixed acetal **8**.[53] In this route the oxidation of the thioglycoside was done before tethering (Scheme 17).

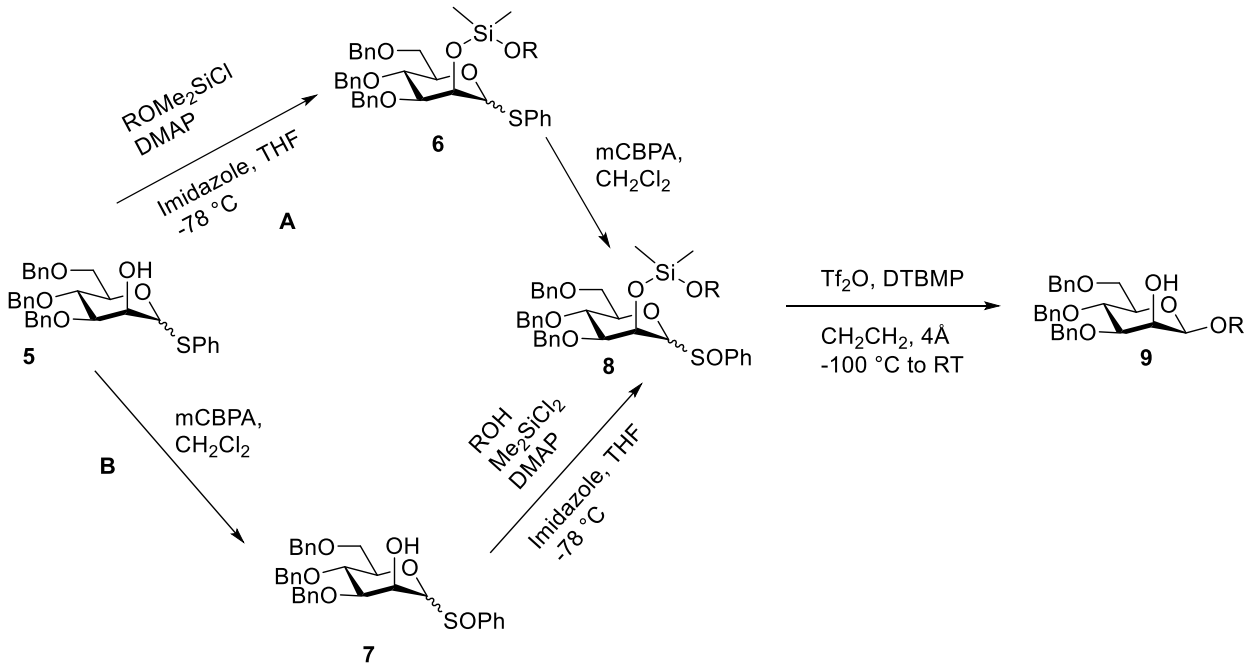

Scheme **23**. Stork's silicon-tethered β-mannosylation

1.6.2 para-Methoxybenzyl Mediated Intramolecular Aglycon Delivery

The synthesis of β-mannosides using IAD was further developed in 1994, soon after the very early communications from Hindsgaul and Stork. Ogawa and Ito introduced a tethering method based on the use of the paramethoxybenzyl (PMB) ether protecting group.[54] The oxidation of a PMB group generates an oxocarbenium ion that can be captured by an alcohol to give a mixed acetal. The resulting mixed acetals can undergo an intramolecular glycosylation reaction to give the 1,2-*cis* glycoside products. The initial paper[54] describes the use of mannosyl fluorides as donors (Scheme 24). Activation of the glycosyl fluorides by AgOTf, $SnCl_2$ in the presence of

DTBMP gave the 1,2-*cis* glycosides as the sole glycosylated products. The tether was lost under the reaction conditions to give the glycoside with a free 2-OH group.

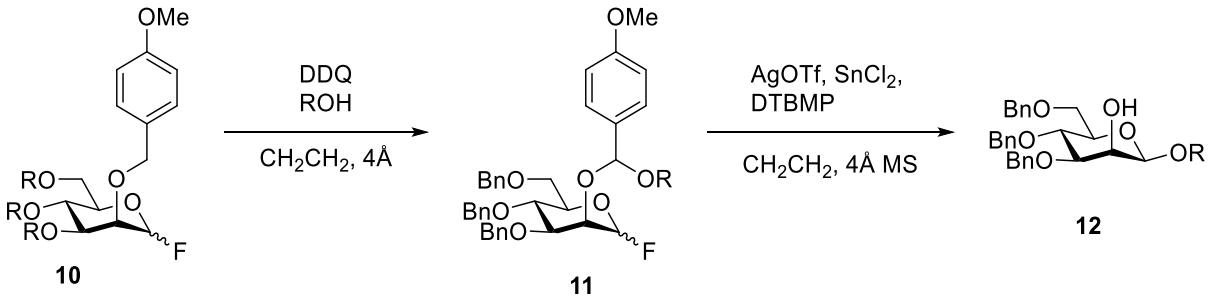

Scheme **24:** Ogawa's p-Methoxybenzyl mediated intramolecular aglycon delivery

The subsequent publications from the Ito/Ogawa group utilized methyl thioglycosides as glycosyl donors (Scheme 25).[55,56] Tethering proceeded very efficiently to give mixed acetals, which were either purified by size-exclusion chromatography or used crude in the next step. In this case, activation with MeOTf, DTBMP, 4Å molecular sieves in DCE or DCM gave the β-mannosides exclusively.

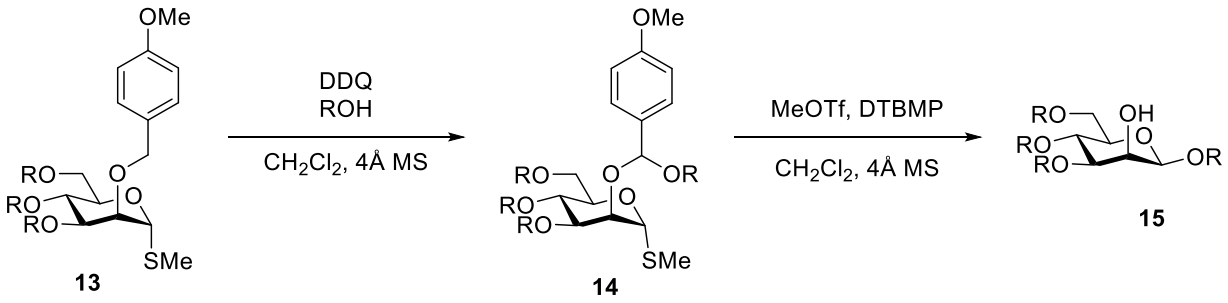

Scheme **25.** Ogawa and Ito's PMB mediated β-mannosylation using thioglycoside donor

The Ogawa group further increased the efficiency in the glycosylation reaction by using O-4 and O-6 cyclic protecting groups like cyclohexylidene and benzylidene, which constrained the system.[57,58] This increased the rigidity of the system forcing a more S_N2-like reaction[59] thereby

suppressing side reactions. The fate of the tether in these glycosylation reactions was addressed by Ito[60] in a series of NMR experiments that revealed that para-methoxybenzaldehyde was formed during the reaction. The use of a PMB acetal as tether, creates a new stereogenic center during the tethering process, so that in theory two diastereomeric mixed acetals can be formed in a tethering reaction, however, only one diastereomer is seen as shown in the Scheme 26.[61]

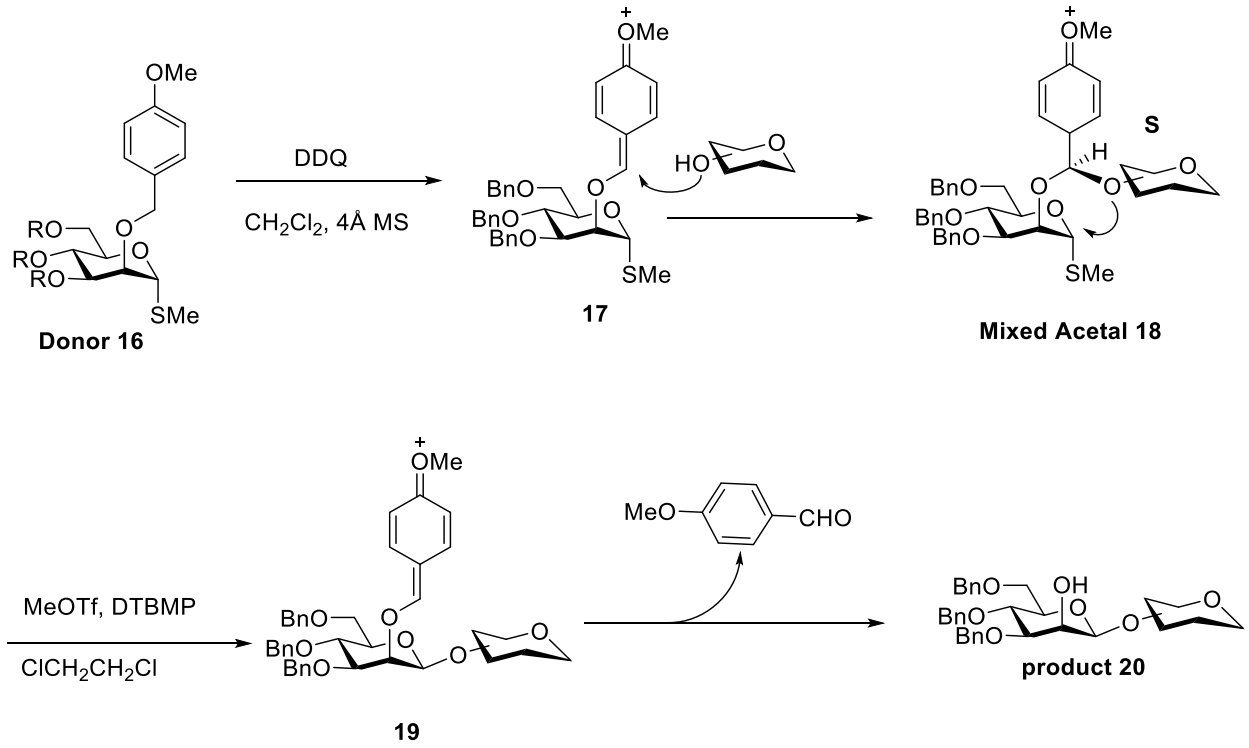

Scheme **26.** Mechanism of 4-methoxybenzylidene- tethered intermediates

The scope of application of PMB acetals was expanded by other groups. In 1996, Oscarson and Krog-Jensen reported the successful application to the synthesis of β-fructofuranoside (Scheme 27),[62] which are commonly found in nature. They activated the thioglycoside by DMTST in dichloromethane. However, the yields were relatively low.

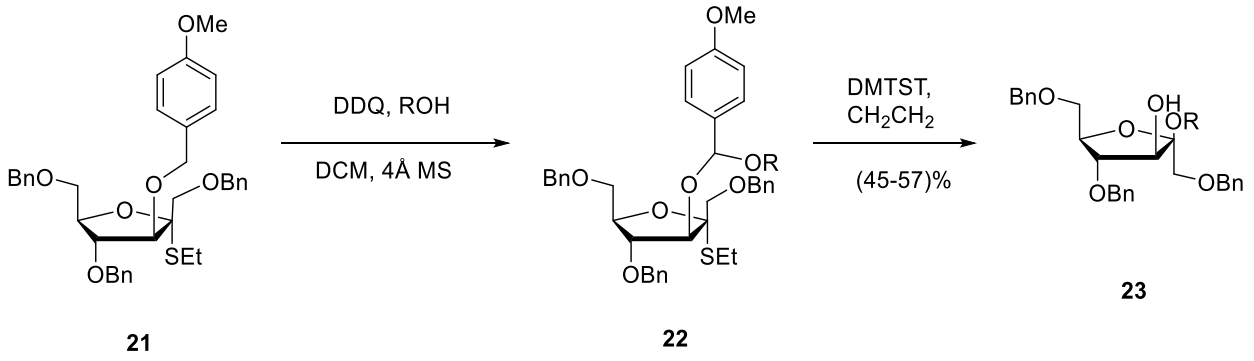

Scheme **27:** β-Fructosylation with the PMB IAD method

Application to the construction of β-arabinofuranoside linkages (Scheme 28) was successful by Prandi group in good yield.[63] Subsequently, the synthesis of oligoarabinofuranosides[64] was conducted by this method with activation of the thioglycoside by IDCP.

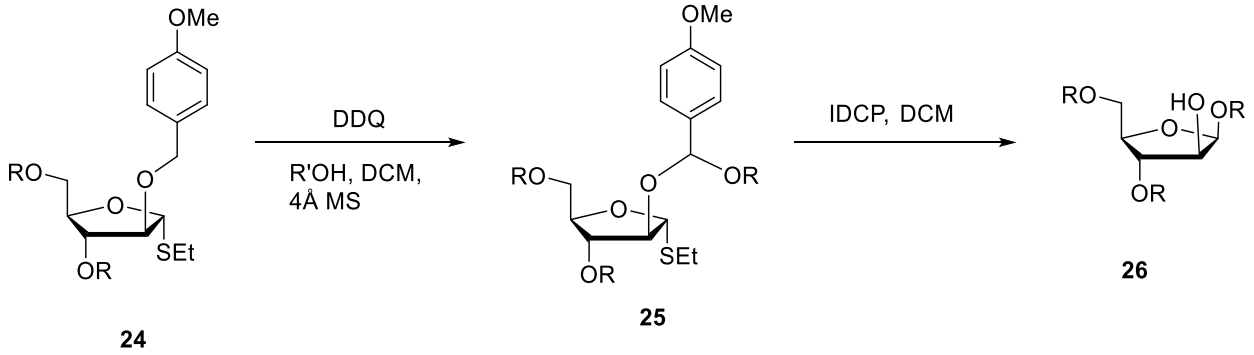

Scheme **28.** β-Arabinofuranosylation with the PMB IAD method

Finally, Bertozzi and co-workers, in their bid to find a high yielding and stereoselective route to symmetrical and unsymmetrical α,α-trehaloses for the synthesis of glycolipids from *Mycobacterium tuberculosis*, modified the PMB approach and used a more electron-rich 3,4-dimethoxybenzyl group (DMB) as a tether (Scheme 29).[65]

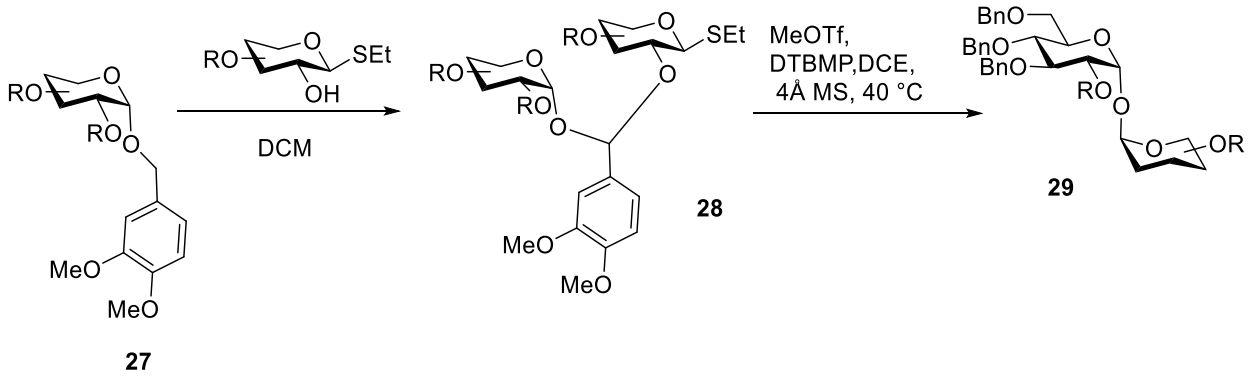

Scheme **29.** Bertozzi's DMB-mediated IAD for the synthesis of trehaloses

1.6.3 Iodonium-mediated Intamolecular Aglycone Delivery

The Fairbanks group investigated many IAD systems,[66] all based on electrophilic tethering to enol ethers to give mixed carbon acetals, similar to the original Hindsgaul route. The use of NIS both for tethering and for activation of the glycosyl donor opened the opportunity for a one-pot tethering–glycosylation reaction. This vinyl ether strategy was applied in *gluco* donor systems and successfully formed α-glycosides in one-pot tethering and glycosylation. Fairbanks also conducted similar reactions in the *manno* series and obtained β-mannosides.[67] The authors noted that reaction only gave the intramolecular products and that no hydrolyzed products were observed (Scheme 30).

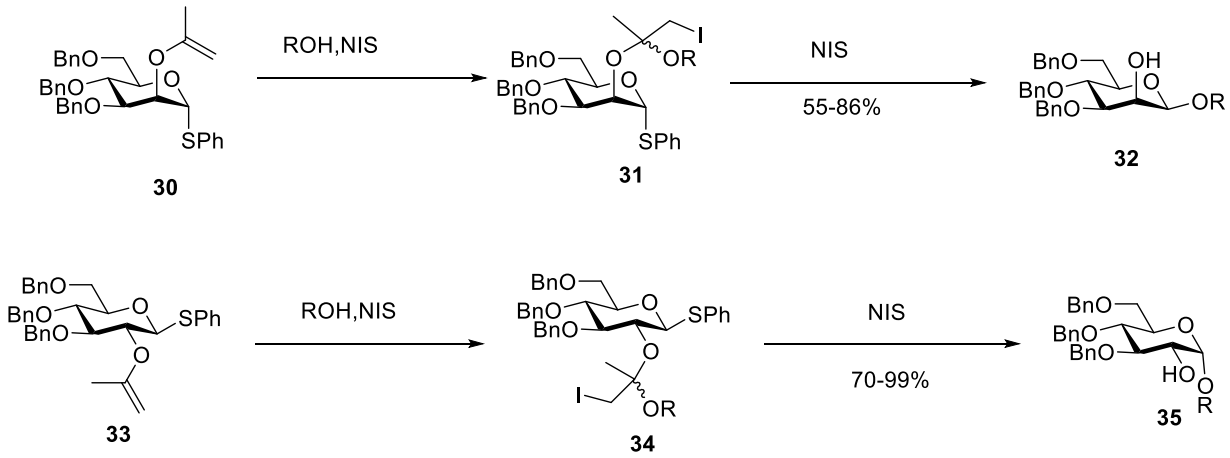

Scheme **30.** Iodinium-mediated tethering and intramolecular glycosylation in gluco and manno systems

Similarly, the Fairbanks group extended the strategy to allyl-derived intramolecular aglycon delivery (Scheme 31).[68] In this strategy, 2-O-allyl protected glycosyl donors were first isomerized to the corresponding vinyl ethers and then treated with NIS in THF under dry conditions to give the mixed acetal. However, it is worth noting that they observed a competitive tethering reaction, resulting in the formation of a succinimide tether in the gluco series. To suppress this, they used IDCT that was generated in situ with I_2 and AgOTf. A similar reaction was successfully reported in the manno series.[69]

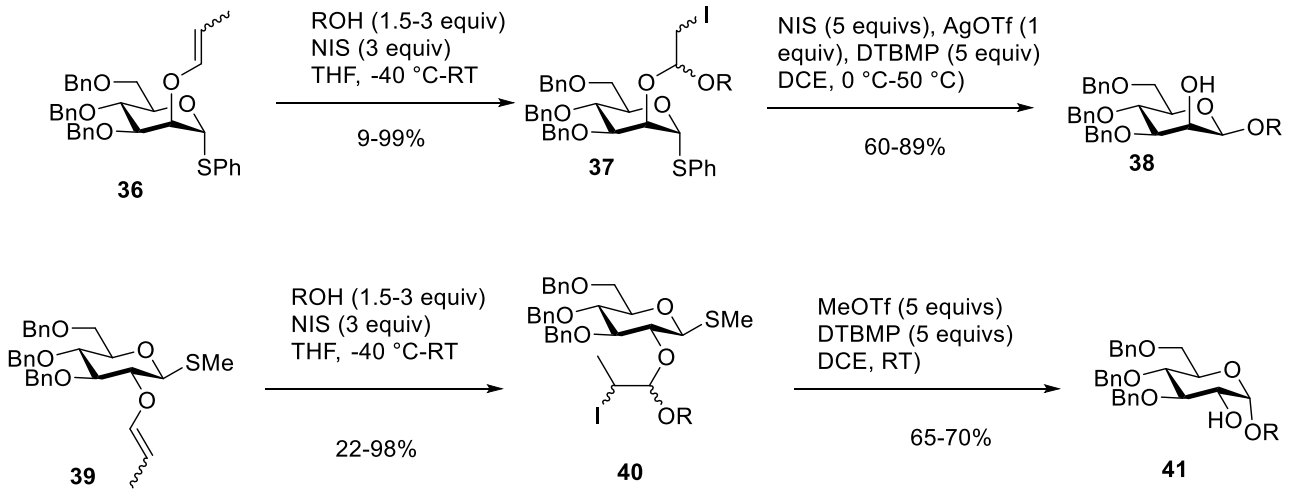

Scheme **31.** Fairbanks' allyl-derived IAD with thioglycoside donors

1.7 The Cyclization Concept

The design of cyclization reactions for use of intramolecular glycosylation clocks was informed by the general concept of intramolecular aglycone delivery[49,52, 54,2b,70] and, more particularly, by two instances in Crich laboratory of cyclization of protecting groups at O2 of glycosyl donors onto the anomeric centre during previous studies (Scheme 32).[71] It was observed that on warming above 5 ^{o}C in deuterated dichloromethane the α-mannosyl triflate **41** underwent decomposition with cyclization onto a benzyl group to give the tricyclic product 4**2**, which was isolated in 56% yield. On the other hand, the corresponding α-mannosyl triflate derived by in situ activation of the sulfoxide **43** underwent cyclization at -78 ^{o}C in dichloromethane onto the naphthylpropargyl system in competition with reaction with an external alcohol,[72] with yields varying as an inverse function of the reactivity of the external alcohol. In contrast, simple allyl ethers[73,74] propargyl ethers ethers[75] and [3-(4-trifluoromethylphenyl)propargyl] ethers,[76,77] may be employed as protecting groups for the O2-postion in mannosylation reactions without complications arising from cyclization. Thus, while the precedent certainly gave rise to the

potential for the use of carbon-carbon bond forming cyclization reaction onto O2 protecting groups as an intramolecular clock reaction for glycosylation reactions, it also highlighted the sensitivity of such cyclizations to the structure and reactivity of the nucleophilic function.

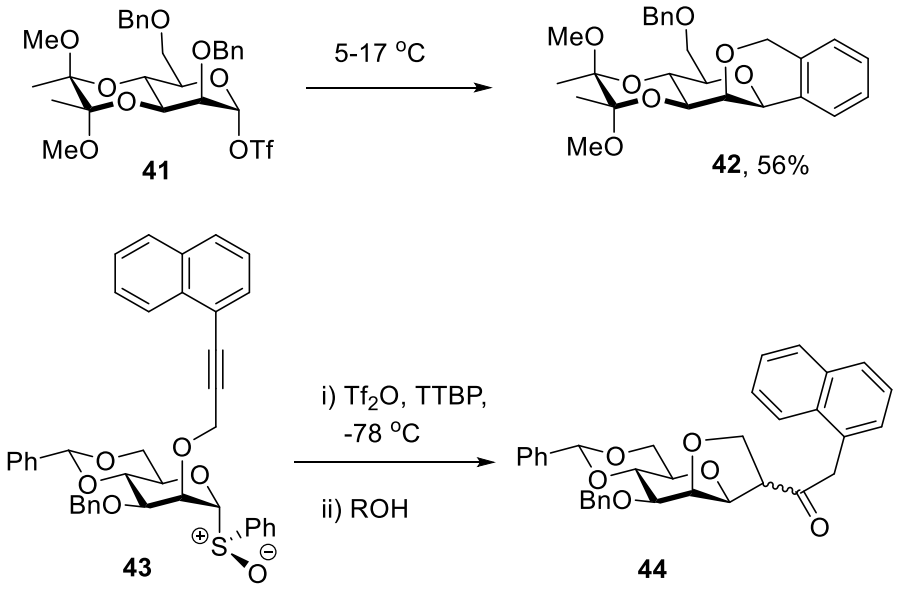

Scheme **32**. Cyclization of protecting groups at the 2-position.

Based on the work of Denmark and coworkers, who showed that allylsilanes can be used as nucleophiles in a series of cyclization-based probes designed to interrogate the mechanism of the Lewis acid promoted reaction of allylsilanes with acetals (Scheme 33)[78] and other instances of the intramolecular Sakurai reaction,[79] Crich and coworkers designed an initial system, employing a 2-*O*-(2-trimethylsilylmethyl)allyl group as intramolecular nucleophile. In addition to excluding the formation of an analysis-complicating additional stereogenic center, as observed in the model cyclization of **45** to **46** (Scheme 34), this system takes advantage of the much increased nucleophilicity of allylsilanes over simple alkenes in their reaction with carbocations,[80] thereby increasing the likelihood that cyclization will compete with trapping by an external alcohol

nucleophile. Finally, the system envisaged found precedent in the well-known *C*-glycoside-forming intermolecular reaction of allylsilanes with putative anomeric oxocarbenium ions.[81,82,83,84]

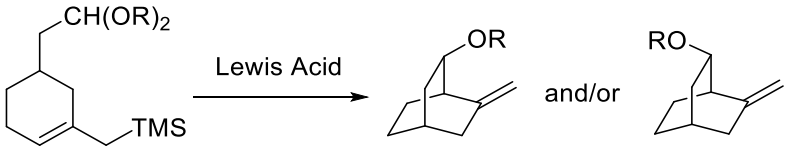

Scheme **33.** Denmark's use of an intramolecular allylsilane-acetal reaction as a probe of mechanism.

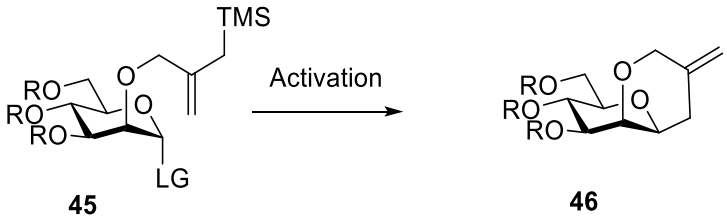

45 **46**

Scheme **34.** Initial clock cyclization design.

1.8 Previous Studies in Cation Clock Reactions for the Determination of Relative Kinetics in Pyranosyl Sulfoxide Systems and their Limitations.

The initial work was focused on the use of the pyranosyl sulfoxides as precursors of the pyranosyl (manno and gluco-type) triflates. Conscious of the ever-widening range of donor types capable of providing β-mannopyranosides when used in conjunction with the 4,6-*O*-benzylidene or related acetals,[85,86] a cation clock method for probing the concentration dependence of the acceptor in glycosylation reactions was applied to 4,6-*O*-benzylidene-protected pyranosyl sulfoxide donor systems in our lab.[87] The design for the experiment was based on the intramolecular Sakurai reaction employing the use of 2-*O*-2-(trimethylsilylmethyl) allyl ethers tether as a nucleophilic arm in the sulfoxide donor provided an efficient clock reaction for mannosyl sulfoxides (Scheme 35).

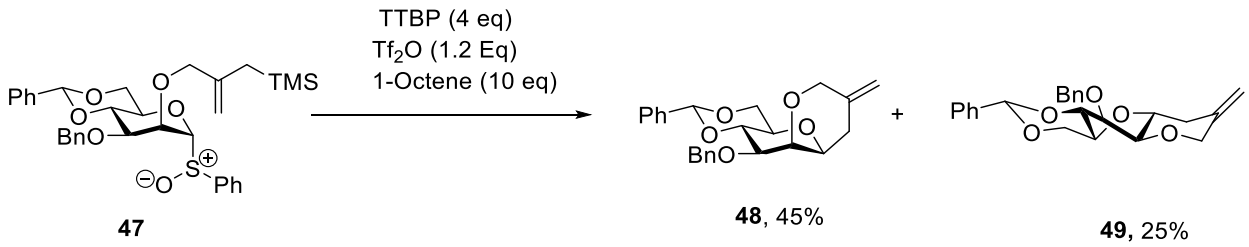

Scheme **35**. Clock reaction for mannosyl sulfoxide donor

In this system, it was reported that the cyclization resulted in the formation of both *cis*- and *trans*-fused tricyclic systems, thereby invoking an intermediate glycosyl oxocarbenium ion reacting in a boat conformation as proposed in Scheme **25**. The rationalization of the formation of the *trans*-fused product **49** invokes a mannosyl oxocarbenium ion, **51**, that exists in equilibrium with α-glycosyl triflate **50**[88] and accesses the $B_{2,5}$ conformation, previously computed.[89] In this conformation, the 2-*O*-silylmethylallyl ether can access both the β-face of the cation, leading to the *cis*-fused product **48**, and the α-face, resulting in the formation of the *trans* isomer **49** initially as the $^{O}S_2$ twist boat **52**, which then relaxes to the observed $^{1}S_5$ conformer (Scheme 36). The observation of the *trans*-fused product provides very strong evidence in support of the existence of a mannosyl oxocarbenium ion in equilibrium with the covalent glycosyl triflate

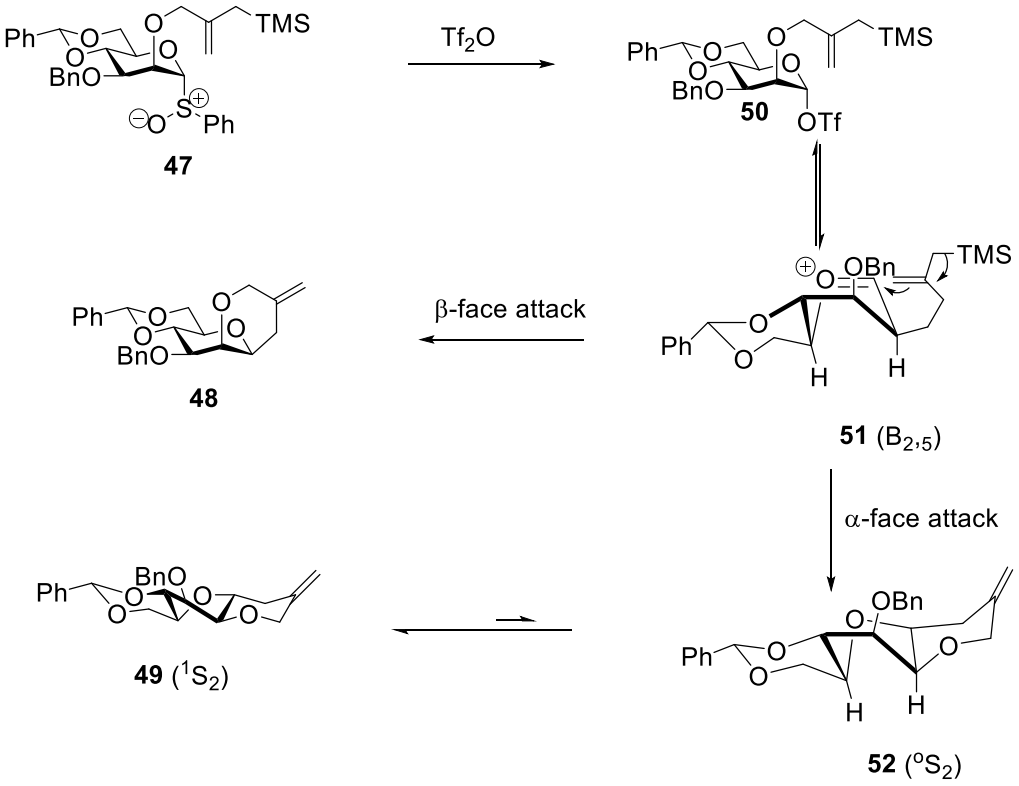

Scheme **36**. Proposed reaction mechanism for the formation of clock products

The concentration dependence of glycosylation was easily determined by performing simple competition reactions in which the putative transient oxocarbenium intermediate, generated on activation, is trapped either by cyclization (clock reaction) or by an external nucleophile (Scheme 37). The increase in the ratio of glycosylation to cyclization products with increasing acceptor concentration reveals an S_N2-like associative mechanism. Whereas, low acceptor concentration dependence is characteristic of an S_N1-like dissociative mechanism.[87]

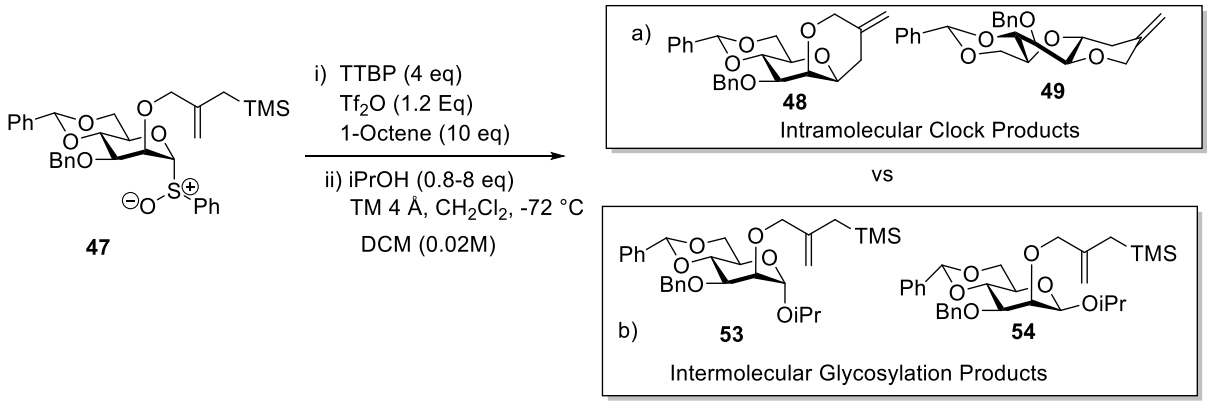

Scheme **37**. Competition glycosylation reaction in mannose system

The kinetic studies were then performed based on the competition glycosylation reaction with isopropanol, and suggested that β-*O*-mannosylation proceeds via an associative S_N2-like mechanism, whereas α-*O*-mannosylation and β-*C*-mannosylation are dissociative and S_N1-like.[87]

1.9 Problem Statement.

The application of the clock reaction to the glucosyl sulfoxide system was characterized by the formation of the cyclized products as well as other byproducts, which were isolated and characterized as sulfenyl transfer products (Scheme 38). This happened despite attempts to use the addition of 1-octene as a scavenger, as was successfully applied in the mannose series to suppress the formation of the byproduct. The explanation for the difference in migration aptitude supposes that it takes place intramolecularly in the glucose system due to the close proximity of the allylic trimethylsilane to the sulfoxide leaving group as was later confirmed.[90]

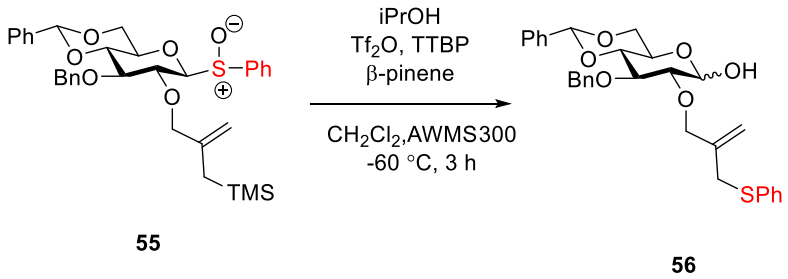

55 **56**

Scheme **38.** The sulfenyl transfer product complicating use of the original clock in the glucose series.

The failure of the intramolecular allylsilane cation clock in glucopyranosylation by the sulfoxide method necessitated more methodological studies to further develop alternative methods to probe the concentration dependence of the nucleophile in glycosylation. This precedence also suggests that ring closure onto appropriately designed substituents in appropriate donor would provide a suitable clock reaction for the determination of the relative kinetics in glycosylation reactions. To this extent we proposed the use of trichloroacetimidates as glycosyl donors for cation clock reaction.

1.10 Main Objectives:

The first part of this work seeks to further develop the simple cation clock method based on the intramolecular Sakurai reaction to probe the concentration dependence of the nucleophiles in glycosylation reactions. It applies the use of trichloroacetimidates as a probable solution to intramolecular sulfenyl transfer in sulfoxide clocks. This study was intended to provide a wider scope for the application of cation clock reaction for the determination of relative kinetics in pyranoside systems (both gluco and mano configurations).

Further parts seek to explore the use of a hydroxyl group attached to O2 as internal nucleophile for cation clocks in arabinofuranoside systems and therefore, further explores the application of the concept of cyclization reactions as simple cation clocks for estimating the molecularity of nucleophilic attack on transient oxocarbenium ions of the furanosyl systems. This work will also

explore the influence of acceptor nucleophilicity on the cation clock reactions as probes of glycosylation reaction mechanism in arabinofuranoside formation.

The last part of the work will explore the selective hydrogenolysis of naphthylmethyl ethers in the presence of sulfide containing molecules.

CHAPTER 2: CATION CLOCK REACTIONS FOR THE DETERMINATION OF RELATIVE KINETICS IN GLYCOSYLATION REACTIONS: APPLICATIONS TO GLUCO AND MANNOPYRANOSYL TRICHLOROACETIMIDATE DONORS

2.1 Introduction

The study of glycosylation reaction mechanisms in chemical synthesis is among the hottest research areas in carbohydrate chemistry.[9,91,92] Several literature reports on previous studies targeting mechanism have been conducted experimentally and supported by theoretical calculation, with the main objective of determining the stereochemical outcome in terms of α or β-anomer selectivity. Most researchers concur that glycosylation with a triflate donor occurs through nucleophilic attacks of a glycosyl acceptor to covalent intermediates, contact ion pairs, and solvent-separated ion pairs, all of which are in equilibrium in solution (Scheme 13).

The characterization of reaction mechanisms is usually based on combinations of stereochemical and kinetic evidence and is often supported whenever possible by the characterization of any intermediates and by computational work as generalized in Figure 7. Central to the mechanistic studies of glycosylation is the glycosyl cation, popularly referred to as the oxocarbenium ion in red. Due to the many variables operating in a glycosylation reaction, the mechanism can best be regarded as a continuum between S_N2-like and S_N1-like substitution. The uncertainty of distinguishing between mechanisms calls for more detailed mechanistic studies to uncover the exact glycosylation mechanism (Figure 7).

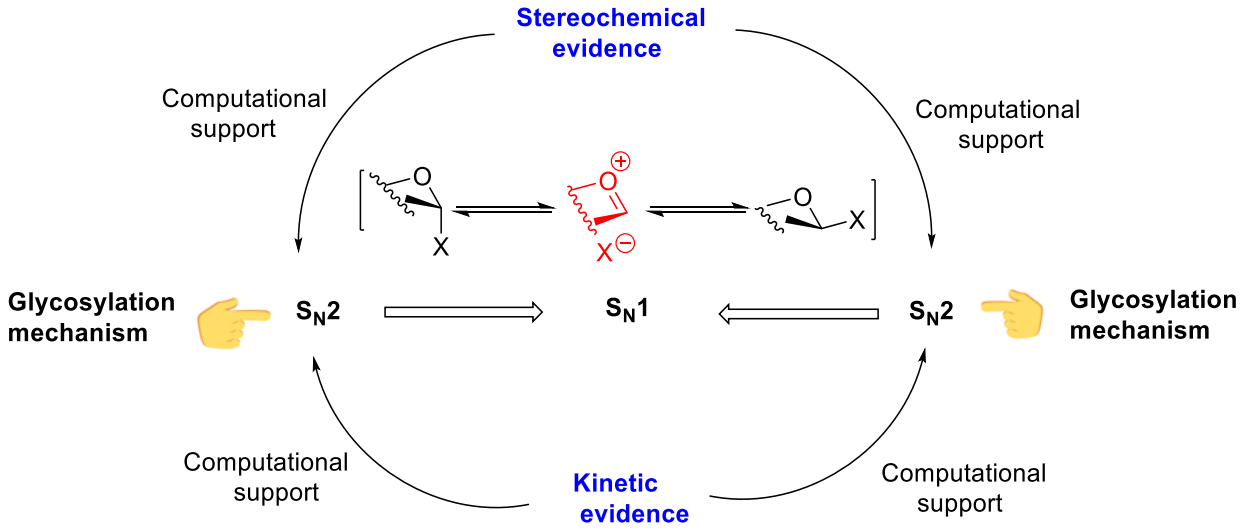

Figure **7**. Possible approaches to the determination of glycosylation reaction mechanism.

As discussed in chapter 1, the recent development of the cation clock method as a simple tool for the determination of relative kinetics of glycosylation reactions, based on the internal attack on the cationic center of a nucleophilic arm strategically bound to the donor provided the basis for the determination of molecularity of glycosylation reactions. The concentration dependence of glycosylation is easily determined by performing simple competition reactions in which the oxocarbenium intermediate, generated on activation, is trapped either by cyclization or an external acceptor (Scheme 39).

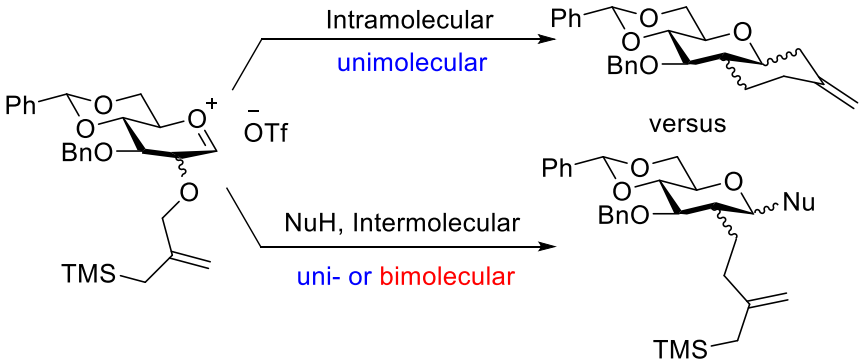

Scheme **39.** The cation clock reaction

In this study we extended the use of the cation clock method to include the use of the very popular glycosyl trichloroacetimidates,[93] with a focus on pyranosides (gluco and manno type) systems.

2.2 Cation Clock Reactions for the Determination of Relative Kinetics in Glycosylation Reactions: Mannopyranosyl clock system.

2.2.1 Synthesis of the 4,6-*O*-Benzylidene-protected Mannopyranosyl Clock

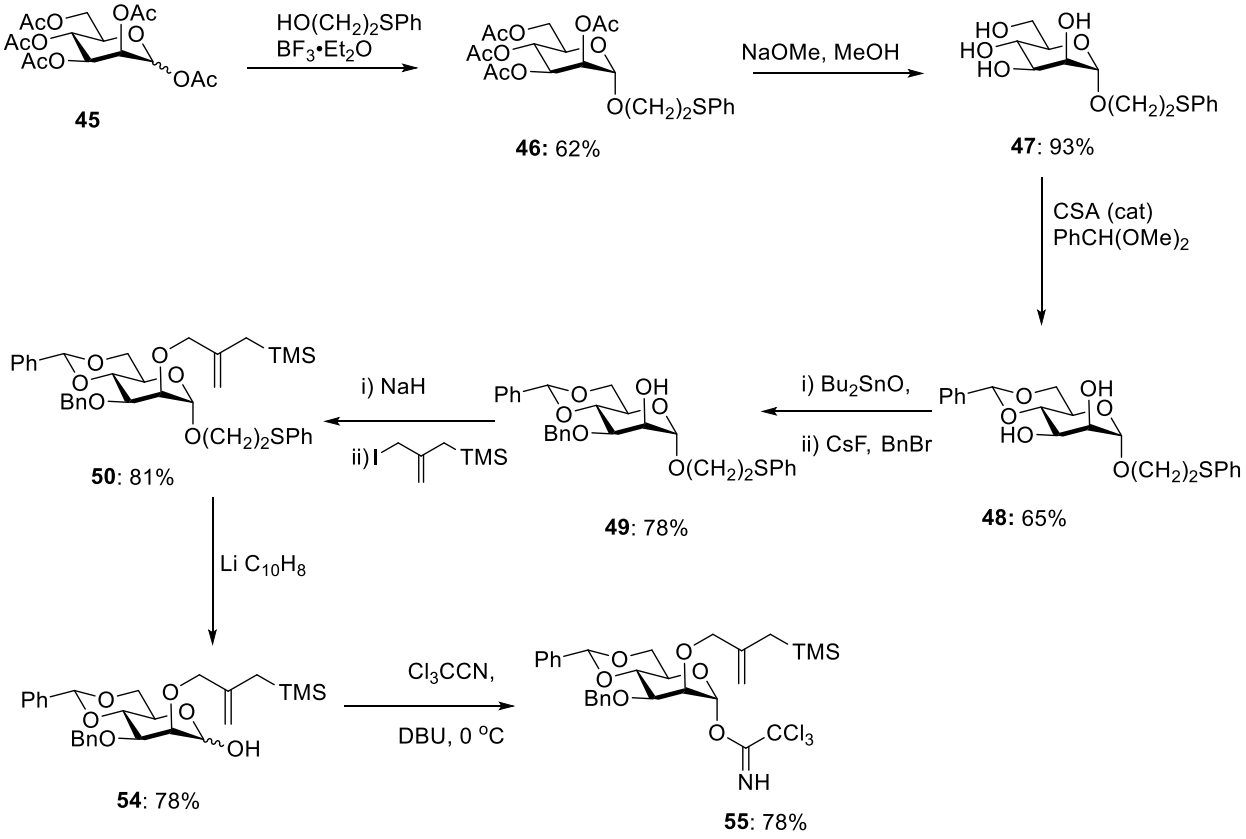

Scheme **40**. Synthesis of a 4,6-*O*-benzylidene-protected mannopyranosyl clock

The synthesis of the 4,6-*O*-benzylidene mannopyranosyl trichoroacetimidate clock began with glycosylation under standard means of phenylthioethanol with pentaacetyl mannopyranose and gave compound **46** in 62% yield. Saponification with catalytic sodium methoxide in methanol

and consequent 4,6-*O*-benzylidene group installation using the dimethyl acetal and catalytic CSA gave compound **48** in 65% yield. Standard[94] regioselective monobenzylation of **48** with dibutyltin oxide, cesium fluoride and benzyl bromide gave **49** in 78% yield, ready for the installation of the allylsilane moiety. In the phenyl thioglycoside series studied initially (Scheme 41),[87] alkylation was achieved with sodium hydride and commercial 2-(chloromethyl)allyl trimethylsilane in hot THF and gave the anticipated product in 47% yield after 7 days. Thus, conversion of chloromethylallysilane to the corresponding iodomethylallylsilane[95] with sodium iodide in acetone was preferred (Scheme 42).

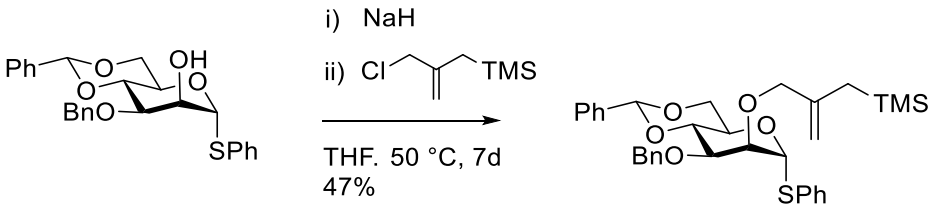

Scheme **41.** Initial alkylation of the thioglycoside

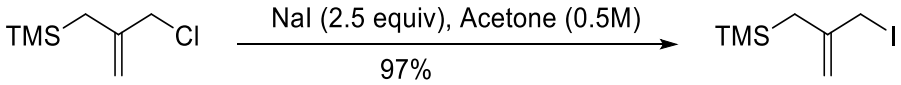

Scheme **42.** Synthesis of iodomethylallylsilane

This set stage for the *O*-alkylation reaction with 2-(chloromethyl)allyl trimethylsilane and sodium hydride in THF at 0 ºC in the presence of 15-crown-5, to obtain 2-(iodomethyl)allyl trimethylsilane in 81% yield with greatly reduced reaction times (Scheme 42). This is attributed to the fact that iodide is a better leaving group than chloride.

2.1.2 Reductive Lithiation

The strategic installation of phenylethyl the thioglycoside **46** was to allow for eventual reductive lithiation of compound **50** (Scheme 43) and installation of the trichloroacetimidates. This key step started by generation of the lithium naphthalenide radical anion (Scheme 44).

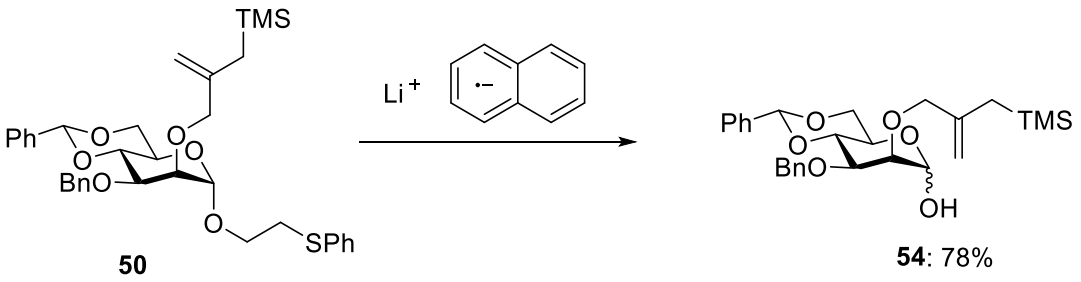

Scheme **43.** Cleavage of the phenylethyl thioglycoside

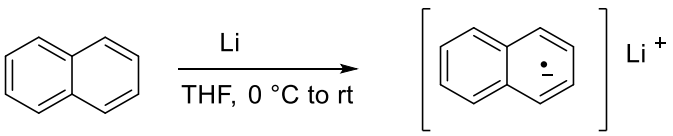

Scheme **44.** Generation of the aromatic radical anion reducing agent

Reductive cleavage of phenyl thioethers using aromatic radical anions as source of electrons is well documented in literature and follows a two-step pathway (Scheme 45). Other widely used aromatic radical anion sources are LDMAN and LDBB (Figure 8),[96] which are used interchangeably depending on the reactivity and selectivity required of a particular reaction. The choice of lithium naphthalenide in this synthesis was largely influenced by its low cost and effectiveness towards the deprotection of phenyl thioethers.

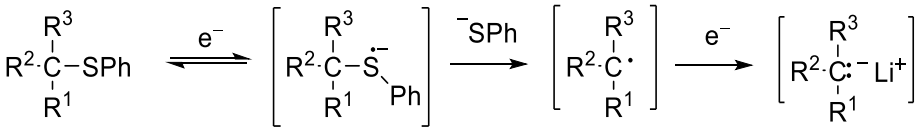

Scheme **45.** General mechanism of reduction cleavage of phenylether thioethers

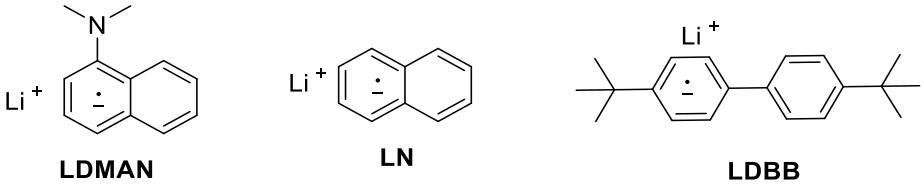

Figure **8.** Common aromatic radical-anions

Applying the concept of reductive cleavage, treatment of the phenylthioethyl glycoside **50** with lithium naphthenalide[97] in THF at -78 ^{o}C gave the mannopyranose **54** in 78% yield. Cleavage of the C-S bond by the lithium naphthalenide reagent is followed by β-elimination of the anomeric alkoxide which on workup, gives the pyranose (Scheme 46)

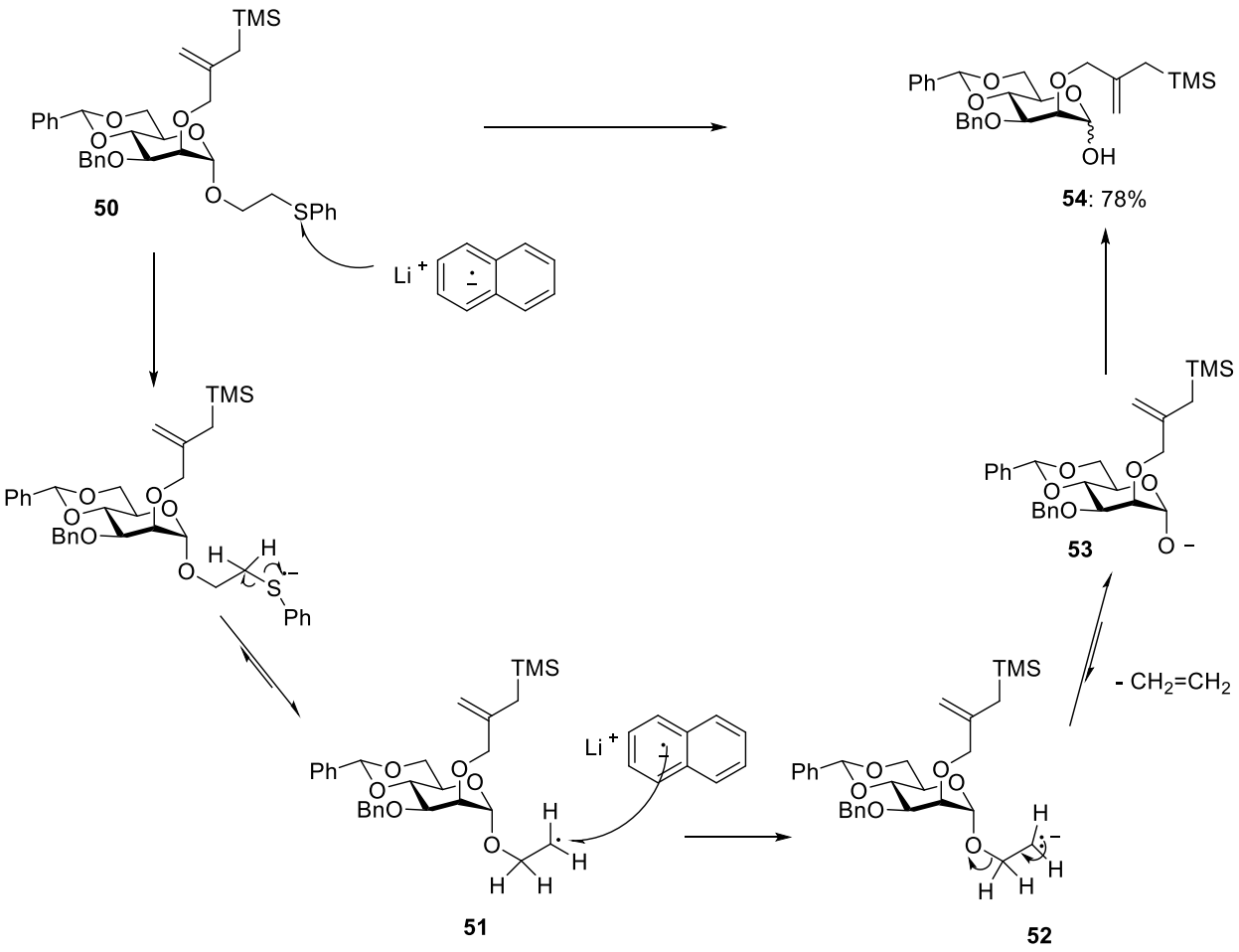

Scheme **46**. Proposed mechanism of reductive cleavage of compound **50**

With the compound **54** in hand, it was easily converted to α-trichloroacetimidate **55** in 78% yield on reaction with trichloroacetonitrile in the presence of DBU (Scheme 40).[98]

2.1.3 Clock Cyclization Reaction

As a preliminary to the kinetics, it was necessary to establish the operation of clock reaction under the new conditions. This was initially attempted by the reaction of the mannosyl trichloroacetimidate donor with catalytic TMSOTf in dichloromethane at -72 ^{o}C in the presence of the hindered non-nucleophilic base 2,4,6-tri-*tert*-butylpyrimidine (TTBP). However, when this reaction was quenched at -72 ^{o}C after stirring for 2.5 h, this gave only low yields. Raising the temperature to -20 ^{o}C enabled a rapid smooth reaction resulting in the isolation of **58** and **59** in 70 and 25 % yields, respectively (Scheme 47). These structures were earlier confirmed by X-ray crystallography.[87] The conformation of **59** does not change on going from the crystal to the solution phase as is apparent from the 10.5 Hz coupling constants of the vicinal *trans*-pseudo-diaxial hydrogen atoms at the bridgehead positions of the newly formed ring. The major *cis*-fused products **58** contains only chair conformers of the three six-membered rings, while the *trans* fused product **49** contains two chairs and a twist boat.

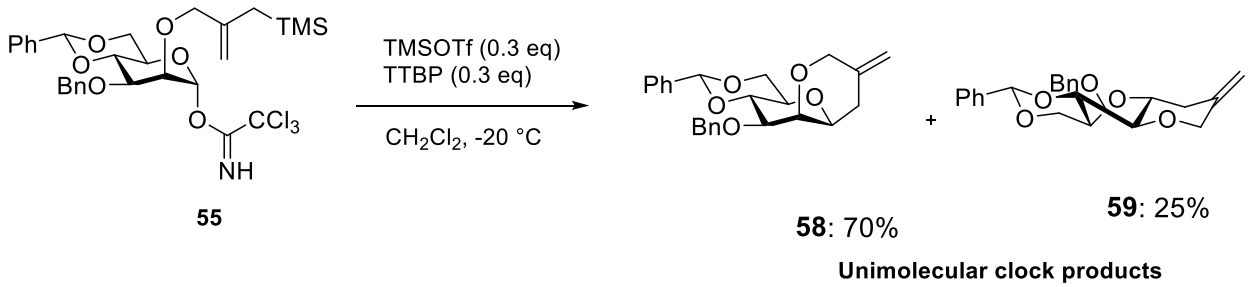

Scheme **47.** Clock cyclization reaction (mannosyl unimolecular clock reaction)

Mechanistically, the mannosyl triflate **56**[88] formed on activation of the donor can be in equilibrium with the mannosyl oxocarbenium/triflate ion pair **57**, which can adopt only $^{4}H_{3}$ and

$B_{2,5}$ conformations (Scheme 48) as a result of the presence of 4,6-*O*-benzylidene acetal which locks the conformation. The $B_{2,5}$ conformation allows the allylsilane to adopt a pseudo equatorial position in which it is poised to react with either the β or α face of the oxocarbenium ion, thereby enabling the formation of the *cis* and *trans*-fused products. The major *cis*-fused product can be formed from nucleophilic attack on the β-face of any of the two accessible conformations. The *trans*-fused products **59** can only be rationalized by the formation of a transient mannopyranosyl oxocarbenium that populates the $B_{2,5}$ conformation. Nucleophilic attack on the α-face then leads to the compound **59** in the $^{o}S_2$ conformation which equilibrates to form the observed final product **59** in the $^{1}S_5$ conformation.

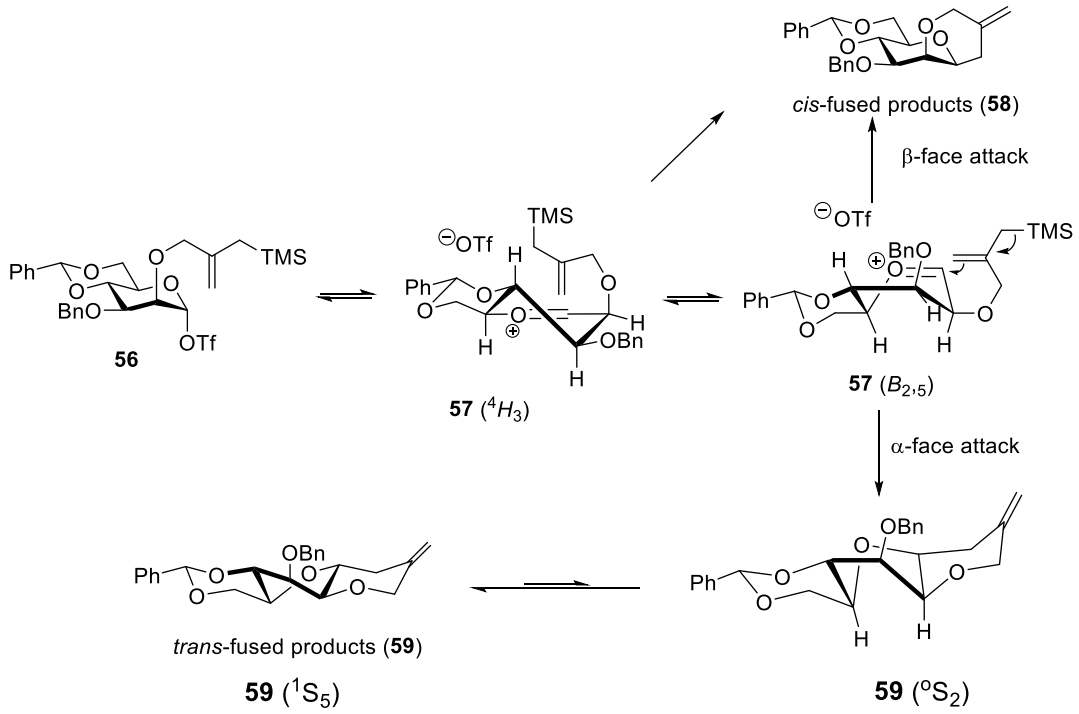

Scheme **48.** Conformation and selectivity of the mannopyranosyl oxocarbenium ion in the cyclization reaction

2.1.4 *O*-Glycoside Formation in Competition with Cyclization

Once the viability of the unimolecular clock reaction was demonstrated, the competition kinetics were conducted. The trichloroacetimidate **55** and 2,4,6-tri-*tert*-butyl pyrimidine were co-

evaporated 3 times in toluene and dried in vacuo for 3 h. Freshly 4Å activated molecular sieves were added, the flask was purged with argon and dry dichloromethane added, followed by addition of 2-propanol (0.81-8.12 equiv). The reaction mixture was stirred for 1 h at room temperature then cooled to -20 °C followed by addition of TMSOTf and stirring for 3 h at -20 °C. The reaction mixture was quenched with triethylamine at that temperature and worked up and the product ratios analyzed by UHPLC. Pooling the crude reaction mixtures from several runs afforded sufficient material for the chromatographic purification and full characterization of the glycosides (Figure 9).

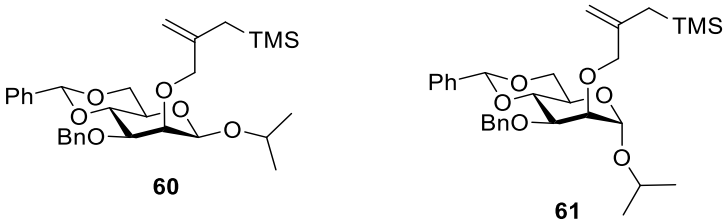

Figure **9**. O-Glycosides from competition kinetics

2.1.5 Kinetic Data

The experimental data was then converted into ratios of the glycoside, β- or α-, with the combined cyclized products as shown in Table **1.**

Table **1**. *O*-Mannosylation with trichloroacetimidates donor **55**.

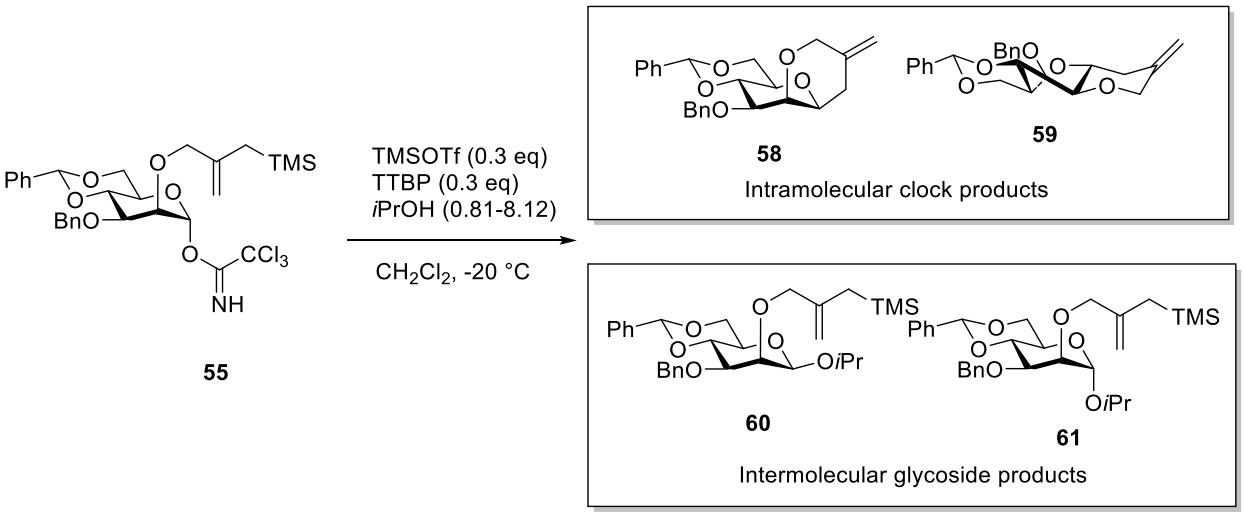

Entry	Nucleophile	Equiv (M conc)	**β-gly/cycl** **60**/(**58** + 59)[b]	**α-gly/cycl** **61**/(**58** + 59)[b]
1[a]	*i*PrOH	0.81 (0.013)	2.5702	0.30827
2[a]	*i*PrOH	1.63 (0.026)	5.0541	0.54899
3[a]	*i*PrOH	2.4 (0.052)	10.1031	1.33043
4[a]	*i*PrOH	3.25 (0.078)	13.3632	1.83040
5[a]	*i*PrOH	4.88 (0.104)	19.7443	3.20719
6[a]	*i*PrOH	8.12 (0.130)	24.2748	4.83401

a) Experimental conditions: TTBP (0.3 equiv), TMSOTf (0.3 equiv.) at -20 °C; molecular sieves 4 Å;
b) Molar ratios were determined by UHPLC/UV/MS

Graphical representation of this data gives a clear picture of the influence of concentration on the ratio of glycoside formation to cyclization (Figure 10)

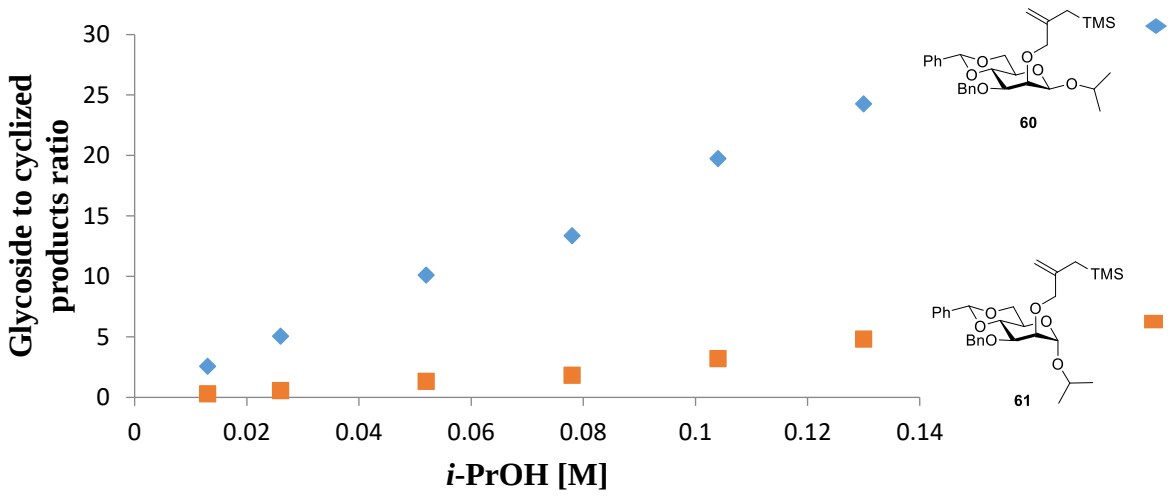

Figure **10.** O-Glycoside in competition with cyclization

The above graph reveals a strong concentration dependence of the nucleophile in the formation of β-*O*-mannosides, compared to a rather weak concentration dependence in the formation of α-*O*-mannosides.

2.1.6 *C*-Glycosylation in competition with cyclization

The protocol for the competition kinetics was repeated using trimethylallylsilane (2.1-32.0) as external nucleophile in place of 2-propanol**.** Again, pooling the crude reaction mixtures afforded sufficient material for the chromatographic purification and full characterization of the *C*-glycoside **62,** which was formed as a single β-anomer**.**

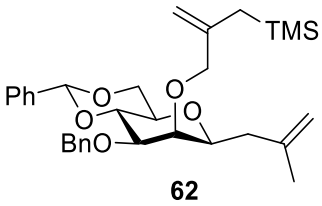

Figure **11.** *C*-glycoside from competition kinetics.

The product ratios were analyzed by UHPLC and reported in Table **2**.

Table **2**. *C*-Mannosylation with trichloroacetimidates donor

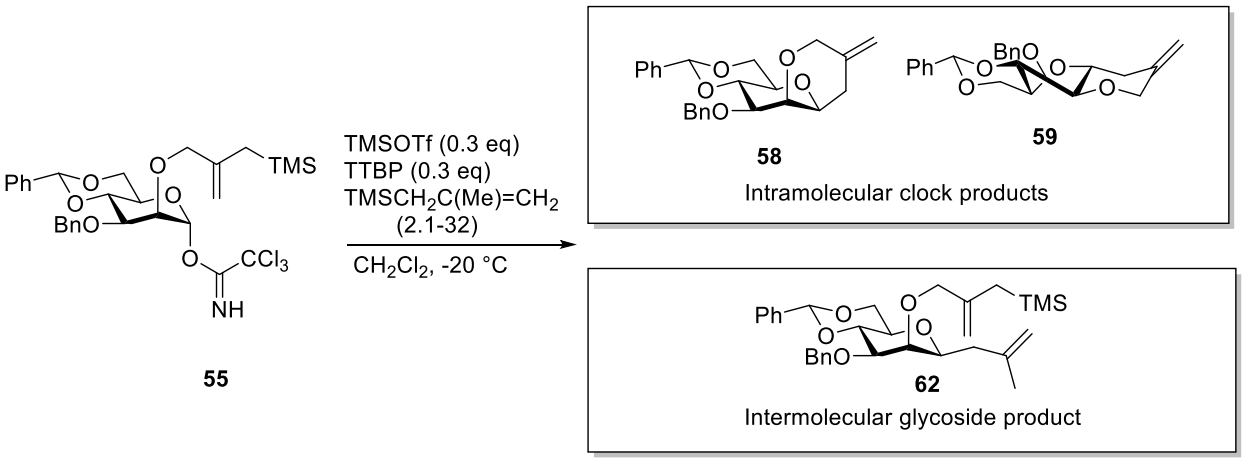

Entry	Nucleophile	Equiv (M conc)	**β-gly / cycl** **62** / (**58**+**59**)[b]	**α-gly / cycl** **62** / (**58**+**59**)[b]
1[a]	$TMSCH_2C(Me)=CH_2$	2.1 (0.032)	0.0729	-
2[a]	$TMSCH_2C(Me)=CH_2$	5.3 (0.085)	0.1046	-
3[a]	$TMSCH_2C(Me)=CH_2$	10.7 (0.171)	0.2996	-
4[a]	$TMSCH_2C(Me)=CH_2$	16.0 (0.256)	0.4712	-
5[a]	$TMSCH_2C(Me)=CH_2$	21.3 (0.341)	0.6673	-
6[a]	$TMSCH_2C(Me)=CH_2$	26.7(0.427)	0.9509	-
7[a]	$TMSCH_2C(Me)=CH_2$	32.0 (0.512)	1.1419	-

a) Experimental conditions: TTBP (0.3 equiv), TMSOTf (0.3 equiv.) at -20 °C; molecular sieves 4 Å;
b) Molar ratios were determined by UHPLC/UV/MS

The graphical representation of the concentration dependence of C-mannosylation is presented in Figure **12**. The lower nucleophilicity of allylsilane compared to the alcohol necessitated the use of higher concentration of in order for *C*-glycosylation to compete with cyclization.

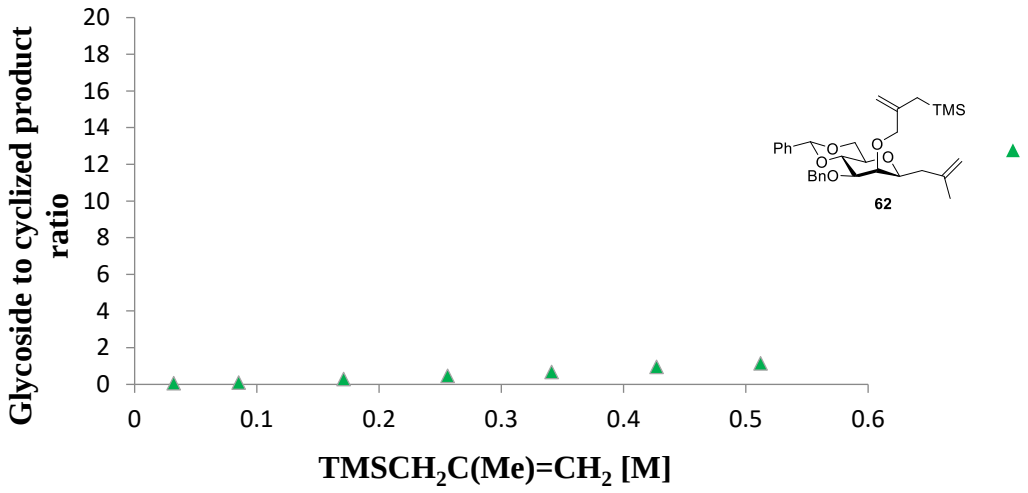

Figure **12.** Concentration dependence of the formation of *C*-mannosides in competition with cyclization.

Proper analysis of acceptor concentration dependence in *O*- and *C*-mannosylation can be best done by superimposition of the *O* and *C*- glycoside data (Figure 13). Clearly, the analysis reveals that, the formation of the β-mannoside **60** has a much stronger concentration dependence than α-anomer **61**. Nevertheless, the α-anomer showed greater concentration dependence than the formation of the β-*C*-mannoside **62**.

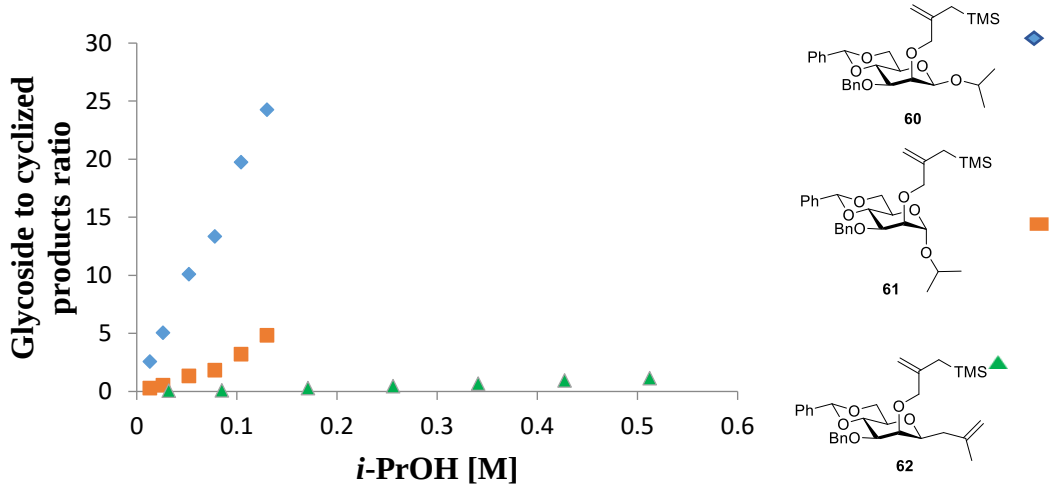

Figure **13.** *O*- and *C*-Mannosylation with trichloroacetimidate donor

Comparing the data obtained from the kinetics using trichloroacetimidate donor and that from the earlier sulfoxide donor (Scheme **37**)[87] revealed a similar trend of concentration dependence in the formation of both *C*- and *O*-glycosides (Figure 15). This indicates that after the initial activation step both the trichloroacetimidate and the sulfoxide donors follow comparable mechanisms. The minor differences between Figure **14a** and **14b** reflect the fact that different reaction temperatures were used for the two donors.

a) ***O*- and *C*-Mannosylation with trichloroacetimidate donor**	**b) *O*- and *C*-Mannosylation with sulfoxide donor**
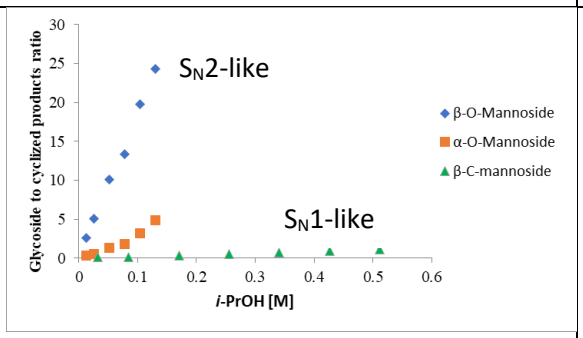	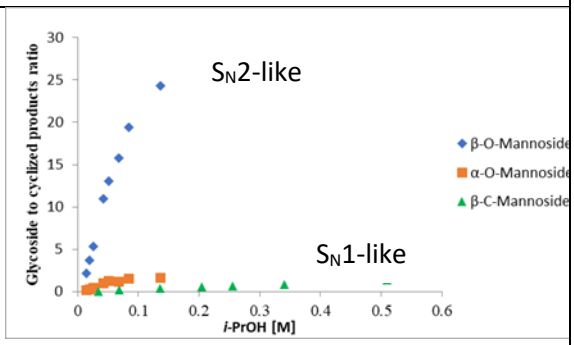

a) Figure **14.** Graphic representation of clock reactions. a) *O*- and *C*-Mannosylation with trichloroacetimidate donor. b) *O*- and *C*-Mannosylation with sulfoxide donor

2.1.7 β-*C*-Mannoside Selectivity

The β-selectivity observed in *C*-glycoside formation reaction confirms the earlier report by Crich and coworkers[84, 99] in which they observed that the formation of *C*-glycosides as exclusively β-isomers in the mannose series. This β-selectivity can be understood in the light of the mannosyl oxocarbenium ion model. The presence of the 4,6-*O*-benzylidene acetal group favors locks the range of conformations of the glycosyl oxocarbenium ions to $B_{2,5,}$ and $^{3}H_{4}$ as shown by computational work of Whitfield and coworkers.[100,101] The $B_{2,5}$ conformation puts the C2− O2 bond in the less hindered position and the C3−O3 bond in a pseudoaxial position from which it maximizes stabilization of the oxocarbenium ion. Therefore, by adopting the oxocarbenium ion

model for the formation of *C*-glycosides, the selective formation of the β-*C*-mannopyranosides is most reasonably explained by β-face attack on the $B_{2,5}$ conformation of the oxocarbenium ion, leading initially to the $^{1}S_{5}$ conformer of the product in which the newly formed bond adopts a pseudoaxial position (Scheme 49). The attack on the α-face, places the product initially in the $^{O}S_{2}$ twist boat conformation, with the newly formed bond pseudoequatorial and suffering from a gauche interaction with the C-2 substituent.

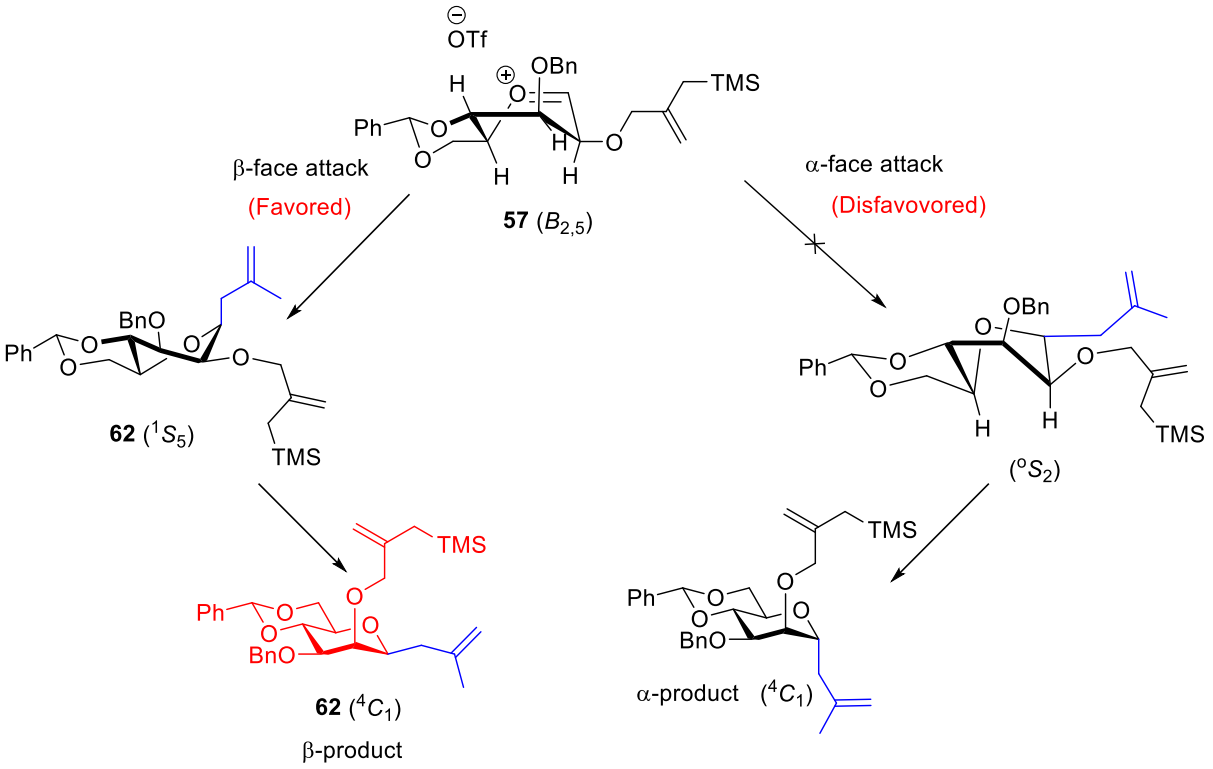

Scheme **49.** Rationalization of selectivity in 4,6-*O*-benzylidene protected β-*C*-mannosyl formation

2.1.8 Conclusions on *O* and *C*-Mannosylation

It is revealed that the 4,6-*O*-benzylidene mannosyl trichloroacetimidates and sulfoxides display largely parallel behavior toward both isopropanol and methylallyltrimethylsilane despite the different reaction temperatures and initialleaving groups. In both cases, the formation of the

β-mannoside **60** shows a much stronger concentration dependence than that of the α-anomer **61**, with the latter showing a slightly greater concentration dependence than the formation of the β-*C*-mannoside **62**. The selectivity in the β-*C*-mannosylation is consistent with earlier observations that only the β-anomer **62** is formed in the 4,6-*O*-benzylidene-directed *C*-mannosylation.[84] The of formation of the β-*O*-mannoside **60** is consistent with an S_N2-like associative displacement of an axial leaving group. While, the formation of the of α-*O*-mannoside **61** is a much more dissociative S_N1-like reaction as determined previously using ^{13}C-primary kinetic isotope effect measurements for the case of triflate as leaving group.[41] The very low concentration dependence observed for the formation of the *C*-mannoside **62** is consistent with a highly dissociative mechanism proceeding via an oxocarbenium ion **59** that is only loosely associated with the counterion.[102] This in turn is consistent with methallyltrimethylsilane being a much weaker nucleophile than isopropanol and requiring the more potent electrophile at the dissociative end of the mechanistic spectrum.[103]

2.3 Cation Clock Reactions for the Determination of Relative Kinetics in Glycosylation Reactions: Glucopyranosyl Clocks

2.3.1 Synthesis of the 4,6-*O*-Benzylidene-protected Glucopyranosyl Clock

The successful relative kinetics study of the mannosyl trichloroacetimidate system inspired comparable application of the method to the glucopyranosyl trichloroacetimidates. In the 4,6-*O*-benzylidene glucopyranose series (Scheme 50) synthesis of the trichloroacetimidate clock began from 1,2:5,6-di-*O*-isopropylidene-α-D-glucofuranose. Protection of the hydroxyl group with benzyl bromide in the presence of sodium hydride, followed by acid hydrolysis of the isopropylidene groups with a cation-exchange resin gave 3-*O*-benzyl-D-glucopyranose, which was acetylated with acetic anhydride/pyridine to give 1,2,4,6-tetra-*O*-acetyl-3-*O*-benzyl-β-D-

glucopyranose. Glucosidation with 2-(phenylthio)ethanol in dry dicholoromethane under BF_3•Et_2O conditions gave 2-phenylthioethyl 1,2,4,6-tetra-*O*-acetyl-β-D-glucopyranoside.[104] Subsequent saponification of **65** gave the triol **67** onto which the benzylidene group was installed in the usual manner to afford 2-phenylthioethyl 3-*O*-benzyl-4,6-*O*-benzilidene-β-D-glucopyranose **68.** Trimethylsilylmethallylation was conducted under the improved conditions where chloromemylallylsilane was first converted to iodomethylallysilane followed by alkylation to give **68** in 89% yield. The reductive cleavage of the phenylthioethyl group was achieved with lithium naphthenalide to give **69**. Finally, the trichloroacetimidate was installed with the aid of sodium hydride[98] affording the trichloroacetimidate clock **70** (Scheme 50).

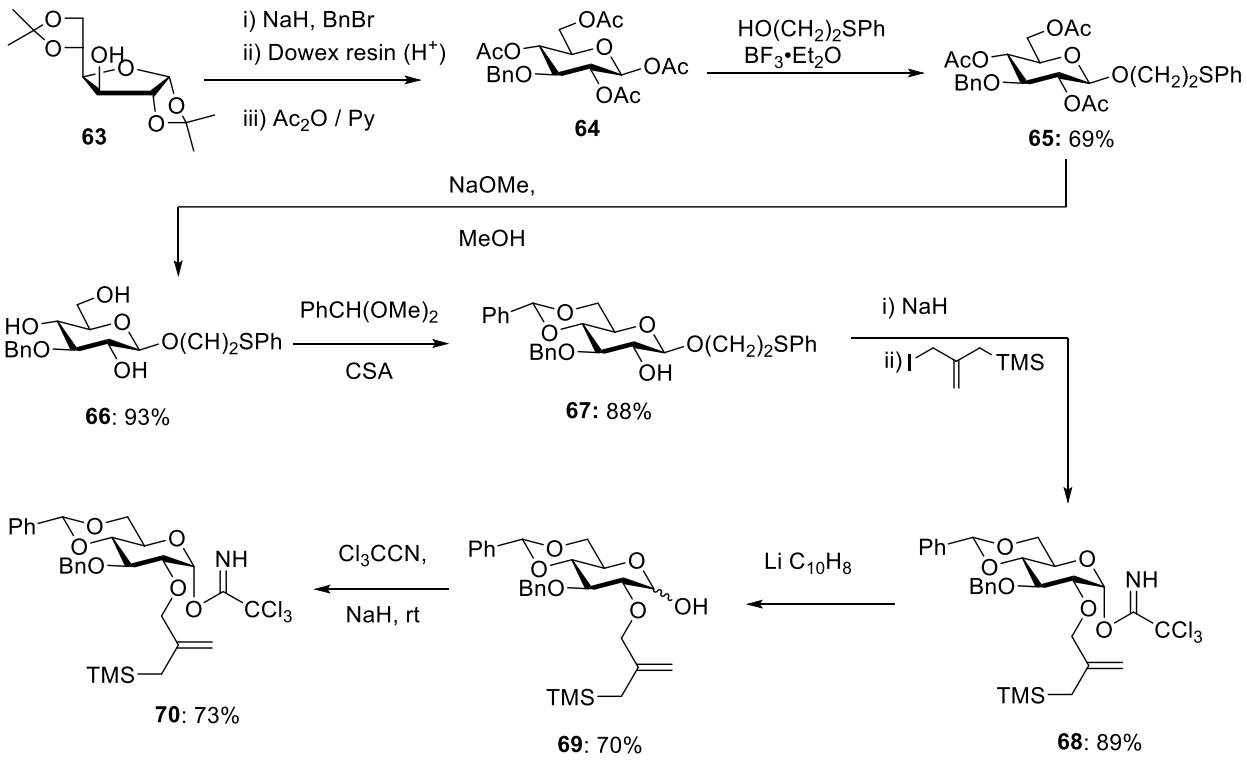

Scheme **50.** Synthesis of the 4,6-O-benzylidene-protected glucopyranosyl clock.

2.3.2 Clock Cyclization Reaction

Glucopyranosyl trichloroacetimidate **70** was first subjected to cyclization without an external nucleophile using the same protocol used for mannosyl tricholoroacetimidate system and gave compound **73** as a single isomer in 90% (Scheme 51).

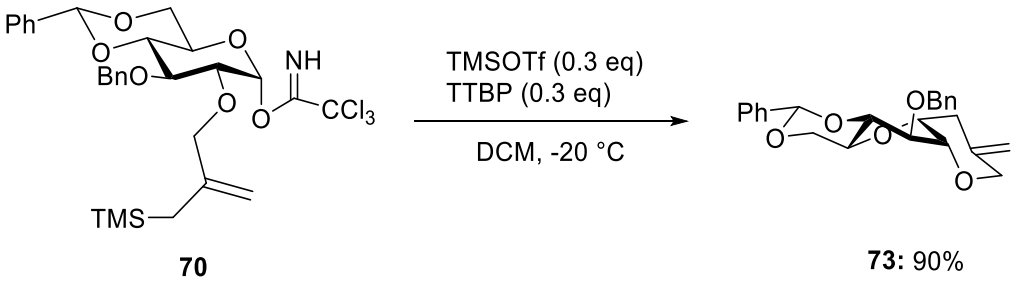

70 **73:** 90%

Scheme **51**. Glucopyranosyl unimolecular clock reaction

2.3.3 Conformation and Selectivity of the Glucopyranosyl Oxocarbenium Ion

The formation of the cyclized product can be understood to go through the activated covalent triflate **71** that adopts two conformations, $^{4}H_{3}$ and $B_{2,5}$, of the oxocarbenium ion/triflate ion pair **72**, which are in equilibrium and which both lead to the *cis*-fused product **73** (Scheme 52). The tricyclic glucose derivative **73** prefers the $^{1}S_{5}$ conformation of the pyranose ring as opposed to the $^{4}C_{1}$ chair. This preference is due to the combination of two unfavorable steric interactions in the chair; namely, the 1,3-diaxial interaction between the axial anomeric C-C bond and the axial C3-H3 bond and the gauche butane interaction illustrated by blue the color in Scheme **52**. This later interaction is determining as other simple 4.6-*O*-benzylidene α-*C*-glucopyranosides retain $^{4}C_{1}$ conformation.[84,83]

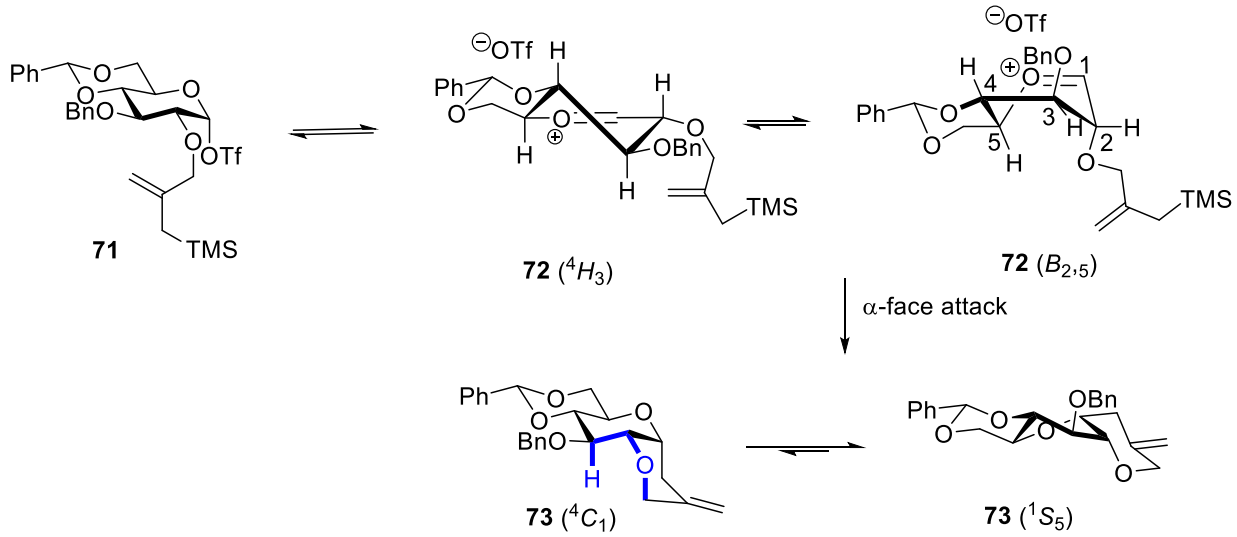

Scheme **52**. Conformation and selectivity of the glucopyranosyl oxocarbenium ion

2.3.4 Competition Kinetics (*O*-Glycoside in Competition with Cyclization)

Use of the trichloroacetimidates glucosyl donor in competition reactions with isopropanol, by the same protocol to the mannose series, gave two *O*-glucosides in addition to the clock product **(**Figure 15).

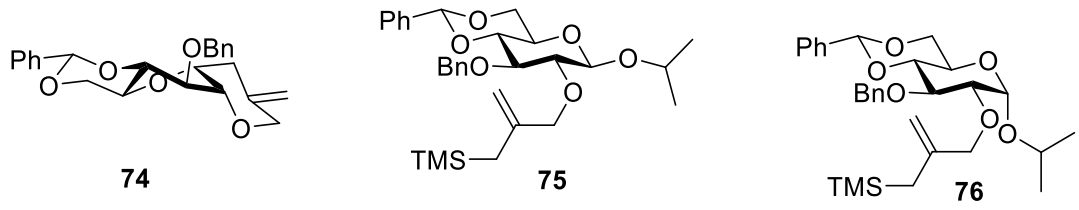

Figure **15.** *O*-Glucoside products from competition reaction

Analysis of the reaction mixtures using HPLC gave the data presented in Table **3**.

Table **3.** *O*-Glucosylation with trichloroacetimidate donor **70**.

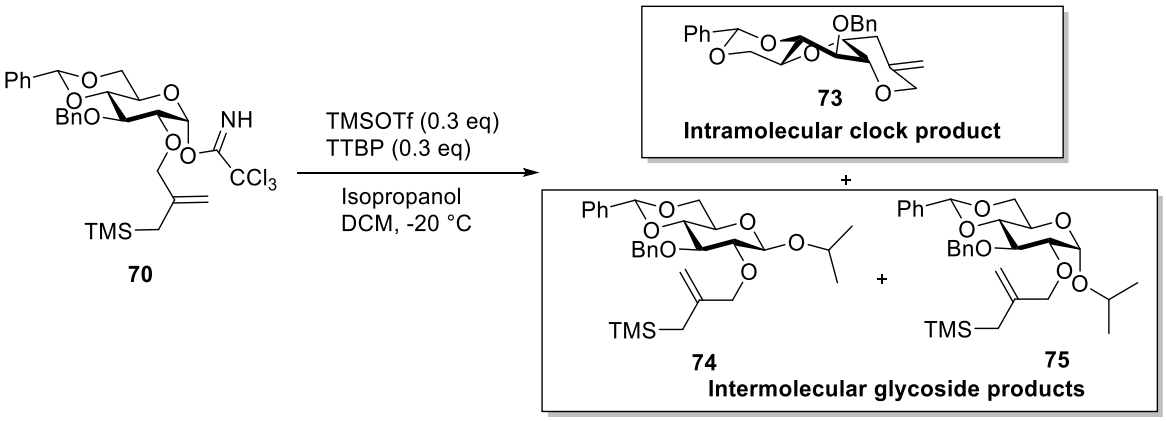

Entry	Nucleophile	Equiv (M conc)	**β-gly/cycl** **74**/(**73**)[b]	**α-gly/cycl** **75**/(**73**)[b]
1[a]	*i*PrOH	1 (0.048)	0.0067	0.0227
2[a]	*i*PrOH	1.5 (0.072)	0.0243	0.0708
3[a]	*i*PrOH	2 (0.096)	0.0550	0.1297
4[a]	*i*PrOH	3 (0.144	0.1143	0.2498
5[a]	*i*PrOH	5 (0.239)	0.4043	0.5135
6[a]	*i*PrOH	8 (0.382)	0.9845	1.0176

a) Experimental conditions: TTBP (0.3 eq), TMSOTf (0.3 equiv.) at -20 °C; molecular sieves 4 Å;
b) Molar ratios were determined by UHPLC/UV/MS

Graphical representation of this data reveals the influence of the concentration of the acceptor on the ratio of glycoside formation to cyclization (Figure 16).

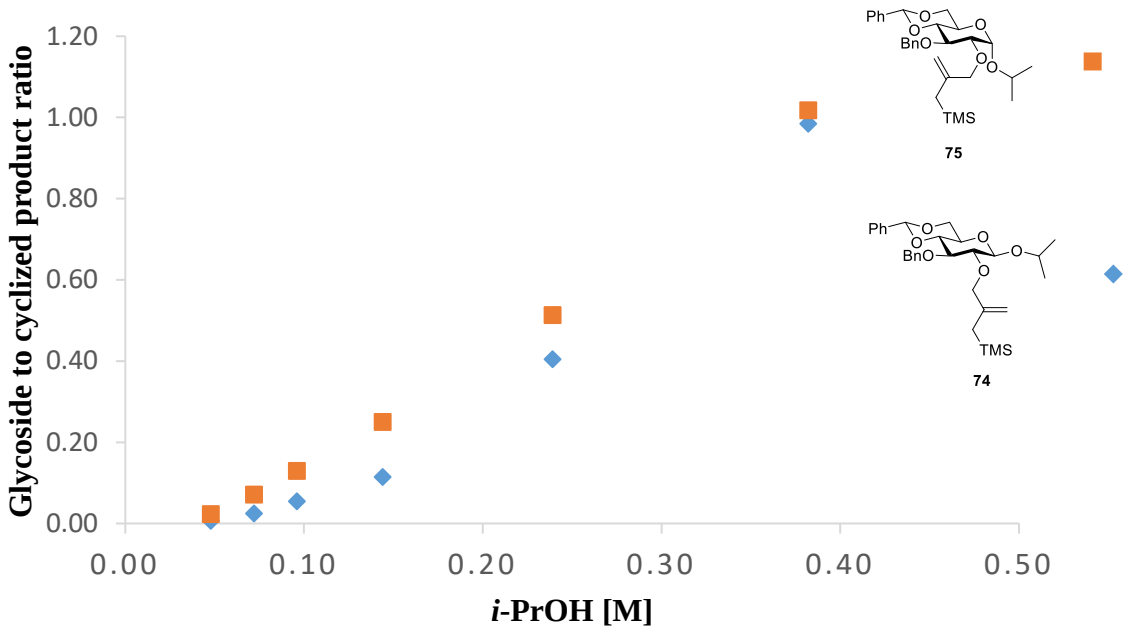

Figure **16.** *O*-Glucosylation in competition with cyclization

2.3.5 Competition Kinetics (*C*-Glucoside Formation in Competition with Cyclization)

With the kinetics of the *O*-glycoside formation at hand, the focus turned to the competition of *C*-glycoside formation with cyclization. The protocol used for the *O*-glycosides was applied by simply replacing 2-propanol with methylallyl trimethylsilane to give single clock product and a single *C*-glycoside **(**Figure 17).

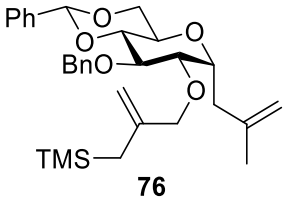

76

Figure **17.** *C*-Glucoside

Analysis of the experimental data gave the ratios as shown in Table 4.

Table **4.** *C*-Glucoside in competition with cyclization

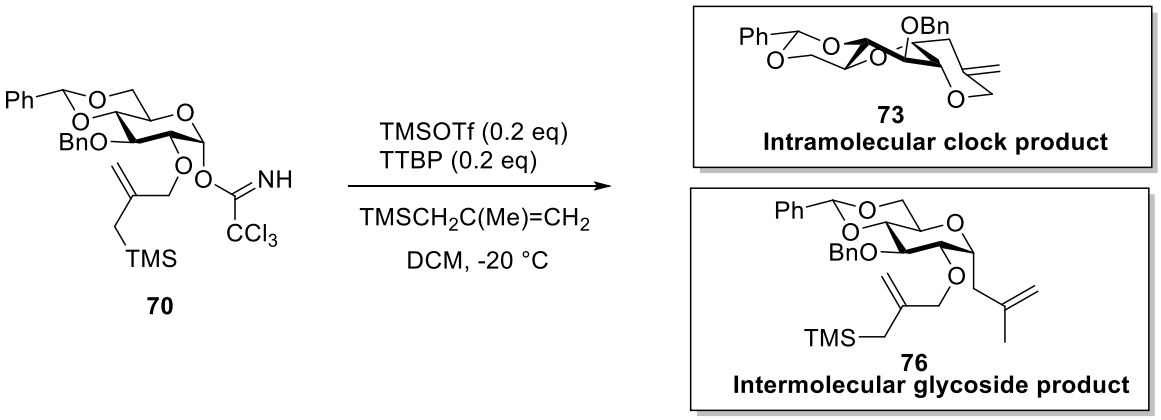

Entry	Nucleophile	Equiv (M conc)	**β-gly/cycl**	**α-gly/cycl**
				76/(**73**)[b]
1[a]	$TMSCH_2C(Me)=CH_2$	23.8 (1.14)	-	0.0899
2[a]	$TMSCH_2C(Me)=CH_2$	35.7 (1.71)	-	0.1078
3[a]	$TMSCH_2C(Me)=CH_2$	47.6 (2.28)	-	0.1273
4[a]	$TMSCH_2C(Me)=CH_2$	59.5 (2.85)	-	0.1957
5[a]	$TMSCH_2C(Me)=CH_2$	71.4 (3.41)	-	0.2331

a) Experimental conditions: TTBP (0.3 equiv), TMSOTf (0.3 equiv.) at -20 °C; molecular sieves 4 Å;
b) Molar ratios were determined by UHPLC/UV/MS

The results were then represented graphically as shown in Figure **18**. It is noteworthy that even the highest ratio for a α-*C*-glycoside to cyclized product was low (0.23).

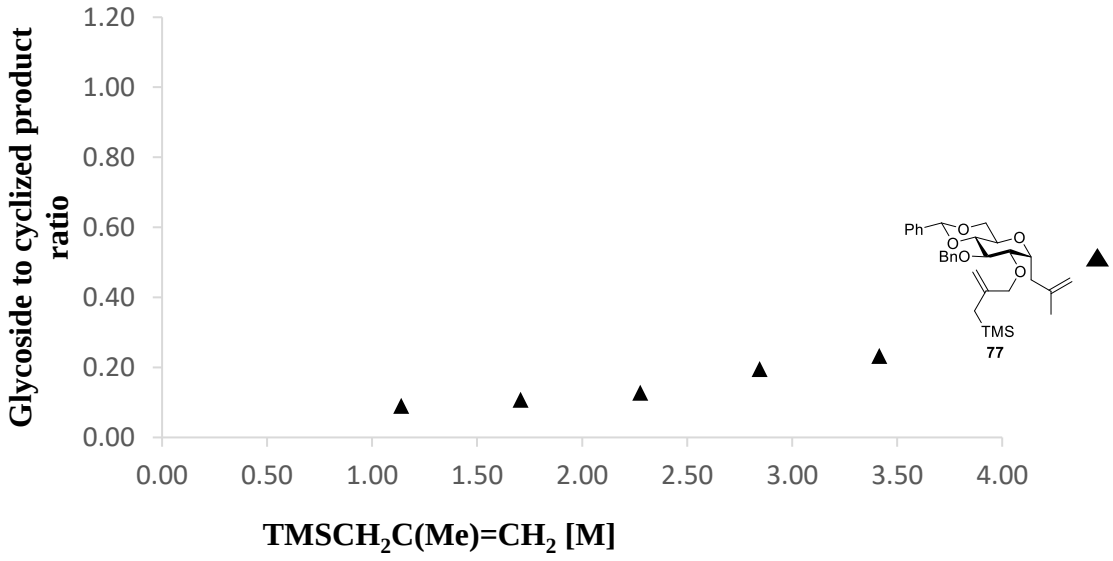

Figure **18.** Graphical representation of *C*-glucoside formation in competition with cyclization as a function of concentration

The significant difference in concentration dependence between *O*- and *C*- glycoside formation is best appreciated by superimposition of the individual plots as shown in Figure **19**

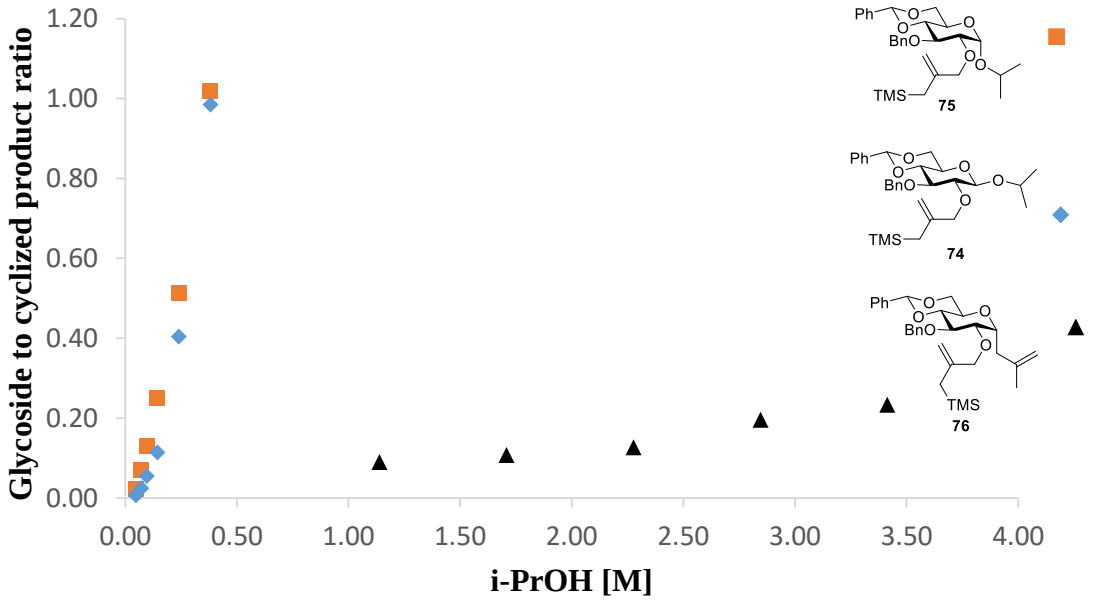

Figure **19**. Graphical representation of concentration dependence in *O*- and *C*-glucosylations with trichloroacetimidate donor **70**

This data (Figure 20) reveals that formation of both β- and α-*O*-glucosides (**74** and **75**) has a much stronger concentration dependence than that of the corresponding *C*-glucoside **76**. A single α-*C* glucoside **76** formed is consistent with previous literature work.[84,83] Considering that the *C*-glucoside formation is interpreted as representative of the concentration dependence of a dissociative S_N1-like mechanism with a weak nucleophile as in the mannose case, these results are again consistent with the primary ^{13}C kinetic isotope effect studies on benzylidene protected *O*-glucosylation with triflate as leaving group, which point to both anomers being formed by associative S_N2-like mechanisms from a pair of rapidly equilibrating anomeric glucosyl triflates.[41]

Superimposing the relative kinetics data for the formation of *C*-glycosides in both mannose and glucose in green and black colors respectively, reveals that the two have different cyclization rates. (Figure 20).

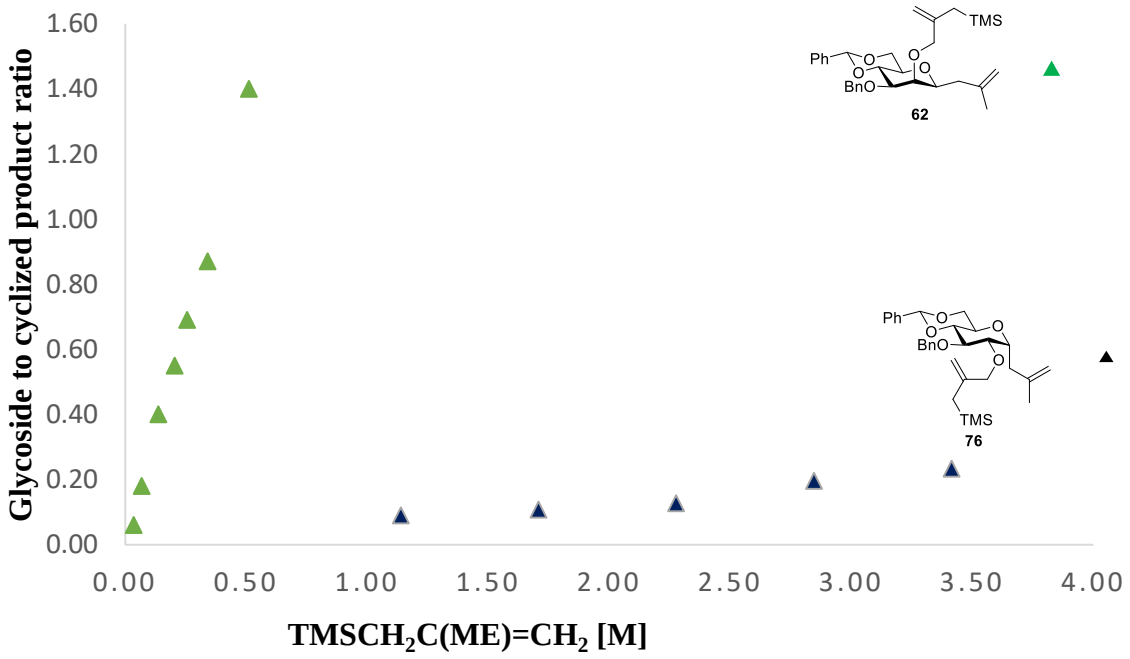

Figure **20.** Superposition of *C*-glycosylation with mannosyl and glucosyl donors

It is also possible to make the comparison between the manno and gluco series as illustrated in the Figure **20.** At first glance, it appears that *C*-mannoside formation in the mano series is more concentration dependent than in the gluco series. However, the analysis ignores the use of different cyclization as clocks with no knowledge of their relative rates. Thus, an alternative explanation of figure **20** simply has the gluco cyclization being more rapid than the manno with little or no difference in concentration. Presumably, the reality is somewhere between these two extremes. Unfortunately, the data does not allow any such distinctions and thus gluco/manno comparisons are avoided.

The data also reveals the differing influences of the 4,6-*O*-benzylidene acetal protecting group in the manno- and glucopyranose series. Thus, in contrast to the benzylidene-protected *O*-mannosylation, both anomers **74** and **75** of the benzylidene-protected glucosides are formed with the same concentration dependence. The formation of both *O*-glucosides **74** and **75** shows a much stronger concentration dependence than that of the corresponding *C*-glucoside **76**, which is confirmed as a single α-*C* glucoside, consistent with previous reports.[84,83] Considering that the *C*-glucoside formation is interpreted as representative of the concentration dependence of a dissociative S_N1-like mechanism with a weak nucleophile as in the mannose case, these results are again consistent with primary ^{13}C kinetic isotope effect studies on benzylidene protected *O*-glucosylation with triflate as leaving group, which point to both anomers being formed by associative S_N2-like mechanisms from a pair of rapidly equilibrating anomeric glucosyl triflates (Scheme 52).

Finally, the absence of phenyl thiol transfer in the trichloroacetimidate donor makes it a better clock in glucose series than thioglycoside donors.

2.4 Overall Conclusions

The further development of a cation clock method based on the intramolecular Sakurai reaction has been demonstrated and used to probe the concentration dependence of representative *O*- and *C*-glycosylation reactions from glycosyl trichloroacetimidate donors on activation by trimethylsilyl triflate. The 4,6-*O*-benzylidene-directed β-mannosylation is demonstrated to proceed with a strong dependence on the concentration of the acceptor alcohol, whereas the α-anomer is much less concentration dependent. Analogous results are observed in 4,6-*O*-benzylidene-directed β-mannosylation conducted by the trichloroacetimidate method (Figure 14a) and sulfoxide method (Figure 14b) suggesting a commonality of mechanism if not necessarily of leaving group. The significant difference in the influence of the 4,6-*O*-benzylidene-acetal in the mannose and glucose series is also demonstrated by the comparison of the *C*-glycosides both the mannose and glucose series. Finally, the formation of *trans*-fused products from the clock reaction in the mannopyranose series is interpreted in terms of a transient glycosyl oxocarbenium ion that is capable of accessing the $B_{2,5}$ and/or $^{3}H_{4}$ conformers.

CHAPTER 3: USE OF CATION CLOCK REACTIONS FOR THE DETERMINATION OF RELATIVE REACTION KINETICS IN ARABINOFURANOSYLATION

3.1 Introduction

Arabinosides are important constituents of natural glycoconjugates and are commonly found in furanose form.[105] Both D and L versions (Figure 21) of arabinofuranosides exist in nature with the L-form being the components of plant cell walls, majorly as α-L-furanosides. The β-L-furanosides though less common, play key roles as building blocks in glycoproteins such as potato lectins.[106] The D-arabinofuranosides are generally less common in nature but are found mostly in the mycobacterial cell wall as both β- and α-configurations.[107] The significance of arabinofuranoside residues in biological processes[108] has attracted many synthetic chemists to develop a proper mechanistic understanding of arabinofuranosylation.

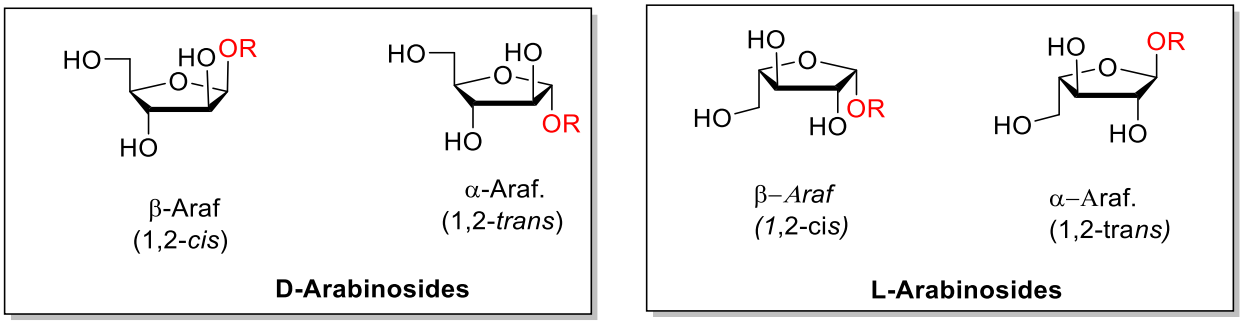

Figure **21**. Structures of D- and L-arabinofuranosides and their anomers

One of the challenges involved in the development of a general method for the stereoselective 1,2-*cis*-arabinofuranosylation is associated with the weak anomeric effects in furanosides, with only slight differences between β and α-anomers, thus making it difficult to exploit thermodynamic selection for anomeric selectivity.[109,110] Moreover, the ability of furanosides to assume several twist and envelope conformations, which can interconvert via pseudorotational itineraries,[107] allows them to glycosylate through multiple but closely

energetically related different transition states, which may further compromise anomeric selectivity.[111] Fortunately, 1,2-*trans* anomers are readily installed through neighboring group participation, whereas, the synthesis of the 1,2-*cis*-arabinofuranosides with a high degree of stereocontrol is generally problematic.[111] The literature solution to this has been the use of indirect methods. For example, Lowary and co-workers employed a 2,3- anhydrofuranosyl donor to achieve 1,2 *cis* selectivity[112] while Ito and coworkers used the intramolecular aglycon delivery methods.[54,64] Boons[113] and Crich[114] accessed β-arabinofuranosylation through 3,5-*O*-silylene protected arabonofuranoside donors inspired by Crich's β-mannosylation.[37]

The successful application of the cation clock method for the determination of relative kinetics of glycosylations reaction in pyranosyl systems and the need to understand the arabinofuranosyl reaction mechanism inspired the further development and application of cation clock reaction to understand the molecularity in the arabinofuranosyl system. The use of the 2-*O*-(2-trimethylsilylmethallyl) group as intramolecular nucleophile provided an efficient clock reaction for mannosylation and glycosylation reactions with trichloroacetimidates. The arabinofuranosyl system, with its predictably faster kinetics, provides the opportunity to explore other nucleophiles in the clock reaction; indeed, the anticipated need for faster cyclization led to the choice of alcohols as nucleophiles. The anticipated overly rapid cyclization of systems providing five and six-membered rings resulted in the choice of a conformationally rigidified system leading to the eight-membered ring.

3.2 Synthesis of Phenyl 3,5-*O*-(di-*tert*-Butylsilylene) 2-*O*-((2-Hydroxymethyl) Benzyl)-1-Thio-α-D-Arabinofuranoside

The synthesis of the 3,5-*O*-di-*tert*-butylsilylene protected acetal **83** began with the preparation of the known compound **80**,[115] which was obtained from D-arabinose per the literature protocol.[116] According to Lowary and coworkers, the methyl arabinofuranoside intermediate obtained was esterified under standard conditions and then transformed into the tetraacetate **78**[116] with sulfuric acid in acidic acetic anhydride. Reaction of **78** as a mixture of anomers with thiophenol in the presence of boron trifluoride etherate gave thioglycoside **79** in 70% (overall yield from compound **77**). Subsequently, deacetylation of compound **79** with sodium methoxide followed by silylation with di-*tert*-butylsilyl bis(trifluoromethanesulfonate) using lutidine as a base gave the 2-*O*-unprotected arabinofuranoside **80**[115] in **79**% yield in two steps.

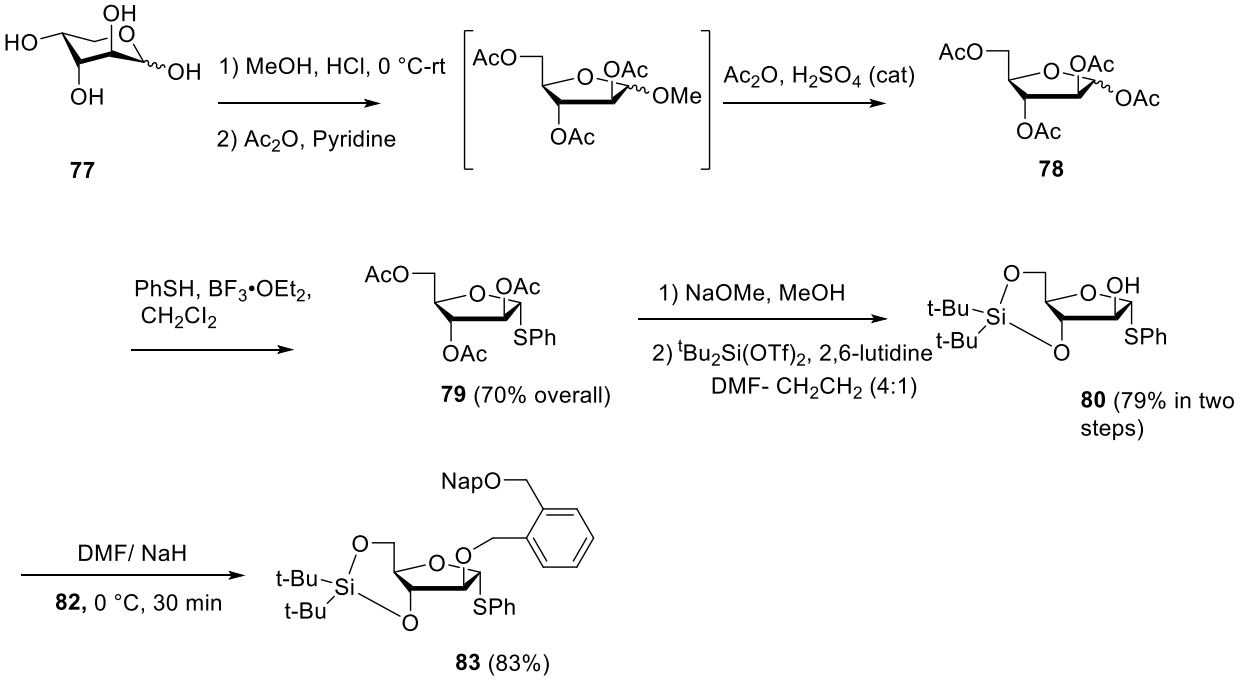

Scheme **53.** Synthesis of a 3,5-*O*-di-*tert*-butylsilylene protected arabinofuranoside donor

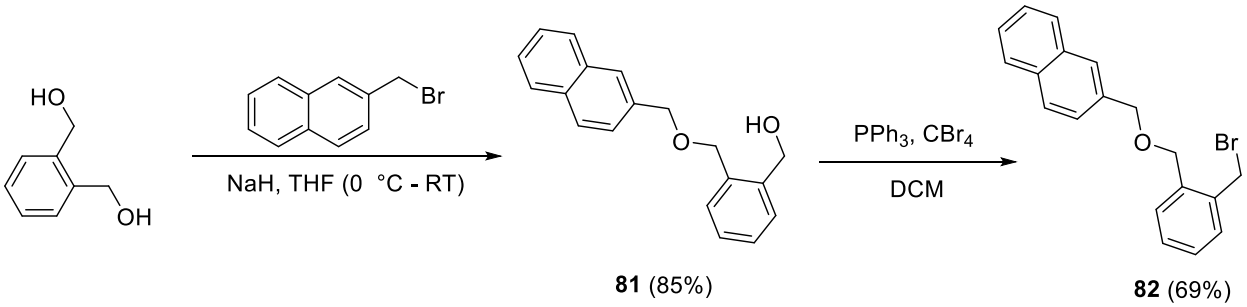

Scheme 54. Synthesis of 2-((naphthalen-2-ylmethoxy) methyl) benzyl bromide

The next step in the synthesis was the strategic installation of the nucleophilic arm on O2. The synthesis of the requisite 2-((naphthalen-2-ylmethoxy) methyl) benzyl bromide began with the selective protection of one hydroxyl group of 1,2-benzene dimethanol by treatment with sodium hydride, followed by careful addition of a solution of 2-(bromomethyl)naphthalene in THF to the milky suspension. Subsequent reflux of the mixture for 2.5 h, followed by cooling and careful quenching at room temperature gave the desired monoprotected compound **81** in 85% yield. The conversion of the remaining hydroxyl group to corresponding bromide **82** was done using carbon tetrabromide and triphenylphosphine in 69% yield (Scheme 54), thereby setting the stage for the alkylation at the O2 of the 3,5- (di-*tert*-butylsilylene) α-D-arabinofuranoside. Treatment of a mixture of compounds **80** and **82** with NaH at 0 ºC gave the desired alkylated product **83** in 83% (Scheme 53).

The final stage of the synthesis of donor **84** was the selective deprotection of the napthylmethyl ether in presence of the sulfide (Scheme 55). This is a key reaction since sulfides are well known catalyst poisons.[117] Fortunately, the different affinities of naphthylmethyl and benzyl groups[118] for heterogenous catalysts allowed for the selective hydrogenolytic cleavage of the naphthylmethyl ether in the presence of the sulfide and the benzyl ether using palladium hydroxide at 1, atmosphere and gave the desired donor **84** in 90% yield.

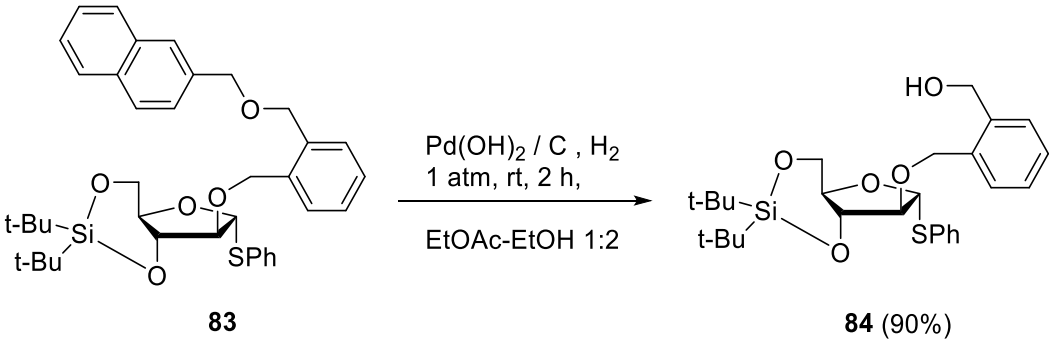

83 **84** (90%)

Scheme **55**. Hydogenolytic cleavage of the naphthymethyl protecting group

3.2.1 Clock Cyclization Reaction

With compound **84** in hand, it was necessary to establish the operation of the clock reaction in the arabinofuranosyl system. Previously, Crich and coworkers investigated various glycosylation conditions and showed the importance of the activation method on the stereoselectivity of glycosylation reaction of the thioglycoside donor in this series.[114] In this work, the use of NIS/AgOTf as a promoter was preferred following the original report by Boons and co-workers[113] in glycosylations with a 3,5-di-*tert*-butylsilylene protected arabinofuranoside donor. Further literature reports by Lowary[119] and coworkers, together with that of Kim and coworkers,[120] suggested the application the thiophilic NIS/AgOTf in 3,5-dibenzylated arabinofuranosyl systems. In the above examples, the pre-activation of the of the donor at low temperatures followed by warming to 0 ºC or room temperature was applied. For the clock reaction, the need to use a temperature that allows for complete activation under competition conditions led to setting up the cyclization clock reaction under the NIS/AgOTf conditions at – 20 ºC, enabling a rapid, smooth reaction and resulting in the isolation of **85** (1,2-*cis* intramolecular product) and **86** (1,2-*trans* intramolecular product) in 90 and 5 % yields, respectively (Scheme 56).

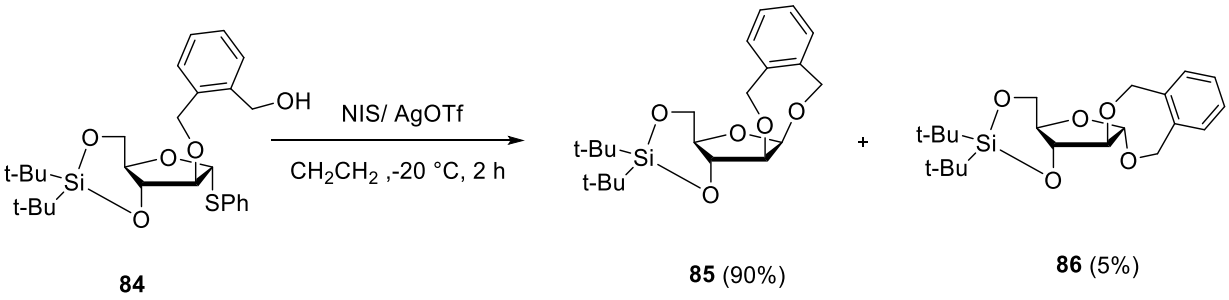

Scheme **56**. Clock cyclization reaction

The anomeric configuration of the cyclic arabinosides was based on the chemical shifts of the anomeric carbons and the size of their $^{3}J_{H1-H2}$ coupling constants. Generally for the arabinofuranosides, the β-isomer resonates upfield in the range of δ(C-1) 97–104 ppm relative to the α-isomer which resonates in the region of δ(C-1) 104–111 pp.[114,121] The anomeric coupling constant in the β-anomer is larger and in the range of ($^{3}J_{H1-H2}$ = 4–6 Hz). The α-counterpart, shows $^{3}J_{H1-H2}$ = 1–3 Hz.[114] Thus, the applying these characteristic features, the 1,2-*cis* anomer (**85**) exhibited δ(C-1) = 101.5 ppm and $^{3}J_{H1-H2}$ = 5.2 Hz Hz, While the minor 1,2-*trans* anomer (**86**) was characterized by, δ(C-1) 104.6 ppm, and $^{3}J_{H1-H2}$ = 3.0 Hz (Scheme 57).

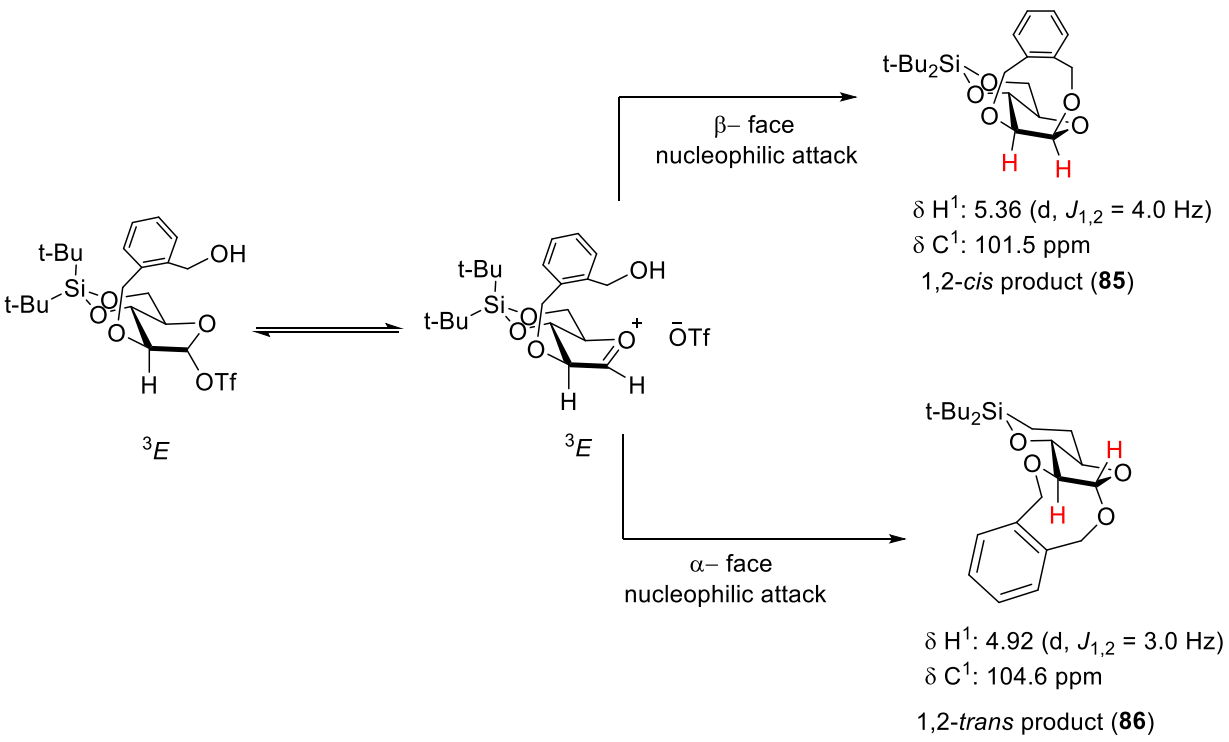

Scheme **57**. Cyclization of the clock system.

The stereoselectivity of reactions involving substituted furanosyl oxocarbenium ions as intermediates was first rationalized by Woerpel and co-workers, who proposed a model in which the equilibrium between the ^3E and E_3 oxocarbenium ions is decisive.[122] Woerpel holds that, the envelope conformations are preferentially attacked on the inside face, in order to minimize eclipsing interactions with substituents at C2 and provide a product featuring a favorable staggered C1-C2 conformation.[123,124] This model is consistent with Boon's proposal for the β-arabinosylation.[113] The stability of the oxocarbenium ion depends mainly on the orientation of the substituents on the furanosyl ring. Notably, the C2-substituent preferentially adopts a pseudoequatorial position to allow hyperconjugative stabilization of the oxocarbenium ion by the pseudoaxial C2-H2 bond. The formation of the major 1,2 *cis* product (**85**) is understood in terms of the effect of the Woerpel model. Indeed Codée and coworkers[122] reported a systematic analysis

of the stereoelectronic effects that govern the highly stereoselective formation of 1,2-*cis* glycosides regardless of the configuration of the furanosyl donor at C2, and confirmed the preference for the inside attack of the nucleophile on the lowest energy conformer of the corresponding oxocarbeniums consistent with Woerpel's theory (Scheme 58).[82a]

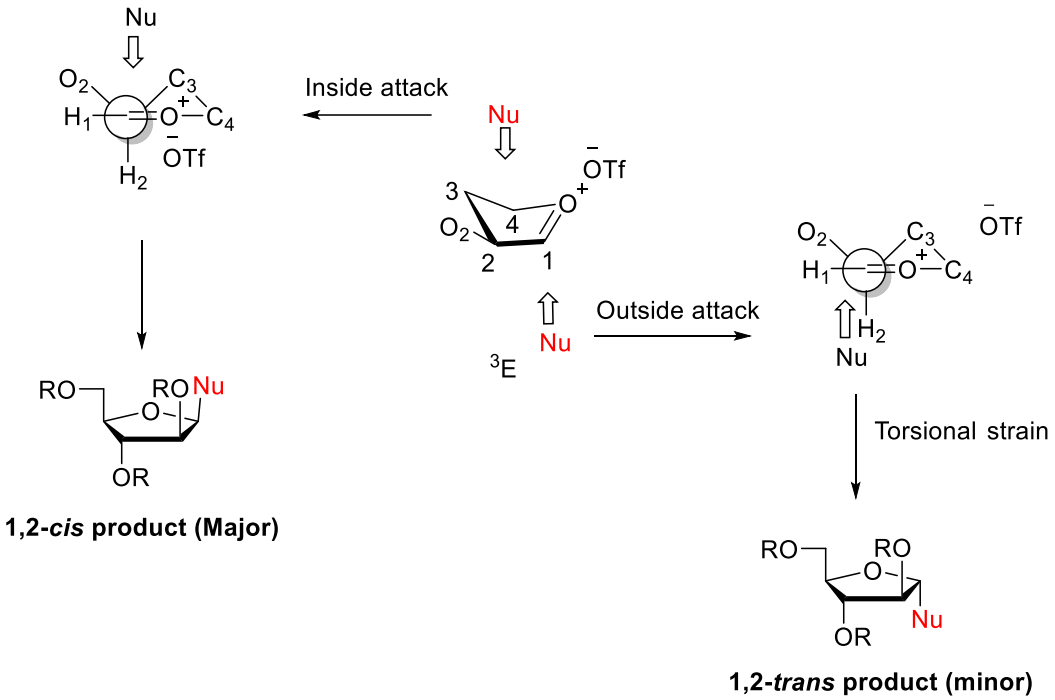

Scheme **58**. Inside attack on the furanosyl oxocarbenium ion leading to the major product, and outside attack leading to the minor product.

3.2.2 Competition Kinetics

The successful cyclization clock reaction paved way for its application in the study of relative kinetics of the glycosylation reaction of 3,5-di-*tert*-butylsilylene protected arabinofuranosides. The kinetic study was executed by conducting multiple experiments at a different alcohol concentration each time, and carrying out chromatographic analysis as done earlier for the pyranosides. Thus, the thioglycoside **84** was co-evaporated with toluene 3 times and kept in vacuo for 3 h. 4Å Molecular sieves and anhydrous dichloromethane then were added and

the reaction mixture was stirred for 1 h at room temperature prior to cooling to -20 °C, under argon. Isopropanol (2.1-9.9 equiv) was added and the reaction mixture stirred for 10 min before solid NIS was added, followed by AgOTf. The reaction mixture was then stirred at the same temperature for 1 h, during which the appearance of a persistent characteristic iodine color was observed. The reaction mixture was quenched with triethylamine at -20 ºC and the suspension was diluted with EtOAc and filtered through Celite. The filtrate was worked up and the product ratios analyzed by HPLC. Pooling the crude reaction mixtures from several runs afforded sufficient material for the chromatographic purification and full characterization of the intermolecular glycosides (Figure 22). The chemical shift of the anomeric carbon and the coupling constants for compound **87** were; δC-1= 104.7 ppm. $^{3}J_{H1\text{-}H2}$ = 3.5 Hz) resulted in the assignment as the α-anomer, while compound **88** was identified by (δC-1= 98 ppm. $^{3}J_{H1\text{-}H2}$ = 5.5 Hz) consistent with the β-configuration.

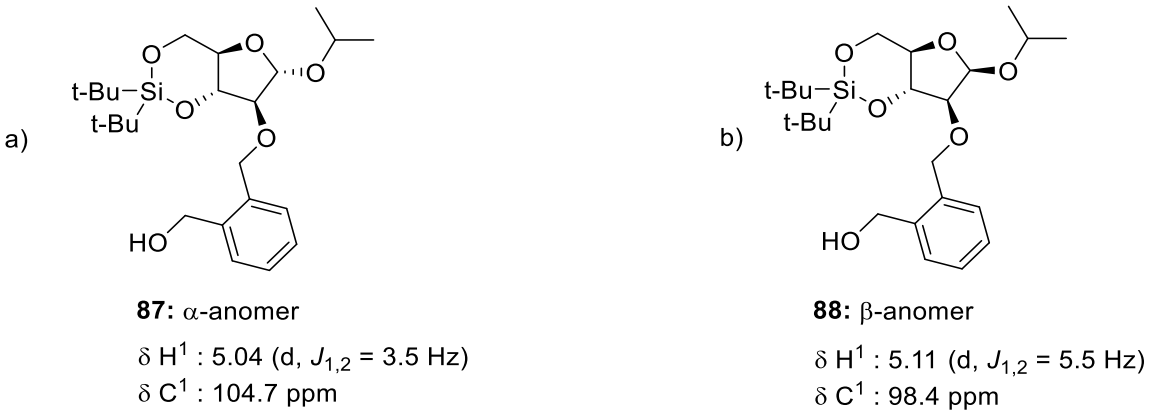

Figure **22**. Isolated 3,5-di-*tert*-butylsilylene protected α- and β-*O*-glycosides

3.2.3 Kinetic Analysis

In the series of competition experiments described above, HPLC analysis was used to determine the ratio of glycosides **87** and **88** formed compared to the amount of the combined cyclization products **85** and **86** as a function of the amount of concentration of isopropanol, resulting in the data presented in Table 5.

Table **5**. *O*-Glycoside formation in competition with cyclization for the 3,5-*O*-di-*tert*-butylsilylene protected donor

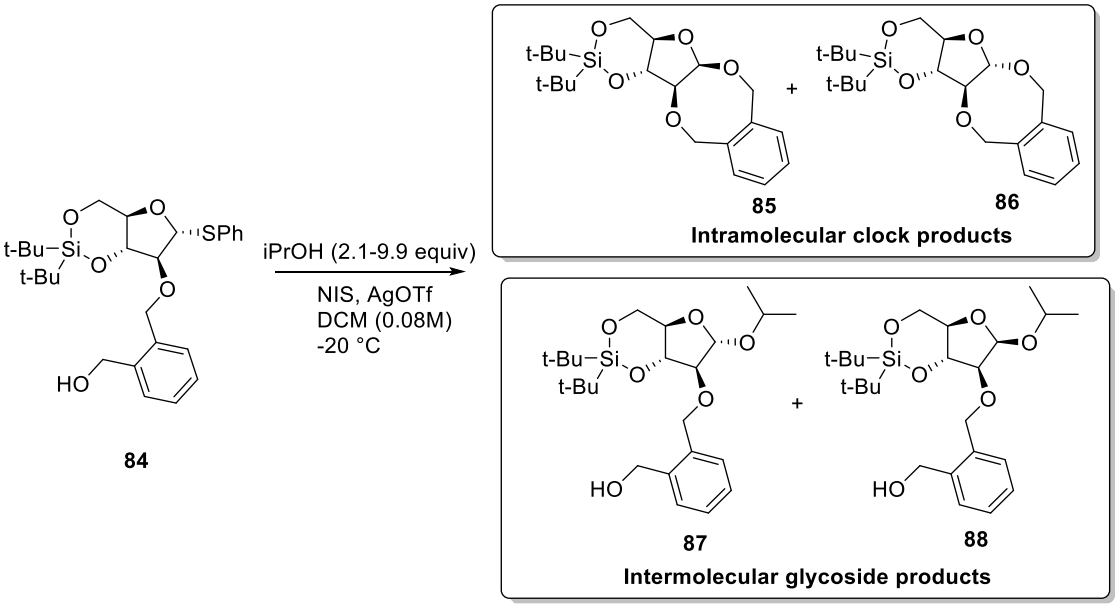

Entry	Equiv (M conc)	**α -gly/cycl** **87**/(**85** + **86**)[b]	**β-gly/cycl** **88**/(**85** + **86**)[b]
1[a]	0.078 (2.11)	0.304	0.544
2[a]	0.117 (3.17)	0.399	0.638
3[a]	0.156 (4.22)	0.509	0.880
4[a]	0.234 (6.33)	0.678	0.987
5[a]	0.273 (7.38)	0.680	1.127
6[a]	0.312 (8.44)	0.727	1.273
7[a]	0.363 (9.85)	0.666	1.304

a) Experimental conditions: NIS (2 equiv), AgOTf (0.5 equiv), at -20 °C; molecular sieves 4 Å;
b) Ratios were determined by HPLC/UV/MS

Graphical representation of the above data gives a clear picture of the influence of concentration on the ratio of glycoside formation to cyclization (Figure 23).

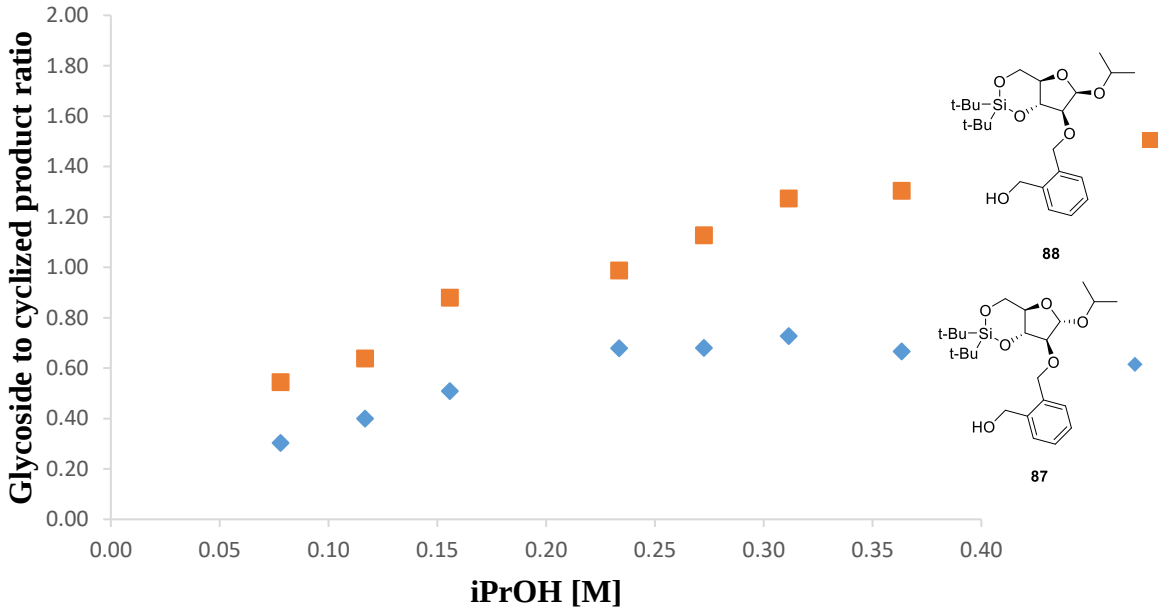

Figure **23**. Graphical representation of *O*-glycoside formation in competition with cyclization reaction for the 3,5-di-*tert*-butylsilylene donor **84**.

The graphical representation of the competition experiments presented in Figure 24, reveals that the rate of formation of the β-*O*-arabinoside **88** has a stronger concentration dependence than that of α-*O*-arabinofuranoside **87**. This suggests that the β-glycosylation is closer to S_N2 end of the mechanistic spectrum.

3.3 Synthesis of Phenyl 3,5-*O*-Dibenzyl-2-*O*-(2-Hydroxymethyl) Benzyl-1-thio-α-D-Arabinofuranoside

Once the data for the conformationally locked phenyl 3,5-*O*-(di-tert-butylsilylene) 2-*O*-((2-hydroxymethyl) benzyl)-1-thio-α-D-arabinofuranoside were in hand, we turned to phenyl 3,5-*O*-dibenzyl-2-*O*-(2-hydroxymethyl) benzyl-1-thio-α-D-arabinofuranoside in order to determine the influence of the cyclic protecting group. Using TBAF deprotection, the silylene protecting group was removed to give compound **89** in 80% yield. Benzylation of compound **89** at the 3,5-*O* positions with NaH and benzyl bromide gave compound **90** in 83% yield. Finally, selective

deprotection of the napthylmethyl group in the presence of the benzyl groups and the thioether was done under hydrogenolytic conditions and gave the desired 3,5-*O*-di-benzyl-2-*O*-(2-hydroxymethyl) benzyl-1-thio-α-D-arabinofuranoside donor **91** in 92% yield (Scheme 59).

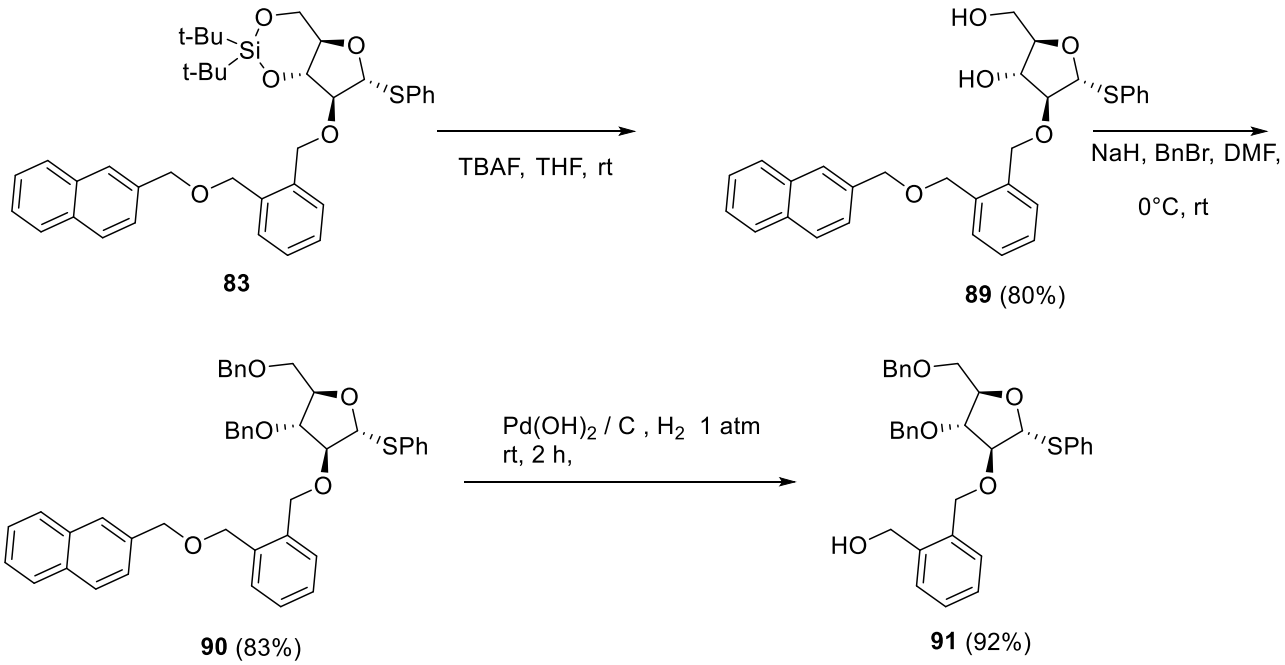

83

89 (80%)

90 (83%)

91 (92%)

Scheme **59**. Synthesis of phenyl 3,5-*O*-dibenzyl-2-*O*-(2-hydroxymethyl) benzyl-1-thio-α-D-arabinofuranoside

3.3.1 Clock cyclization reaction with donor 91

As described earlier for the 3,5-di-*tert*-butylsilylene protected compound **84**, the cyclization of compound **91** was initially conducted without external nucleophile using the protocol employed for the cyclization reaction of compound **84** and gave a single isomer **92** in 92% yield (Scheme 60). The anomeric configuration was assigned based on the ^{13}C chemical shift of (δC-1 = 102.3 ppm) and anomeric proton coupling ($^{3}J_{H1–H2}$ = 4.5 Hz) constant, which were consistent with the β-anomer.

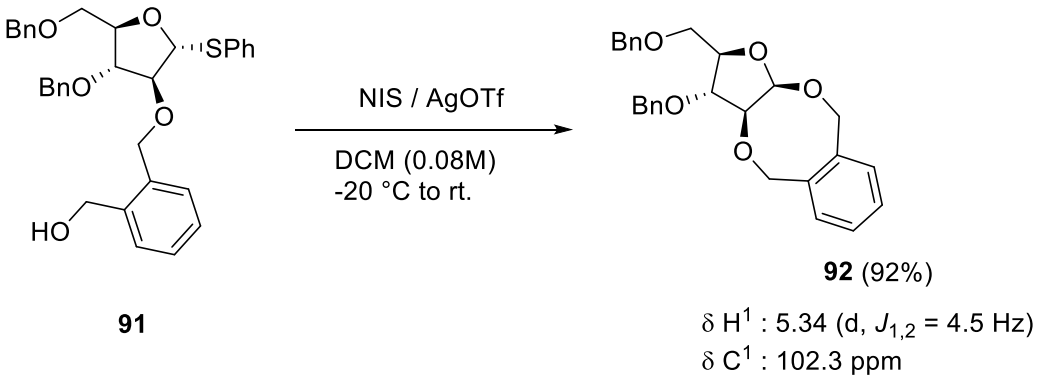

Scheme **60** The clock cyclization reaction in the 3,5-di-*O*-benzyl series

Again, the excellent stereoselectivity for the cyclic 3,5-dibenzylated compound **92** can be understood in terms of the preferential inside attack on the ^{3}E conformation of the oxocarbenium ion leading to the formation of 1,2-*cis* product (Scheme 61).

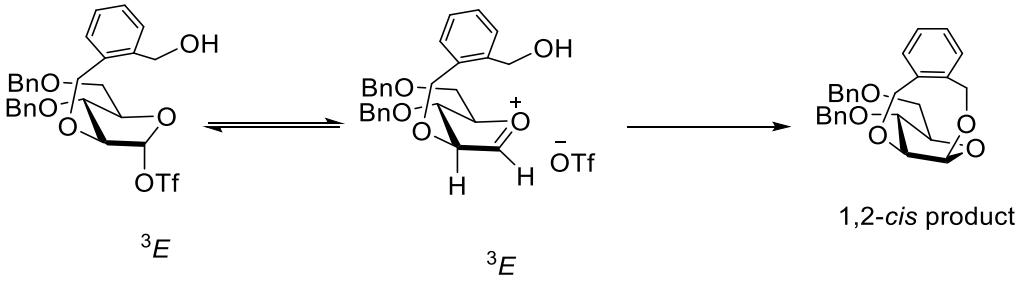

Scheme **61**. Model for the selectivity of the cyclization

3.3.2 *O*-Glycoside Synthesis

Due to the high rate of the cyclization reaction as a result of the internal hydroxyl nucleophilic arm,[90] synthesis and characterization of the *O*-glycosides was necessary prior to the competition reaction. Thus, the reaction was setup with a large excess of isopropanol resulting in a 1:1 mixture of two compounds with a combined yield of 91%. HPLC purification of the mixture gave **93** and **94** (Scheme 62). The differences in the chemical shifts of the anomeric carbons and the coupling constants for the two isomers were used to assign their configurations; (δC-1= 97.9

ppm. $^{3}J_{H1\text{-}H2}$ = 4.0 Hz) and δC-1= 103.7 ppm. $^{3}J_{H1\text{-}H2}$ = 1.4 Hz) are consistent with β-anomer (**94**) and α-anomer (**94**), respectively.

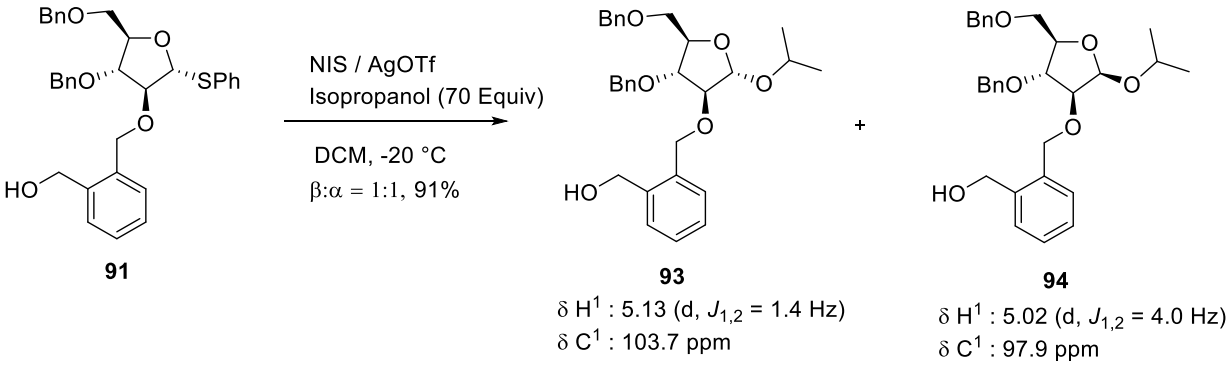

Scheme **62**. The synthesis and characterization of *O*-glycosides in the 3,5-di-*O*-benzyl arabinofuranoside series.

After the optimization of the glycosylation protocol, the competition kinetics were conducted in the same manner as for the 3,5-di-*tert*-butylsilane protected donor with analysis using HPLC and giving the ratios shown in Table **6**.

Table **6**. *O*-Glycoside formation in competition with cyclization reaction for the 3,5-dibenzyl protected donor **91**

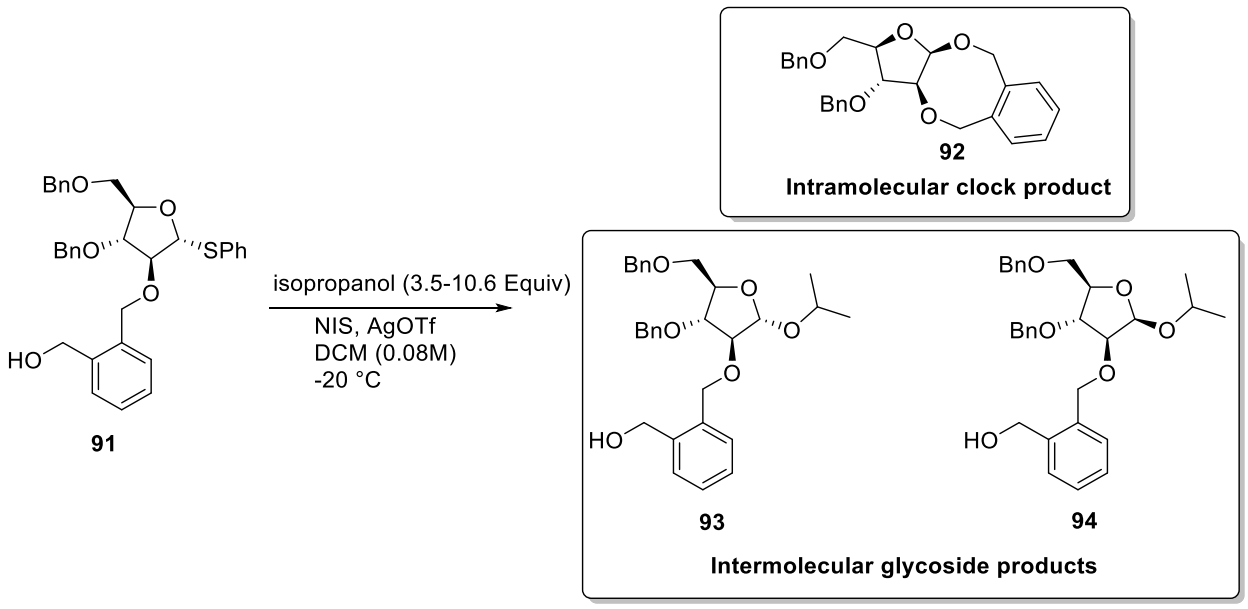

Entry	Equiv (M conc)	**α -gly/cycl** **93**/(**92**)[b]	**β-gly/cycl** **94**/(**92**)[b]
1[a]	0.130 (3.52)	0.055	0.066
2[a]	0.195 (5.28)	0.072	0.097
3[a]	0.260 (7.03)	0.079	0.108
4[a]	0.325(8.79)	0.111	0.139
5[a]	0.389(10.55)	0.120	0.166

a) Experimental conditions: NIS (2 equiv), AgOTf (0.5 equiv), at -20 °C; molecular sieves 4 Å;
b) Ratios were determined by HPLC/UV/MS

Graphical representation of the above data gives a clearer picture of the influence of concentration on the ratio of glycoside formation to cyclization (Figure 24).

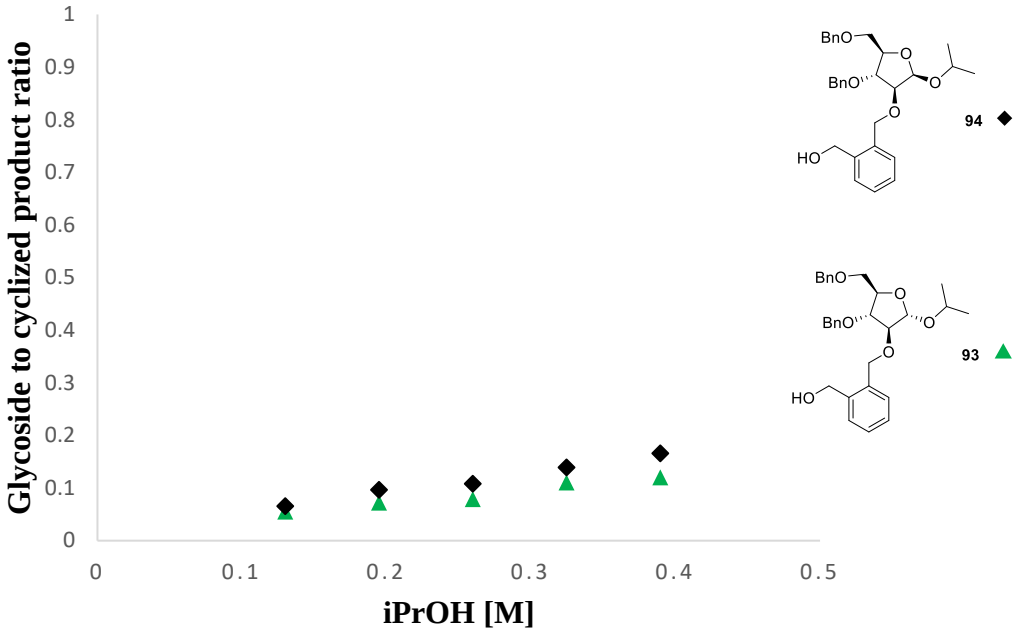

Figure **24**. Graphical representation of *O*-glycoside formation in competition with cyclization reaction in 3,5-dibenzyl protected arabinofuranosyl donor series.

Figure 24, reveals that the formation of both the β- and α-arabinosides **93** and **94** from **91** on coupling to isopropanol display essentially the same concentration dependence. This lack of selectivity may arise from diffusion-controlled unselective attack of the external nucleophile on either face of the oxocarbenium ion as explained by Woerpel.[125] Alternatively, an extension of the Lemieux hypothesis[12a] can be advanced in which two rapidly equilibrating anomeric triflates are displaced with comparable rates by the nucleophile. As the anomeric effect in the furanosides is minimal, the two triflates can be considered to have similar energies leading to comparable rates for the formation of the two anomeric products.

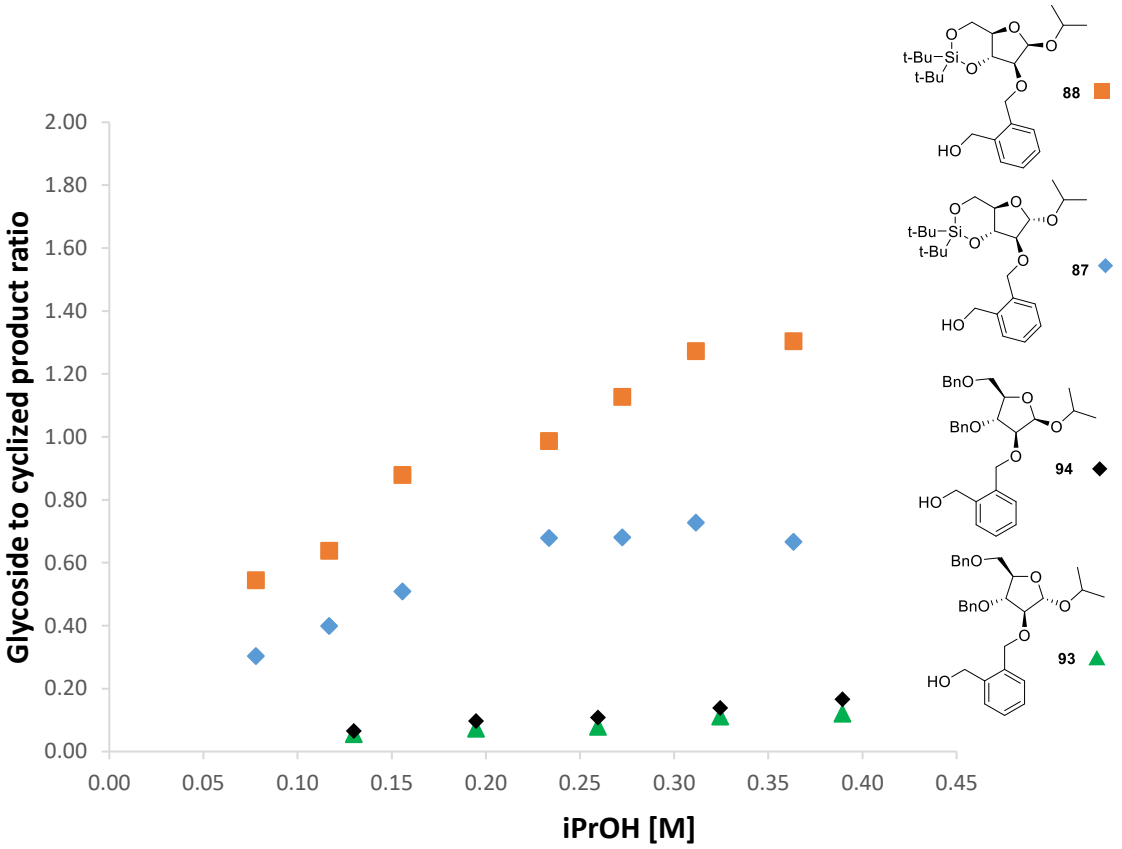

Figure **25**. Comparison of graphical representation of *O*-glycoside formation in competition with cyclization reaction in both 3,5-di-tert-butylsilylene donor and 3,5-dibenzyl donor series

Superimposition of the two graphs (Figures 22 and 24) in Figure 25 reveals a difference in the initial concentration of the external nucleophile. This suggests that trapping of the external nucleophile in the 3,5-dibenzyl protected arabinofuranoside series requires a higher concentration of acceptor alcohol than the cyclic 3,5-silylene protected arabinofuranoside series, thus indicating that the rate of cyclization in 3,5-dibenzyl series is much higher than that in the cyclic 3,5- silylene protected series. This difference in the rate of clock cyclization does not allow for the direct comparison of the concentration dependence in the formation of their respective *O*-glycosides in the two series. However, the graph does suggest that the formation of both α- and β-*O*-glycosides

in the 3,5-di-*O*-benzyl protected is via a more cation-like intermediate as shown by low of concentration dependence on the acceptor alcohol. The formation of β-arabinofuranosides in the 3,5-silylene acetals protected are more concentration dependent so closer to the S_N2 end of the spectrum.

3.4 Conclusions

The further development of the concept cation clock reactions for the determination of relative reaction kinetics in arabinofuranosylation has been demonstrated. The use of intramolecular hydroxyl groups as candidates for clock reactions has been shown, leading to the formation of cyclic clock products in both 3,5-*O*-di-*tert*-butylsilylene and 3,5-di-*O*-benzyl arabinofuranoside series. The study also revealed that, formation of the β-arabinofuranoside is more concentration dependent than the α-isomers in the 3,5-*O*-di-*tert*-butylsilylene protected donor. The unselective formation of formation of both, β and α-*O*-glycosides in the 3,5-di-*O*-benzyl protected arabinofuranosides can be understood in terms of a more of S_N1-like mechanism with a strong nucleophile. The high nucleophilicity of the internal hydroxyl group favors rapid formation of the cyclized product consequently only low ratios of the *O*-glycoside products are formed.

CHAPTER 4: USE OF THE CATION CLOCK METHOD TO DETERMINE THE INFLUENCE OF ACCEPTOR NUCLEOPHILICITY ON THE ARABINOFURANOSYLATION MECHANISM

4.1 Introduction

Glycosylation as described earlier is a complex substitution reaction that involves a donor (electrophile) and an acceptor (nucleophile) in the presence of a promoter and is characterized by the major challenge of low or unpredictable selectivity.[126] The influence of the reactivity of the donor on the stereochemical outcome and effect of the functional and protecting groups have been studied extensively.[127,128,129,130] However, the influence of the reactivity (nucleophilicity) of the acceptor on the glycosylation stereoselectivity remains poorly explored.[131,132]

Woerpel and co-workers in 2009[103] correlated the nucleophilicities and selectivities of several carbon nucleophiles and observed erosions in stereoselectivities with increasing nucleophilicity, which they attributed to rates of nucleophilic additions to oxocarbenium ion intermediates that approach the diffusion-controlled limit. They immediately followed up with another set of studies, using a set of alcohol acceptors and observed results which were consistent with the earlier ones.[125] Codée and co-workers, inspired by Woerpel's, work, conducted a systematic study of the influence of acceptor nucleophilicity on various glycopyranosyl donors; benzylidene-protected gluco- and mannopyranosyl donors and mannuronic acid donors with alcohols of varying nucleophilicity obtained from ethanol derivatives.[133,134,135] Their studies revealed that the stereochemical outcome of glycosylation depends on the acceptor nucleophilicity. The data for each of the three systems revealed that the more reactive alcohols were more β-selective than their less reactive counterparts.[133] The general interpretation of these results was in terms of the more reactive alcohols being capable of S_N2-like displacement of covalent glycosyl

triflates in contrast to their less nucleophilic counterparts, which follow a more S_N1-like mechanism. The other information revealed by their study was that for each of the three donors, the change from S_N2-like to S_N1-like mechanisms and selectivity occurred at a different point on the scale of alcohol nucleophilicity, consistent with the general pattern of stability of the glycosyl triflates. It is also noteworthy that there was little influence of acceptor nucleophilicity on the *O*-glycoside formation in the benzylidene-protected mannosides and mannuronic acid systems.[133]

The application of the cation clock method as a simple toolset for the distinctions between the mechanisms of α- and β-*O*-glycoside formation in manno and glucopyranoside systems,[87,136] and its successful application in the 3,5-arabinofuranoside system in Chapter 3, provide an excellent platform to extend the use of the cation clock method to determine the influence of acceptor nucleophilicity on the arabinofuranosylation mechanism. In this investigation, in addition to isopropanol, the use of fluorinated alcohols like 1,3-difluoroisopronanol and fluoroethanol in the in the kinetics study of arabinofuranosylation is presented (Figure 26).

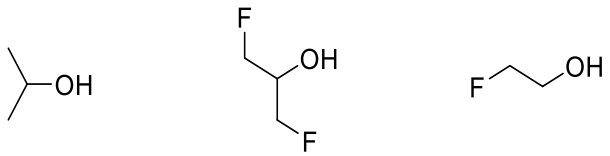

Figure **26**. Selected acceptors for the kinetics study.

4.2 Synthesis of 1,3-Difluoropropan-2-yl 3,5-*O*-(Di-*tert*-Butylsilylene)-2-*O*-((2-Hydroxymethyl) Benzyl)-1-Thio-D-Arabinofuranosides.

After the establishment of kinetics of arabinofuranosylation in the 3,5-*O*-di-*tert*-butylsilylene protected acetal **84** using isopropanol as the acceptor, the investigation was switched to the use of 1,3-difluoropropan-2-ol as external nucleophile. Again, the synthesis and characterization of the *O*-glycosides was necessary prior to the competition reaction. Therefore, the glycosylation reaction was setup with 1,3-difluoropropan-2-ol (72 equivs.) using the same protocol as for the synthesis of compounds **87** and **88** (isopropyl aglycon) to give compounds **95** and **96** in as 1:2.7 ratio with a combined yield of 56%. HPLC purification of the mixture gave samples of pure **95** and **96** (Figure 27). The characterization and the assignment of the configurations of both isomers were based on the differences in the chemical shifts of the anomeric carbons and the coupling constants. The values of δC-1= 99.9 ppm, $^{3}J_{H1\text{-}H2}$ = 4.0 Hz, and δC-1= 106.8 ppm. $^{3}J_{H1\text{-}H2}$ = 1.4 Hz are consistent with the β-anomer (**95**) and the α-anomer (**96**), respectively.

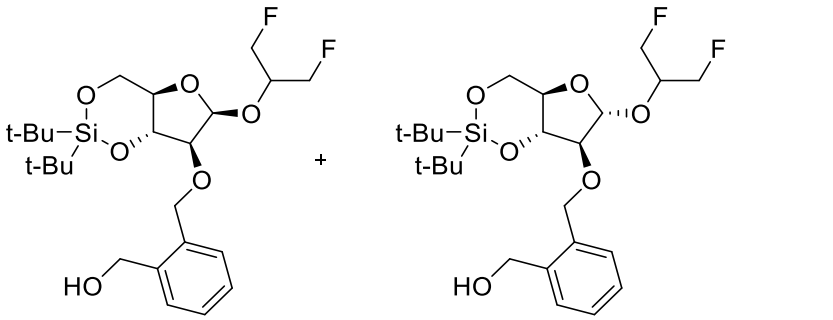

95

δ H^1 : 5.02 (d, $J_{1,2}$ = 5.1 Hz)
δ C^1 : 99.9 ppm

96

δ H^1 : 5.13 (d, $J_{1,2}$ = 3.2 Hz)
δ C^1 : 106.8 ppm

Figure **27**. 1,3-Difluoroisopropyl glycosides in the 3,5-di-*O*-*tert*-butylsilylene protected arabinofuranosyl system.

4.3 Competition Kinetics Using 1,3-Difluoroisopropanol as Acceptor in the 3,5-Di-*O*-*tert*-Butylsilylene Protected Arabinofuranosyl System

The initial stage of the kinetics study involved establishing the detection limit for the formation of both the α- and β-*O*-glycosides by HPLC. The use of 2.06 equivalents of 1,3-difluoroisopropanol was sufficient for the glycosides to be detected. Thus, after the optimization of the glycosylation protocol, the competition kinetics were conducted as previously described with the analysis HPLC leading to the ratios shown in Table **7**.

Table **7**. *O*-Glycoside formation in competition with cyclization reaction for the 3,5-di-*tert*-silylene protected donor **84** using 1,3-difluoroisopronol as acceptor.

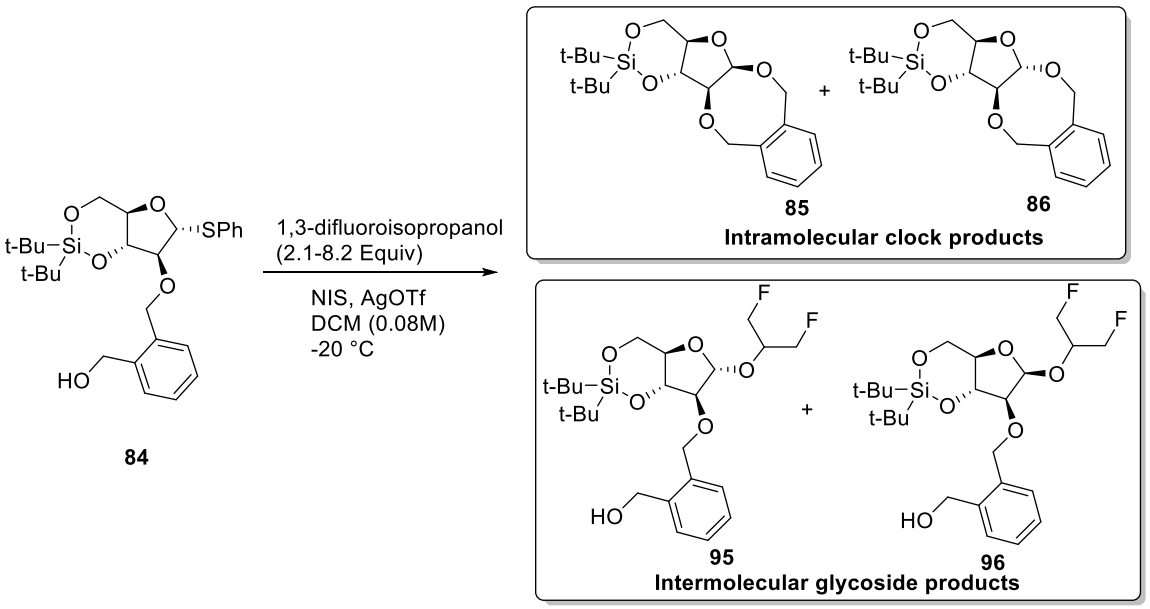

Entry	Equiv (M conc)	**α -gly/cycl** **95**/(**85** + **86**)[b]	**β-gly/cycl** **96**/(**85** + **86**)[b]
1[a]	0.076 (2.06)	0.020	0.052
2[a]	0.152 (4.11)	0.107	0.208
3[a]	0.190 (5.14)	0.156	0.312
4[a]	0.228 (6.17)	0.175	0.437
5[a]	0.266 (7.20)	0.184	0.467
6[a]	0.303 (8.22)	0.247	0.565

a) Experimental conditions: NIS (2 equiv), AgOTf (0.5 equiv), at -20 °C; molecular sieves 4 Å;
b) Ratios were determined by HPLC/UV/MS

The kinetics data in the above table was then represented graphically for clearer analysis (Figure 28).

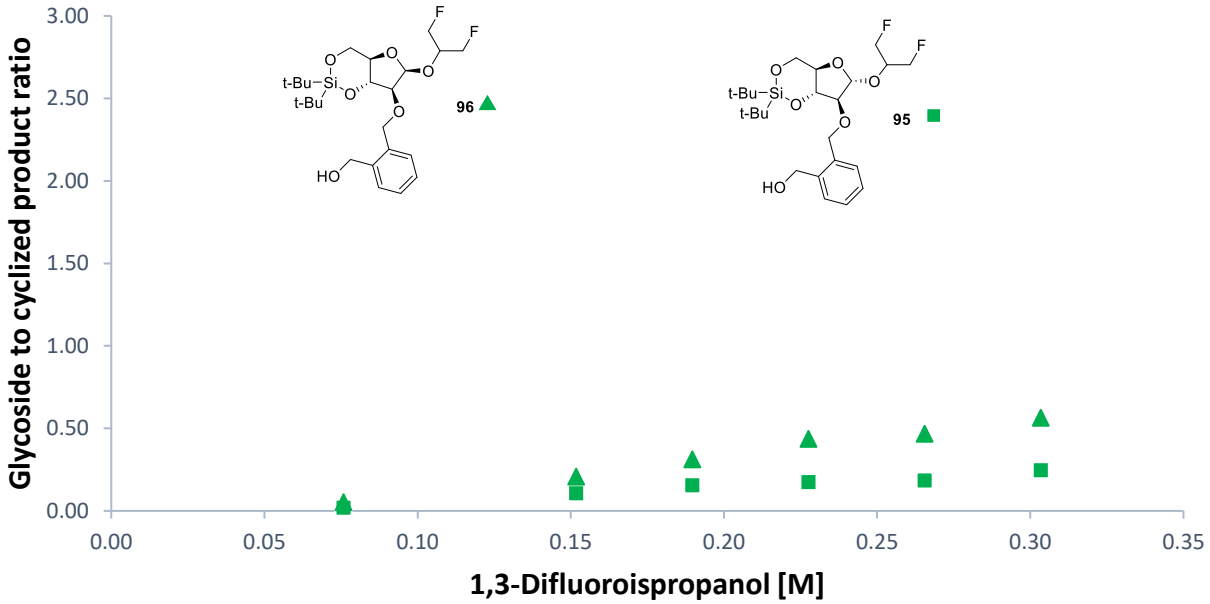

Figure **28**. Graphical representation of *O*-glycoside formation in competition with cyclization reaction in 3, 5-di-*tert*-butylsilylene protected arabinofuranosyl donor series using 1,3-difluoroisopronanol as the acceptor.

Figure 28, reveals that the formation of both the β- and α-arabinosides **95** and **96** from **84** on coupling to 1,3-difluoroisopropanol display essentially the same concentration dependence. Again, it shows lack of selectivity in the glycoside formation which may arise from diffusion-controlled unselective attack of the external nucleophile on either face of the oxocarbenium ion as explained by Woerpel.[125]

4.4 Competition Kinetics Using 2-Fluoroethenol as an Acceptor in the 3,5-Di-*O*-*tert*-Butylsilylene Protected Arabinofuranosyl System

The next investigation of the influence of the acceptor nucleophilic was done with fluoroethanol as acceptor. The synthesis of the *O*-glycoside compounds **97** and **98** from 3,5-*O*-di-*tert*-butylsilylene protected acetal **84** was conducted following the same similar used protocol used

for the synthesis of 1,3-difluoroispropyl glycosides **95** and **97** (Figure 28), to give the desired compounds in 20% and 52% yield respectively (Figure 31). The assignment of the anomeric configuration showed the data for **97** (δC-1= 106.8 ppm. $^{3}J_{H1\text{-}H2}$ = 3.2 Hz) consistent with α-anomer, while compound **98** (δC-1= 100.1 ppm. $^{3}J_{H1\text{-}H2}$ = 5.3 Hz) was assigned as β-anomer.

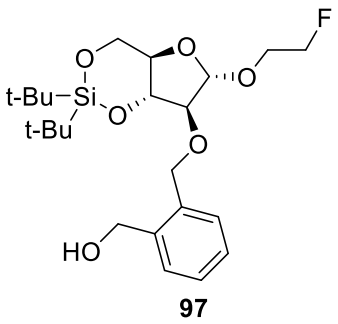

97

δ H^1 : 5.13 (d, $J_{1,2}$ = 3.2 Hz)
δ C^1 : 106.8 ppm

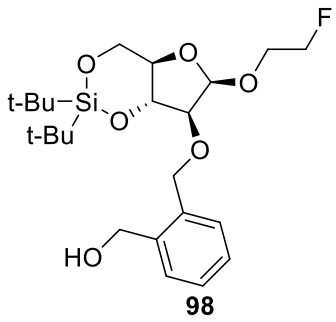

98

δ H^1 : 5.02 (d, $J_{1,2}$ = 5.3 Hz)
δ C^1 : 100.1 ppm

Figure **29**. 2-Fluoroethanol glycosides in the 3,5-di-*O*-*tert*-butylsilylene protected arabinofuranosyl system

A series of competition kinetics were conducted in the same manner as for the 3,5-*O*-di-*tert*-butylsilylene protected donor **84** in the isopropanol case**.** HPLC analysis of the crude samples gave ratios as shown in Table **8**.

Table **8**. *O*-Glycoside formation in competition with cyclization reaction for the 3,5-di-*tert*-butylsilylene protected donor **84** using 2-fluoroethanol acceptor.

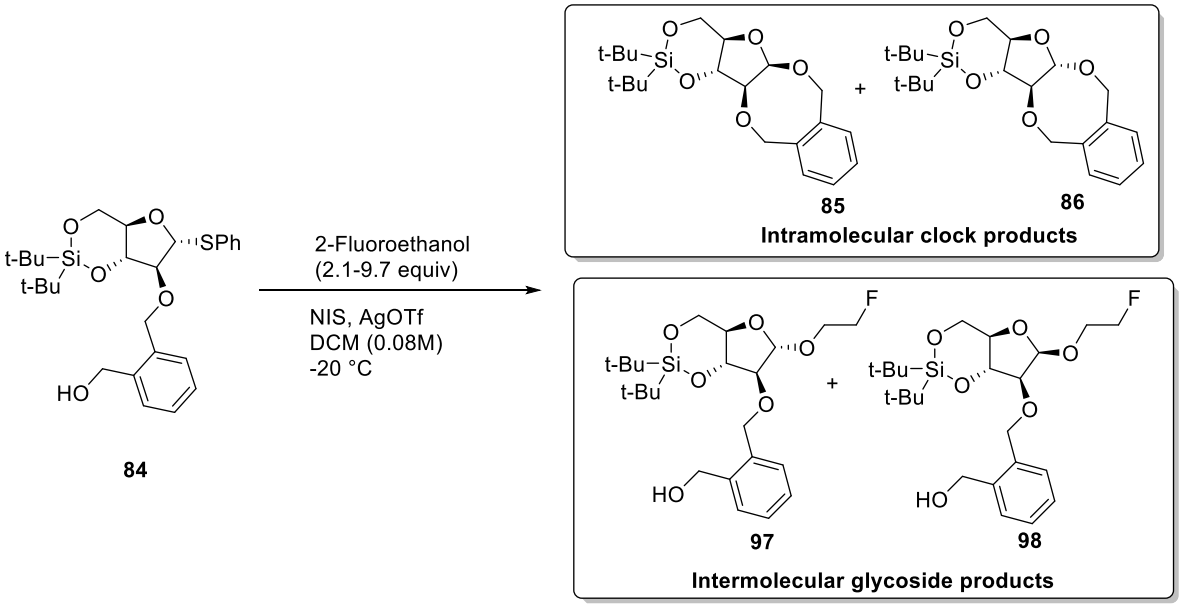

Entry	Equiv (M conc)	**α -gly/cycl** **97**/(**85** + **86**)[b]	**β-gly/cycl** **98**/(**85** + **86**)[b]
1[a]	0.077 (2.08)	0.325	0.708
2[a]	0.119 (3.22)	0.470	0.767
3[a]	0.170 (4.61)	0.466	0.820
4[a]	0.221 (5.99)	0.598	1.084
5[a]	0.272 (7.38)	0.820	1.298
6[a]	0.323 (8.76)	0.854	1.409
7[a]	0.357 (9.68)	0.861	1.453

a) Experimental conditions: NIS (2 equiv), AgOTf (0.5 equiv), at -20 °C; molecular sieves 4 Å;
b) Ratios were determined by HPLC/UV/MS

Graphical representation of the above kinetics data as shown in Figure 32, gives a clear picture of the influence concentration of 2-fluoroethanol on the ration of the glycosides formed.

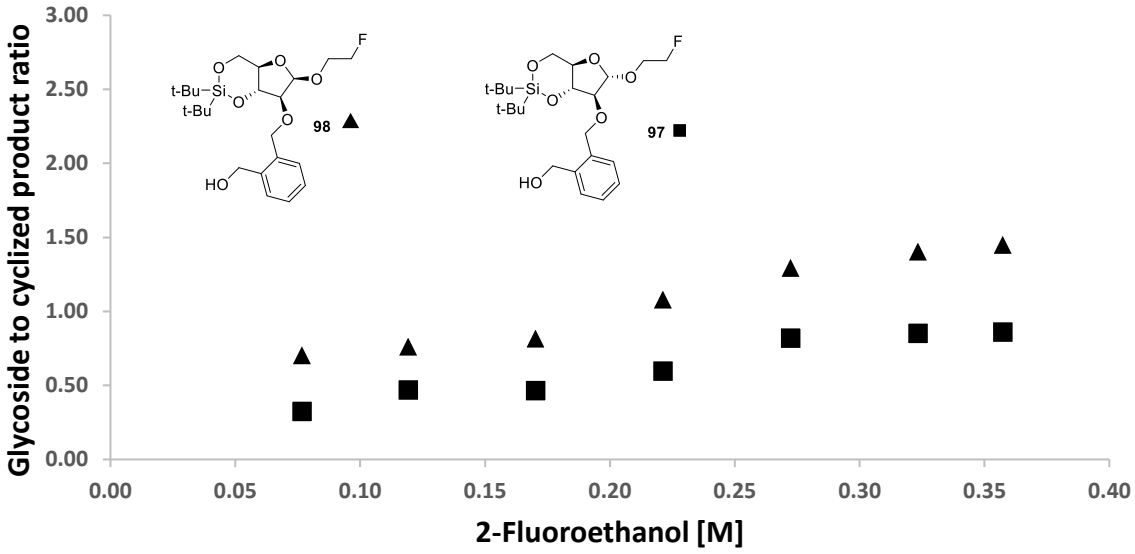

Figure **30**. Graphical representation of *O*-glycoside formation in competition with cyclization reaction in 3,5-di-*tert*-butylsilylene protected arabinofuranosyl donor series using 2-fluoroethanol as the acceptor.

The above Figure 30, indicates an essentially similar trend of concentration dependence of acceptor alcohol in the formation of both β- and α-anomers. However, the formation of β-arabinosides is marginally more concentration dependence, suggesting that β-glycosylation is a little closer to S_N2 end of the mechanistic spectrum than the formation of α-arabinofuranosides.

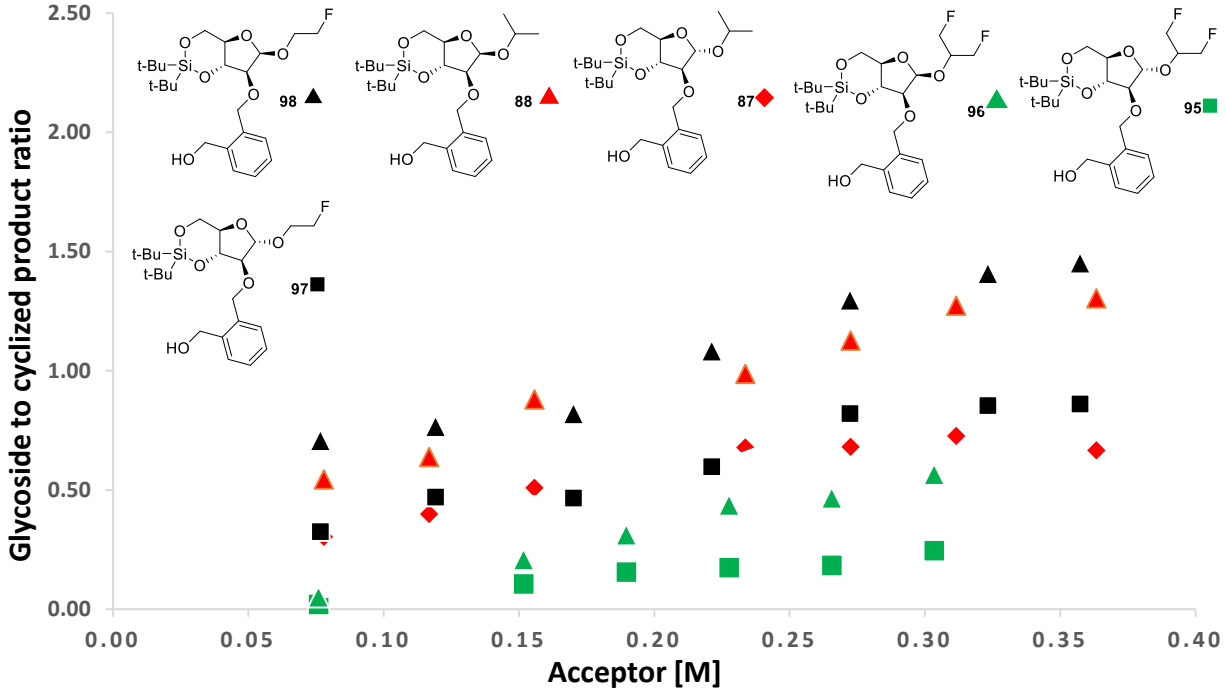

Figure **31**. The influence of acceptor nucleophilicity on arabinofuranosylation mechanism

In the Figure 32, the concentration dependence of 3,5-di-*tert*-butylsilylene protected arabinofuranosylation is shown for each of the three alcohols studied; isopropyl alcohol, 1,3-difluoroisppropanol, and 2-fluoroethanol. The greatest concentration dependence is seen with primary alcohol 2-fluoroethanol. This is followed by secondary alcohol (isopropanol) and finally 1,3-difluoro-2-propanol. This trend is consistent with the least sterically hindered alcohol exhibiting the greatest reactivity. For the two secondary alcohols with very similar steric environments, the installation of the electron with drawing groups reduces the reactivity. This overall pattern is consistent with a loose S_N2-like mechanism for glycosylation. As the acceptor becomes less active due to steric hindrance and the electron withdrawing nature of the substituents the transition becomes looser and moves closer to the S_N1 end of the spectrum. The very similar

concentration dependence seen for both anomers of any of the three glycosylation suggests the involving a pair of rapidly equilibration glycosyl triflates both with very similar reactivity.

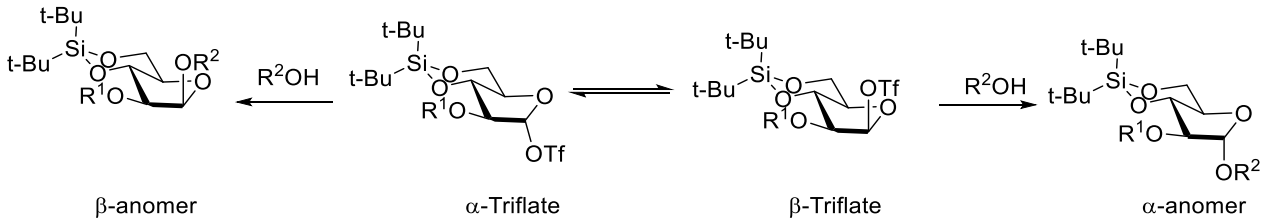

Scheme **63**. The formation of both β- and α-glycosides due to rapidly equilibrating arabinofuranosyl triflates.

4.5 Conclusions

The cation clock method has once again been demonstrated to be a good tool for the probing of glycosylation mechanisms. In this instance, through the use of acceptors of varying nucleophilicity, it was found that 3,5-di-*tert*-butylsilylene protected arabinofuranosylation is likely to occur vial a loose S_N2 mechanism from each of the two rapidly equilibrating glycosyl triflates.

CHAPTER 5: HYDROGENOLYTIC CLEAVAGE OF NAPHTHYLMETHYL ETHERS IN THE PRESENCE OF SULFIDES

5.1 Introduction

The significance of protecting groups in synthetic organic chemistry cannot be underestimated.[137] Benzyl-type ethers are very widely employed as temporary protecting groups in organic chemistry and carbohydrate chemistry and are typically removed by hydrogenolysis at the end of a synthetic sequence.[138,139] However, the major problem in the catalytic hydrogenolysis of benzyl ethers is catalyst poisoning, which can occur when the substrate contains thioethers.[139] Such problems, which frequently go unreported, are widespread and are typically solved by the use of large amount of catalyst.[140,141] This leads to the use of the far less convenient reductive cleavage of benzyl ethers with sodium in liquid ammonia as reported for example by Crich and coworkers.[141]

2-Naphthylmethyl ethers have enjoyed widespread use in carbohydrate chemistry as substitutes for *p*-methoxybenzyl (PMB) ethers since their introduction to the field by Matta,[142] because of their greater stability to Brønsted acids but comparable ease of removal under oxidative condition with dichlorodicyanoquinone (DDQ).[142,143] Spencer and co-workers confirmed[144] Matta's findings and even went further to selectively remove both PMB and Nap using ceric ammonium nitrate (CAN) and DDQ respectively.[144] In 2015, Codée and coworkers also selectively cleaved both Nap and PMB in presence of benzyl ethers in hexafluoro-2-propanol (HFIP).[145] In 2017, Bennett and co-workers improved the conditions of oxidative cleavage.[146] However, oxidative cleavage is not compatible with acid labile functionalities. Therefore, Spencer's initial report of selective hydrogenolytic removal of Nap ethers in presence of benzyl ethers (Scheme 64),[118] and the further work on the selective hydrogenolysis of benzyl carbamates (Scheme 65),[147]

suggested the possibly of their use in place of benzyl ethers for hydrogenolytic cleavage in the presence of sulfides.

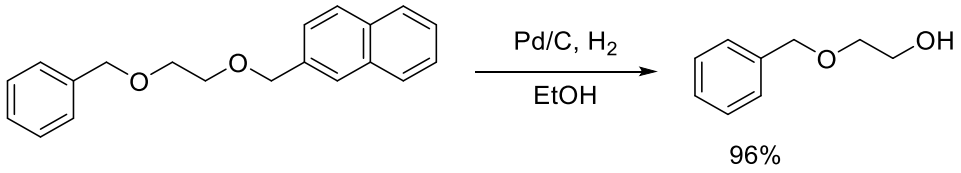

Scheme **64.** Selective hydrogenolysis of a naphthylmethyl ether in presence of a benzyl ether

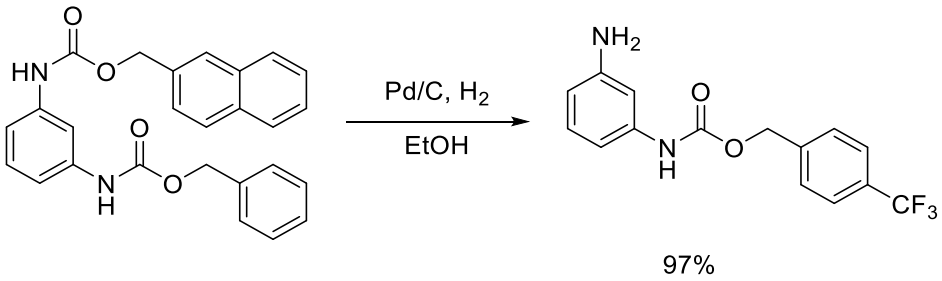

Scheme **65**. Selective hydrogenolytic cleavage of a naphthylmethyl carbamate in presence of a benzyl carbamate.

The selective hydogenolytic cleavage of the naphthymethyl protecting group in the synthesis of a 3,5-*O*-di-*tert*-butylsilylene protected arabinofuranoside donor **83** (Scheme 66) to give compound **84**, which was reported in Chapter 3, provided a clear evidence of selective deprotection and inspired the further explorations reported in this chapter.

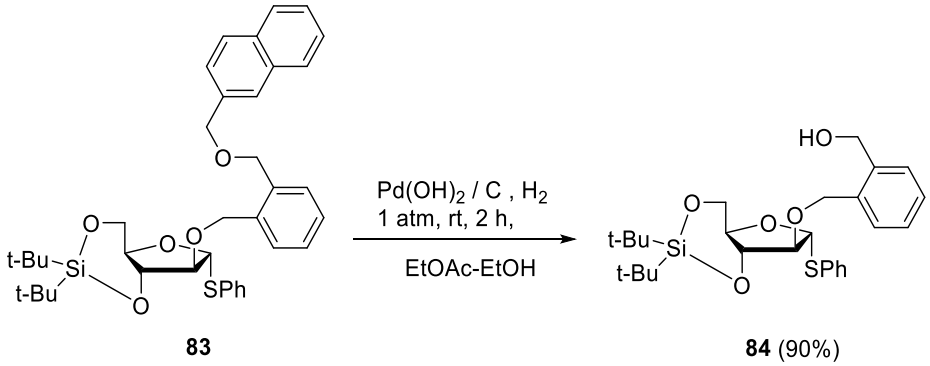

Scheme **66**. Hydogenolytic cleavage of the naphthymethyl ether in presence of benzyl ether and phenyl thioether.

Accordingly, in this chapter, we report the synthesis of a series of compounds containing benzyl and Nap ethers together with either thioethers or thioglycosides and further demonstrate that indeed the Nap ethers are removed selectively under these conditions.

5.2 Chemistry

5.2.1 Synthesis and Hydrogenolytic Cleavage of Naphthylmethyl Ethers in Aliphatic Model Substrates

The synthesis of the aliphatic thioether substrate, 2-(2-naphthalen-2-ylmethoxy)ethyl-2-(benzyloxy)ethyl) sulfide began with the selective protection of one hydroxyl group of 2,2-thiodiglycol by naphthylmethyl bromide as described for the monoprotection of 1,2-benzene dimethanol (Chapter 3), to give the desired monoprotected compound **99** in 75% yield. This was followed by the installation of the benzyl protecting group on the remaining hydroxyl functionality to give desired compound **100** in 81% yield (Scheme 67).

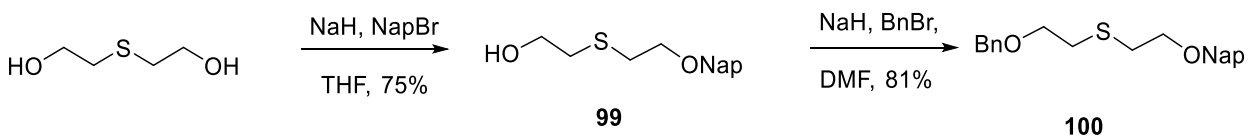

Scheme **67**. Model aliphatic substrate synthesis

Hydrogenolysis of the model aliphatic compound over palladium hydroxide on carbon in ethanolic ethyl acetate under the 3 atmospheres of hydrogen successfully cleaved the naphthylmethyl ether in 72% yield (Scheme 68).

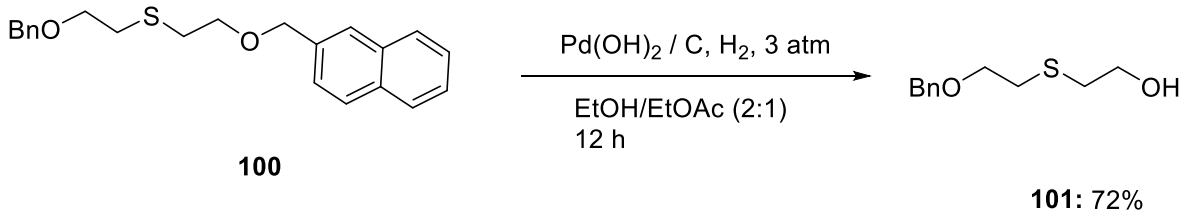

Scheme **68**. Hydrogenolytic cleavage of aliphatic a naphthylmethyl ether in presence of a sulfide.

5.2.2 Synthesis and Hydrogenolytic Cleavage of Napthylmethyl Ethers in Thiomannoside Substrates

Investigation of the selective hydrogenolysis turned to the thiomomannosides, and began by the regioselective ring opening of phenyl 4,6-*O*-benzylidene-2,3-di-*O*-benzyl-D-mannopyranoside **102**[141] using BH_3•THF in the presence of a catalytic amount of yttrium trifluoromethanesulfonate to give the corresponding 6-alcohol, *O*-benzyl ether **103**[148] in 87% yield. The installation of the naphthylmethyl ether under basic conditions gave compound **104**[149] in 77% yield.

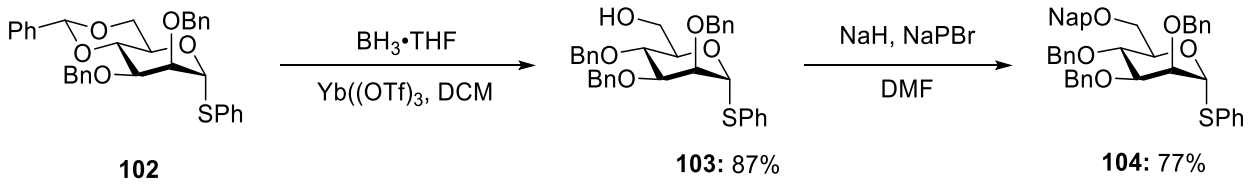

Scheme **69**. Synthesis of phenyl 2, 3, 4-tri-*O*-benzyl-6-*O*-(2-naphthyl)methyl-1-thio-α-D-mannopyranoside

Next, a further thiomomannoside substrate was synthesized from compound **105**.[150] Deprotection of the benzylidene acetal with tosic acid gave compound **106** in 89% yield. Treatment with benzyl bromide and sodium hydride gave the desired compound **107** in 88% yield (Scheme 69).

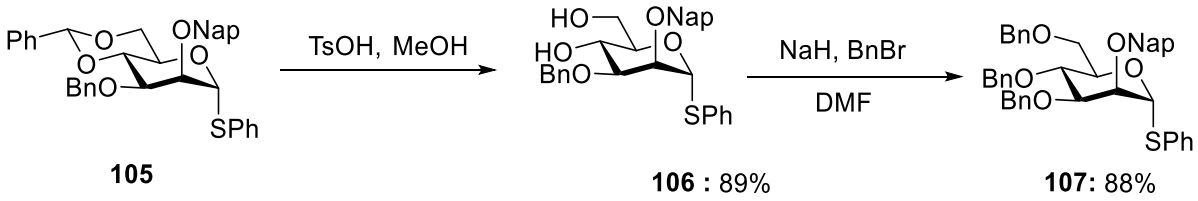

105 **106 :** 89% **107:** 88%

Scheme **70**. Synthesis of phenyl 3, 4, 6-tri-*O*-benzyl-2-*O*-(2-naphthyl)methyl-1-thio-α-D-mannopyranoside

The failed global removal of benzyl ethers in compound **108**[141] with sodium in liquid ammonia presented a further an opportunity for the application of the naphthylmethyl ether in substrate **111**. The synthesis followed the regioselective deprotection described earlier to give compound **110** in 94% yield. Naphthylmethyl ether installation completed the synthesis in 72% yield (Scheme 71).

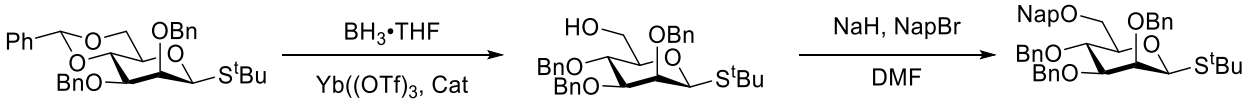

108 **110 :** 94% **111:** 72%

Scheme **71**. *tert*-Butyl 2,3,4-tri-*O*-benzyl-6-*O*-(2-naphthyl)methyl-1-thio-β-D-mannopyranoside

The hydrogenolytic cleavage of the naphylmethyl group in the three substrates, **106**, **109** and **113** is presented in Table **9**.

Table **9**. Hydrogenolytic cleavage of napthylmethyl ethers in thiomannoside systems

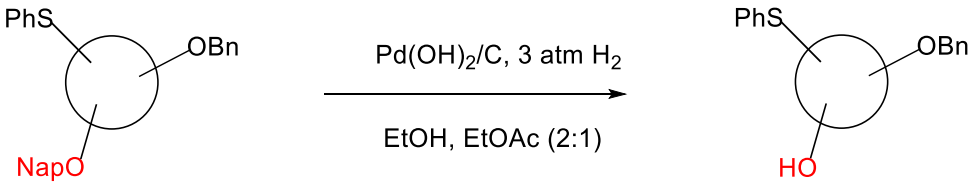

Entry	Substrate	Product	Time (h)	% Yield
1	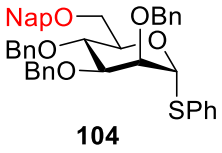 **104**	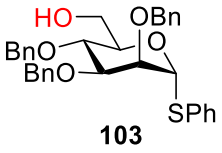 **103**	2	92
2	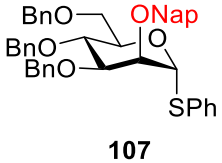 **107**	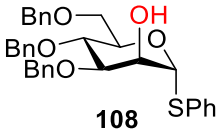 **108**	16	65
3	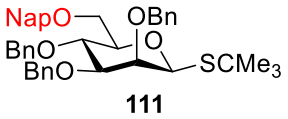 **111**	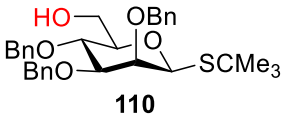 **110**	3	89

From Table **9**, it is evident that selective deprotection of naphylmethyl ethers in the primary substrate is much faster than that of the secondary naphthylmethyl ethers. This can be understood in terms reduced steric interactions in the primary substrates and increased catalytic access.

5.2.3 Synthesis and Hydrogenolytic Cleavage of Naphthylmethyl Ethers in Thioglucoside Substrates

After successful hydrogenolysis of the mannosyl substrates, we turned to the glucosyl substrates. Selective deprotection of benzylidene protected glucoside **112** gave the 6-hydroxyl compound **113** and the 4-hydroxyl compound **115**, respectively. Treatment of both compounds,

with naphthylmethyl bromide and sodium hydride gave desired the products **114** and **116,** respectively (Scheme 72).

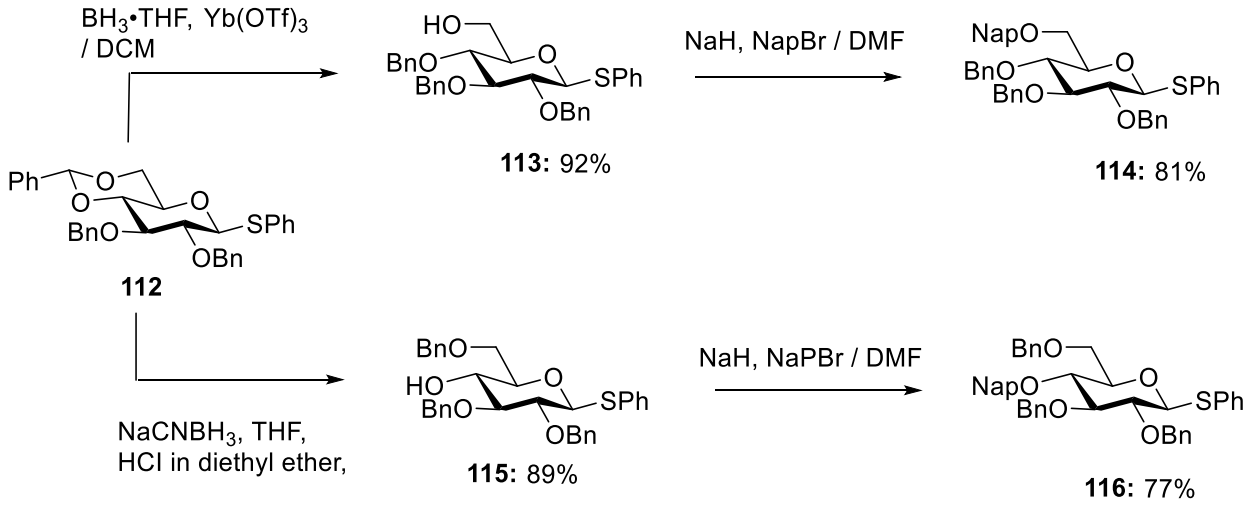

Scheme **72**. Synthesis of naphthylmethyl and benzyl ethers containing thioglucosides **116** and **118.**

Glucosides **114** and **116** were separately subjected to hydrogenolysis conditions to give selective cleavage products **113** and **115** in 88% and 70% yields (Scheme 73). Again, the primary naphthymethyl ether was cleaved more readily than the secondary one. Closer inspection of both the gluco- and mannosyl systems reveals that the cleavage of the naphthylmethyl protecting group is independent of the nature, axial or equatorial, of the phenyl thioglycosides.

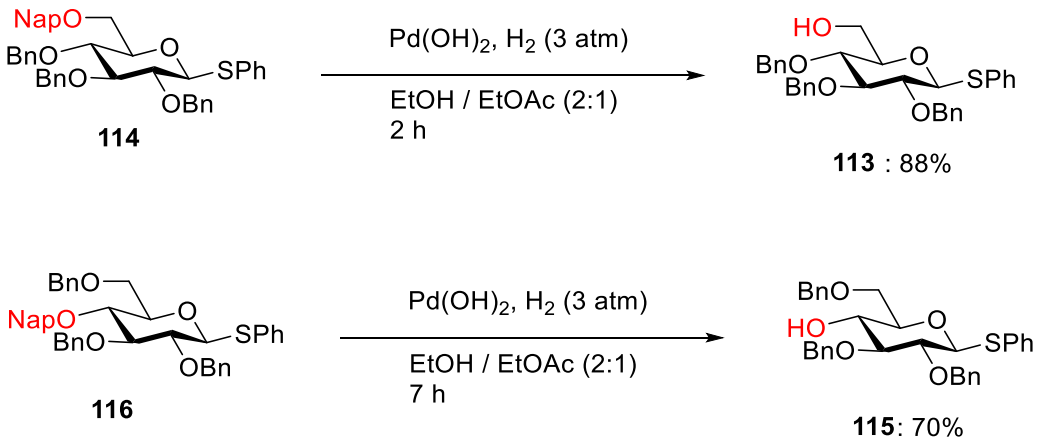

Scheme **73**. Hydrogenolytic cleavage of napthylmethyl ethers in thioglucosides

5.2.4 Synthesis and Hydrogenolytic Cleavage of Naphthylmethyl Ethers in Peptides

The investigation of the selective hydrogenolysis of naphthylmethyl in presence of sulfides was extended to peptides. We began the peptide synthesis by naphthylmethyl installation on *N*-Boc-protected serine **117**, followed by esterification using methyl iodide with potassium carbonate to give desired compound **118** in 60% yield in two steps. Boc-removal with trifluoroacetic acid gave the intermediate **119**, which was coupled with *N*-Boc-*O*-benzyl-L serine **120** using HATU to give dipeptide **121** in 69%. The introduction of the sulfide functionality was achieved by the deprotection of Boc group with trifluoracetic acid and gave the dipeptide **122,** which was again coupled with *N*-Boc-methionine **123** to give the expected tripeptide **124** in 70% yield (Scheme 74).

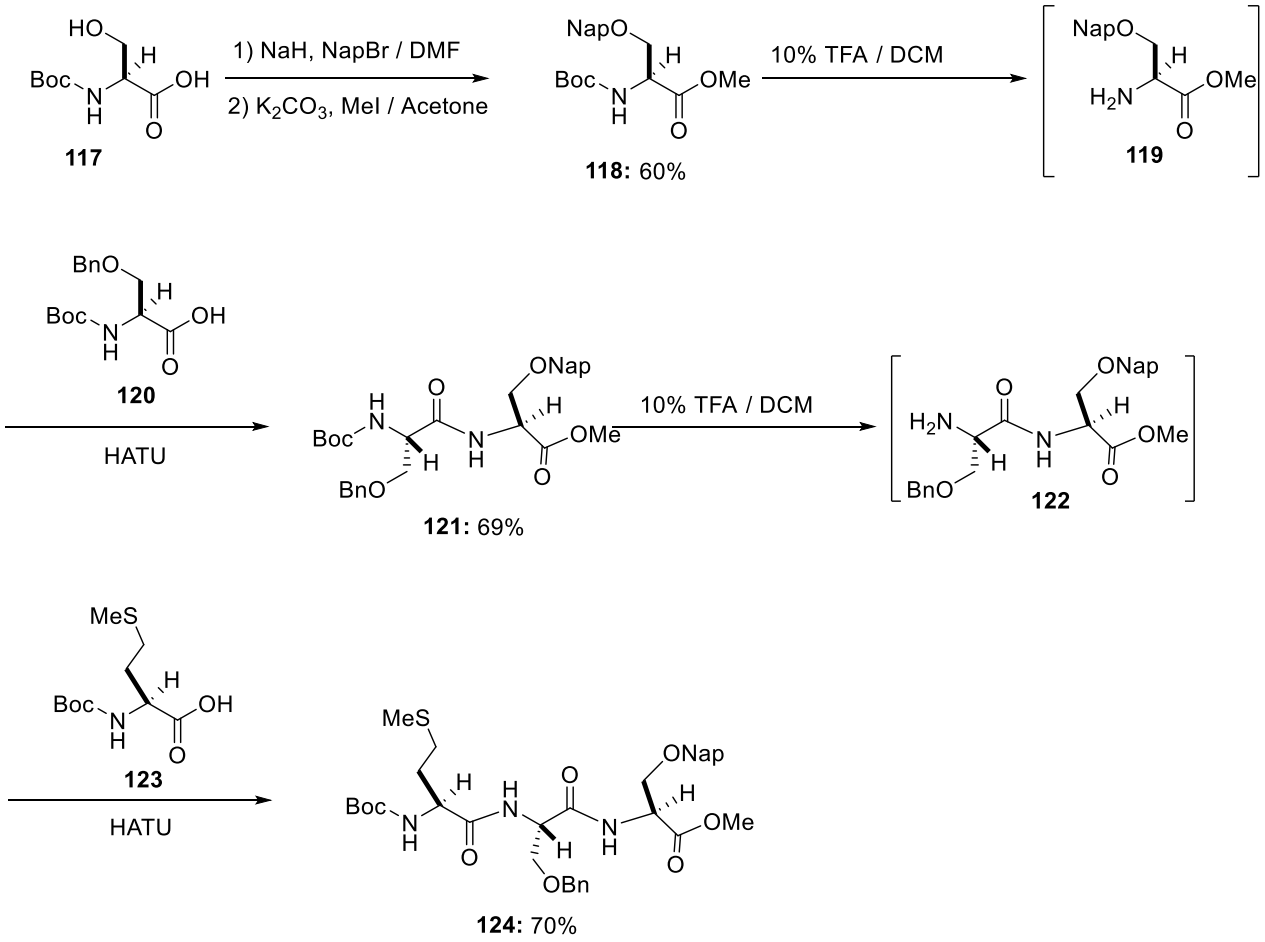

Scheme **74**. Synthesis of the naphthylmethyl and benzyl containing tripeptide **124**.

With the tripeptide in hand, the hydrogenolytic cleavage of naphthylmethyl ether was set up. After 7 h, the reaction was complete and gave compound **125** in 82% yield (Scheme 75).

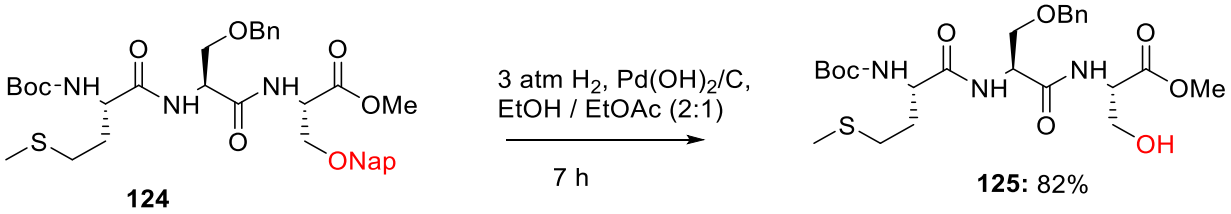

Scheme **75**. Hydrogenolytic cleavage of napthylmethyl ethers peptides.

5.3 Conclusions

This chapter demonstrates with aid of a series of model thioethers or thioglycosides protected with combinations of benzyl ethers and 2-naphthylmethyl ethers, that the latter are readily cleaved selectively under hydrogenolytic conditions in the presence of the frequently catalyst-poisoning sulfides. These results therefore, suggest the possibility of using 2-naphthylmethyl ethers in place of benzyl ethers in synthetic schemes whenever hydrogenolytic deprotection is anticipated in the presence of thioether type functionality.

CHAPTER 6: EXPERIMENTAL SECTION

General

All experimental were carried out under atmosphere of argon unless otherwise specified. all extracts were dried over sodium sulfate, filtered, and evaporated under reduced pressure at room temperature. Unless otherwise stated column chromatography was carried out over silica gel. Specific optical rotations were measured on an automatic polarimeter with a path length of 10 cm. High-resolution (HRMS) electrospray (ESI-TOF) mass spectra were recorded using a Micromass LCT instrument. UHPLC analysis was performed with a BEH C18 1.7 µm (2.1 × 50 mm) equipped with mass and a UV detector. Extracts were dried over anhydrous sodium sulfate and chromatography was carried out over silica gel. Specific rotations were measured on an automatic polarimeter with a path length of 10 cm in chloroform solution unless otherwise stated. High-resolution (HRMS) mass spectra were recorded in the electrospray mode using a time of flight mass analyzer (ESI-TOF)

2-Phenylthioethyl 2,3,4,6-tetra-*O*-acetyl-α-D-mannopyranoside (46). A solution of α-D-mannopyranose 1,2,3,4,6-pentaacetate (10 g, 25.64 mmol) and 2-(phenylthio)ethanol (4.74 g, 30.7 mmol, 4.15 mL) in dry CH_2Cl_2 (100 mL) was treated slowly with BF_3•Et_2O (9.66 mL, 76.92 mmol) at 0 °C and stirred at room temperature for 20 h. The reaction mixture was cooled to 0 °C and slowly quenched with trimethylamine (15 mL) before being allowed to stir at room temperature for 30 minutes. The reaction mixture was diluted with CH_2Cl_2 (200 mL), and washed with saturated $NaHCO_3$, water and brine, dried and filtered. The filtrate was evaporated and the residue was subjected to flash chromatography (hexane: ethyl acetate, 2:1) to give **46** (12.4 g, 62%) as a colorless gel. $[\alpha]^{RT}_{D}$ = +45 (*c* 1.27, $CHCl_3$); ^{1}H NMR (600 MHz, $CDCl_3$) δ 7.37 – 7.33 (m, 2H), 7.30 – 7.26 (m, 2H), 7.21 – 7.16 (m, 1H), 5.27 (dd, *J* = 10.0, 3.3 Hz, 1H), 5.23 (t, *J* = 10.0

Hz, 1H), 5.20 (dd, *J* = 3.2, 1.8 Hz, 1H), 4.79 (d, *J* = 1.8 Hz, 1H), 4.22 (dd, *J* = 12.2, 5.3 Hz, 1H), 4.03 (dd, *J* = 12.2, 2.4 Hz, 1H), 4.02 – 3.98 (m, 1H), 3.82 (dt, *J* = 10.3, 7.0 Hz, 1H), 3.72 – 3.67 (m, 1H), 3.15 – 3.12 (m, 2H), 2.13 (s, 3H), 2.04 (s, 3H), 2.03 (s, 3H), 1.97 (s, 3H). ^{13}C NMR (150 MHz, $CDCl_3$) δ 170.6, 169.9, 169.7, 169.6, 135.3, 129.5, 129.0, 126.4, 97.6, 69.4, 68.9, 68.6, 67.3, 65.9, 62.3, 32.9, 20.8, 20.7, 20.6. ESIHRMS calcd for $C_{22}H_{28}O_{10}SNa$ $[M + Na]^+$, 507.1301; found; 507.1303.

2-Phenylthioethyl α-D-mannopyranoside (47). Compound **46** (200 mg, 0.413 mmol) was dissolved in NaOMe–MeOH (8 mL, 0.05 M,) and stirred for 45 min at room temperature and then neutralized using Amberlyst IR-120 hydrogen form. The reaction mixture was filtered, concentrated and chromatographed (CH_2Cl_2: MeOH 5:1) to give **46** as a colorless form (121 mg, 93%). $[\alpha]^{RT}_D$ +58 (*c* 0.93, $CHCl_3$); ^{1}H NMR (600 MHz, $CDCl_3$) δ 7.25 – 7.22 (m, 2H), 7.19 – 7.15 (m, 2H), 7.10 – 7.06 (m, 1H), 4.75 (d, *J* = 1.6 Hz, 1H), 3.85 (dd, *J* = 3.2, 1.6 Hz, 1H), 3.81 (dd, *J* = 12.4, 3.0 Hz, 1H), 3.77 (t, *J* = 9.5 Hz, 1H), 3.74 – 3.69 (m, 2H), 3.63 (dd, *J* = 12.4, 2.2 Hz, 1H), 3.55 – 3.44 (m, 2H), 2.99 (t, *J* = 6.7 Hz, 2H). ^{13}C NMR (150 MHz, $CDCl_3$) δ 135.5, 129.1, 129.0, 126.20, 100.0, 72.50, 71.0, 70.4, 66.0, 65.9, 60.5, 32.8. ESIHRMS calcd for $C_{14}H_{20}O_6SNa$ $[M + Na]^+$, 339.0878; found; 339.0879.

2-Phenylthioethyl 4,6-*O*-benzylidene-α-D-mannopyranoside (48). To a suspension of **47** (2.1 g, 6.64 mmol) in acetonitrile (21 mL) was added CSA (0.3 g, 1.33 mmol) and benzaldehyde dimethyl acetal (1.09 mL, 7.31 mmol) at room temperature. A white precipitate formed during the addition of the reagent. After 2 h the reaction mixture was quenched with triethylamine (2 mL), diluted with an ethyl acetate: water mixture (3:1, 50 mL), and extracted with ethyl acetate. The combined organic layers were washed with brine, dried, filtered and concentrated. The crude product was purified by chromatography (hexane: ethyl acetate 1:2) to give **48** as colorless oil

(1.74 g, 65%). $[\alpha]^{RT}_D$ +40.4 (*c* 1.00, $CHCl_3$); ^1H NMR (600 MHz, $CDCl_3$) δ 7.50 – 7.47 (m, 2H), 7.41 – 7.33 (m, 5H), 7.28 (m, 2H), 7.22 – 7.16 (m, 1H), 5.54 (s, 1H), 4.82 (d, *J* = 1.3 Hz, 1H), 4.17 (dd, *J* = 9.9, 4.4 Hz, 1H), 4.02 – 3.95 (m, 2H), 3.91 – 3.81 (m, 3H), 3.77 (t, *J* = 10.2 Hz, 1H), 3.64 (dt, *J* = 10.3, 6.6 Hz, 1H), 3.12 (t, *J* = 6.6 Hz, 2H). ^{13}C NMR (150 MHz, $CDCl_3$) δ 137.1, 135.5, 134.4, 129.7, 129.5, 129.43, 129.2, 129.0, 128.3, 126.3, 126.3, 126.2, 102.2, 100.1, 78.7, 70.7, 68.7, 68.5, 66.5, 63.1, 33.2. ESIHRMS calcd for $C_{21}H_{24}O_6SNa$ $[M + Na]^+$, 427.1191; found 427.1198.

2-Phenylthioethyl 3-*O*-benzyl 4,6-*O*-benzylidene-α-D-mannopyranoside (49). A mixture of compound **48** (1.66 g 4.12 mmol) and Bu_2SnO (1.08 g, 4.33 mmol) in toluene (17 mL) was heated at 110 °C for 3 h. The solvent was removed under reduced pressure to obtain the stannylene acetal which was kept under high vacuum for 2 h, then was dissolved in DMF (17 mL), and treated with cesium fluoride (0.66 g, 4.33 mmol) and finally slowly with benzyl bromide (0.53 mL, 4.45 mmol) under an argon atmosphere. The reaction mixture was stirred for 6 h then was quenched by addition of trimethylamine (1 mL), concentrated and the residue was purified by chromatography over silica gel containing 10 % K_2CO_3 (hexane: ethyl acetate 3:1) to give **49** as a colorless oil (2.03 g, 78%). $[\alpha]^{RT}_D$ +32 (*c* 1.81, $CHCl_3$); ^1H NMR (600 MHz, $CDCl_3$) δ 7.53 – 7.47 (m, 2H), 7.33 (13, 6H), 7.21 – 7.14 (m, 1H), 5.60 (s, 1H), 4.85 (d, *J* = 1.5 Hz, 1H), 4.83 (d, *J* = 11.8 Hz, 1H), 4.68 (d, *J* = 11.8 Hz, 1H), 4.23 – 4.18 (m, 1H), 4.07 (t, *J* = 9.2 Hz, 1H), 3.99 (dd, *J* = 3.5, 1.5 Hz, 1H), 3.92 – 3.77 (m, 4H), 3.65 (dt, *J* = 10.3, 6.5 Hz, 1H), 3.12 (t, *J* = 6.6 Hz, 2H). ^{13}C NMR (150 MHz, $CDCl_3$) δ 138.0, 137.5, 135.6, 129.5, 128.9, 128.91, 128.4, 128.2, 127.8, 127.7, 126.3, 126.0, 101.5, 100.0, 78.7, 75.6, 73.0, 69.7, 68.7, 66.6, 63.4, 33.1. ESIHRMS calcd for $C_{21}H_{24}O_6SNa$ $[M + Na]^+$, 517.1661; found; 517.1663.

2-Phenylthioethyl 3-*O*-benzyl-4,6-*O*-benzylidene-2-*O*-[2-(trimethysilylmethyl)allyl]-α-D-mannopyranoside (50). To a stirred solution of compound **49** (2.8 mg, 5.71 mmol) in anhydrous THF (23 mL, 0.25 M), NaH (0.46 mg, 60% mineral oil dispersion) was added at 0 °C under argon. After 10 min, 2-iodomethyl-3-trimethylsilyl-1-propane[151] (2.4 g, 9.45 mmol) was added and the reaction mixture was further stirred for 10 minutes at the same temperature, before 15-crown-5 (1.1 mL, 5.71 mol) was added and stirring continued for 1 h at 0 ˚C. The reaction mixture was diluted with diethyl ether, washed with sat. $Na_2S_2O_3$ and brine, dried, filtered and concentrated. The crude product was purified by chromatography (hexane:diethyl ether 100:0~86:14 containing 0.5% triethylamine) to give **50** as a colorless oil (2.84 mg, 81%) $[\alpha]^{RT}_D$ +12 (*c* 0.17, CH_2Cl_2); ^{1}H NMR (600 MHz, CD_2Cl_2) δ 7.60 – 7.49 (m, 2H), 7.45 – 7.39 (m, 12H), 7.38 – 7.31 (m, 1H), 7.28 – 7.16 (m, 1H), 5.66 (s, 1H), 4.21 (dd, *J* = 8.1, 2.9, 1H), 4.20 – 4.16 (m, 1H), 4.12 (dd, *J* = 12.8, 1.1 Hz, 1H), 4.02 (dd, *J* = 12.9, 1.1 Hz, 1H), 3.94 – 3.88 (m, 2H), 3.87 – 3.84 (m, 2H), 3.79 (dd, *J* = 3.3, 1.6 Hz, 1H), 3.69 (dt, *J* = 10.5, 6.6 Hz, 1H), 3.19 (t, *J* = 6.6 Hz, 2H), 1.62 (s, 2H), 0.07 (s, 9H). ^{13}C NMR (150 MHz, CD_2Cl_2) δ 144.1, 138.9, 138.0, 129.3, 128.9, 128.7, 128.2, 128.1, 127.4, 127.3, 126.2, 126.1, 109.4, 101.4, 99.3, 79.0, 76.6, 76.4, 75.83, 72.8, 68.7, 66.5, 64.3, 33.1, 23.0, -1.7. ESIHRMS calcd for $C_{35}H_{44}NaO_6SSi$ $[M + Na]^+$, 643.2526; found; 643.2529.

3-*O*-Benzyl-4,6-*O*-benzylidene-2-*O*-[2-(trimethysilylmethyl)allyl]-α-D-mannopyranose (51). Lithium wire (41 mg, 6.01 mmol) was added under argon to a solution of naphthalene (0.81 g, 5.23 mmol) in dry tetrahydrofuran (11.3 mL, 0.46 M) and the reaction mixture was stirred at room temperature for 4 h to give a dark green solution. This solution was cooled to 0 °C then was added slowly via a syringe pump to a solution of **50** (0.79 g, 1.27 mmol) in dry tetrahydrofuran (3 mL) under argon at -78 °C. The reaction was monitored by TLC to avoid over-

reduction and was quenched by addition of brine (50 µL), concentrated and directly purified chromatographically (hexane:ethyl acetate 100:0~75:25 containing 0.5% triethylamine) to give compound **51** as a colorless oil. (0.49 g 78%) in the form of an α:β mixture consisting mainly of the α-anomer. **51α**: ^{1}H NMR (600 MHz, CD_2Cl_2) δ 7.52 – 7.44 (m, 2H), 7.42 – 7.24 (m, 8H), 5.63 (s, 1H), 5.25 (s, 1H), 4.96 (s, 1H), 4.80 (d, *J* = 12.0 Hz, 1H), 4.73 (d, *J* = 1.8 Hz, 1H), 4.70 (d, *J* = 12.0 Hz, 1H), 4.21 (dd, *J* = 9.9, 4.8 Hz, 1H), 4.16 (t, *J* = 9.7 Hz, 1H), 4.11 – 4.08 (d, *J* =12.8, 1H) 4.04 – 3.97 (m, 3H), 3.86 – 3.80 (m, 2H), 1.58 (s, 2H), 0.03 (s, 9H). ^{13}C NMR (150 MHz, CD_2CL_2) δ 144.1, 138.8, 137.9, 128.7, 128.1, 128.0, 127.5, 127.5, 17.3, 126.0, 109.3, 101.44, 94.0, 79.1, 76.8, 75.8, 75.7, 72.7, 68.8, 64.2, 22.9, -1.7. ESIHRMS calcd for $C_{27}H_{36}NaO_6Si$ $[M + Na]^+$, 507.2179; found; 507.2177.

3-*O*-Benzyl-4,6-*O*-benzylidene-2-*O*-[2-(trimethysilylmethyl)allyl]-α-D-mannopyranosyl trichloroacetimidate (52). Compound **51 (**327 mg, 0.68 mmol) was stirred with $CC1_3CN$ (0.61 mL, 6.70 mmol) and DBU (0.10 mL, 0.0.135 mmol) in dry CH_2C1_2 (3.4 mL) at 0 °C for 1 h. The reaction mixture was transferred directly to a pre-packed silica gel column and eluted with (hexane:diethyl ether (100:0~90:10, containing 0.5% trimethylamine) to give **52** as a colorless oil (330 mg, 78%). $[\alpha]^{RT}_{D}$ +26 (*c* 0.16, CH_2Cl_2); ^{1}H NMR (400 MHz, CD_2Cl_2) δ 8.68 (s, 1H), 7.68 – 7.09 (m, 10H), 6.27 (d, *J* = 1.8 Hz, 1H), 5.67 (s, 1H), 5.01 (d, *J* = 1.8 Hz, 1H), 4.85 (d, *J* = 11.9 Hz, 1H), 4.77 (br s, 1H), 4.72 (d, *J* = 12.0 Hz, 1H), 4.33 – 4.24 (m, 2H), 4.16(d, *J* = 12.0 Hz, 1H), 4.08 (d, *J* = 12.0 Hz, 1H), 4.03 (dd, *J* = 10.1, 3.3 Hz, 1H), 4.01 – 3.95 (m, 1H), 3.90 (dd, *J* = 3.3, 1.8 Hz, 1H), 3.86 (t, *J* = 10.2 Hz, 1H), 1.63 (s, 2H), 0.06 (s, 9H). ^{13}C NMR (100 MHz, CD_2Cl_2) δ 160.1, 143.7, 138.4, 137.6, 128.8, 128.26, 128.0, 127.8, 127.5, 126.0, 109.7, 101.4, 96.5, 78.3, 75.9, 75.3, 75.3, 73.0, 68.4, 66.8, 22.9, -1.7. ESIHRMS calcd for $C_{29}H_{36}Cl_3NNaO_6SiCl_3$ $[M + Na]^+$, 650.1275; found; 650.1265.

Cyclization of Mannosyl Trichloroacetimidate (55)1,5;4,8-Bisanhydro-6-*O*-benzyl-7,9-*O*-benzylidene-2,3-dideoxy-2-methylene-D-glycero-D-galacto-2-nonulose (58) and 1,5;4,8-Bisanhydro-6-*O*-benzyl-7,9-*O*-benzylidene-2,3-dideoxy-2-methylene-D-glycero-D-talo-2-nonulose (59). To a mixture of dry trichloroacetimidate **15** (0.15 g, 0.24 mmol) and anhydrous 2,4,6-tri-*tert*-butyl pyrimidine (20 mg, 0.08 mmol), freshly activated molecular sieves 4Å (0.22 g) were added and the flask purged with argon. Dry dichloromethane (10 mL) was added and the reaction mixture was stirred for 1 h at room temperature. The mixture was cooled to -20 °C followed by addition of TMSOTf (15 µL, 0.08 mmol) and stirring for 2 h at the same temperature. The reaction mixture was quenched with triethylamine (0.3 mL) and allowed to warm to room temperature. It was then diluted with dichloromethane (10 mL), filtered and washed with saturated aqueous $NaHCO_3$ and brine, dried, filtered, and concentrated. The crude mixture was then chromatographed (Heptane: Ethyl acetate 99:1~75:25) to give **58** as a white solid (0.066 g, 70%) and **59** as colorless needles with spectral data identical to the literature.[152]

Competition Kinetics with Mannosyl Trichloroacetimidate (55). Trichloroacetimidate **55** (10 mg, 16 µmol) and 2,4,6-tri-*tert*-butyl pyrimidine (1.4 mg, 5.5 µmol), were co-evaporated 3 times in toluene and dried in vacuo for 3 h. Freshly 4Å activated molecular sieves (50 mg) were added, the flask was purged with argon and dry dichloromethane (1 mL) added, followed by 2-propanol (0.81-8.12 equiv). The reaction mixture was stirred for 1 h at room temperature then cooled to -20 °C followed by addition of TMSOTf (1.22 µL, 5.5, µmol) and stirring for 3 h at -20 °C. The reaction mixture was quenched with triethylamine (20 µL) and allowed to warm to room temperature. It was diluted with dichloromethane, filtered and washed with saturated aqueous $NaHCO_3$ and with brine, dried, filtered, and concentrated. The crude mixture was dissolved in dichloromethane (0.5 mL) from which aliquots (10 µL) were withdrawn and diluted in acetonitrile

for UHPLC analysis (flow rate: 0.4 mL/min; Initial: H_2O 65/CH_3CN 35; 5.5 min: H_2O 50/CH_3CN 50; 5 min: H_2O 24/CH_3CN 76; 15 min: H_2O 20/CH_3CN 80; 5 min: H_2O 0/CH_3CN 100; 5 min). The protocol was repeated using trimethylallylsilane (2.1-32.0 equiv) in place of 2-propanol.

Isopropyl 3-*O*-benzyl-4,6-*O*-benzylidene-2-*O*-[2-(trimethysilylmethyl)allyl]-β-D-mannopyranoside (60). An analytical sample of this compound was isolated from the combined kinetics runs of **52** with isopropanol and had spectral data identical with the literature.[152]

Isopropyl 3-*O*-benzyl-4,6-*O*-benzylidene-2-*O*-[2-(trimethysilylmethyl)allyl]-α-D-mannopyranoside (61). An analytical sample of this compound was isolated from the combined kinetics runs of **52** with isopropanol and had spectral data identical with the literature.[152]

2-Phenylthioethyl 2,4,6-tri-*O*-acetyl 3-*O*-benzyl-β-D-glucopyranoside (65). To a solution of 1,2,4,6-tetra-*O*-acetyl-3-*O*-benzyl-β-D-glucopyranose (0.7 g, 1.59 mmol) and 2-(phenylthio)ethanol (0.3 mL, 2.08 mmol) in dry CH_2Cl_2 (7 mL) was added BF_3•Et_2O (0.60 mL 4.86 mmol,) slowly at 0 °C. The mixture was stirred at room temperature for 20 h then was slowly quenched with trimethylamine (0.7 mL) at 0 °C, diluted with CH_2Cl_2 (2 mL), and the organic layer was washed with saturated $NaHCO_3$, water and brine, dried, filtered, and evaporated. The residue was subjected to flash chromatography (hexane: ethyl acetate, 5:1) to give **65** (0.61 g, 69%) as a colorless oil $[\alpha]^{RT}_D$ -2 (*c* 1.23, $CHCl_3$); ^{1}H NMR (600 MHz, $CDCl_3$) δ 7.34 – 7.16 (m, 10H), 5.10 (t, *J* = 9.6 Hz, 1H), 5.04 (dd, *J* = 9.4, 8.0 Hz, 1H), 4.59 (d, *J* = 11.6 Hz, 1H), 4.56 (d, *J* = 11.6 Hz, 1H), 4.42 (d, *J* = 7.9 Hz, 1H), 4.18 (dd, *J* = 12.3, 5.2 Hz, 1H), 4.09 (dd, *J* = 12.2, 2.5 Hz, 1H), 4.00 – 3.94 (m, 1H), 3.67 (t, *J* = 10.0 Hz, 1H), 3.65 (dt, *J* = 10.5, 7.3 Hz, 1H). 3.58 – 3.54 (m, 1H), 3.15 – 3.03 (m, 2H), 2.05 (s, 3H), 2.00 (s, 3H), 1.96 (s, 3H). ^{13}C NMR (150 MHz, $CDCl_3$) δ 170.7, 169.3, 169.2, 137.6, 135.56, 129.4, 128.9, 128.4, 127.8, 127.7, 126.3, 101.2, 79.8, 73.7, 72.3, 72.1,

69.5, 68.4, 62.2, 33.1, 20.9, 20.8, 20.7. ESIHRMS calcd for $C_{27}H_{32}O_9SNa$ $[M + Na]^+$, 555.1665; found 555.1669.

2-Phenylthioethyl 3-*O*-benzyl β-D-glucopyranoside (66). Compound **65** (2.5 g, 4.7 mmol) was dissolved in dry methanol (28 mL), treated with NaOMe (126 mg, 2.35 mmol), and stirred at room temperature for 5 h. The reaction mixture was neutralized with Amberlyst IR-120 HC, filtered, concentrated and purified chromatographically (Hexane:Ethyl acetate 1:2) to give **23** in 93% as a colorless oil**.** $[\alpha]^{RT}_D$ -31 (*c* 0.67, $CHCl_3$); ^{1}H NMR (600 MHz, $CDCl_3$) δ 7.41 – 7.19 (m, 10H), 5.00 (d, *J* = 11.6 Hz, 1H), 4.72 (d, *J* = 11.6 Hz, 1H), 4.28 (d, *J* = 7.7 Hz, 1H), 4.07 (dt, *J* = 10.3, 6.2 Hz, 1H), 3.90 – 3.81 (m, 1H), 3.77 – 3.68 (m, 2H), 3.55 (dt, *J* = 9.3, 2.4 Hz, 1H), 3.49 (ddd, *J* = 9.5, 7.7, 1.9 Hz, 1H), 3.38 (t, *J* = 9.0 Hz, 1H), 3.32 (ddd, *J* = 9.2, 5.0, 3.6 Hz, 1H), 3.19 – 3.10 (m, 2H). ^{13}C NMR (150 MHz, $CDCl_3$) δ 138.4, 135.2, 129.8, 129.0, 128.6, 128.0, 126.6, 103.2, 83.4, 75.2, 74.6, 74.6, 70.0, 68.7, 62.6, 33.7. ESIHRMS calcd for $C_{27}H_{32}O_9SNa$ $[M + Na]^+$, 429.1348 found 429.1352.

2-Phenylthioethyl 3-*O*-benzyl 4,6-*O*-benzylidene-β-D-glucopyranoside (67). The compound was synthesized using the same procedure as compound **49** in 88% yield as a colorless oil. $[\alpha]^{RT}_D$ -31 (*c* 0.55, $CHCl_3$) 1H NMR (600 MHz, CDCl3) δ 7.51 – ^{1}H NMR (600 MHz, $CDCl_3$) δ 7.51 – 7.44 (m, Hz, 2H), 7.42 – 7.24 (m, Hz, 12H), 7.23 – 7.18 (m, 1H), 5.56 (s, 1H), 4.95 (d, *J* = 11.7 Hz, 1H), 4.81 (d, *J* = 11.7 Hz, 1H), 4.38 (d, *J* = 7.7 Hz, 1H), 4.32 (dd, *J* = 10.5, 5.0 Hz, 1H), 4.05 (dt, *J* = 10.4, 6.6 Hz, 1H), 3.78 (t, *J* = 10.3 Hz, 1H), 3.75 – 3.71 (m, 1H), 3.68 (t, *J* = 9.1 Hz, 1H), 3.65 (t, *J* = 8.7 Hz, 1H), 3.56 (td, *J* = 8.3, 1.9 Hz, 1H), 3.41 (td, *J* = 9.5, 5.0 Hz, 1H), 3.16 (t, *J* = 6.9 Hz, 2H). ^{13}C NMR (150 MHz, $CDCl_3$) δ 138.3, 137.2, 129.8, 129.0, 129.0, 128.4, 128.2,

128.0, 127.8, 126.5, 126.0, 103.6, 101.3, 81.2, 80.1, 74.56, 74.3, 68.8, 68.6, 66.5, 33.5. ESIHRMS calcd for $C_{21}H_{24}O_6SNa$ $[M + Na]^+$, 517.1661; found; 517.1661.

2-Phenylthioethyl 3-*O*-benzyl-4,6-*O*-benzylidene-2-*O*-[2-(trimethysilylmethyl)allyl]-β-D-glucopyranoside (68). The protocol employed for the synthesis **50** was used to convert **67** to **68** in 89% yield as a colorless oil. $[\alpha]^{RT}_D$ -41 (*c* 0.56, CH_2Cl_2) ^{1}H NMR (600 MHz, CD_2Cl_2) δ 7.71 – 7.10 (m, 15H), 5.57 (s, 1H), 4.97 (s, 1H), 4.87 (d, *J* = 11.4 Hz, 1H), 4.80 (d, *J* = 11.4 Hz, 1H), 4.68 (s, 1H), 4.48 (d, *J* = 7.7 Hz, 1H), 4.30 (dd, *J* = 10.4, 5.0 Hz, 1H), 4.24 (d, *J* = 12.5 Hz, 1H), 4.07 (d, *J* = 12.5 Hz, 1H), 4.02 – 3.97 (m, 1H), 3.79 – 3.73 (m, 2H), 3.70 – 3.63 (m, 2H), 3.41 – 3.36 (m, 1H), 3.30 (t, *J* = 8.0 Hz, 1H), 3.16 (t, *J* = 7.5 Hz, 2H), 1.57 (d, *J* = 13.7 Hz, 1H), 1.54 (d, *J* = 13.7 Hz, 1H), 0.02 (s, 9H). ^{13}C NMR (150 MHz, CD_2Cl_2) δ 144.3, 138.8, 137.6, 135.8, 129.2, 128.9, 128.8, 128.1, 127.9, 127.4, 126.2, 126.0, 108.3, 104.1, 101.0, 81.9, 81.3, 80.7, 76.8, 74.7, 68.7, 68.6, 65.9, 33.2, 23.2, -1.7. ESIHRMS calcd for $C_{35}H_{44}NaO_6SSi$ $[M + Na]^+$, 643.2526; found; 643.2528.

3-*O*-Benzyl-4,6-*O*-benzylidene-2-*O*-[2-(trimethysilylmethyl)allyl]-D-glucopyranose (26). The aglycone was cleaved from **68** with lithium naphthenalide by the protocol used for the synthesis of compound **54** and gave **69** in 70% yield as an anomeric mixture (α:β = 1.1:1).

β-anomer (26): ^{1}H NMR (600 MHz, CD_2Cl_2) δ 7.53 – 7.48 (m, 2H), 7.43 – 7.37 (m, 5H), 7.35 – 7.25 (m, 3H), 5.60 (s, 1H), 5.01 (d, *J* = 1.6 Hz, 1H), 4.92 (d, *J* = 11.5 Hz, 1H), 4.84 (d, *J* = 11.5 Hz, 2H), 4.73 (s, 1H), 4.34 (dd, *J* = 10.4, 5.0 Hz, 1H), 4.26 (d, *J* = 12.5 Hz, 1H), 4.16 (d, *J* = 12.6 Hz, 1H), 3.78 (t, *J* = 10.3 Hz, 1H), 3.74 (t, *J* = 9.0 Hz, 1H), 3.66 (t, *J* = 9.5 Hz, 1H), 3.49 – 3.41 (m, 1H), 3.29 (t, *J* = 8.0 Hz, 1H), 1.61 (d, *J* = 13.6 Hz, 3H), 1.58 (d, *J* = 13.7 Hz, 1H), 0.05 (s, 9H).

^{13}C NMR (150 MHz, CD_2Cl_2) δ 144.4, 138.8, 137.6, 128.8, 128.1, 127.9, 127.4, 126.1, 109.6, 101.1, 97.9, 83.1, 81.5, 80.7, 76.8, 74.7, 68.7, 66.1, 23.3, -1.7.

α-anomer (26): ^{1}H NMR (600 MHz, CD_2Cl_2) δ 7.53 – 7.48 (m, 2H), 7.43 – 7.37 (m, 5H), 7.35 – 7.25 (m, 3H), 5.60 (s, 1H), 5.34 (d, *J* = 3.7 Hz, 1H), 4.99 (d, *J* = 1.4 Hz, 1H), 4.92 (d, *J* = 11.5 Hz, 1H), 4.84 (d, *J* = 11.5 Hz, 1H), 4.77 (s, 1H), 4.30 (dd, *J* = 10.2, 5.0 Hz, 1H), 4.12 (d, *J* = 12.7 Hz, 1H), 4.08 (d, *J* = 12.7 Hz, 1H), 4.06 (dt, *J* = 10.0, 5.0 Hz, 1H), 3.96 (t, *J* = 9.2 Hz, 1H), 3.70 (t, *J* = 9.2 Hz, 1H), 3.56 (dd, *J* = 9.1, 3.7 Hz, 1H), 1.61 (d, *J* = 13.7 Hz, 1H), 1.58 (d, *J* = 13.7 Hz, 1H), 0.06 (s, 9H). ^{13}C NMR (150 MHz, CD_2Cl_2) δ 143.8, 138.9, 137.7, 128.8, 128.1, 127.9, 127.4, 126.1, 108.5 101.2, 91.9, 81.9, 79.4, 78.0, 75.3, 74.8, 69.0, 62.5, 62.4, 23.0, -1.7. ESIHRMS calcd for $C_{27}H_{36}NaO_6Si$ $[M + Na]^+$, 507.2179; found; 507.2177.

3-*O*-Benzyl-4,6-*O*-benzylidene-2-*O*-[2-(trimethysilylmethyl)allyl]-α-D-glucopyranosyl trichloroacetimidate (70). Compound **69** (220 mg, 0.454 mmol) was dissolved in dry dichloromethane (2.2 mL) and trichloroacetonitrile (327 µL, 5 eq) was added, followed by NaH (4 mg, 0.091 mmol). The reaction mixture was stirred for 0.25 h at room temperature followed by NaH (36 mg, 0.9 mmol) for 3 hr, filtered through celite, concentrated and directly purified chromatographically (Hexane:Diethyl ether 100:0~90:10, containing 0.5% trimethylamine) to give **70** as colorless oil (0.21, 73%) $[\alpha]^{RT}_D$ +25 (*c* 0.56, CH_2Cl_2) ^{1}H NMR (600 MHz, CD_2Cl_2) δ 8.68 (s, 1H), 7.52 – 7.47 (m, 2H), 7.44 – 7.35 (m, *J* = 7.2 Hz, 5H), 7.34 – 7.22 (m, *J* = 7.5 Hz, 3H), 6.50 (d, *J* = 3.7 Hz, 1H), 5.61 (s, 1H), 4.96 (s, 1H), 4.91 (d, *J* = 11.4 Hz, 1H), 4.86 (d, *J* = 11.4 Hz, 1H), 4.72 (s, 1H), 4.30 (dd, *J* = 10.3, 5.0 Hz, 1H), 4.11 – 3.98 (m, 4H), 3.78 – 3.69 (m, 3H), 1.58 (d, *J* = 13.7 Hz, 1H), 1.54 (d, *J* = 13.7 Hz, 1H). 0.01 (s, 9H). ^{13}C NMR (150 MHz, CD_2Cl_2) δ 161.1, 143.7, 138.8, 137.4, 128.8, 128.1, 127.8, 127.4, 126.0, 109.4, 101.2, 94.6,

81.4, 78.5, 77.9, 75.5, 74.9, 68.6, 65.0, 22.8, -1.8. ESIHRMS calcd for $C_{29}H_{36}Cl_3NNaO_6SiCl_3$ [M + Na]$^+$, 650.1275; found; 650. 1266.

Prepartive Cyclization of Glucosyl Trichloroacetimidate (27). 1,5;4,8-Bisanhydro-6-*O*-benzyl-7,9-*O*-benzylidene-2,3-dideoxy-2-methylene-D-glycero-D-ido-2-nonulose (32). A mixture of trichloroacetimidate **70** (0.077 mg, 0.12 mmol) and 2,4,6-tri-*tert*-butyl pyrimidine (10 mg, 0.042 mmol) was co-evaporated with toluene 3 times, dried in vacuo for 3 h before freshly activated 4Å molecular sieves (0.11 g) were added. The flask was sealed and purged with argon and dry dichloromethane (6 mL) was added. The mixture was then stirred for 1 h at room temperature and cooled to -20 °C followed by addition of TMSOTf (7 µL, 0.042 mmol). After stirring for 2 h at same temperature, the reaction mixture was quenched with triethylamine (0.15 mL) and allowed to warm to room temperature. It was then diluted with dichloromethane, filtered and washed with saturated aqueous $NaHCO_3$ and brine, dried, filtered, and concentrated. The crude mixture was purified by chromatography (Hexane: Diethyl ether 10:1~5:1 containing 0.5% triethylamine) to give the tricyclic product **73** as a light white solid (0.45 mg, 92%) with data identical to the literature.[87] Mp 102-103 °C; $[\alpha]^{RT}_D$ +143 (*c* 1.00, $CHCl_3$); ^{1}H NMR (600 MHz, CD_2Cl_2) δ 7.50-7.47 (m, 2H), 7.40-7.36 (m, 5H), 7.34-7.31 (m, 2H), 7.29-7.27 (m, 1H), 5.56 (s, 1H), 4.93 (br s, 1H), 4.88-4.87 (bs d, *J* = 1.1 Hz, 1H), 4.81-4.79 (d, *J* = 11.8 Hz, 1H), 4.77-4.75 (d, *J* = 11.6 Hz, 1H), 4.27-4.24 (dd, *J* = 4.8, 9.7 Hz, 1H), 4.15-4.13 (m, *J* = 3.6 Hz, 1H), 4.04-4.02 (d, *J* = 12.8 Hz, 1H), 3.96-3.94 (d, *J* = 12.8 Hz, 1H), 3.93-3.90 (m, 1H), 3.86-3.81 (m, 2H), 3.79-3.75 (td, *J* = 4.7, 9.5 Hz, 1H), 3.68-3.64 (t, *J* = 9.9 Hz, 1H), 2.62-2.58 (dd, *J* = 7.4, 13.6 Hz, 1H), 2.40-2.37 (dd, *J* = 4.4, 13.9 Hz, 1H); ^{13}C NMR (150 MHz, CD_2Cl_2) δ 140.9, 138.9, 138.2, 129.3, 128.7, 128.5, 128.3, 128.0, 126.5, 112.2, 101.6, 82.3, 77.3, 76.5, 73.1, 70.7, 70.2, 69.2, 64.5, 35.2, 30.1; ESIHRMS calcd for $C_{24}H_{26}O_5Na$ [M + Na]$^+$, 417.1678; found, 417.1681

Competition Kinetics with Glucosyl Trichloroacetimidate 70. Trichloroacetimidate **70** (30 mg, 48 µmol) and 2,4,6-tri-*tert*-butyl pyrimidine (3.2 mg, 13 µmol) were co-evaporated 3 times in toluene and dried in vacuo for 3 h. Freshly activated 4Å molecular sieves (100 mg) were added, the flask was purged with argon and dry dichloromethane (2.4 mL) added followed by 2-propanol (0.81-8.12 equiv). The reaction mixture was stirred for 1 h at room temperature then cooled to -20 °C followed by addition of TMSOTf (2.3 µL, 13, µmol) and stirring for 3 h at -20 °C. The reaction mixture was quenched with triethylamine (20 µL), allowed to warm to room temperature. It was diluted with dichloromethane, filtered and washed with saturated aqueous $NaHCO_3$ and with brine, dried, filtered, and concentrated. The crude mixture was dissolved in dichloromethane (1 mL) from which aliquots (10 µL) were withdrawn and diluted in acetonitrile (1 mL) for UHPLC (flow rate: 0.4 mL/min; Initial: H_2O 65/CH_3CN 35; 5.5 min: H_2O 50/CH_3CN 50; 5 min: H_2O 24/CH_3CN 76; 15 min: H_2O 20/CH_3CN 80; 8 min H_2O 10/CH_3CN 90; 5 min: H_2O 0/CH_3CN 100; 5 min). The protocol was repeated using trimethylallylsilane (2.1-32.0 equiv) in place of 2-propanol. The same protocol was applied using trimethylallylsilane (23.8-71.4 equiv) as nucleophile in place of 2-propanol.

Isopropyl 3-*O*-benzyl-4,6-*O*-benzylidene-2-*O*-[2-(trimethysilylmethyl)allyl]-α,β-D-glucopyranoside (74 and 75). Pooling of the kinetic runs of trichloroacetimidate **70** with isopropanol followed by chromatographic purification (Petroleum ether:diethyl ether 8:1 containing 0.5% triethylamine) gave a mixture of **74** and **75** in the form of an oil ESIHRMS calcd for $C_{30}H_{42}O_6SiNa$ $[M + Na]^+$, 549.2648; found 549.2642.

β-anomer (**74**): ^1H NMR (600 MHz, CD_2Cl_2) δ 7.50 – 7.46 (m, 2H), 7.40 – 7.34 (m, 5H), 7.31 – 7.24 (m, 3H), 5.57 (s, 1H), 4.96 (br s, 1H), 4.87 (d, *J* = 11.4 Hz, 1H), 4.81 (d, *J* = 11.4 Hz, 1H),

4.67 (s, 1H), 4.53 (d, *J* = 7.7 Hz, 1H), 4.30 (dd, *J* = 10.4, 5.0 Hz, 1H), 4.23 (d, *J* = 11.8 Hz, 1H), 4.07 (d, *J* = 11.8 Hz, 1H), 3.98 (sept, *J* = 6.2 Hz, 1H), 3.76 (t, *J* = 10.3 Hz, 1H), 3.71 (t, *J* = 9.8 Hz, 1H), 3.68 (t, 1H), 3.61 (t, *J* = 9.4 Hz, 1H), 3.42 – 3.35 (m, 1H), 3.25 (t, *J* = 8.1 Hz, 1H), 1.59 (d, *J* = 13.5 Hz, 1H), 1.54 (d, *J* = 13.6 Hz, 1H), 0.02 (s, 9H). ^{13}C NMR (150 MHz, CD_2Cl_2) δ 144.3, 144.3, 138.9, 137.7, 128.7, 128.1, 127.9, 127.3, 126.0, 108.3, 102.3, 101.0, 82.0, 81.5, 80.9, 76.9, 74.6, 72.0, 68.8, 65.8, 23.3, 23.2, 21.7, -1.7.

α-anomer (75): ^{1}H NMR (600 MHz, CD_2Cl_2) δ 7.52 – 7.45 (m, *J* = 7.0, 5.4, 1.7 Hz, 2H), 7.40 – 7.34 (m, 5H), 7.31 – 7.23 (m, 3H), 5.57 (s, 1H), 5.04 (d, *J* = 3.8 Hz, 1H), 4.95 (br s, 1H), 4.86 (d, *J* = 11.4 Hz, 1H), 4.82 (d, *J* = 11.5 Hz, 1H), 4.72 (br s, 1H), 4.30 (dd, *J* = 10.4, 5.0 Hz, 1H), 4.24 (dd, *J* = 10.1, 5.0 Hz, 1H), 4.07 (d, *J* = 12.5 Hz, 1H), 4.00 (d, *J* = 12.7 Hz, 1H), 3.93 (t, *J* = 9.5 Hz, 1H), 3.92 – 3.87 (m, 1H), 3.71 (t, *J* = 9.8 Hz, 1H), 3.64 (t, *J* = 9.2 Hz, 1H), 3.47 (dd, *J* = 9.3, 3.8 Hz, 1H), 1.59 (br s, 1H), 1.53 (br s, 1H), 1.27 (d, *J* = 6.3 Hz, 1H), 1.21 (d, *J* = 6.2 Hz, 3H), 0.02 (s, 9H). ^{13}C NMR (150 MHz, CD_2Cl_2) δ 144.2, 139.2, 137.8, 128.7, 128.1, 127.7, 127.3, 126.0, 109.3, 101.1, 95.9, 82.3, 79.3, 78.31, 75.0, 74.8, 69.8, 69.1, 62.4, 23.1, 22.95, 21.2, -1.8.

4,8-Anhydro-6-*O*-benzyl-7,9-*O*-benzylidene-1,2,3-trideoxy-2-methylene-D-glycero-D-ido-2-nonulose (76). Pooling of the kinetic runs of trichloroacetimidate **27** with methallyl trimethylsilane followed by chromatographic purification (Petroleum ether: Diethyl ether 10:1 containing 0.5% triethylamine) gave an analytical sample of **76** as a colorless oil $[\alpha]^{RT}_{D}$ +6 (*c* 0.24, CH_2Cl_2) ^{1}H NMR (400 MHz, $CDCl_3$) δ 7.73 – 7.19 (m, 10H), 5.57 (s, 1H), 4.95 (d, *J* = 1.5 Hz, 1H), 4.92 (d, *J* = 11.6 Hz, 1H), 4.85 (s, 1H), 4.83 (d, *J* = 11.9 Hz, 1H), 4.72 (s, 1H), 4.30 (ddd, *J* = 9.7, 5.6, 3.5 Hz, 1H), 4.24 (dd, *J* = 8.7, 2.9 Hz, 1H), 4.07 (d, *J* = 12.6 Hz, 1H), 3.98 (d, *J* = 12.8 Hz, 1H), 3.84 (t, *J* = 8.6 Hz, 1H), 3.75 – 3.61 (m, 4H), 2.57 (dd, *J* = 15.1, 11.8 Hz, 1H), 2.42

(dd, *J* = 15.1, 2.8 Hz, 2H), 1.79 (s, 2H), 1.62 – 1.51 (m, 2H), 0.03 (s, 9H). ^{13}C NMR (101 MHz, $CDCl_3$) δ 143.7, 142.0, 137.5, 128.84, 128.27, 128.20, 127.88, 127.53, 125.96, 113.01, 109.68, 101.12, 82.79, 79.14, 78.63, 75.5, 74.8, 73.4, 69.5, 63.5, 33.8, 23.2, 22.0, -1.4. ESIHRMS calcd for $C_{31}H_{42}O_5SiNa$ $[M + Na]^+$, 545.2699; found 545.2679.

2-((Naphthalen-2-ylmethoxy) methyl) benzyl alcohol (81) Sodium hydride (0.58 g, 14.5 mmol, 60% dispersion in mineral oil) was washed with anhydrous hexanes (3 × 10 mL), then suspended in anhydrous THF (20 mL) under Argon, and cooled to 0 °C. To this suspension, 1,2-benzenedimethanol (3.2 g, 14.5 mmol) in THF (30 mL) was slowly added over 10 min. After the addition was complete, the milky white suspension was removed from the ice bath, and stirred for an additional 10 min. 2-(Bromomethyl)naphthalene (3.2 g, 14.5 mmol) dissolved in THF (20 mL) was added dropwise via syringe. The mixture was refluxed for 2.5 h, then was cooled to room temperature and carefully quenched by slow addition of water (5 mL). The reaction mixture was diluted with ethyl acetate (100 mL) and washed with brine and dried on anhydrous Na_2SO_4. The organic layer was evaporated under reduced pressure. Chromatographic purification of the residue (hexanes/ethyl acetate 3:1) afforded the title compound (3.4 g, 85%) as a colorless oil. ^{1}H NMR (600 MHz, $CDCl_3$) δ 7.92 – 7.75 (m, 4H), 7.58 – 7.47 (m, 3H), 7.43 – 7.40 (m, 1H), 7.38 – 7.28 (m, 3H), 4.75 (s, 2H), 4.69 (s, 4H).^{13}C NMR (151 MHz, $CDCl_3$) δ 140.5, 135.8, 134.8, 133.2, 133.1, 130.1, 129.7, 128.9, 128.4, 128.0, 127.9, 127.7, 127.0, 126.2, 126.1, 125.8, 72.6, 71.3, 63.8. ESIHRMS calcd for $C_{19}H_{18}O_2Na$, 301.1204 $[M + Na]^+$, found; 301.1202.

2-((Naphthalen-2-ylmethoxy) methyl) benzyl bromide (82) A solution of 2-((naphthalen-2-ylmethoxy) methyl) benzyl alcohol (1.66 g, 5.97 mmol) in anhydrous CH_2Cl_2 (20 mL) was treated with CBr_4 (2.55 g, 7.6 mmol) and stirred for 5 min at room temperature. PPh_3 (2.06 g, 6.56 mmol)

in anhydrous CH_2Cl_2 (20 mL) was added dropwise and the reaction mixture was stirred for 1 h. The reaction mixture was quenched with saturated aqueous $NaHCO_3$ and extracted with CH_2Cl_2. The organic layer was washed with brine and dried over anhydrous Na_2SO_4, filtered and concentrated. Silica gel column chromatography of the residue (hexanes/ethyl acetate, 95:5) afforded the title compound (1.41 g, 69%) as a pale yellow oil. ^{1}H NMR (400 MHz, $CDCl_3$) δ 7.90 – 7.81 (m, 4H), 7.54 – 7.47 (m, 3H), 7.44 – 7.37 (m, 2H), 7.35 – 7.30 (m, 2H), 4.78 (s, 2H), 4.76 (s, 2H), 4.66 (s, 2H). ^{13}C NMR (101 MHz, $CDCl_3$) δ 136.7, 136.4, 135.4, 133.3, 133.0, 130.7, 129.8, 128.9, 128.5, 128.3, 127.9, 127.7, 126.7, 126.1, 125.9, 125.8, 72.7, 69.8, 31.0. ESIHRMS calcd for $C_{19}H_{17}BrONa$ $[M + Na]^+$, 363.0360; found; 363.0360.

Phenyl 3,5-*O*-(di-*tert*-butylsilylene)-2-*O*-(2-((naphthalen-2-ylmethoxy) methyl) benzyl)-1-thio-α-D-arabinofuranoside (83). A mixture of phenyl 3,5-*O*-(di-*tert*-butylsilylene)-1-thio-α-D-arabinofuranoside[153] (1.3 g, 3.41 mmol) and 2-((naphthalen-2-ylmethoxy) methyl) benzyl bromide (1.3 g, 3.82 mmol) was dissolved in dry DMF (17 mL) and cooled to 0 ºC. Sodium hydride (0.26 g, 60% suspension in mineral oil, 6.80 mmol) was carefully added and reaction mixture stirred for 30 min. The reaction mixture was diluted with ethyl acetate (50 mL), washed with brine, and dried over anhydrous Na_2SO_4 and concentrated. Chromatographic purification of the residue (hexane/ethyl acetate 100:0-95:5) gave the title compound **4** (1.75g, 83%) as a colorless oil. $[\alpha]^{RT}_{D=}$ +77 (*c* 1.08, $CHCl_3$); ^{1}H NMR (400 MHz, $CHCl_3$) δ 7.93 – 7.66 (m, 4H), 7.52 – 7.46 (m, 5H), 7.42 – 7.39 (m, 2H), 7.38 – 7.30 (m, 2H), 7.29 – 7.22 (m, 3H), 5.41 (d, *J* = 5.4 Hz, 1H), 4.94 (d, *J* = 12.2 Hz, 1H), 4.85 (d, *J* = 12.1 Hz, 1H), 4.80 – 4.72 (m, 4H), 4.36 – 4.28 (m, 1H), 4.16 – 4.08 (m, 1H), 3.99 – 3.87 (m, 3H), 1.06 (s, 9H), 0.98 (s, 9H). ^{13}C NMR (151 MHz, $CDCl_3$) δ 136.8, 135.7, 135.6, 134.4, 133.3, 133.0, 131.1 (2 carbons), 129.3, 128.9(2 carbons), 128.8, 128.2, 128.1, 127.9, 127.7, 127.7, 127.3, 126.4, 126.1, 125.8, 125.8, 89.7, 86.8, 81.0, 73.6, 72.5,

70.2, 70.0, 67.2, 27.4, 27.1, 22.6, 20.1. ESIHRMS calcd for $C_{38}H_{46}O_5SSiNa$ $[M + Na]^+$, 665.2733; found; 665.2728.

Phenyl 3,5-*O*-(di-*tert*-butylsilylene) 2-*O*-((2-hydroxymethyl) benzyl)-1-thio-α-D-arabinofuranoside (84). 20% Pd $(OH)_2$ /C (0.35 g, 0.54 mmol) was dispersed in EtOAc-EtOH (1:2, 22 mL) under argon. The mixture was degassed, purged and saturated with hydrogen. After 1 h of vigorous stirring, a solution of compound **83** (0.35 g, 0.54 mmol) in EtOAc-EtOH 1:2, 4 ml) was added to the suspension. The reaction mixture was purged with H_2 a second time and allowed to stir at room temperature for 2 h under a hydrogen atmosphere (balloon), after which TLC (hexane-ethyl acetate, 10:1) indicated the completion of the reaction. The catalyst was removed by filtration through Celite and washed with EtOAc. The filtrate was concentrated, and the resulting crude product was purified by silica gel column chromatography (ethyl acetate/hexane, 10:1-5:1) to give the title compound (0.25 g, 90%) as a white powder. $[\alpha]^{RT}_D$ = +109 (*c* 0.42, $CHCl_3$); ^{1}H NMR (600 MHz, $CDCl_3$) δ 7.47 – 7.42 (m, 3H), 7.41 – 7.35 (m, 2H), 7.33 – 7.23 (m, 4H), 5.38 (d, *J* = 5.6 Hz, 1H), 4.94 (d, *J* = 11.7 Hz, 1H), 4.87 (d, *J* = 11.7 Hz, 1H), 4.75 (d, *J* = 6.4 Hz, 2H), 4.35 – 4.29 (m, 1H), 4.13 (dd, *J* = 9.2, 7.3 Hz, 1H), 4.00 – 3.93 (m, 2H), 3.92 – 3.87 (m, 1H), 2.66 (t, *J* = 6.5 Hz, 1H), 1.07 (s, 9H), 0.97 (s, 9H). ^{13}C NMR (151 MHz, $CDCl_3$) δ 140.5, 134.8, 133.9, 131.5 (2 carbons), 130.5, 129.9, 129.1, 129.0(2 carbons), 127.8, 127.6, 89.5, 85.9, 80.7, 73.6, 71.2, 67.2, 63.3, 27.4, 27.0, 22.6, 20.1. ESIHRMS calcd for $C_{27}H_{38}NaO_5SSi$ $[M + Na]^+$, 525.2107; found; 525.2106.

1,2-Di-*O*-(1,2-xylylene)-3,5-*O*-di-*tert*-butylsilylene- β/α -D-arabinofuranoside (85 and 86). The thioglycoside **84** (160 mg, 0.32 mmol) was coevaporated with toluene 3 times and kept in vacuo for 3 h. 4Å Molecular sieves (160 mg) and anhydrous dichloromethane (18.6 mL) were

added and the reaction mixture was stirred for 1 h at room temperature prior to cooling to -20 °C. Solid NIS (87 mg, 0.39 mmol) was added followed by AgOTf (38 mg, 0.15 mmol). The reaction mixture was then stirred at the same temperature for 1 h during which the appearance of persistent characteristic iodine color was observed. The reaction was quenched by the addition of Et_3N (120 µL). The suspension was diluted with EtOAc and filtered through Celite, and the filtrate was washed successively with saturated aqueous $Na_2S_2O_3$ and brine. The organic layer was dried over anhydrous Na_2SO_4 and concentrated under reduced pressure to give a crude product, which was purified by flash column chromatography (hexane/ ethyl acetate 99:1-95:5) to afford a major isomer **85**, (112 mg, 90%) as white needles and minor isomer **86** (6.4 mg, 5%) as colorless oil.

Major product **85**: (m.p, 145 ˚C) $[\alpha]^{RT}_{D}$ = +25 (*c* 0.17, $CHCl_3$); ^{1}H NMR (600 MHz, $CDCl_3$) δ 7.28 – 7.22 (m, 2H), 7.and a minor product – 7.14 (m, 2H), 5.36 (d, *J* = 5.2 Hz, 1H), 5.32 (d, *J* = 13.3 Hz, 1H), 4.97 (d, *J* = 13.3 Hz, 1H), 4.83 (d, *J* = 13.3 Hz, 1H), 4.64 (d, *J* = 13.3 Hz, 1H), 4.41 – 4.33 (m, 1H), 4.22 (dd, *J* = 7.2, 5.3 Hz, 1H), 4.08 (dd, *J* = 9.5, 7.2 Hz, 1H), 3.64 – 3.46 (m, 1H), 1.04 (s, 9H), 1.00 (s, 9H). ^{13}C NMR (151 MHz, $CDCl_3$) δ 137.2, 137.0, 129.1, 128.5, 128.1, 127.9, 101.5, 83.6, 80.6, 71.8, 71.1, 69.7, 67.6, 27.4, 27.1, 22.6, 20.1 ESIHRMS calcd for $C_{21}H_{32}NaO_5Si$ $[M + Na]^+$, 415.1917; found; 415.1920.

Minor product **86** (6.4 mg, 5%) as colorless: $[\alpha]^{RT}_{D}$ = -43 (*c* 0.37, $CHCl_3$); ^{1}H NMR (600 MHz, $CDCl_3$) δ 7.43 – 7.35 (m, 4H), 4.99 (d, *J* = 12.7 Hz, 1H), 4.92 (s, 1H), 4.93 (d, *J* = 12.8 Hz, 1H), 4.86 (d, *J* = 12.8 Hz, 1H), 4.81 (d, *J* = 12.7 Hz, 1H), 4.28 (dd, *J* = 9.3, 5.1 Hz, 1H), 4.07 – 4.02 (m, 2H), 4.02 – 3.95 (m, 1H), 3.83 (t, *J* = 9.8 Hz, 1H), 1.03 (s, 9H), 1.03 (s, 9H), ^{13}C NMR (151 MHz, $CDCl_3$) δ 135.5, 135.1, 131.8, 131.7, 129.8, 129.8, 104.6, 86.5, 79.5, 74.4, 70.8, 67.3, 66.0, 27.4, 27.1, 27.0, 22.6, 20.1. ESIHRMS calcd for $C_{21}H_{32}NaO_5Si$ $[M + Na]^+$, 415.1917; found; 415.1927.

Isopropyl 3,5-*O*-(di-*tert*-butylsilylene)-2-*O*-((2-hydroxymethyl) benzyl)-1-thio-α/β-D-arabinofuranoside (87 and 88). The thioglycoside **84** (140 mg, 0.28 mmol) was coevaporated with toluene 3 times and kept in vacuo for 3 h. 4Å Molecular sieves (350 mg) and anhydrous dichloromethane (17 mL) were added and the reaction mixture was stirred for 1 h at room temperature prior to cooling to -20 °C under argon. 2-Propanol (1.3 mL, 16.95 mmol) was added and the reaction mixture stirred for 10 min before solid NIS (125 mg, 0.56 mmol) was added followed by AgOTf (35 mg, 0.14 mmol). The reaction mixture was then stirred at the same temperature for 1 h during which the appearance of persistent characteristic iodine color was observed. The reaction was quenched by the addition of Et_3N (100 µL) at -20 °C. The suspension was diluted with EtOAc and filtered through Celite. The filtrate was washed successively with saturated aqueous $Na_2S_2O_3$ and brine. The organic layer was dried over anhydrous Na_2SO_4 and concentrated under reduced pressure to give the crude product, which was purified by flash column chromatography (hexane/ ethyl acetate 99:1-80-20) to afford two compounds, **87** (33 mg, 26%) and **88** (58 mg. 46%) as colorless oils.

Minor α- isomer **87**: $[\alpha]^{RT}_{D}$ = -62 (*c* 0.55, $CHCl_3$);^{1}H NMR (600 MHz, $CDCl_3$) δ 7.44 – 7.40 (m, 1H), 7.37 – 7.32 (m, 2H), 7.30 – 7.26 (m, 1H), 5.04 (d, *J* = 3.5 Hz, 1H), 4.86 (d, *J* = 11.6 Hz, 1H), 4.79 (d, *J* = 11.6 Hz, 1H), 4.72 – 4.65 (m, 2H), 4.30 (dd, *J* = 8.2, 4.2 Hz, 1H), 4.06 (t, *J* = 8.3 Hz, 1H), 3.95 – 3.86 (m, 3H), 3.84 (hept, *J* = 6.2 Hz, 1H), 2.80 (t, *J* = 6.6 Hz, 1H). 1.20 (d, *J* = 6.2 Hz, 3H), 1.16 (d, *J* = 6.1 Hz, 3H), 1.06 (s, 9H), 0.97 (s, 9H). ^{13}C NMR (151 MHz, $CDCl_3$) δ 140.5, 135.2, 130.4, 130.1, 129.0, 127.9, 104.7, 87.2, 80.6, 73.5, 71.1, 70.8, 67.6, 63.4, 27.4, 27.1, 23.6, 22.6, 21.6, 20.1. ESIHRMS calcd for $C_{24}H_{40}NaO_6Si$ $[M + Na]^+$, 475.2492; found; 475.2490.

Major β-isomer **87:** $[\alpha]^{RT}_{D}$ = +27 (*c* 1.22, $CHCl_3$); ^{1}H NMR (600 MHz, $CDCl_3$) δ 7.45 – 7.41 (m, 1H), 7.38 – 7.33 (m, 1H), 7.30 – 7.27 (m, 2H), 5.11 (d, *J* = 5.5 Hz, 1H), 5.04 (d, *J* = 11.3 Hz, 1H), 4.77 (d, *J* = 11.3 Hz, 1H), 4.74 (dd, *J* = 12.1, 6.0 Hz, 1H), 4.59 (dd, *J* = 12.1, 8.3 Hz, 1H), 4.38 (t, *J* = 9.0 Hz, 1H), 4.31 (dd, *J* = 9.1, 5.0 Hz, 1H), 3.95 (dd, *J* = 8.8, 5.5 Hz, 1H), 3.91 (dd, *J* = 10.6, 9.1 Hz, 1H), 3.88 – 3.81 (m, 1H), 3.73 (dd, *J* = 8.2, 6.2 Hz, 1H), 3.65 (ddd, *J* = 10.6, 9.2, 5.1 Hz, 1H), 1.20 (d, *J* = 6.2 Hz, 3H), 1.13 (d, *J* = 6.2 Hz, 3H), 1.07 (s, 9H), 1.00 (s, 9H). ^{13}C NMR (151 MHz, $CDCl_3$) δ 141.2, 135.7, 130.9, 130.0, 129.1, 127.8, 98.4, 80.6, 79.2, 73.2, 71.6, 71.6, 68.5, 63.7, 27.5, 27.1, 23.5, 22.5, 21.6, 20.1. ESIHRMS calcd for $C_{24}H_{40}NaO_6Si$ $[M + Na]^+$, 475.2492; found; 475.2488.

Competition kinetics with 3,5-*O*-di-*tert*-butyl arabinosyl thioglycoside (84). The thioglycoside **5** (18.5 mg, 0.037 mmol) was coevaporated with toluene 3 times, and kept in vacuo for 3 h. Anhydrous dichloromethane (0.46 mL, 0.08 M) was added. The solution was cooled to -20 °C under argon. The corresponding acceptor (2.1-10 Eq) was added and the reaction stirred for a further 10 min before NIS (16.5 mg, 0.074 mmol) was added followed by AgOTf (4 mg, 0.014 mmol). The reaction mixture was then stirred at the same temperature for 1 h during which the appearance of a persistent brown color was observed. The reaction was quenched by the addition of Et_3N (5 µL) at -20 °C. The suspension was then diluted with dichloromethane (2 mL) and filtered through Celite. The filtrate was washed successively with aqueous $Na_2S_2O_3$ (2 mL) and brine (2 mL). The organic layer was dried over anhydrous Na_2SO_4 and concentrated under reduced pressure to give a residue which was used for HPLC analysis.

Phenyl 2-*O*-(2-((naphthalen-2-ylmethoxy) methyl) benzyl)-1-thio-α-D-arabinofuranoside (89). To a solution of compound **83** (1.55 g, 2.41 mmol) in THF (5.2 mL) was

carefully added TBAF (6 mL, 1.0 M in THF) at 0 ˚C. The resulting mixture was warmed gradually to room temperature and stirred for 3 h, after which TLC (hexane ethyl acetate 2:1) indicated the reaction was complete. The crude reaction mixture was then evaporated, and the residue was dissolved in CH_2Cl_2 (40 mL) and washed with saturated aqueous NH_4Cl and brine, and then dried over anhydrous Na_2SO_4 and concentrated to dryness. The crude material was purified by column chromatography (2:1, hexane/ ethyl acetate) to afford the tittle compound (0.97 g, 80%) as a white amorphous solid. $[\alpha]^{RT}_{D}$ = +78 (*c* 0.50, $CHCl_3$); ^{1}H NMR (400 MHz, $CDCl_3$) δ 7.77 – 7.70 (m, 4H), 7.43 – 7.34 (m, 5H), 7.32 – 7.27 (m, 2H), 7.26 – 7.15 (m, 5H), 5.39 (d, *J* = 3.8 Hz, 0H), 4.72 (d, *J* = 12.0 Hz, 1H), 4.64 – 4.61 (m, 3H), 4.61 – 4.59 (m, 1H), 4.52 (d, *J* = 11.6 Hz, 1H), 4.01 (dd, *J* = 7.3, 4.4 Hz, 1H), 3.93 (dt, *J* = 7.2, 3.6 Hz, 0H), 3.84 (dd, *J* = 4.5, 3.8 Hz, 0H), 3.65 (dd, *J* = 12.1, 3.3 Hz, 1H), 3.53 (dd, *J* = 12.2, 3.9 Hz, 1H). ^{13}C NMR (101 MHz, $CDCl_3$) δ 136.1, 135.9, 135.2, 134.1, 133.2, 133.0, 131.5 (2 carbons), 130.0, 129.5, 129.0 (2 carbons), 128.4, 128.3, 128.3, 127.9, 127.7, 127.5, 126.9, 126.2, 126.0, 126.0, 89.6, 89.2, 82.2, 75.5, 72.5, 70.2, 70.0, 61.5. ESIHRMS calcd for $C_{30}H_{30}NaO_5S$ $[M + Na]^+$, 525.1712; found; 525.1720.

Phenyl 3, 5-*O*-dibenzyl-2-*O*-(2-((naphthalen-2-ylmethoxy) methyl) benzyl)-1-thio-α-D-arabinofuranoside (91). Compound **90** (0.8 g, 1.61 mmol) was dissolved in DMF (6.7 mL), cooled to 0 ˚C and treated with benzyl bromide (0.68 mL, 4.0 mmol) followed by portion wise addition of sodium hydride (0.31 mg, 60% suspension in mineral oil, 7.24 mmol). The reaction mixture was allowed to warm to room temperature and stirred for 3 h. After diluting with ethyl acetate, the mixture was washed with brine, dried over anhydrous Na_2SO_4 and concentrated under reduced pressure to dryness. Chromatographic purification of the residue (ethyl acetate/hexanes, 10:1) afforded the title compound as a colorless oil (0.90 g, 83%). $[\alpha]^{RT}_{D}$ = +34 (*c* 0.48, $CHCl_3$); ^{1}H NMR (400 MHz, $CDCl_3$) δ 7.86 – 7.70 (m, 4H), 7.52 – 7.42 (m, 7H), 7.36 – 7.19 (m, 14H),

5.61 (d, *J* = 2.9 Hz, 1H), 4.76 (d, *J* = 12.0 Hz, 1H), 4.70 – 4.58 (m, 5H), 4.57 – 4.43 (m, 4H), 4.39 (dt, *J* = 6.5, 4.5 Hz, 1H), 4.12 (t, *J* = 3.1 Hz, 1H), 4.03 (dd, *J* = 6.6, 3.3 Hz, 1H), 3.68 (dd, *J* = 10.9, 3.9 Hz, 1H), 3.63 (dd, *J* = 10.9, 4.9 Hz, 1H). ^{13}C NMR (101 MHz, $CDCl_3$) δ 138.1, 137.7, 136.3, 135.8, 135.6, 134.8, 133.3, 133.0, 131.2 (2 Carbons), 129.1, 129.1, 128.9(2 Carbons), 128.4 (2 Carbons), 128.3 (2 Carbons), 128.2, 128.1, 128.0, 127.9, 127.8 (2 Carbons), 127.7(4 Carbons), 127.6, 127.1, 126.5, 126.1, 125.9, 125.8, 90.2, 88.6, 83.5, 80.6, 73.3, 72.4, 72.2, 70.0, 69.8, 69.1. ESIHRMS calcd for $C_{44}H_{42}NaO_5S$ $[M + Na]^+$, 705.2651; found; 705.2679.

Phenyl 3, 5-*O*-dibenzyl-2-*O*-(2-hydroxymethyl) benzyl-1-thio-α-D-arabinofuranoside (91). Compound **90** (0.84 g, 1.23 mmol) was subjected to the hydrogenolysis protocol employed for the synthesis of compound **84.** Chromatographic purification the residue after work-up ((ethyl acetate/hexanes, 4:1) afforded the title compound (0.61 g, 92%) as an amorphous solid. $[\alpha]^{RT}_{D}$ = +106 (*c* 0.85, $CHCl_3$); ^{1}H NMR (600 MHz, $CDCl_3$) δ 7.50 – 7.44 (m, 2H), 7.40 (d, *J* = 7.5 Hz, 1H), 7.36 – 7.22 (m, 16H), 5.57 (d, *J* = 2.8 Hz, 1H), 4.72 (d, *J* = 11.5 Hz, 1H), 4.67 (d, *J* = 12.5 Hz, 1H), 4.64 (d, *J* = 12.6 Hz, 1H), 4.60 (d, *J* = 11.5 Hz, 1H), 4.56 (d, *J* = 12.1 Hz, 1H), 4.53 (d, *J* = 11.9 Hz, 1H), 4.50 (d, *J* = 11.7 Hz, 2H), 4.38 (dt, *J* = 6.1, 4.2 Hz, 1H), 4.15 (t, *J* = 3.0 Hz, 1H), 4.03 (dd, *J* = 6.4, 3.2 Hz, 1H), 3.66 (dd, *J* = 10.9, 3.9 Hz, 1H), 3.61 (dd, *J* = 10.9, 4.7 Hz, 1H). ^{13}C NMR (101 MHz, $CDCl_3$) δ 139.9, 138.0, 137.6, 135.1, 134.5, 131.4 (2 carbons), 129.9, 129.3, 129.0 (2 carbons), 128.9, 128.4 (4 carbons), 128.0 (2 carbons), 127.9 (2 carbons), 127.8(2 carbons), 127.8, 127.6, 127.3, 90.0, 88.7, 83.6, 80.8, 73.4, 72.4, 70.9, 69.0, 63.3. ESIHRMS calcd for $C_{33}H_{34}NaO_5S$ $[M + Na]^+$, 565.2025; found; 565.2037.

Isopropyl 3,5-*O*-dibenzyl-2-*O*-(2-hydroxymethyl) benzyl-β-D-arabinofuranoside (94). Pooling of the kinetic runs of thioglycoside donor **91** with isopropanol followed by HPLC purification gave an analytical sample product as a white amorphous solid. $[\alpha]^{RT}_{D}$ = -17 (*c* 0.16,

$CHCl_3$); ^1H NMR (600 MHz, $CDCl_3$) δ 7.42 – 7.17 (m, 14H), 5.02 (d, *J* = 4.0 Hz, 1H), 4.74 (d, *J* = 11.1 Hz, 1H), 4.65 (d, *J* = 10.9 Hz, 2H), 4.62 – 4.57 (m, 3H), 4.56 – 4.52 (m, 2H), 4.13 (q, *J* = 6.0 Hz, 1H), 4.10 – 4.03 (m, 2H), 3.88 (sept, *J* = 6.2 Hz, 1H), 3.57 – 3.45 (m, 3H), 1.11 (d, *J* = 6.2 Hz, 3H), 1.03 (d, *J* = 6.1 Hz, 3H). ^{13}C NMR (151 MHz, $CDCl_3$) δ 140.9, 137.9, 135.8, 130.5, 129.9, 129.0, 128.4, 127.9, 127.8, 127.7, 97.9, 84.7, 83.9, 80.4, 73.3, 72.7, 72.4, 72.1, 69.0, 63.6, 23.2, 20.6. ESIHRMS calcd for $C_{30}H_{36}NaO_6$ $[M + Na]^+$, 515.2410; found; 515.2415.

Isopropyl 3, 5-*O*-dibenzyl-2-*O*-(2-hydroxymethyl) benzyl-α-D-arabinofuranoside (93). Pooling of the kinetic runs of donor with isopropanol followed by HPLC purification (hexane/ethyl acetate, 95:5-75:25) gave an analytical sample product as a white amorphous solid. $[\alpha]^{RT}_{D=}$ +43 (*c* 0.07, $CHCl_3$); ^1H NMR (600 MHz, Chloroform-*d*) δ 7.41 – 7.22 (m, 14H), 5.13 (d, *J* = 1.4 Hz, 1H), 4.68 – 4.58 (m, 4H), 4.56 (d, *J* = 12.2 Hz, 1H), 4.54 – 4.50 (m, 2H), 4.46 (d, *J* = 12.0 Hz, 1H), 4.17 (ddd, *J* = 6.9, 5.0, 3.5 Hz, 1H), 4.02 (dd, *J* = 3.3, 1.5 Hz, 1H), 3.95 – 3.88 (m, 2H), 3.61 (dd, *J* = 10.8, 3.6 Hz, 1H), 3.55 (dd, *J* = 10.8, 5.1 Hz, 1H), 1.20 (d, *J* = 6.2 Hz, 3H), 1.14 (d, *J* = 6.1 Hz, 3H).^{13}C NMR (151 MHz, $CDCl_3$) δ 140.0, 138.1, 137.9, 135.4, 130.0, 129.4, 128.8, 128.3, 128.0, 127.8, 127.7, 127.6, 103.7, 89.0, 83.6, 80.2, 73.3, 72.2, 70.7, 69.6, 69.1, 63.4, 23.6, 21.4. ESIHRMS calcd for $C_{30}H_{36}NaO_6$ $[M + Na]^+$, 515.2410; found; 515.2408.

3, 5-*O*-dibenzyl-1,2-di-(1,2-xylylene)-β-D-arabinofuranoside. The protocol employed for the synthesis cyclized product **85** and **86** was used to convert thioglycoside donor **91** (60 mg, 0.11mmol) to give cyclized product **92** (43 mg, 92%,) as white needles (m.p 112 ˚C), $[\alpha]^{RT}_{D=}$ +45 (*c* 0.31, $CHCl_3$);^1H NMR (600 MHz, $CDCl_3$) δ 7.34 – 7.28 (m, 7H), 7.28 – 7.25 (m, 5H), 7.19 – 7.12 (m, 2H), 5.40 (d, *J* = 13.5 Hz, 1H), 5.34 (d, *J* = 4.5 Hz, 1H), 4.99 (d, *J* = 13.4 Hz, 1H), 4.75 (d, *J* = 13.3 Hz, 1H), 4.68 (d, *J* = 11.8 Hz, 1H), 4.61 – 4.56 (m, 4H), 4.21 (t, *J* = 4.3 Hz, 1H), 4.06

– 3.94 (m, 2H), 3.75 – 3.60 (m, 2H). ^{13}C NMR (151 MHz, $CDCl_3$) δ 138.1, 137.8, 137.1, 137.0, 129.3, 128.5, 128.4, 128.3, 128.0, 128.0, 127.8, 127.7, 127.7, 127.5, 102.3, 85.5, 83.4, 78.4, 73.4, 72.3, 72.2, 70.5, 69.1. ESIHRMS calcd for $C_{27}H_{28}NaO_5$ $[M + Na]^+$, 455.1834; found; 455.1834.

Competition kinetics with 3,5-*O*-dibenzyl arabinosyl thioglycoside (91). The thioglycoside **91** (20 mg, 0.037 mmol) was coevaporated with toluene 3 times; 4Å molecular sieves (30 mg), and anhydrous dichloromethane (0.46 mL, 0.08 M) were added. The solution was cooled to -20 °C under argon and the corresponding acceptor (2.1-10 Eq) was added. After stirring for a further 10 min NIS (16.5 mg, 0.074 mmol) was added followed by AgOTf (4 mg, 0.014 mmol). The reaction mixture was then stirred at the same temperature for 1 h during which the appearance of persistent characteristic iodine color was observed. The reaction was quenched at -20 °C by the addition of Et_3N (5 µL). The suspension was diluted with dichloromethane (2 mL) and filtered through Celite. The filtrate was washed successively with aqueous $Na_2S_2O_3$ (2 mL) and brine (2 mL). The organic layer was dried over anhydrous Na_2SO_4 and concentrated under reduced pressure to give a residue which was used for HPLC analysis

1,3-Difluoropropan-2-yl 3,5-*O*-(di-*tert*-butylsilylene)-2-*O*-((2-hydroxymethyl) benzyl)-1-thio-α/β-D-arabinofuranoside (95 and 96). Prepared from thioglycoside **84** (23 mg, 0.05 mmol) and 1, 3-difluoropropan-2-ol (50 µL) using the same glycosylation protocol as for compounds **86** and **87** above. Careful chromatographic purification (hexane/ ethyl acetate 8:1-4:1) afforded minor α-isomer **95** (5 mg, 15 %) as colorless oils and major β-isomer **96** (9 mg, 41%)

β-isomer **96**: $[\alpha]^{RT}_{D}$ = -62 (*c* 0.06, $CHCl_3$) ^{1}H NMR (600 MHz, $CDCl_3$) δ 7.45 – 7.40 (m, 1H), 7.38 – 7.33 (m, 1H), 7.30 – 7.27 (m, 2H), 5.19 (d, *J* = 5.1 Hz, 1H), 4.96 (d, *J* = 11.3 Hz, 1H), 4.81 (d, *J* = 11.3 Hz, 1H), 4.70 (dd, *J* = 12.1, 6.8 Hz, 1H), 4.63 (dd, *J* = 12.2, 7.0 Hz, 1H), 4.59 – 4.42 (m,

4H), 4.40 – 4.33 (m, 1H), 4.30 (ddd, *J* = 9.1, 5.1, 0.8 Hz, 1H), 4.11 – 4.00 (m, 1H), 3.97 (ddd, *J* = 9.1, 5.2, 0.8 Hz, 1H), 3.88 (d, *J* = 9.8 Hz, 1H), 3.69 (ddd, *J* = 10.3, 9.3, 5.0 Hz, 1H), 3.37 (t, *J* = 7.0 Hz, 1H), 1.05 (s, 9H), 0.98 (s, 9H). ^{13}C NMR (151 MHz, $CDCl_3$) δ 141.1, 135.4, 130.7, 130.0, 129.2, 127.9, 99.9, 82.4, 81.9 (dd, *J* = 171.4, 6.0 Hz), 81.3 (dd, *J* =172.3, 8.2 Hz), 80.7, 78.3, 75.2 (t, *J* = 20.3 Hz), 73.8, 71.6, 68.3, 63.6, 27.4, 27.1, 22.5, 20.1. ESIHRMS calcd for $C_{24}H_{38}F_2NaO_6Si$ $[M + Na]^+$, 511.2303; found; 511.2303.

α-isomer **95**. $[\alpha]^{RT}_{D}$ = +16 (*c* 0.17, $CHCl_3$) ^{1}H NMR (600 MHz, $CDCl_3$) δ 7.45 – 7.41 (m, 1H), 7.38 – 7.31 (m, 2H), 7.31 – 7.27 (m, 1H), 5.13 (d, *J* = 3.2 Hz, 1H), 4.83 (s, 2H), 4.74 – 4.68 (m, 2H), 4.65 – 4.41 (m, 4H), 4.32 – 4.29 (m, 1H), 4.06 (dd, *J* = 8.9, 7.6 Hz, 1H), 4.04 – 4.00 (m, 0H), 3.98 (dd, *J* = 7.6, 3.2 Hz, 1H), 3.95 – 3.88 (m, 2H), 1.05 (s, 9H), 0.97 (s, 9H). ^{13}C NMR (151 MHz, $CDCl_3$) δ 140.4, 135.0, 130.3, 129.9, 129.0, 127.9, 106.8, 87.0, 81.67 (dd, *J* = 171.8, 5.9 Hz), 81.48 (dd, *J* = 172.2, 8.1 Hz), 80.5, 75.32 (t, *J* = 20.0 Hz), 73.7, 71.2, 67.3, 63.4, 27.4, 27.0, 22.6, 20.1. ESIHRMS calcd for $C_{24}H_{38}F_2NaO_6Si$ $[M + Na]^+$, 511.2303; found; 511.2303.

2-Fluoroethyl 3,5-*O*-(di-*tert*-butylsilylene)-2-*O*-((2-hydroxymethyl) benzyl)-1-thio-α/β-D-arabinofuranoside (97 and 98). The thioglycoside **84** (60 mg, 0.12 mmol) was coevaporated with toluene 3 times and kept in vacuo for 3 h. 4Å Molecular sieves (100 mg) and anhydrous dichloromethane (7.4 mL) were added and the reaction mixture was stirred for 1 h at room temperature prior to cooling to -20 °C under argon. 2-Fluoroethanol (1.1 mL, 16.95 mmol) was added and the reaction mixture stirred for 10 min before solid NIS (54 mg, 0.24 mmol) was added followed by AgOTf (15 mg, 0.06 mmol). The reaction mixture was then stirred at the same temperature for 1 h during which the appearance of persistent characteristic brown color was observed. The reaction was quenched at -20 °C by the addition of Et_3N (50 µL). The suspension

was diluted with EtOAc and filtered through Celite, The filtrate was washed successively with saturated aqueous $Na_2S_2O_3$ and brine. The organic layer was dried over anhydrous Na_2SO_4 and concentrated under diminished pressure to give the crude product, which was purified by flash column chromatography (hexane/ ethyl acetate 9:1-4:1) to afford a major isomer **98** (28 mg, 52%) and minor isomer **97** (11 mg, 20%) as colorless oils.

Major β-isomer **98**: $[\alpha]^{RT}_{D}$ = -56 (*c* 0.40, $CHCl_3$); ^{1}H NMR (600 MHz, $CDCl_3$) δ 5.04 (d, *J* = 5.3 Hz, 1H), 5.01 (d, *J* = 11.3 Hz, 1H), 4.79 (d, *J* = 11.3 Hz, 1H), 4.72 (dd, *J* = 12.1, 6.1 Hz, 1H), 4.62 (dd, *J* = 12.2, 7.8 Hz, 1H), 4.59 – 4.53 (m, 1H), 4.52 – 4.46 (m, 1H), 4.37 (t, *J* = 9.1 Hz, 1H), 4.30 (dd, *J* = 9.1, 5.1 Hz, 1H), 3.98 (dd, *J* = 9.0, 5.3 Hz, 1H), 3.90 (dd, *J* = 10.7, 9.0 Hz, 1H), 3.87 – 3.82 (m, 1H), 3.75 – 3.63 (m, 2H), 3.51 (dd, *J* = 7.9, 6.2 Hz, 1H), 1.06 (s, 9H), 0.99 (s, 9H). ^{13}C NMR (151 MHz, $CDCl_3$) δ 141.1, 135.6, 130.8, 130.0, 129.2, 127.8, 100.1, 82.5 (d, *J* = 169.4 Hz), 80.9, 78.6, 73.6, 71.7, 68.3, 67.6 (d, *J* = 20.4 Hz), 63.6, 27.5, 27.1, 22.5, 20.1. ESIHRMS calcd for $C_{23}H_{37}FNaO_6Si$ $[M + Na]^+$, 479.2241; found; 479.2241

Minor α-isomer **97:** (11 mg, 20%) as a colorless oil. $[\alpha]^{RT}_{D}$ = +17 (*c* 0.40, $CHCl_3$) ^{1}H NMR (600 MHz, $CDCl_3$) δ 7.44 – 7.41 (m, 1H), 7.37 – 7.32 (m, 2H), 7.31 – 7.26 (m, 1H), 4.97 (d, *J* = 3.2 Hz, 1H), 4.86 (d, *J* = 11.7 Hz, 1H), 4.79 (d, *J* = 11.7 Hz, 1H), 4.71 (br,s, 2H), 4.63 – 4.57 (m, 1H), 4.55 – 4.51 (m, 1H), 4.33 – 4.27 (m, 1H), 4.07 (dd, *J* = 9.0, 7.5 Hz, 1H), 3.98 (dd, *J* = 7.5, 3.2 Hz, 1H), 3.95 – 3.88 (m, 3H), 3.88 – 3.83 (m, 1H), 3.74 – 3.62 (m, 1H), 2.68 (br,s, 1H), 1.05 (s, 9H), 0.97 (s, 9H). ^{13}C NMR (151 MHz, $CDCl_3$) δ 140.4, 135.1, 130.4, 129.9, 129.0, 127.9, 106.8, 87.1, 82.6 (d, *J* = 169.2 Hz), 80.7, 73.7, 71.2, 67.7 (d, *J* = 20.1 Hz), 63.4, 27.4, 27.0, 22.6, 20.1. ESIHRMS calcd for $C_{23}H_{37}FNaO_6Si$ $[M + Na]^+$, 479.2241; found; 479.2239

General hydrogenolytic cleavage procedure. 20% $Pd(OH)_2$ /C was dispersed in EtOAc-EtOH (40 mL/mmol, 1:2) under argon. The mixture was degassed, purged 4 times and saturated with hydrogen. After 40-60 min of vigorous stirring, the substrate was quickly added as a solution of EtOH-EtOAc (2:1, 0.05M) to the suspension. The reaction mixture was purged again 4 times, and allowed to stir at room temperature under a hydrogen atmosphere (3 atm) until complete by TLC. The catalyst was removed by filtration through Celite and washed with EtOAc. The filtrate were concentrated, and the resulting crude product was purified by silica gel column chromatography (ethyl acetate/hexane) to give desired compounds **99**, **101,106, 113, 115 and 121**

2-((2-(Naphthalen-2-ylmethoxy)ethyl)thio) ethanol (99). To the suspension of sodium hydride (0.43 g, 10.9 mmol, 60% in mineral oil) in dry THF (30 mL), under argon, cooled to 0 °C, was slowly added 2,2-thiodiethanol (3.3 g, 27.15 mmol). The reaction was stirred for 1 h. 2–(Bromomethyl) naphthalene (2.0 g, 9.05 mmol) in dry THF (20 ml) was added dropwise, and the reaction mixture was stirred an additional 5 h. The reaction mixture was diluted with water (50 mL).The solution was extracted diethyl ether (50 mL x 2). The organic layer was washed with water and brine and dried over Na_2SO_4, and the solvent was evaporated under reduced pressure. Chromatographic purification (hexane ethyl acetate 6:1-2:1) gave the title compound **1** (1.78 g, 75%) as a pale yellow oil. ^{1}H NMR (400 MHz, $CDCl_3$) δ 7.87 – 7.76 (m, 4H), 7.53 – 7.43 (m, 3H), 4.71 (s, 2H), 3.71 (t, *J* = 6.0 Hz, 2H), 3.69 (t, *J* = 6.4 Hz, 2H), 2.78 (t, *J* = 6.4 Hz, 2H). 2.76 (t, *J* = 6.0 Hz, 2H). ^{13}C NMR (101 MHz, $CDCl_3$) δ 135.3, 133.2, 133.0, 128.3, 127.9, 127.7, 126.6, 126.2, 126.0, 125.7, 73.3, 69.9, 60.8, 35.9, 31.6. ESIHRMS calcd for $C_{22}H_{24}O_2SNa$ $[M + Na]^+$, 385.0925; found; 385.0921.

2-(2-Naphthalen-2-ylmethoxy)ethyl-2-(benzyloxy)ethyl) sulfide (100). A solution of compound 1(1.2 g, 4.58 mmol) was dissolved in dry DMF (22 mL) under argon, cooled to 0 ˚C and treated with NaH (0.27 g, 60% dispersion in mineral oil). The mixture was stirred for 10 minutes followed by slow addition of benzyl bromide (0.61 ml, 5.04 mmol,). The reaction mixture was warmed to room temperature and stirred for 2 h before it was cooled to 0 ˚C and quenched with MeOH (1 mL) and concentrated in *vacuo*. The concentrate was dissolved in ethyl acetate, washed with water and brine, dried over Na_2SO_4 and concentrated. The residue was purified by silica gel column chromatography (hexane-ethyl acetate (9:1)) to give the title compound (1.3 g, 81%) as a colorless oil. ;^{1}H NMR (600 MHz, $CDCl_3$) δ 7.85 – 7.81 (m, 3H), 7.80 – 7.76 (m, 1H), 7.51 – 7.43 (m, 3H), 7.36 – 7.31 (m, 4H), 7.30 – 7.26 (m, 1H), 4.69 (s, 2H), 4.51 (s, 2H), 3.69 (t, *J* = 6.7 Hz, 2H), 3.65 (t, *J* = 6.7 Hz, 2H), 2.82 (t, *J* = 6.1 Hz, 2H), 2.80 (t, *J* = 6.1 Hz, 2H). ^{13}C NMR (151 MHz, $CDCl_3$) δ 138.1, 135.6, 133.2, 133.0, 128.4, 128.2, 127.9, 127.8, 127.7, 127.6, 126.4, 126.1, 125.9, 126.0, 73.1, 73.0, 70.0, 32.1, 32.1. ESIHRMS calcd for $C_{22}H_{24}O_2SNa$ $[M + Na]^+$, 375.1395; found; 375.1396.

Phenyl 2,3,4-tri-*O*-benzyl-6-*O*-(2-naphthyl)methyl-1-thio-α-D-mannopyranoside (104). A solution of **6**[154] (0.30 g, 0.57 mmol) in anhydrous DMF (6 mL), was cooled to 0 ˚C, treated with NaH (60% dispersion in mineral oil, 33 mg,) under argon, and stirred for 20 min. A solution 2–(bromomethyl) naphthalene (0.33 mg, 1.5 mmol,) in DMF (2 mL) was added slowly followed by TBAI (40 mg, 0.11 mmol). The reaction mixture was stirred for 12 h after which it was quenched with methanol (0.2 mL) and water (10 mL). The mixture was extracted with ethyl acetate, and the combined organic phase was washed with HCl (1 M), saturated $NaHCO_3$, brine, dried over Na_2SO_4, filtered and concentrated in *vacuo*. The resulting brown oil was purified by silica chromatography, eluting with hexane-ethyl acetate (9:1) to give the desired compound **4**

(0.29 g, 74%) as colorless oil. $[\alpha]^{RT}_{D}$ = +44 (*c* 0.24, $CHCl_3$); ^{1}H NMR (600 MHz, $CDCl_3$) δ 7.83 – 7.80 (m, 1H), 7.78 – 7.75 (m, 3H), 7.49 – 7.44 (m, 5H), 7.40 – 7.27 (m, 10H), 7.25 – 7.15 (m, 6H), 7.14 – 7.09 (m, 2H), 5.64 (d, *J* = 1.7 Hz, 1H), 4.91 (d, *J* = 10.7 Hz, 1H), 4.82 (d, *J* = 12.4 Hz, 1H), 4.75 (d, *J* = 12.4 Hz, 1H), 4.66 (d, *J* = 12.4 Hz, 1H), 4.64 (d, *J* = 12.4 Hz, 1H), 4.62 (d, *J* = 11.7 Hz, z1H), 4.60 (d, *J* = 11.7 Hz, 1H), 4.52 (d, *J* = 10.7 Hz, 1H), 4.32 (ddd, *J* = 9.9, 5.1, 1.9 Hz, 1H), 4.10 (t, *J* = 9.6 Hz, 1H), 4.02 (dd, *J* = 3.2, 1.7 Hz, 1H), 3.91 – 3.87 (m, 2H), 3.80 (dd, *J* = 10.9, 1.9 Hz, 1H). ^{13}C NMR (151 MHz, $CDCl_3$) δ 138.3, 138.2, 137.9, 135.8, 134.4, 133.2, 132.9, 131.6, 129.0, 128.4, 128.4, 128.3, 128.0, 127.9, 127.9, 127.8, 127.7, 127.7, 127.6, 127.4 126.4, 126.0, 125.9, 125.7, 85.8, 80.2, 76.3, 75.2, 75.0, 73.4, 72.8, 72.1, 71.9, 69.1 ESIHRMS calcd for $C_{44}H_{42}O_5SNa$ $[M + Na]^+$,705.2651; found; 705.2654.

Phenyl 3, *O*-benzyl-2-*O*-(2-naphthyl)methyl-1-thio-α-D-mannopyranoside (106). A solution of phenyl 3-*O*-benzyl-4,6-*O*-benzyliden-2-(2-naphtylmethyl)-1-thio-α-D-mannopiranoside[155] (0.6 g, 1.02 mmol) in $CHCl_3$-MeOH (4:1, 16 mL) was treated with p-TsOH monohydrate (0.2 g, 1.02 mmol) and stirred under argon at room temperature for 2 h, after which, it was quenched with triethylamine (0.2 mL) and concentrated. The crude mixture was purified by flash column chromatography (hexane/ethyl acetate 1:1) to give the desired product (0.44 g, 89%) as a colorless oil. $[\alpha]^{RT}_{D}$ = +0.4 (*c* 0.55, $CHCl_3$); ^{1}H NMR (600 MHz, $CDCl_3$) δ 7.83 – 7.79 (m, 1H), 7.78 – 7.75 (m, 2H), 7.74 – 7.71 (m, 1H), 7.50 – 7.44 (m, 3H), 7.38 – 7.35 (m, 2H), 7.34 – 7.28 (m, 5H), 7.27 – 7.23 (m, 3H), 5.55 (d, *J* = 1.5 Hz, 1H), 4.82 (d, *J* = 12.3 Hz, 1H), 4.72 (d, *J* = 12.3 Hz, 1H), 4.57 (d, *J* = 11.7 Hz, 1H), 4.49 (d, *J* = 11.7 Hz, 1H), 4.16 (t, *J* = 9.1Hz 1H), 4.14 – 4.10 (m, 1H), 4.05 (dd, *J* = 3.0, 1.5 Hz, 1H), 3.92 – 3.80 (m, 2H), 3.71 (dd, *J* = 9.1, 3.0 Hz, 1H). ^{13}C NMR (151 MHz, $CDCl_3$) δ 137.7, 135.1, 133.8, 133.2, 133.1, 131.9, 129.1, 128.6 128.3, 128.0,

127.9, 127.9, 127.7, 127.7, 126.8, 126.2, 126.1, 125.9, 86.2, 79.6, 75.5, 73.3, 72.33, 71.8, 67.3, 62.7. ESIHRMS calcd for $C_{30}H_{30}O_5SNa$ $[M + Na]^+$, 525.1712; found; 525.1719.

Phenyl 3,4,6-tri-*O*-benzyl-2-*O*-(2-naphthyl)methyl-1-thio-α-D-mannopyranoside (107). To a solution of phenyl 3-*O*-benzyl-2-*O*-(2-naphthyl)methyl-1-thio-α-D-mannopyranoside **7** (0.27 g, 0.54 mmol) in anhydrous DMF (2.6 mL) was added NaH (86 mg, 60% dispersion in mineral oil) at -15 °C. After stirring for 5 min BnBr (0.15 mL, 1.23 mmol) was added, and the mixture was warmed to room temperature and stirred for 6 h. The reaction mixture was carefully quenched with MeOH (0.4 mL, at 0 °C) and diluted with ethyl acetate, washed with water and brine. The organic layer was dried over Na_2SO_4 and concentrated. The residue was purified by column chromatography on silica gel (hexane: ethyl acetate 9:1) to afford compound **107** as a colorless oil (0.32 g, 88%). $[\alpha]^{RT}_{D =}$ +33 (*c* 0.42, $CHCl_3$); ^{1}H NMR (600 MHz, $CDCl_3$) δ 7.85 – 7.81 (m, 1H), 7.80 – 7.71 (m, 3H), 7.52 (dd, *J* = 8.4, 1.7 Hz, 1H), 7.50 – 7.46 (m, 2H), 7.44 – 7.41 (m, 2H), 7.37 – 7.27 (m, 12H), 7.23 (dt, *J* = 9.3, 7.3 Hz, 5H), 5.65 (d, *J* = 1.7 Hz, 1H), 4.95 (d, *J* = 10.8 Hz, 1H), 4.91 (d, *J* = 12.5 Hz, 1H), 4.81 (d, *J* = 12.5 Hz, 1H), 4.69 (d, *J* = 12.0 Hz, 1H), 4.65 (d, *J* = 11.7 Hz, 1H), 4.62 (d, *J* = 11.7 Hz, 1H), 4.58 (d, *J* = 10.8 Hz, 1H), 4.52 (d, *J* = 12.0 Hz, 1H), 4.31 (ddd, *J* = 9.9.6, 5.1, 1.9 Hz, 1H), 4.13 (t, *J* = 9.6 Hz, 1H), 4.07 (dd, *J* = 3.1, 1.7 Hz, 1H), 3.92 – 3.85 (m, 2H), 3.78 (dd, *J* = 9.6, 3.1 Hz, 1H). ^{13}C NMR (151 MHz, $CDCl_3$) δ 138.4, 138.4, 138.2, 135.4, 134.4, 133.2, 133.0, 131.7, 129.0, 128.4, 128.4, 128.3, 128.2, 128.0, 128.0, 127.8, 127.8, 127.7, 127.6, 127.5, 127.4, 126.8, 126.1, 126.0, 126.0, 85.9, 80.2, 76.2, 75.2, 75.0, 73.3, 72.8, 72.2, 72.0, 69.2. ESIHRMS calcd for $C_{44}H_{42}O_5SNa$ $[M + Na]^+$, 705.2651; found; 705.2654.

***tert*-Butyl 2,3,4-tri-*O*-benzyl-1-thio-β-D-mannopyranoside (110).** To a solution of *tert*-butyl 2,3-*O*-benzyl-4,6-*O*-benzylidene-1-thio-*β*-D-mannopyranoside **14**[156] (130 mg, 0.25 mmol)

in dry DCM (3 mL) was added BH_3.THF (1.0 M in THF, 1.3 mL, 1.25 mmol) under argon with stirring. After 10 mins yttrium (III) trifluoromethanesulfonate (15.5mg, 0.025 mmol) was added and the reaction mixture was stirred under argon at room temperature for 2 h. The reaction mixture was cooled to 0 ˚C, then triethylamine (50 µL, 0.04 mmol) was added dropwise followed by slow addition of methanol (100 µL). The solvent was removed under reduced pressure and the crude mixture was co-evaporated with methanol to give a residue, which was purified by flash column chromatography on silica gel using hexane-ethyl acetate (4:1) as eluent. The product was obtained as a light yellow oil (117 mg, 90 %). $[\alpha]^{RT}_{D=}$ -23 (*c* 1.78, $CHCl_3$); ^{1}H NMR (600 MHz, $CDCl_3$) δ 7.59 – 7.04 (m, 15H), 4.94 (d, *J* = 11.3 Hz, 1H), 4.91 (d, *J* = 11.3 Hz, 1H), 4.79 (d, *J* = 10.9 Hz, 1H), 4.72 (d, *J* = 11.8 Hz, 1H), 4.67 (d, *J* = 11.8 Hz, 2H), 4.66 (d, *J* = 1.0 Hz, 1H), 4.64 (d, *J* = 10.9 Hz, 1H), 4.00 (dd, *J* = 3.0, 1.0 Hz, 1H), 3.90 (t, *J* = 9.5 Hz, 1H), 3.84 (dd, *J* = 11.9, 3.0 Hz, 1H), 3.40 – 3.33 (m, 1H), 1.36 (s, 9H). ^{13}C NMR (151 MHz, $CDCl_3$) δ 138.3, 138.1, 128.4, 128.4, 128.2, 128.1, 128.1, 127.8, 127.7, 127.5, 127.4, 84.5, 82.3, 79.9, 78.5, 77.2, 77.0, 76.9, 75.3, 75.2, 74.9, 72.3, 62.7, 43.3, 31.6. ESIHRMS calcd for $C_{31}H_{38}O_5SNa$ $[M + Na]^+$, 545.2338; found; 545.2341.

***tert*-Butyl 2,3,4-tri-*O*-benzyl-6-*O*-(2-naphthyl)methyl-1-thio-β-D-mannopyranoside (111).** This compound was synthesized from **15**, using the same procedure as used in the preparation of compound **7**, in 72% yield as a pale yellow oil. $[\alpha]^{RT}_{D=}$ -19.7 (*c* 0.62, $CHCl_3$) ^{1}H NMR (600 MHz, $CDCl_3$) δ 7.83 – 7.68 (m, 4H), 7.54 – 7.38 (m, 5H), 7.33 – 7.12 (m, 13H), 4.93 (d, *J* = 11.5 Hz, 1H), 4.86 (d, *J* = 10.9 Hz, 1H) 4.84 (d, *J* = 11.5 Hz, 1H), 4.73 (d, *J* = 12.1 Hz, 1H), 4.71 (d, *J* = 12.1 Hz, 1H) 4.69 (d, *J* = 11.8 Hz, 1H), 4.66 (d, *J* = 1.0 Hz, 1H) 4.63 (d, *J* = 11.8 Hz, 1H), 4.55 (d, *J* = 10.9 Hz, 1H), 3.99 (dd, *J* = 3.1, 1.0 Hz, 1H), 3.88 (t, *J* = 9.5 Hz, 1H), 3.80 (dd, *J* = 10.8, 1.8 Hz, 1H), 3.72 (dd, *J* = 10.8, 6.5 Hz, 1H), 3.64 (dd, *J* = 9.5, 3.0 Hz, 1H), 3.54 –

3.50 (m, 1H), 1.39 (s, 9H). ^{13}C NMR (151 MHz, $CDCl_3$) δ 138.2, 138.2, 136.0, 132.9, 128.4, 128.2, 128.1, 128.0, 128.0, 127.9, 127.6, 127.6, 127.5, 127.4, 126.3, 125.9, 125.9, 125.6, 84.7, 82.1, 79.8, 78.2, 75.1, 75.0, 74.9, 73.4, 72.2, 69.9, 43.4, 31.7. ESIHRMS calcd for $C_{31}H_{38}O_5SNa$ $[M + Na]^+$, 685.2964; found; 685.2969.

Phenyl 2,3,4-tri-*O*-benzyl-6-*O*-(2-naphthyl)methyl-1-thio-β-D-glucopyranoside (114). This compound was synthesized from **112,** using the same protocol for the synthesis of **108**, in 81% yield as a colorless oil. $[\alpha]^{RT}_{D}$ = +3 (*c* 1.78, $CHCl_3$); ^{1}H NMR (600 MHz, $CDCl_3$) δ 7.86 – 7.78 (m, 4H), 7.63 – 7.58 (m, 2H), 7.49 – 7.45 (m, 3H), 7.41 – 7.37 (m, 2H), 7.36 – 7.26 (m, 8H), 7.26 – 7.18 (m, 6H), 7.15 – 7.10 (m, 2H), 4.90 (d, *J* = 10.3 Hz, 2H), 4.85 (d, *J* = 10.9 Hz, 1H), 4.82 (d, *J* = 10.9 Hz, 1H), 4.77 (d, *J* = 12.2 Hz, 1H), 4.74 (d, *J* = 10.2 Hz, 1H), 4.71 (d, *J* = 9.9 Hz, 1H), 4.69 (d, *J* = 7.7 Hz, 1H), 4.58 (d, *J* = 10.8 Hz, 1H), 3.83 (dd, *J* = 10.9, 1.9 Hz, 1H), 3.77 (d, *J* = 4.7 Hz, 1H), 3.72 (t, *J* = 8.9 Hz, 1H), 3.67 (t, *J* = 9.4 Hz, 1H), 3.57 – 3.50 (m, 2H). ^{13}C NMR (151 MHz, $CDCl_3$) δ 138.4, 138.0, 137.9, 135.7, 133.8, 133.3, 133.0, 131.9, 128.9, 128.4, 128.4, 128.4, 128.2, 128.1, 127.9, 127.9, 127.8, 127.8, 127.8, 127.7, 127.4, 126.4, 126.1, 125.8, 125.8, 87.5, 86.7, 80.8, 79.1, 77.8, 75.8, 75.4, 75.0, 73.5, 69.0. ESIHRMS calcd for $C_{44}H_{42}O_5SNa$ $[M + Na]^+$, 705.2651; found; 705.2651.

***N*-(*tert*-Butoxycarbonyl)-*O*-(2-naphthyl)methyl-L-serine Methyl Ester (118).** A solution of *N*-Boc-L-serine (2.1 g, 10.2 mmol) in anhydrous DMF (20 mL) was cooled to -15 ˚C, treated with NaH (0.6 g, 10.5 mmol, 60% dispersion in mineral oil) under argon and stirred for 30 min. A solution 2–(bromomethyl)naphthalene (2.26 mg, 10.24 mmol,) in DMF (5 mL) was slowly added followed by TBAI (0.36 g, 0.1 mmol). The reaction mixture was stirred for 12 h after which it was diluted with ethyl acetate (20 mL) and poured into water, and extracted with ethyl acetate. The organic layer was washed with HCl (0.5M), and water, dried (MgSO4) and concentrated in

vacuo. The residue (2.0 g) was dissolved in acetone (40 mL), cooled to 0 ˚C and slowly added K_2CO_3 (1.1 g, 8.6 mmol) followed by MeI (0.8 mL, 5.7 mmol). The reaction mixture was warmed to room temperature and stirred for 10 h, then was filtered and diluted with ethyl acetate, washed with $Na_2S_2O_5$, water, brine and dried over Na_2SO_4, and concentrated in *vacuo*. Chromatographic purification (hexane: ethyl acetate 85:15) the title compound (2.2 g, 60% in 2 steps) as a colorless oil. $[\alpha]^{RT}_{D}$ = +12 (*c* 2.80, $CHCl_3$) ^{1}H NMR (600 MHz, $CDCl_3$) δ 7.84 – 7.78 (m, 3H), 7.71 (s, 1H), 7.51 – 7.44 (m, 2H), 7.38 (dd, *J* = 8.5, 1.7 Hz, 1H), 5.42 (d, *J* = 8.8 Hz, 0H), 4.70 (d, *J* = 12.3 Hz, 1H), 4.63 (d, *J* = 12.3 Hz, 1H), 4.50 – 4.37 (m, 1H), 3.89 (dd, *J* = 9.4, 3.3 Hz, 1H), 3.73 (s, 3H), 3.71 (dd, *J* = 9.7, 3.7 Hz, 1H), 1.43 (s, 9H). ^{13}C NMR (151 MHz, $CDCl_3$) δ 171.2, 155.4, 135.0, 133.2, 133.0, 128.2, 127.8, 127.7, 126.4, 126.2, 126.0, 125.5, 80.0, 73.3, 70.0, 54.0, 52.4, 28.3 ESIHRMS calcd for $C_{20}H_{25}NO_5Na$ $[M + Na]^+$, 382.1630; found; 382.1632.

***N*-(*tert*-Butoxycarbonyl)-(*O*-benzyl-L-serinyl)-*O*-(2-naphthyl)methyl)-L-serine methyl ester (121).** A solution of compound **118** (175 mg, 0.49 mmol) in dichloromethane (5 mL) was treated with trifluoroacetic acid (0.5 mL) at room temperature and stirred for 2 h. The volatiles were removed in *vacuo*. The crude product was dissolved in ethyl acetate, washed with saturated Na_2CO_3, followed by brine. The organic layer was dried over Na_2SO_4 and concentrated in *vacuo* to give the crude amine **119** (120 mg, 0.46 mmol) which was used without further purification. In a separate dry round bottom flask, a solution of *N*-Boc-*O*-benzyl-L-serine **120** (155 mg, 0.52 mmol) in DMF (3 mL) was treated with HATU (200 mg, 0.52 mmol) and DIPEA (0.3 mL). The reaction mixture was stirred for 30 min at room temperature followed by addition of the solution of compound **119** (120 mg, 0.46 mmol) in dry DMF (1 mL). The resulting reaction mixture was stirred for a further 3 h, then cooled to 0 ˚C and quenched with trimethylamine (100 µL), diluted with H_2O (2 mL) and extracted with EtOAc (4 mL x 2). The organic layers were dried

over Na_2SO_4 and concentrated in *vacuo* then purified by silica gel chromatography (hexane-ethyl acetate 2:1) to give the title compound (77 mg, 69 %) as colorless oil. $[\alpha]^{RT}_{D=}$ +21 (*c* 0.90, $CHCl_3$); ^{1}H NMR (400 MHz, CD_3OD) δ 7.83 – 7.78 (m, 3H), 7.72 (br s, 1H), 7.48 – 7.43 (m, 2H), 7.38 (dd, *J* = 8.5, 1.7 Hz, 1H), 7.32 – 7.19 (m, 6H), 4.70 (t, *J* = 3.9 Hz, 1H), 4.64 (d, *J* = 12.2 Hz, 1H), 4.57 (d, *J* = 12.2 Hz, 1H), 4.50 (d., *J* = 12.0 Hz, 1H), 4.47 (d, *J* = 12.1 Hz, 1H), 4.38 (t, *J* = 5.4 Hz, 1H), 3.88 (dd, *J* = 9.8, 4.3 Hz, 1H), 3.75 – 3.68 (m, 3H), 3.67 (s, 3H), 1.42 (s, 9H). ^{13}C NMR (101 MHz, CD_3OD) δ 171.4, 170.3, 156.3, 137.8, 135.2, 133.3, 133.1, 128.0, 127.8, 127.7, 127.5, 127.4, 127.4, 127.3, 126.2, 125.8, 125.6, 125.4, 79.5, 72.8, 72.8, 72.7, 69.7, 69.1, 54.4, 52.8, 51.6, 27.3. ESIHRMS calcd for $C_{30}H_{36}N_2O_7Na$ $[M + Na]^+$, 559.2420; found; 559.2421.

***N*-(*tert*-Butoxycarbonyl)-L-methionyl)-(*O*-benzyl-L-serinyl)-(*O*-(2-naphthyl)methyl)-L-serine methyl ester (124).** A solution of compound **121** (70 mg, 0.13 mmol) in dichloromethane (2 mL) was treated with trifluoroacetic acid (0.2 mL) at room temperature and stirred for 2 h. The volatiles were removed in *vacuo*. The crude product was dissolved in ethyl acetate, washed with saturated Na_2CO_3, followed by brine. The organic layer was dried over Na_2SO_4 and concentrated in *vacuo* to give the crude amine **122** (57 mg, 0.13 mmol) which was used without further purification. In a separate dry round bottom flask, a solution of *N*-Boc-L-methionine (42 mg, 0.17 mmol) in dry DMF (1 mL) was treated with HATU (65 mg, 0.17 mmol) and DIPEA (0.1 mL,). The mixture was stirred for 30 minutes at room temperature followed by the addition of compound **122** (57 mg, 0.13 mmol) in dry DMF (0.5 mL). The resulting reaction mixture was stirred for a further 3 h, then cooled to 0 ˚C and quenched with trimethylamine (50 µL), diluted with H_2O (1 mL) and extracted with EtOAc (2 mL x 2). The organic layers were dried over Na_2SO_4 and concentrated in *vacuo* then purified by silica gel chromatography (hexane-ethyl acetate 2:1) to give the title compound (60 mg, 70 %) as colorless oil. $[\alpha]^{RT}_{D=}$ -3 (*c* 0.75, $CHCl_3$);

^{1}H NMR (600 MHz, CD_3OD) δ 7.81 – 7.75 (m, 3H), 7.70 (s, 1H), 7.47 – 7.40 (m, 2H), 7.39 – 7.34 (m, 1H), 7.30 – 7.17 (m, 5H), 4.72 – 4.66 (m, 2H), 4.65 – 4.60 (m, 1H), 4.59 – 4.53 (m, 2H), 4.50 (d, *J* = 11.8 Hz, 1H), 4.47 (d, *J* = 11.8 Hz, 1H), 4.41 (s, 1H), 4.25 – 4.18 (m, 1H), 2.55 – 2.39 (m, 2H), 2.09 – 1.95 (m, 4H), 1.91 – 1.78 (m, 1H), 1.38 (s, 9H). ^{13}C NMR (151 MHz, CD_3OD) δ 173.3, 170.4, 170.3, 156.5, 137.7, 135.2, 135.2, 133.3, 133.3, 133.1, 128.0, 127.8, 127.8, 127.5, 127.5, 127.4, 127.3, 126.2, 126.2, 125.8, 125.6, 125.4, 79.4, 72.9, 72.8, 72.8, 72.8, 69.4, 69.1, 69.0, 53.9, 53.7, 52.9, 52.9, 51.6, 31.4, 29.7, 3.4, 13.9. ESIHRMS calcd for $C_{35}H_{45}N_3O_8SNa$ $[M + Na]^+$, 690.2825; found; 690.2819.

***N*-(*tert*-Butoxycarbonyl)-L-methionyl)-(*O*-benzyl-L-serinyl-L-serine (125).** The compound was synthesized from **25** (40 mg, 0.06 mmol) using the general hydrogenolysis protocol to give the title compound (26 mg, 82%) as colorless oil.^{1}H NMR (600 MHz, CD_3OD) δ 7.56 – 7.02 (m, 5H), 4.63 (t, *J* = 5.3 Hz, 1H), 4.58 – 4.49 (m, 3H), 4.22 – 4.14 (m, 1H), 3.91 – 3.85 (m, 1H), 3.81 – 3.76 (m, 2H), 3.74 – 3.71 (m, 1H), 3.71 (s, 3H), 2.61 – 2.47 (m, 2H), 2.08 – 2.01 (m, 4H), 1.89 – 1.82 (m, 1H), 1.41 (s, 9H). ^{13}C NMR (151 MHz, CD_3OD) δ 173.2, 170.5, 170.4, 156.6, 137.8, 128.0, 127.5, 127.3, 79.4, 72.9, 72.8, 69.3, 61.4, 61.4, 54.9, 54.8, 54.0, 53.8, 53.0, 51.4, 31.3, 29.7, 27.3, 13.8. ESIHRMS calcd for $C_{24}H_{37}N_3O_8SNa$ $[M + Na]^+$, 550.2199; found; 550.2195.

2-((2-Benzyloxyethyl)thio) ethanol (101). Compound **100** (10 mg, 0.028 mmol) was subjected to hydrogenolysis according to the standard conditions using 20% $Pd(OH)_2$ (40 mg, 0.056 mmols). After chromatography on silica gel (hexane / ethyl acetate 2:1) the title compound was obtained as a colorless oil, 4.3 mg, 72 %) with spectral data identical to the literature.[157]

Phenyl 2,3,4-tri-*O*-benzyl-1-thio-α-D-mannopyranoside (103). Compound **102** (10 mg, 0.015 mmol) was subjected to hydrogenolysis according to the standard conditions using 20% $Pd(OH)_2$ (15 mg, 0.022 mmol). After chromatography on silica gel (hexane / ethyl acetate 4:1) the title compound was obtained as a colorless oil (7.1 mg, 92 %) with spectral data identical to the literature[158].

Phenyl 3,4,6-tri-*O*-benzyl-1-thio-α-D-mannopyranoside (108). Compound **107** (11 mg, 0.016 mmol) was subjected to hydrogenolysis according to the standard conditions using 20% $Pd(OH)_2$ (22 mg, 0.032 mmol). After chromatography on silica gel (hexane / ethyl acetate 4:1) the title compound was obtained as a colorless oil (5.7 mg, 65 %) with spectral data identical to the literature[159]

***S*-*tert*-Butyl 2, 3, 4-tri-*O*-benzyl-1-thio-β-D-mannopyranoside (110).** Compound **111** (15 mg, 0.02 mmol) was subjected to hydrogenolysis according to the standard conditions using 20% $Pd(OH)_2$ (24 mg, 0.03 mmol). Chromatographic purification (hexane / ethyl acetate 4:1) the title compound (10.5 mg, 89 %) as a colorless oil. The spectral data identical to the literature compound **110** above.

Phenyl 2,3,4-tri-*O*-benzyl-1-thio-β-D-glucopyranoside (103). Compound **104** (10 mg, 0.015 mmol) was subjected to hydrogenolysis according to the standard conditions using 20% $Pd(OH)_2$ (15 mg, 0.022 mmol). After chromatography on silica gel (hexane / ethyl acetate 5:1) the title compound was obtained as a white powder, (7 mg, 88%) with spectral data identical to the literature.[160]

Phenyl 2,3,6-tri-*O*-benzyl-1-thio- β-D-glucopyranoside (115). Compound **116**[161] (10 mg, 0.015 mmol) was subjected to hydrogenolysis according to the standard conditions using 20%

$Pd(OH)_2$ (15 mg, 0.022 mmol). After chromatography on silica gel (hexane / ethyl acetate 4:1) the title compound was obtained as a powder, (5.5 mg, 70 %) with spectral data identical to the literature.[162]

REFERENCES

1. Montreuil, J., *Adv. Carbohydr. Chem. Biochem.* **1980,** *37*, 157-223.
2. (a) Bertozzi, C. R.; Kiessling; L., L., *Science* **2001,** *291*, 2357-2364; (b) Jung, K.-H.; Müller, M.; Schmidt, R. R., *Chem. Rev.* **2000,** *100*, 4423-4442.
3. (a) Davis, B. G., *Chem. Rev.* **2002,** *102*, 579-602; (b) Bishop, J. R.; Schuksz, M.; Esko, J. D., *Nature* **2007,** *446*, 1030-1037; (c) Linhardt, R. J., *J. Med. Chem.* **2003,** *46*, 2551-2564.
4. Wu, C.-Y.; Wong, C.-H., *Chem. Commun.* **2011,** *47*, 6201-6207.
5. Seeberger, P. H., *Nat Chem Biol* **2009,** *5*, 368-372.
6. Boltje, T. J.; Buskas, T.; Boons, G.-J., *Nat. Chem.* **2009,** *1*, 611-622.
7. Chlubnová, I.; Sylla, B.; Nugier-Chauvin, C.; Daniellou, R.; Legentil, L.; Kralová, B.; Ferrieres, V., *Nat. Prod. Rep.* **2011,** *28*, 937-952.
8. Stallforth, P.; Lepenies, B.; Adibekian, A.; Seeberger, P. H., *J. Med. Chem.* **2009,** *52*, 5561-5577.
9. Crich, D., *Acc. Chem. Res.* **2010,** *43*, 1144-1153.
10. Mydock, L. K.; Demchenko, A. V., *Org. Biomol. Chem.* **2010,** *8*, 497-510.
11. Koenigs, W.; Knorr, E., *Ber. Dtsch. Chem. Ges.* **1901,** *34*, 957-981.
12. (a) Lemieux, R. U.; Hendriks, K. B.; Stick, R. V.; James, K., *J. Am. Chem. Soc.* **1975,** *97*, 4056-4062; (b) Kaeothip, S.; Yasomanee, J. P.; Demchenko, A. V., *J. Org. Chem.* **2012,** *77*, 291-299.
13. Hanessian, S.; Ponpipom, M. M.; Lavallee, P., *Carbohydr. Res.* **1972,** *24*, 45-56.
14. Schmidt, R. R.; Michel, J., *Angew. Chem., Int. Ed. Engl.* **1980,** *19*, 731-732.
15. Mukaiyama, T.; Murai, Y.; Shoda, S.-i., *Chem. Lett.* **1981,** *10*, 431-432.

16. (a) Mukaiyama, T.; Jona, H.; Takeuchi, K., *Chem. Lett.* **2000,** *29*, 696-697; (b) Jona, H.; Mandai, H.; Chavasiri, W.; Takeuchi, K.; Mukaiyama, T., *Bull. Chem. Soc. Jpn* **2002,** *75*, 291-309; (c) Jona, H.; Takeuchi, K.; Mukaiyama, T., *Chem. Lett.* **2000,** *29*, 1278-1279.

17. Douglas, S. P.; Whitfield, D. M.; Krepinsky, J. J., *J. Carbohydr. Chem.* **1993,** *12*, 131-136.

18. Guazzelli, L.; Ulc, R.; Oscarson, S., *Carbohydr. Res.* **2014,** *389*, 57-65.

19. Lian, G.; Gao, Q.; Lin, F., *Carbohydr. Res.* **2008,** *343*, 2992-2996.

20. Li, M.; Han, X.; Yu, B., *J. Org. Chem.* **2003,** *68*, 6842-6845.

21. Mattson, A. L.; Michel, A. K.; Cloninger, M. J., *Carbohydr. Res.* **2012,** *347*, 142-146.

22. Yang, W.; Sun, J.; Yang, Z.; Han, W.; Zhang, W.-D.; Yu, B., *Tetrahedron Lett.* **2012,** *53*, 2773-2776.

23. Li, Y.; Mo, H.; Lian, G.; Yu, B., *Carbohydr. Res.* **2012,** *363*, 14-22.

24. Adinolfi, M.; Barone, G.; Iadonisi, A.; Mangoni, L.; Schiattarella, M., *Tetrahedron Lett.* **2001,** *42*, 5967-5969.

25. Adinolfi, M.; Iadonisi, A.; Ravidà, A.; Valerio, S., *Tetrahedron Lett.* **2006,** *47*, 2595-2599.

26. Danishefsky, S. J.; Bilodeau, M. T., *Angew. Chem., Int. Ed. Engl.* **1996,** *35*, 1380-1419.

27. Lemieux, R. U.; Huber, G., *J. Am. Chem. Soc.* **1953,** *75*, 4118-4118.

28. Winstein, S.; Grunwald, E.; Ingraham, L. L., *J. Am. Chem. Soc.* **1948,** *70*, 821-828.

29. Olah, G. A.; Baker, E. B.; Evans, J. C.; Tolgyesi, W. S.; McIntyre, J. S.; Bastien, I. J., *J. Am. Chem. Soc.* **1964,** *86*, 1360-1373.

30. Olah, G. A., *Angew. Chem., Int. Ed. Engl.* **1995,** *34*, 1393-1405.

31. Martin, A.; Arda, A.; Désiré, J.; Martin-Mingot, A.; Probst, N.; Sinaÿ, P.; Jiménez-Barbero, J.; Thibaudeau, S.; Blériot, Y., *Nat. Chem.* **2016,** *8*, 186-191.

32. Whitfield, D. M., *Adv. Carbohydr. Chem. Biochem.* **2009,** *62*, 83-159.

33. Whitfield, D. M., *Carbohydr. Res.* **2012,** *356*, 180-190.

34. Li, Z., *Carbohydr. Res.* **2010,** *345*, 1952-1957.

35. Litjens, R. E. J. N.; van den Bos, L. J.; Codée, J. D. C.; Overkleeft, H. S.; van der Marel, G. A., *Carbohydr. Res.* **2007,** *342*, 419-429.

36. Crich, D.; Sun, S., *J. Org. Chem.* **1996,** *61*, 4506-4507.

37. Crich, D.; Sun, S., *J. Org. Chem.* **1997,** *62*, 1198-1199.

38. Hosoya, T.; Kosma, P.; Rosenau, T., *Carbohydr. Res.* **2015,** *401*, 127-131.

39. Singleton, D. A.; Thomas, A. A., *J. Am. Chem. Soc.* **1995,** *117*, 9357-9358.

40. Crich, D.; Chandrasekera, N. S., *Angew. Chem., Int. Ed.* **2004,** *43*, 5386-5389.

41. Huang, M.; Garrett, G. E.; Birlirakis, N.; Bohé, L.; Pratt, D. A.; Crich, D., *Nat. Chem.* **2012,** *4*, 663-667.

42. E.-Badri, M. H.; Willenbring, D.; Tantillo, D. J.; Gervay-Hague, J., *J. Org. Chem.* **2007,** *72*, 4663-4672.

43. Amyes, T. L.; Jencks, W. P., *J. Am. Chem. Soc.* **1989,** *111*, 7888-7900.

44. Horenstein, B. A.; Bruner, M., *J. Am. Chem. Soc.* **1998,** *120*, 1357-1362.

45. Zhu, J.; Bennet, A. J., *J. Org. Chem.* **2000,** *65*, 4423-4430.

46. Griller, D.; Ingold, K. U., *Acc. Chem. Res.* **1980,** *13*, 317-323.

47. Beckwith, A. L. J.; Schiesser, C. H., *Tetrahedron* **1985,** *41*, 3925-3941.

48. Newcomb, M., *Tetrahedron* **1993,** *49*, 1151-1176.

49. Barresi, F.; Hindsgaul, O., *J. Am. Chem. Soc.* **1991,** *113*, 9376-9377.

50. Tebbe, F. N.; Parshall, G. W.; Reddy, G. S., *J. Am. Chem. Soc.* **1978,** *100*, 3611-3613.

51. Lakhlifi, T.; Sedqui, A.; Fathi, T.; Laude, B.; Robert, J.-F., *Can. J. Chem.* **1994,** *72*, 1417-1423.

52. Stork, G.; Kim, G., *J. Am. Chem. Soc.* **1992,** *114*, 1087-1088.

53. Stork, G.; La Clair, J. J., *J. Am. Chem. Soc.* **1996,** *118*, 247-248.

54. Ito, Y.; Ogawa, T., *Angew. Chem., Int. Ed. Engl.* **1994,** *33*, 1765-1767.

55. Dan, A.; Ito, Y.; Ogawa, T., *J. Org. Chem.* **1995,** *60*, 4680-4681.

56. Dan, A.; Ito, Y.; Ogawa, T., *Tetrahedron Lett.* **1995,** *36*, 7487-7490.

57. Ito, Y.; Ohnishi, Y.; Ogawa, T.; Nakahara, Y., *Synlett* **1998,** *1998*, 1102-1104.

58. Seifert, J.; Lergenmüller, M.; Ito, Y., *Angew. Chem., Int. Ed.* **2000,** *39*, 531-534.

59. Dan, A.; Lergenmüller, M.; Amano, M.; Nakahara, Y.; Ogawa, T.; Ito, Y., *Chem. Eur. J.* **1998,** *4*, 2182-2190.

60. Ito, Y.; Ando, H.; Wada, M.; Kawai, T.; Ohnish, Y.; Nakahara, Y., *Tetrahedron* **2001,** *57*, 4123-4132.

61. Lergenmüller, M.; Nukada, T.; Kuramochi, K.; Dan, A.; Ogawa, T.; Ito, Y., *Eur. J. Org. Chem.* **1999,** *1999*, 1367-1376.

62. Krog-Jensen, C.; Oscarson, S., *J. Org. Chem.* **1996,** *61*, 4512-4513.

63. Sanchez, S.; Bamhaoud, T.; Prandi, J., *Tetrahedron Lett.* **2000,** *41*, 7447-7452.

64. Marotte, K.; Sanchez, S.; Bamhaoud, T.; Prandi, J., *Eur. J. Org. Chem.* **2003,** *2003*, 3587-3598.

65. Pratt, M. R.; Leigh, C. D.; Bertozzi, C. R., *Org. Lett.* **2003,** *5*, 3185-3188.

66. Fairbanks, A. J., *Synlett* **2003,** *2003*, 1945-1958.

67. Ennis, S. C.; Fairbanks, A. J.; Slinn, C. A.; Tennant-Eyles, R. J.; Yeates, H. S., *Tetrahedron* **2001,** *57*, 4221-4230.

68. Seward, C. M. P.; Cumpstey, I.; Aloui, M.; Ennis, S. C.; Redgrave, A. J.; Fairbanks, A. J., *Chem. Commun.* **2000**, 1409-1410.

69. Aloui, M.; Chambers, D. J.; Cumpstey, I.; Fairbanks, A. J.; Redgrave, A. J.; Seward, C. M., *Chem. Eur. J.* **2002,** *8*, 2608-2621.

70. Ishiwata, A.; Lee, Y. J.; Ito, Y., *Org. Biomol. Chem.* **2010,** *8* (10), 3596-3608.

71. Crich, D.; Cai, W.; Dai, Z., *J. Org. Chem.* **2000,** *65*, 1291-1297.

72. Crich, D.; Wu, B., *Org. Lett.* **2006,** *8*, 4879-4882.

73. Crich, D.; Barba, G. R., *Tetrahedron Lett.* **1998,** *39*, 9339-9342.

74. Crich, D.; de la Mora, M. A.; Cruz, R., *Tetrahedron* **2002,** *58*, 35-44.

75. Crich, D.; Jayalath, P., *Org. Lett.* **2005,** *7*, 2277-2280.

76. Crich, D.; Karatholuvhu, M. S., *J. Org. Chem.* **2008,** *73*, 5173-5176.

77. Matsui, R.; Seto, K.; Sato, Y.; Suzuki, T.; Nakazaki, A.; Kobayashi, S., *Angew. Chem.* **2011,** *123*, 706-709.

78. Denmark, S. E.; Willson, T. M., *J. Am. Chem. Soc.* **1989,** *111*, 3475-3476.

79. Schinzer, D., *Synthesis* **1988,** *1988*, 263-273.

80. Mayr, H.; Kempf, B.; Ofial, A. R., *Acc. Chem. Res.* **2003,** *36*, 66-77.

81. Lewis, M. D.; Cha, J. K.; Kishi, Y., *J. Am. Chem. Soc.* **1982,** *104*, 4976-4978.

82. (a) Smith, D. M.; Woerpel, K. A., *Org. Biomol. Chem.* **2006,** *4*, 1195-1201; (b) Danishefsky, S.; Kerwin, J. F., *J. Org. Chem.* **1982,** *47*, 3803-3805.

83. McGarvey, G. J.; LeClair, C. A.; Schmidtmann, B. A., *Org. Lett.* **2008,** *10*, 4727-4730.

84. Crich, D.; Sharma, I., *Org. Lett.* **2008,** *10*, 4731-4734.

85. Zhang, Z.; Ollmann, I. R.; Ye, X.-S.; Wischnat, R.; Baasov, T.; Wong, C.-H., *J. Am. Chem. Soc.* **1999,** *121*, 734-753.

86. (a) Fraser-Reid, B.; Wu, Z.; Andrews, C. W.; Skowronski, E.; Bowen, J. P., *J. Am. Chem. Soc.* **1991,** *113*, 1434-1435; (b) Andrews, C. W.; Rodebaugh, R.; Fraser-Reid, B., *J. Org. Chem.* **1996,** *61*, 5280-5289; (c) Bülow, A.; Meyer, T.; Olszewski, Tomasz K.; Bols, M., *Eur. J. Org. Chem.* **2004,** *2004*, 323-329.

87. Huang, M.; Retailleau, P.; Bohé, L.; Crich, D., *J. Am. Chem. Soc.* **2012,** *134*, 14746-14749.

88. Crich, D.; Sun, S., *J. Am. Chem. Soc.* **1997,** *119*, 11217-11223.

89. Nukada, T.; Bérces, A.; Whitfield, D. M., *Carbohydr. Res.* **2002,** *337*, 765-774.

90. Huang, M.; Furukawa, T.; Retailleau, P.; Crich, D.; Bohé, L., *Carbohydr. Res.* **2016,** *427*, 21-28.

91. Crich, D., *J. Org. Chem.* **2011,** *76*, 9193-9209.

92. Walvoort, M. T. C.; Dinkelaar, J.; van den Bos, L. J.; Lodder, G.; Overkleeft, H. S.; Codée, J. D. C.; van der Marel, G. A., *Carbohydr. Res.* **2010,** *345*, 1252-1263.

93. Schmidt, R. R., Oligosaccharide Synthesis with Trichloroacetimidates. In *Preparative Carbohydrate Chemistry*, Hanessian, S., Ed. Dekker: New York, 1997; pp 283-312.

94. David, S.; Hanessian, S., *Tetrahedron* **1985,** *41*, 643-663.

95. Lu, L.; Zhang, W.; Nam, S.; Horne, D. A.; Jove, R.; Carter, R. G., *J. Org. Chem.* **2013,** *78*, 2213-2247.

96. Kulkarni, V.; Cohen, T., *Tetrahedron* **1997,** *53*, 12089-12100.

97. Screttas, C. G.; Micha-Screttas, M., *J. Org. Chem.* **1978,** *43*, 1064-1071.

98. Schmidt, R. R.; Michel, J.; Roos, M., *Liebigs Ann. Chem.* **1984**, 1343-1357.

99. Moumé-Pymbock, M.; Crich, D., *J. Org. Chem.* **2012,** *77*, 8905-8912.

100. Nukada, T.; Bérces, A.; Wang, L.; Zgierski, M. Z.; Whitfield, D. M., *Carbohydr. Res.* **2005,** *340*, 841-852.

101. Ionescu, A. R.; Whitfield, D. M.; Zgierski, M. Z.; Nukada, T., *Carbohydr. Res.* **2006,** *341*, 2912-2920.

102. Sammakia, T.; Smith, R. S., *J. Am. Chem. Soc.* **1994,** *116*, 7915-7916.

103. Krumper, J. R.; Salamant, W. A.; Woerpel, K. A., *J. Org. Chem.* **2009,** *74*, 8039-8050.

104. Koeppen, B. H., *Carbohydr. Res.* **1972,** *24*, 154-158.

105. Houseknecht, J. B.; Lowary, T. L., *Curr. Opin. Chem. Biol.* **2001,** *5*, 677-682.

106. Allen, A. K.; Desai, N. N.; Neuberger, A.; Creeth, J. M., *Biochem. J.* **1978,** *171*, 665-674.

107. Lowary, T. L., *Curr. Opin. Chem. Biol.* **2003,** *7*, 749-756.

108. Lowary, T. L., *Acc. Chem. Res.* **2016,** *49* (7), 1379-1388.

109. Ellervik, U.; Magnusson, G., *J. Am. Chem. Soc.* **1994,** *116*, 2340-2347.

110. Houseknecht, J. B.; Lowary, T. L.; Hadad, C. M., *J. Phys. Chem. A* **2003,** *107*, 5763-5777.

111. Imamura, A.; Lowary, T., *Trends Glycosci. Glycotechnol.*, **2011,** *23*, 134-152.

112. Gadikota, R. R.; Callam, C. S.; Wagner, T.; Del Fraino, B.; Lowary, T. L., *J. Am. Chem. Soc.* **2003,** *125*, 4155-4165.

113. Zhu, X.; Kawatkar, S.; Rao, Y.; Boons, G.-J., *J. Am. Chem. Soc.* **2006,** *128*, 11948-11957.

114. Crich, D.; Pedersen, C. M.; Bowers, A. A.; Wink, D. J., *J. Org. Chem.* **2007,** *72*, 1553-1565.

115. Wang, Y.; Maguire-Boyle, S.; Dere, R. T.; Zhu, X., *Carbohydr. Res.* **2008,** *343*, 3100-3106.

116. Ayers, J. D.; Lowary, T. L.; Morehouse, C. B.; Besra, G. S., *Bioorg. Med. Chem. Lett.* **1998,** *8*, 437-442.

117. Chauhan, B. P. S.; Rathore, J. S.; Bandoo, T., *J. Am. Chem. Soc.* **2004,** *126*, 8493-8500.

118. Gaunt, M. J.; Yu, J.; Spencer, J. B., *J. Org. Chem.* **1998,** *63*, 4172-4173.

119. Yin, H.; D'Souz, F. W.; Lowary, T. L., *J. Org. Chem.* **2002,** *67*, 892-903.

120. Lee, Y. J.; Lee, K.; Jung, E. H.; Jeon, H. B.; Kim, K. S., *Org. Lett.* **2005,** *7*, 3263-3266.

121. Taha, H. A.; Richards, M. R.; Lowary, T. L., *Chem. Rev.* **2013,** *113*, 1851-1876.

122. Rijssel, E. R. v.; Delft, P. v.; Lodder, G.; Overkleeft, H. S.; Marel, G. A. v. d.; Filippov, D. V.; Codée, J. D. C., *Angew. Chem., Int. Ed.* **2014,** *53*, 10381-10385.

123. Larsen, C. H.; Ridgway, B. H.; Shaw, J. T.; Woerpel, K. A., *J. Am. Chem. Soc.* **1999,** *121*, 12208-12209.

124. Larsen, C. H.; Ridgway, B. H.; Shaw, J. T.; Smith, D. M.; Woerpel, K. A., *J. Am. Chem. Soc.* **2005,** *127*, 10879-10884.

125. Beaver, M. G.; Woerpel, K. A., *J. Org. Chem.* **2010,** *75*, 1107-1118.

126. Zhu, X.; Schmidt, R. R., *Angew. Chem., Int. Ed.* **2009,** *48*, 1900-1934.

127. Paulsen, H.; Lockhoff, O., *Chem. Ber.* **1981,** *114*, 3079-3101.

128. Schumann, B.; Parameswarappa, S. G.; Lisboa, M. P.; Kottari, N.; Guidetti, F.; Pereira, C. L.; Seeberger, P. H., *Angew. Chem., Int. Ed.* **2016,** *55*, 14431-14434.

129. Crich, D.; Dudkin, V., *J. Am. Chem. Soc.* **2001,** *123*, 6819-6825.

130. Kaeothip, S.; Akins, S. J.; Demchenko, A. V., *Carbohydr. Res.* **2010,** *345*, 2146-2150.

131. Pedersen, C. M.; Olsen, J.; Brka, A. B.; Bols, M., *Chem. Eur.J.* **2011,** *17*, 7080-7086.

132. Kalikanda, J.; Li, Z., *Carbohydr. Res.* **2011,** *346*, 2380-2383.

133. van der Vorm, S.; Hansen, T.; Overkleeft, H. S.; van der Marel, G. A.; Codee, J. D. C., *Chem. Sci.* **2017,** *8*, 1867-1875.

134. Hagen, B.; Ali, S.; Overkleeft, H. S.; van der Marel, G. A.; Codée, J. D. C., *J. Org. Chem.* **2017,** *82*, 848-868.

135. Hagen, B.; van Dijk, J. H. M.; Zhang, Q.; Overkleeft, H. S.; van der Marel, G. A.; Codée, J. D. C., *Org. Lett.* **2017,** *19*, 2514-2517.

136. Adero, P. O.; Furukawa, T.; Huang, M.; Mukherjee, D.; Retailleau, P.; Bohé, L.; Crich, D., *J. Am. Chem. Soc.* **2015,** *137*, 10336-10345.

137. Wuts, P. G.; Greene, T. W., *Greene's protective groups in organic synthesis*. John Wiley & Sons: 2006.

138. Green, T. W.; Wuts, P. G. M., In *Protective Group in Organic Synthesis*, Third ed.; Wiley: New York, 1999.

139. Kocienski, P. J., In *Protecting Groups*, 3 ed.; Thieme: Stuttgart, 2005.

140. Moreau, V.; Norrild, J. C.; Driguez, H., *Carbohydr. Res.* **1997,** *300*, 271-277.

141. Crich, D.; Li, H., *J. Org. Chem.* **2000,** *65*, 801-805.

142. Xia, J.; Abbas, S. A.; Locke, R. D.; Piskorz, C. F.; Alderfer, J. L.; Matta, K. L., *Tetrahedron Lett.* **2000,** *41*, 169-173.

143. Liao, W.; Locke, R. D.; Matta, K. L., *Chem. Commun.* **2000**, 369-370.

144. Wright, J. A.; Yu, J.; Spencer, J. B., *Tetrahedron Lett.* **2001,** *42*, 4033-4036.

145. Volbeda, A. G.; Kistemaker, H. A. V.; Overkleeft, H. S.; van der Marel, G. A.; Filippov, D. V.; Codée, J. D. C., *J. Org. Chem.* **2015,** *80*, 8796-8806.

146. Lloyd, D.; Bylsma, M.; Bright, D. K.; Chen, X.; Bennett, C. S., *J. Org. Chem.* **2017,** *82*, 3926-3934.

147. Papageorgiou, E. A.; Gaunt, M. J.; Yu, J.-q.; Spencer, J. B., *Org. Lett.* **2000,** *2*, 1049-1051.

148. Tani, S.; Sawadi, S.; Kojima, M.; Akai, S.; Sato, K.-i., *Tetrahedron Lett.* **2007,** *48*, 3103-3104.

149. Zhang, Y.-M.; Brodzky, A.; Sinaÿ, P.; Saint-Marcoux, G.; Perly, B., *Tetrahedron: Asymmetry* **1995,** *6*, 1195-1216.

150. Yajima, A.; Kawajiri, A.; Mori, A.; Katsuta, R.; Nukada, T., *Tetrahedron Lett.* **2014,** *55*, 4350-4354.

151. Lu, L.; Zhang, W.; Nam, S.; Horne, D. A.; Jove, R.; Carter, R. G., *J. Org. Chem.* **2013,** *78*, 2213-2247.

152. Huang, M.; Retailleau, P.; Bohé, L.; Crich, D., *J. Am. Chem. Soc.* **2012,** *134*, 14746-14749.

153. Wang, Y.; Maguire-Boyle, S.; Dere, R. T.; Zhu, X., *Carbohydr. Res.* **2008,** *343*, 3100-3106.

154. Waschke, D.; Leshch, Y.; Thimm, J.; Himmelreich, U.; Thiem, J., *Eur. J. Org. Chem.* **2012,** *2012*, 948-959.

155. Yajima, A.; Kawajiri, A.; Mori, A.; Katsuta, R.; Nukada, T., *Tetrahedron Lett.* **2014,** *55* , 4350-4354.

156. Crich, D.; Li, H., *J. Org. Chem.* **2000,** *65*, 801-805.

157. Morellato-Castillo, L.; Acharya, P.; Combes, O.; Michiels, J.; Descours, A.; Ramos, O. H. P.; Yang, Y.; Vanham, G.; Ariën, K. K.; Kwong, P. D.; Martin, L.; Kessler, P., *J. Med. Chem.* **2013,** *56*, 5033-5047.

158. Pothukanuri, S.; Winssinger, N., *Org. Lett.* **2007,** *9*, 2223-2225.

159. Zhang, Y.-M.; Brodzky, A.; Sinaÿ, P.; Saint-Marcoux, G.; Perly, B., *Tetrahedron: Asymmetry* **1995,** *6*, 1195-1216.

160. Chan, T.; He, X., *Synthesis* **2006,** *2006*, 1645-1651.

161. Herczeg, M.; Mező, E.; Eszenyi, D.; Antus, S.; Borbás, A., *Tetrahedron* **2014,** *70*, 2919-2927.

162. Motawia, M. S.; Olsen, C. E.; Enevoldsen, K.; Marcussen, J.; Møller, B. L., *Carbohydr. Res.* **1995,** *277*, 109-123.

ABSTRACT

CATION CLOCK REACTIONS FOR THE DETERMINATION OF RELATIVE REACTION KINETICS IN GLYCOSYLATION REACTIONS

by

PHILIP OUMA ADERO

December 2018

Advisor: Dr. David Crich

Major: Chemistry

Degree: Doctor of Philosophy

This dissertation presents the development of cyclization reactions as clocks for the determination of the molecularity of glycosylation reactions in individual pyranoside systems and extends it to the arabinofuranoside systems. It also describes the development of selective hydrogenolytic cleavage of naphthylmethyl ethers in the presence of sulfides.

The first part of chapter one gives an overview of the significance of glycochemistry and the challenges involved. The second part describes some selected glycosylation methods and extends this to the general mechanistic studies of glycosylation. This is followed by the discussion of the general clock reactions in literature which initiates a further discussion of the concept of cyclization as a clock for probing reaction mechanism and providing specific previous studies as well as the limitations involved and finally proposes the possible solution.

The second chapter discusses the cation clock method based on the intramolecular Sakurai reaction to probe the concentration dependence of representative *O*- and *C*-glycosylation reactions from glycosyl trichloroacetimidate donors on activation by trimethylsilyl triflate. The 4,6-*O*-benzylidene-directed β-mannosylation, and both α and β-glucosylation demonstrated to proceed

with a strong dependence on the concentration of the acceptor alcohol, whereas the α-mannosylation is much less concentration dependent.

In the third chapter, the further development of the concept cation clock reactions for the determination of relative reaction kinetics in arabinofuranosylation is discussed. The use of intramolecular hydroxyl groups as candidates for clock reactions has been shown, leading to the formation of cyclic clock products in both 3,5-*O*-di-*tert*-butylsilylene and 3,5-di-*O*-benzyl arabinofuranoside series. In the study, formation of the β-arabinofuranoside is more concentration dependent than the α-isomers in the 3,5-*O*-di-*tert*-butylsilylene protected donor. The unselective formation of both, β and α-*O*-glycosides in the 3,5-di-*O*-benzyl protected arabinofuranosides is also understood in terms of a more of S_N1-like mechanism with a strong nucleophile.

Chapter four discusses the use of the cation clock method to determine the influence of acceptor nucleophilicity on the arabinofuranosylation mechanism. The use of acceptors of varying nucleophilicity, revealed that 3,5-di-*tert*-butylsilylene protected arabinofuranosylation is likely to occur vial a loose S_N2 mechanism from each of the two rapidly equilibrating glycosyl triflate.

In chapter five, hydrogenolytic cleavage of naphthylmethyl ethers in the presence of sulfides is described. The series of model thioethers or thioglycosides protected with combinations of benzyl ethers and 2-naphthylmethyl ethers, that the latter are readily cleaved selectively under hydrogenolytic conditions in the presence of the frequently catalyst-poisoning sulfides.

Finally, chapter six documents the experimental procedures and characterization data for the synthesized compounds

AUTOBIOGRAPHICAL STATEMENT

PHILIP OUMA ADERO

EDUCATION

2012-Present	PhD in Organic Chemistry Wayne State University, Detroit, Michigan, USA Research Advisor: Professor David Crich
2011-2012	M.Sc. in Organic Chemistry, Youngstown State University, Youngstown, Ohio, USA **Thesis**: Heterocycle synthesis via rhodium (II)-catalyzed azido carbenoid cyclization Research Advisor: Professor Peter Norris
2004-2009	B.Sc. (Hons) Chemistry, University of Eastern Africa Baraton, Eldoret Kenya.

RESEARCH PUBLICATIONS

1. **Adero, P. O**.; Amarasekara, H.; Wen, P.; Bohé, L.; Crich, D. (**2018**), The experimental evidence in support of glycosylation mechanisms at the S_N1–S_N2 Interface. *Chem. Rev*. DOI: 10.1021/acs.chemrev.8b00083
2. **Adero, P. O**., Jarois, D. R., and Crich, D. (**2017**) Hydrogenolytic cleavage of naphthylmethyl ethers in the presence of sulfides. *Carbohydr. Res*. 449, 11–16.
3. **Adero, P. O**., Furukawa, T., Huang, M., Mukherjee, D., Retailleau, P., Bohé, L., and Crich, D. (**2015**). Cation clock reactions for the determination of relative reaction kinetics in glycosylation reactions: Applications to gluco- and mannopyranosyl sulfoxide and trichloroacetimidate type donors. *J. Am. Chem. Soc.*, 137, 10336–10345.
4. Ramachandran, E., Kalaivani, P., Prabhakaran, R., Zeller, M., Bartlett, J. H., **Adero, P.O** O.,….Natarajan, K. (**2012**). Synthesis, characterization, crystal structure and DNA binding studies of Pd(II) complexes containing thiosemicarbazone and triphenylphosphine/ triphenylarsine. *Inorg. Chim. Acta*. 385, 94–99.
5. Yamuna, E., Zeller, M., **Adero, P. O**., and Prasad, K. J. R. (**2012**). Synthesis of thieno- and benzocyclohepta[b]indoles: Gewald reaction and regioselective cycloaddition of acetylenic esters. *Arkivoc*, 2012(6), 326–342.